

Call - 858
FAP-21/22

GOVERNMENT OF PEOPLE'S REPUBLIC OF BANGLADESH
MINISTRY OF WATER RESOURCES
WATER RESOURCES PLANNING ORGANIZATION

FEDERAL REPUBLIC OF GERMANY

KREDITANSTALT FÜR
WIEDERAUFBAU (KfW)

FRENCH REPUBLIC

AGENCE FRANÇAISE DE
DÉVELOPPEMENT (AFD)



8

PAH - 711
A - 858 (1)

**BANK PROTECTION AND
RIVER TRAINING (AFPM)
PILOT PROJECT
FAP 21/22**

**FINAL PROJECT
EVALUATION REPORT**



VOLUME IV

**Annex 6: The Groyne Test Structure;
Monitoring Report**

**Annex 7: The Groyne Test Structure;
Evaluation of Hydraulic
Loads and River Response**

DECEMBER 2001



JAMUNA TEST WORKS CONSULTANTS, JOINT VENTURE
CONSULTING CONSORTIUM FAP 21/22

RHEIN-RUHR ING.GES.MBH, DORTMUND/GERMANY
COMPAGNIE NATIONALE DU RHONE, LYON/FRANCE
PROF.DR. LACKNER & PARTNERS, BREMEN/GERMANY
DELFT HYDRAULICS, DELFT/NETHERLANDS

In association with:
BANGLADESH ENGINEERING &
TECHNOLOGICAL SERVICES LTD. (BETS)
DESH UPODESH LIMITED (DUL)

2

**BANK PROTECTION AND RIVER TRAINING (AFPM)
PILOT PROJECT FAP 21/22**

FINAL PROJECT EVALUATION REPORT

VOLUME IV

- Annex 6: The Groyne Test Structure; Monitoring Report**
**Annex 7: The Groyne Test Structure; Evaluation of Hydraulic
Loads and River Response**

MAY 2001

6

CONTENTS OF FINAL PROJECT EVALUATION REPORT

Volume I	Main Report	
	Part A:	Bank Protection Pilot Project FAP 21
	Part B:	River Training (AFPM) Pilot Project FAP 22
Volume II	Annex 1	Morphological Investigations
	Annex 2	Socio-Economic Aspects
	Annex 3	Ecological Assessment
Volume III	Annex 4	The Groyne Test Structure; Design Report
	Annex 5	The Groyne Test Structure; Procurement and Construction Report
Volume IV	Annex 6	The Groyne Test Structure; Monitoring Report
	Annex 7	The Groyne Test Structure; Evaluation of Hydraulic Loads and River Response
Volume V	Annex 8	The Revetment Test Structure; Design Report
	Annex 9	The Revetment Test Structure; Procurement and Construction Report
Volume VI	Annex 10	The Revetment Test Structure; Monitoring Report
	Annex 11	The Revetment Test Structure; Evaluation of Hydraulic Loads and River Response

BANK PROTECTION PILOT PROJECT

FAP 21/22

Important General Remark

The results presented and discussed in the Annexes of the Final Evaluation Report of the Bank Protection Pilot Project provides the state of the studies during the course of analysis and writing by the individual project partners. After a final review subsequent to the completion of the Annexes during the concluding stages of the Main Reports and the Guidelines and Manual some modifications and adjustments were felt necessary, also for covering more generalized structural measures in addition to the given case studies. For that reason, with respect to design formulae, recommended structure types, etc., reference should be made to the Main Reports and the Guidelines and Design Manual only.

DECEMBER 2001

BANK PROTECTION PILOT PROJECT

FAP 21

FINAL PROJECT EVALUATION REPORT

ANNEX 6

THE GROUYNE TEST STRUCTURE; MONITORING REPORT

MAY 2001

FAP 21 - BANK PROTECTION PILOT PROJECT

FINAL PROJECT EVALUATION REPORT

ANNEX 6

Table of Contents

	<u>Page</u>
List of Acronyms	A-1
Glossary	G-1
SUMMARY	0-1
1 INTRODUCTION	1-1
1.1 INTRODUCTION TO THE PROJECT	1-1
1.2 SCOPE OF THE PRESENT ANNEX	1-1
1.3 OVERVIEW OF THE TEST SITE AND THE LAYOUT OF THE STRUCTURE	1-2
1.4 OBJECTIVES OF THE MONITORING	1-5
1.4.1 General	1-5
1.4.2 Field Tasks	1-6
1.4.3 Definition of Survey Areas	1-7
1.4.4 Definition of Survey Intervals	1-8
1.4.5 Dhaka Office Tasks	1-8
2 ORGANIZATION / IMPLEMENTATION	2-1
2.1 ORGANIZATION OF THE MONITORING TEAM	2-1
2.2 LOGISTICS	2-1
2.3 GEODESY	2-2
2.3.1 Horizontal Reference	2-2
2.3.2 Vertical Reference	2-3
2.3.3 Benchmarks	2-4
2.4 SURVEY EQUIPMENT	2-4
2.5 SURVEY BOATS	2-6
2.6 WATER LEVEL GAUGES	2-10
3 FIELD SURVEYS	3-1
3.1 HYDROGRAPHIC SOFTWARE	3-1
3.2 BATHYMETRY	3-2
3.3 FLOW MEASUREMENTS	3-3
3.3.1 DGPS Float Tracking	3-3
3.3.2 Advanced DGPS Float Tracking	3-3
3.3.3 Current Point Measurements	3-4
3.4 Discharge Measurements	3-4
3.5 Land Surveys	3-4
3.6 Monitoring Station	3-5



	<u>Page</u>
4 POST PROCESSING	4-1
4.1 GENERAL	4-1
4.2 PROCESSING OF BATHYMETRIC DATA	4-3
4.3 PROCESSING OF FLOAT TRACKS	4-3
4.4 PROCESSING OF CURRENT POINT MEASUREMENTS	4-3
4.5 PROCESSING OF TOPOGRAPHIC DATA	4-4
4.6 PROCESSING OF DATA FROM THE MONITORING STATION	4-4
5 THE GROUYNE TEST STRUCTURE	5-1
5.1 SUMMARY	5-1
5.2 LOGBOOK OBSERVATIONS	5-1
5.2.1 Chronology of Events	5-1
5.2.2 Floating Debris	5-3
5.3 BATHYMETRY AND FLOW CONDITIONS	5-3
5.3.1 Site Surveys	5-3
5.3.2 Development of Scour Holes	5-5
5.3.3 Flow Pattern in the Groyne Fields	5-22
5.3.4 Groyne Surveys	5-28
5.3.5 Cross-Sections at Eroded Embankments	5-29
6 STATISTICAL EVALUATIONS	6-1
6.1 WATER LEVEL RECORDS	6-1
6.1.1 Staff Gauges	6-1
6.1.2 Water Level Auto Gauge	6-1
6.2 DATA COLLECTED BY MONITORING STATION	6-4
6.2.1 Wind and Waves Statistics	6-4
6.2.2 Test Pile Inclination and Acceleration	6-5
6.3 PRECIPITATION	6-10
6.4 TEMPERATURE AND RELATIVE HUMIDITY	6-10
6.5 PIEZOMETER MEASUREMENTS	6-12
6.5.1 Water Level Difference at G-2	6-12
6.5.2 Embankment at G-A	6-12
7 THE KAMARNAJI MAIN CHANNEL	7-1
7.1 MAIN SURVEYS	7-1
7.2 CROSS SECTIONS AT MAIN RIVER	7-1
7.3 DISCHARGE	7-9
8 THE KAMARNAJI MAIN CHANNEL	8-1
8.1 NECESSARY	8-1
8.2 INTENSITY	8-1
8.3 LOGISTICS	8-2
8.4 ORGANISATION	8-4

Page**REFERENCES**

R - 1

LIST OF TABLES

Table 2.3-1:	Horizontal reference applied by FAP 21	2-3
Table 2.3-2:	Definition of water levels at Kamarjani	2-4
Table 2.4-1:	Instrumentation specifications	2-5
Table 2.5-1:	Instrumentation of the survey boats	2-7
Table 2.5-2:	Specifications of survey boats	2-7
Table 2.6-1:	Water level gauges	2-10
Table 5.2-1:	Chronology of events reported in the logbook	5-1
Table 5.2-2:	Observations on floating debris	5-3
Table 5.3-1:	Description of hydrographic conditions at Test Site I during monsoon 1995	5-4
Table 5.3-2:	Description of hydrographic conditions at Test Site I during monsoon 1996 and 1997	5-5
Table 5.3-3:	Development of scour holes d/s from G-1, G-2 and G-3	5-6
Table 5.3-4:	Observations from Groyne Surveys	5-28
Table 5.3-5:	Bank erosion rates d/s from G-1, G-2 and G-3	5-29
Table 6.1-1:	Maximum recorded water levels from 1995 to 1999	6-1
Table 6.3-1:	Maximum daily rainfalls	6-10
Table 6.5-1:	Water level difference at G-2	6-12
Table 7.3-1:	Discharge Kamarjani channel vs Kundarapara channel relative to SHW	7-9

LIST OF FIGURES

Fig. 1.3-1:	Original Test Structure June 1995	1-3
Fig. 1.3-2:	Adapted Test Structure September 1998	1-3
Fig. 1.3-3:	Jamuna overview at Test Site-I in January 1999	1-3
Fig. 1.3-4:	Progressive bank erosion from Test Site to Balashi Ghat	1-4
Fig. 2.5-1:	Survey boat Obelix during Valeport operation	2-8
Fig. 2.5-2:	Survey boat Asterix	2-8
Fig. 2.5-3:	Details of survey boats	2-9
Fig. 3.1-1:	Masterchart on-line survey display	3-1
Fig. 3.2-1:	GPS-reference station and survey boat setup for bathymetric surveys	3-2
Fig. 3.3-1:	GPS drifter float with Drogue	3-3
Fig. 3.6-1:	Schematic diagram of monitoring station located at groyne G-2, Test Site I	3-5
Fig. 4.1-1:	Flowchart – Processing of digital monitoring data	4-2
Fig. 5.3-1:	Bathymetry at the test site area on May 18, 1995	5-8
Fig. 5.3-2:	Bathymetry at the test site area on June 10, 1995	5-8
Fig. 5.3-3:	Bathymetry at the test site area on June 24, 1995	5-9
Fig. 5.3-4:	Bathymetry and flow at the test site area on June 26, 1995	5-9

	<u>Page</u>	
Fig. 5.3-5:	Bathymetry at the test site area on June 29, 1995	5-10
Fig. 5.3-6:	Bathymetry at the test site area on July 09-10, 1995	5-10
Fig. 5.3-7:	Bathymetry at the test site area on July 11, 1995	5-11
Fig. 5.3-8:	Bathymetry and flow at the test site area on July 17, 1995	5-11
Fig. 5.3-9:	Bathymetry and flow at the test site area on July 31, 1995	5-12
Fig. 5.3-10:	Bathymetry at the test site area on August 05, 1995	5-12
Fig. 5.3-11:	Bathymetry at the test site area on August 16, 1995	5-13
Fig. 5.3-12:	Bathymetry and flow at the test site area on August 20, 1995	5-13
Fig. 5.3-13:	Bathymetry and flow at the test site area on August 20, 1995	5-14
Fig. 5.3-14:	Bathymetry at the test site area on August 27, 1995	5-14
Fig. 5.3-15:	Bathymetry and flow at the test site area on September 11, 1995	5-15
Fig. 5.3-16:	Bathymetry at the test site area on September 24, 1995	5-15
Fig. 5.3-17:	Bathymetry and flow at the test site area on June 11-12, 1996	5-16
Fig. 5.3-18:	Bathymetry and flow at the test site area on June 25-27, 1996	5-17
Fig. 5.3-19:	Bathymetry and flow at the test site area on July 13-16, 1996	5-18
Fig. 5.3-20:	Bathymetry and flow at the test site area on July 27-28, 1996	5-19
Fig. 5.3-21:	Bathymetry and flow at the test site area on August 17-19, 1996	5-20
Fig. 5.3-22:	Bathymetry and flow at the test site area on July 24-25, 1997	5-21
Fig. 5.3-23:	Flow pattern d/s of G-3 in July 1996	5-23
Fig. 5.3-24:	Flow pattern d/s of G-3 in August 1996	5-24
Fig. 5.3-25:	Float tracking d/s of G-3 in August 1996	5-25
Fig. 5.3-26:	Iso-velocities evaluated from float tracks in August 1996	5-25
Fig. 5.3-27:	Flow pattern d/s of G-A in August 1996	5-26
Fig. 5.3-28:	Flow pattern d/s of G-A in August 1996	5-27
Fig. 5.3-29:	Cross-sections at 10 m d/s from groyne G-1	5-30
Fig. 5.3-30:	Bathymetry at groyne G-1 on June 08, 1995	5-31
Fig. 5.3-31:	Bathymetry at groyne G-1 on June 20, 1995	5-31
Fig. 5.3-32:	Bathymetry at groyne G-1 on June 29, 1995	5-32
Fig. 5.3-33:	Bathymetry at groyne G-1 on July 11, 1995	5-32
Fig. 5.3-34:	Cross-sections at 10 m d/s from groyne G-2	5-33
Fig. 5.3-35:	Bathymetry at groyne G-2 on July 08, 1995	5-34
Fig. 5.3-36:	Bathymetry at groyne G-2 on July 09, 1995	5-34
Fig. 5.3-37:	Bathymetry at groyne G-2 on July 10, 1995	5-35
Fig. 5.3-38:	Bathymetry at groyne G-2 on July 11, 1995	5-35
Fig. 5.3-39:	Bathymetry at groyne G-2 on July 12, 1995	5-36
Fig. 5.3-40:	Bathymetry at groyne G-2 on July 14, 1995	5-36
Fig. 5.3-41:	Cross-sections at 10 m d/s from groyne G-3	5-37
Fig. 5.3-42:	Bathymetry at groyne G-3 on August 10, 1995	5-38
Fig. 5.3-43:	Bathymetry at groyne G-3 on August 14, 1995	5-38
Fig. 5.3-44:	Bathymetry at groyne G-3 on August 16, 1995	5-39
Fig. 5.3-45:	Bathymetry at groyne G-3 on August 20, 1995	5-39
Fig. 5.3-46:	Bathymetry at groyne G-3 on August 23, 1995	5-40
Fig. 5.3-47:	Bathymetry at groyne G-3 on September 24, 1995	5-40
Fig. 5.3-48:	Cross-sections at 10 m d/s from groyne G-A (before adaptation)	5-41
Fig. 5.3-49:	Bathymetry at groyne G-A on January 15, 1996	5-42
Fig. 5.3-50:	Bathymetry at groyne G-A on March 08, 1996	5-42
Fig. 5.3-51:	Cross-sections at 10 m d/s from groyne G-A (after adaptation)	5-43
Fig. 5.3-52:	Bathymetry at groyne G-A on April 19, 1996	5-44
Fig. 5.3-53:	Bathymetry at groyne G-A on July 13, 1996	5-44
Fig. 5.3-54:	Bathymetry at groyne G-A on August 17, 1996	5-45
Fig. 5.3-55:	Bathymetry at groyne G-A on September 23, 1996	5-45

	<u>Page</u>
Fig. 5.3-56: Cross-sections at 10 m d/s from groyne G-A/2	5-46
Fig. 5.3-57: Bathymetry at groyne G-A/2 on February 23, 1997	5-47
Fig. 5.3-58: Bathymetry at groyne G-A/2 on March 06, 1997	5-47
Fig. 5.3-59: Bathymetry at groyne G-A/2 on March 13, 1997	5-48
Fig. 5.3-60: Bathymetry at groyne G-A/2 on March 26, 1997	5-48
Fig. 5.3-61: Cross-sections at 70 m d/s from groyne G-1	5-49
Fig. 5.3-62: Cross-sections at 80 m d/s from groyne G-2	5-50
Fig. 5.3-63: Cross-sections at 30 m d/s from groyne G-3	5-51
Fig. 6.1-1: Hydrographs from June to September in 1995 to 1999	6-2
Fig. 6.1-2: Water level at G-A during two peak levels in 1996 vs water level slope between G-B/1 and downstream from Manos river	6-2
Fig. 6.1-3: Water level at G-A during two peak levels in 1997 vs water level slope between G-B/1 and G-A	6-3
Fig. 6.1-4: Rise to water level peak in July 1997 10 minutes interval recordings of auto gauge at G-2	6-3
Fig. 6.2-1: The Groyne Test Structure; Monthly mean wind speed measured at G-2	6-4
Fig. 6.2-2: Wave height during storm measurement 02/09/95 (4:46 – 11:11)	6-6
Fig. 6.2-3: Wave height during storm measurement 14/09/96 (15:40 – 16:07)	6-6
Fig. 6.2-4: Wave height during storm measurement 25/08/97 (18:25 – 19:53)	6-7
Fig. 6.2-5: Average wave heights in relative to wind speed and wind direction (1996)	6-7
Fig. 6.2-6: Movements of Test Pile # 30 at G-2 (02/09/95)	6-8
Fig. 6.2-7: Movements of Test Pile # 30 at G-2 (14/09/96)	6-9
Fig. 6.3-1: The Groyne Test Structure; Comparison of monthly rainfalls	6-10
Fig. 6.4-1: Temperature and Relative Humidity	6-11
Fig. 6.5-1: Under ground and surface water level at G-A, June to July 1997	6-13
Fig. 7.1-1: Bathymetry and flow at main channel in June 1995	7-2
Fig. 7.1-2: Bathymetry and flow at main channel in July 1995	7-2
Fig. 7.1-3: Bathymetry and flow at main channel in September 1995	7-3
Fig. 7.1-4: Differential DGM Model July 1995 – September 1995	7-3
Fig. 7.2-1: Cross-section Kamarjani channel starting from 150 m upstream of G-B/2	7-5
Fig. 7.2-2: Cross-section Kamarjani channel starting from G-2	7-6
Fig. 7.2-3: Cross-section Kamarjani channel starting from Syedpur	7-7
Fig. 7.2-4: Cross-section Kamarjani channel starting from Rasulpur	7-8
Fig. 7.3-1: Discharge measurement Kundarapara channel on August 19, 1997	7-10
Fig. 7.3-2: Discharge measurement Kamarjani channel on August 19, 1997	7-11
Fig. 7.3-3: Discharge measurement Kamarjani channel on July 31, 1998	7-12
Fig. 7.3-4: Discharge measurement Kundarapara channel on July 31, 1998	7-13
Fig. 7.3-5: Discharge measurement Kamarjani channel on August 26, 1999	7-14
Fig. 7.3-6: Discharge measurement Kundarapara channel on August 26, 1999	7-15

ATTACHMENTS

Attachment 1:	Logbook Form Sheet
Attachment 2:	Data Archive System FAP 21
Attachment 3:	Inventory of Monitoring Data



LIST OF ACRONYMS

BWDB	-	Bangladesh Water Development Board
DGPS	-	Differential Global Positioning System
DHW	-	Design High Water Level
DXF	-	AutoCAD compatible format of digital data
EGIS	-	Environmental and GIS Support Project for water sector planning (formerly FAP 19)
FAP	-	Flood Action Plan
GIS	-	Geographic Information System
GPS	-	Global Positioning System
HF	-	High Frequency
HP-GL/2	-	Hewlett Packard's standard graphics language for its plotters
MDL	-	Measurement Devices Engineering Limited
MSL	-	Mean Sea Level
PWD	-	Public Works Department (datum level)
SHW	-	Standard High Water
SLW	-	Standard Low Water
TPA	-	Test Pile Acceleration
TPI	-	Test Pile Inclination
UHF	-	Ultra High Frequency
VHF	-	Very High Frequency
WGS'84	-	World Geodetic System defined in 1984

GLOSSARY

TERM	DEFINITION
AutoCAD	Auto Computer Aided Design, Release 14 used in this Project
BTM	Bangladesh Transverse Mercator (common projection used in Bangladesh)
DTM	Digital Terrain Model
Gauge	A gauge in its simplest form consists of a vertical staff, graduated in centimeters and placed in such a position that the surface level of the water may be read from the scale at any time. The gauge must be connected to land elevations
Geodesy	Geodesy is the science, which deals with the investigations of the shape and dimensions of the earth's surface.
Geoid	Definition of earth surface assuming the continuation of the mean sea water level, depending on local gravity field.
GIS	Geographical Information System
Height	The elevation of a point is its vertical distance above or below the vertical datum
Projection	Mathematics method to project spheroid coordinates (geographic coordinates) on a plain surface (grid coordinates)
Soundings	Mathematically defined shape of earth, which fits best for a defined area. The spheroid is defined by two parameters (major axis and inverse flattening). The Everest Modified 1830 Spheroid is applied by this Project.
Transducer	Part of an Echo Sounder, which transmit and receive an acoustic pulse
REC-module	Memory Card for storage of digital data. The data can be transferred to a computer by a REC-module reader



SUMMARY

The monitoring of the Brahmaputra-Jamuna river provides information for all river engineering fields. This information is substantial for the planning, the design, the implementation and adaptation works of bank protection structures.

The structure at Kamarjani was monitored under FAP 21/22 from June 1995 to the end of the year 2000. The collected monitoring data of 5 years were the basis to extend the knowledge on the river engineering fields of the Project. The data cover information about hydrography, hydraulic action, hydrology, topography and meteorology. During the monitoring period the survey and processing techniques were continuously developed to optimise the output. The techniques used in this Project are described in the present Annex.

Bathymetry and float tracking surveys were the most appropriate methods to describe the prevailing river conditions. These surveys were carried out using DGPS technology, a survey echo sounder and hydrographic PC-based software. Other types of surveys and data collection related to river engineering tasks practiced in the Project are presented as well. Besides the collection of data the processing and mapping was an important topic. The graphical layout of the presentations should be attractive for the user. Standard layouts were developed for better comparison of consequent surveys. It is also essential to define a well-organised database, which enables the user an easy and quick access to the required data. The structure of the database and an inventory of all monitoring data are presented in the Attachments to this Annex.

To organise and to combine all river survey data from other projects and agencies in the past and in the future in one complex database remains a future topic for research. A geographical information system (GIS) related to river geo-data could be a suitable database for future research and analysis of rivers in Bangladesh.

1 INTRODUCTION

1.1 INTRODUCTION TO THE PROJECT

The objectives of the Project were to find improved solutions for bank protection works against erosion by designing, specifying and constructing different types of groynes and revetments using different materials and protective layers and investigating at the same time the suitability of local materials and construction methods. After construction of the test structures their behaviour had been monitored from the monsoon season 1995 till the end of 2000. The final objective was to develop and to optimise design criteria, cost-effective construction and maintenance methods, which shall serve as future standards, most appropriate for the prevailing conditions at the Jamuna river and other rivers of Bangladesh. Hence, the test structures were to be designed in such a way and with such a level of safety that certain damages of the structures were allowed, were even required, because a test work, which does not suffer any damage in the course of the monitoring and adaptation period may be oversized and therefore not be suitable to identify the limits and to develop new standards.

To achieve the above objectives, regular monitoring of the test structures is a must after their completion as well as preventive maintenance and adaptation of the structures taking into account the results and observations of each monitoring period. For the development of suitable adaptation measures, however, further studies and investigations are possibly required.

1.2 SCOPE OF THE PRESENT ANNEX

This Annex 6 presents the findings of the monitoring at Test Site I. The methods of monitoring are described and the main results are illustrated. The basis of this Annex are the yearly Monitoring and Adaptation Reports and the monthly Monitoring Reports (see list of references). It is to be noted however, that some differences between this report and the above mentioned former reports of the Project are possible. Because of new experiences gained during the monitoring period and new developed processing software it was necessary for some evaluations to refer to the raw data, which had been collected in the field. In case the existing results were found doubtful, the data were checked, partly reprocessed and the results corrected accordingly, if necessary.

The organisation and logistics like the used survey instrumentation in this Project are reported in Chapter 2. Chapter 3 explains the practised survey techniques, whereas the processing of data is described in Chapter 4.

Chapter 5 contains results and observations made by the monitoring team with respect to the Groyne Test Structures. Section 5.3 illustrates the prevailing morphology in combination with the flow conditions. Obviously, not all data collected by the monitoring team can be reported in this Annex. Therefore, an inventory of all collected monitoring data is listed in Attachment 3. Emphasis is laid on the first monitoring year 1995, when the Jamuna river has threatened the test structures more than in the following years. These results occupy the central position of this Annex.

Evaluated hydrodynamic and meteorological statistics are given in Chapter 6. Chapter 7 shows results from bathymetry and flow investigations of the main channels in the area of the Test Structures. In Chapter 8 recommendations are given for future monitoring. It provides, based on the experience of 5 continuous years of monitoring, the information how to optimise but not to oversize monitoring of bank protection works. The organisation of economic and professional monitoring by using modern technology is described and new ideas for future monitoring are given as well.

1.3 OVERVIEW OF THE TEST SITE AND THE LAYOUT OF THE STRUCTURE

The layout of the test structures after completion in June 1995 (the beginning of the monitoring) is shown in Fig. 1.3-1, whereas Fig. 1.3-2 illustrates the adapted layout of the test structures after the first year of testing by the Jamuna. The layout shows the crest of the BWDB embankment including the impermeable parts of the groynes and their axes to the last pile of the permeable part. The prevailing river bed morphology in front of the structures and the actual bankline are presented in these figures as well.

Fig. 1.3-3 shows a general overview of the Jamuna river from the test site area to its opposite bank in January 1999. The figure is based on a Landsat Image, which has been overlaid by the maximum bathymetry survey area carried out by the monitoring team. The names of the main chars and of locations along the bank upstream and downstream from the test site are defined. Benchmarks used by the monitoring team are shown in that chart as well.

The progressive bank erosion since 1988 from the Test Site to Balashi Ghat is presented in Fig. 1.3-4. During the Planning Study Phase of the Project surveys were carried out under the services of Hydroland (1992 and 1993) followed by regular surveys by the monitoring team since 1995. The bankline presentation of 1988 is taken from the map published by the General Survey Department of Bangladesh in 1991 (sheet 78 G/11, 1:50000).

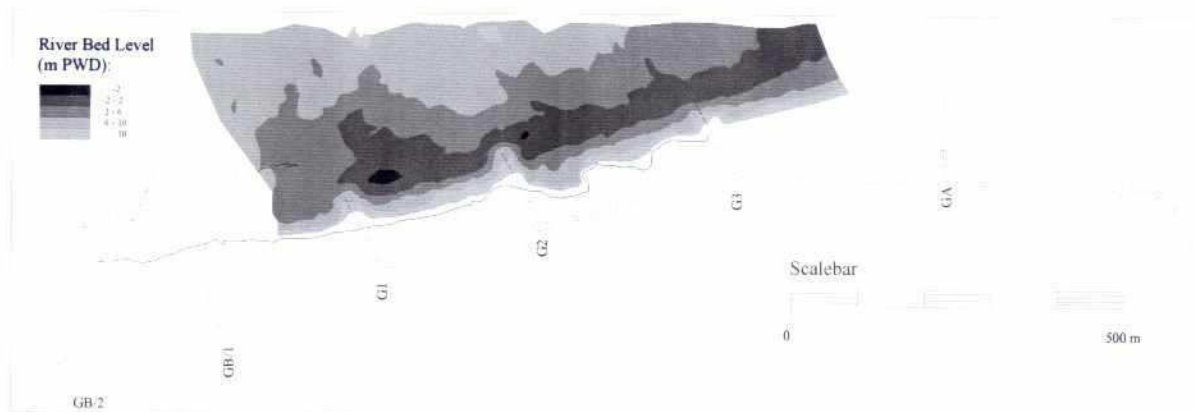


Fig. 1.3-1: Original Test Structure June 1995

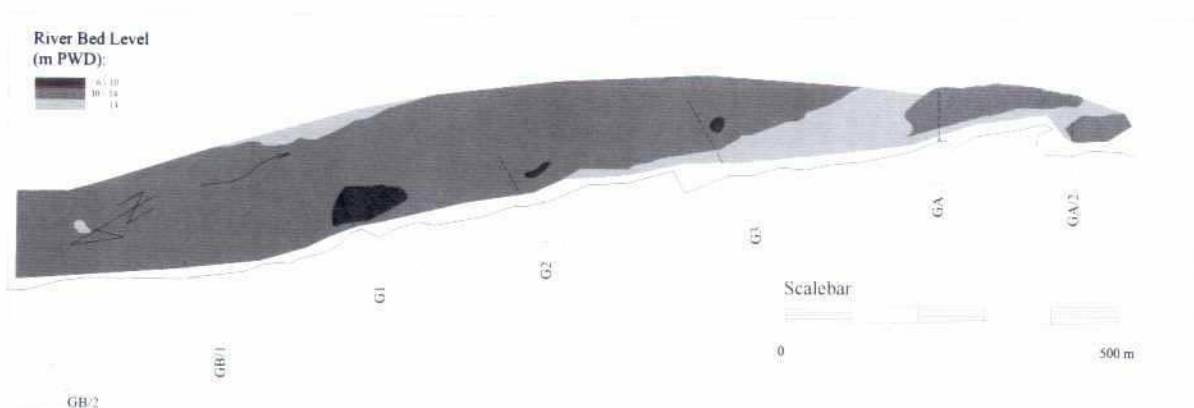


Fig. 1.3-2: Adapted Test Structure September 1998

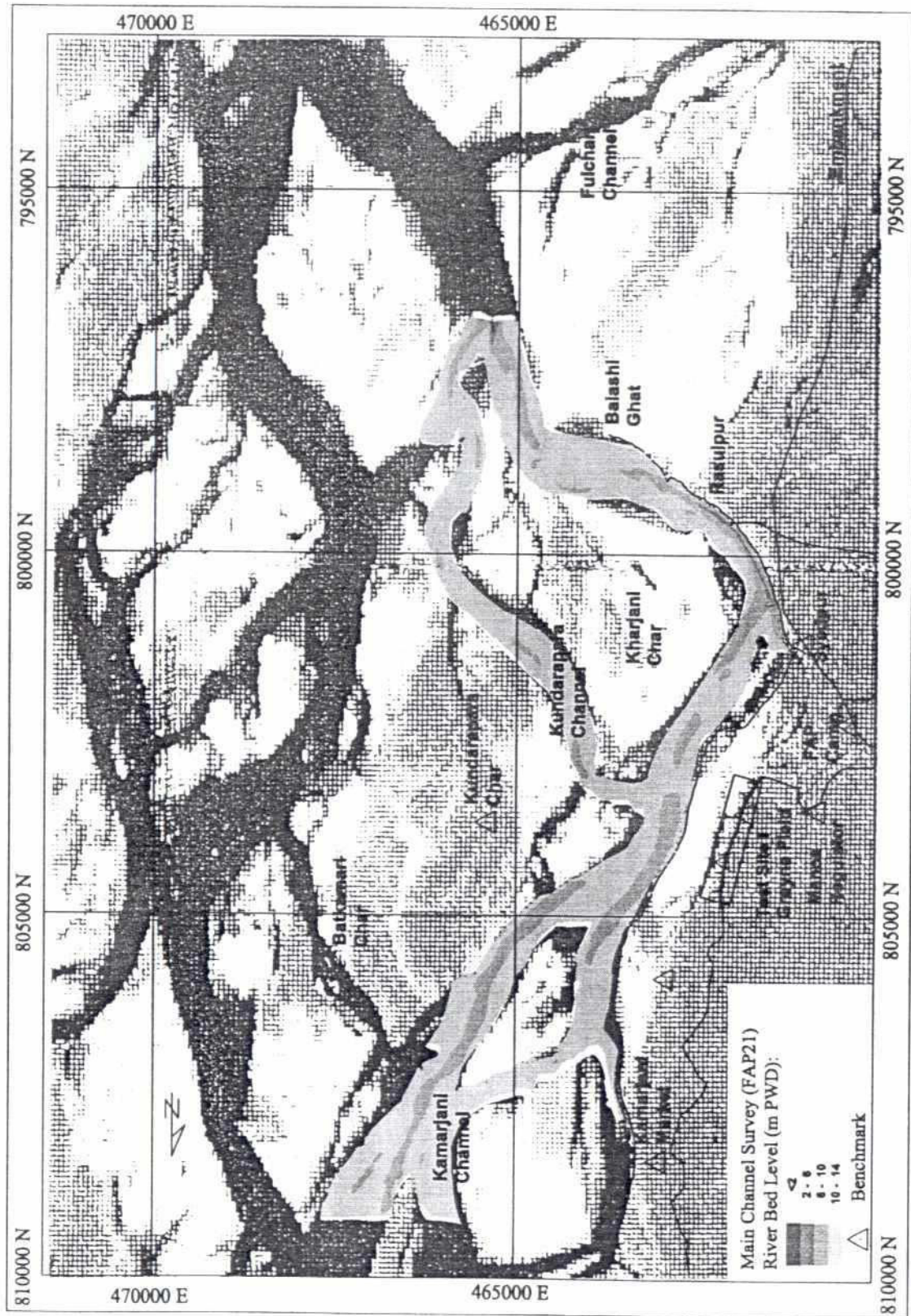


Fig. 1.3-3: Jamuna overview at Test Site-I in January 1999

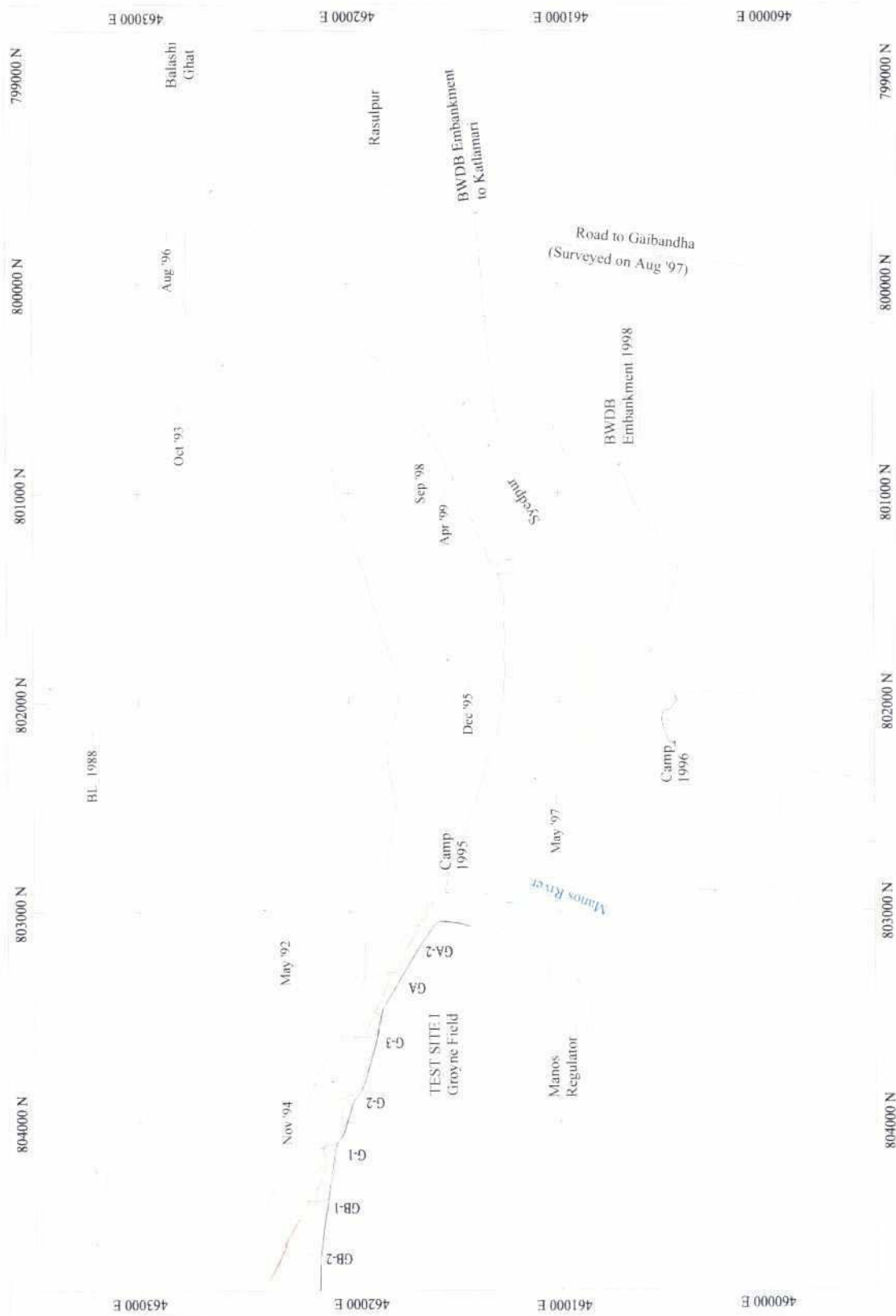


Fig. 1.3-4: Progressive bank erosion from Test Site to Balashi Ghat (1988 – 1999)

1.4 OBJECTIVES OF THE MONITORING

1.4.1 General

The objectives of the monitoring were defined in a monitoring programme before completion of the Groyne Test Structures (Consulting Consortium FAP 21/22, 1993 b). The monitoring started in June 1995. The programme was adapted to the prevailing river conditions concerning the necessity and quantity of data collection. Due to the modification and extension of the test structures during the dry season 1995/1996 and due to new survey equipment the monitoring programme was adapted as well. During the monitoring period till the end of 2000 the monitoring team could continuously optimise the programme by the experience on the job, the experience with the survey equipment and by improving the monitoring procedures (online and offline).

Monitoring of the works undertaken at the test site was aimed to

- identify river changes (e.g. morphology, hydraulic loads etc.) that could endanger the stability of the respective structure;
- detect damages at an early stage;
- understand failure mechanisms, and
- plan suitable adaptation / repair works.

However, monitoring was not only restricted to detect damages to the structure but to observe their behaviour under load and to relate the loads to the structures and river response. This required on the one hand to monitor the loads (especially flow velocities, wave action etc.) and on the other hand to adapt the design rules and the design. Hence, the requirements of monitoring were to take care of the structures features as well as on the loads and natural effects, which may influence the structures.

The monitoring programme developed for the Project included that records were to be taken by the monitoring team of

- the natural conditions at the structures (water level rise and fall, waves, currents, precipitation, wind etc.);
- the morphological changes of the river in the area of the test structures;
- the movements of structures and important structural parts in vertical and horizontal direction;
- the deterioration of materials used;
- the variations of surrounding river bed and bankline, and
- any damage by human and / or animal action.

Thereby it was of utmost importance to alert and train the monitoring team for drawing right conclusions and to record the above information with respect to the

- exact location (referred to fixed points established in the hinterland);
- exact time of occurrence / survey;
- method of recording and equipment used;
- staff involved, and
- special observations etc.

All observations and activities had to be entered daily in logbooks developed for this particular purpose. A logbook form is presented in Attachment 1. These logbooks served at the same time as a checklist for completeness of monitoring. Besides the results of regular hydrographic surveys, the logbooks became the basis for evaluation and selection of necessary measures to be taken. The logbooks and associated records represent a continuous record of events showing the development of failure mechanisms and interrelation with acting forces.

Apart from daily routine observations, regular and periodic inspection programmes were carried out for each and every subject. However, time intervals had to be adapted always in line with the occurring circumstances and river's response. Additional inspections were required after extraordinary loading conditions, accidents etc.

The monitoring activities were subdivided into two main categories:

- survey of the properties and the behaviour of the structures, and
- reference measurements of physical phenomena that produce the loads on the structure.

1.4.2 Field Tasks

The different tasks at site carried out under the monitoring programme are listed below:

(1) Hydrographic/Hydrodynamic Surveys

- bathymetric surveys;
- surface flow direction and velocity measurements by float tracking;
- current point measurements along the water column;
- side scan sonar measurements,
- water level recordings;
- wave recordings;
- test pile recordings, and
- Piezometer measurements.

(2) Land Surveys

- establishment of benchmarks;
- topographic surveys;
- bankline surveys;
- char surveys;
- structures alignment, pile positioning, and
- detailed damage surveys during / after the flood period.

(3) Meteorological Measurements

- wind speed and direction measurements;
- precipitation;
- temperature, and
- relative humidity.

(4) Reporting

- logbook of activities and daily observations;
- reporting to Dhaka office by radio communication;
- floating debris at groynes;
- visual wave observations, and
- data transfer to Dhaka office;

(5) Processing

- priority information of critical situation/conditions to Dhaka Office;
- site processing quality control of data;
- plotting of critical profiles, and
- preliminary charting / presentation of results.

1.4.3 Definition of Survey Areas

The bathymetric survey areas were subdivided in three main categories:

- Groyne Survey
 - 50 m upstream to 50 m downstream from the test structure surveyed parallel to the groyne axes.
 - line separation: 5 to 10 m
- Site Survey
 - 50 m upstream from groyne G-1 to 50 m downstream from groyne G-3 in 1995
 - from monsoon 1996 onward the area was extended from upstream from groyne G-B/2 to downstream from groyne G-A/2.
 - line separation: 10 to 20 m
- Main Channel Survey
 - 1 km upstream from groyne G-B/2 to 2 km downstream from groyne G-A/2 (4 km x 2 km)
 - from the monsoon 1996 onward the area was continuously extended due to less importance of the test site area (Fig. 1.3-3).
 - maximum north: Kamarjani Market
 - maximum south: Balashi Ghat
 - maximum surveyed area: 10 km x 4 km
 - line separation: 100 m

The Groyne Surveys were carried out to analyse changes of the riverbed morphology around the respective groynes. From calculated cross sections it could be checked whether the groyne structure was endangered by the river loads (Fig 5.3-29, 5.3-34, 5.3-41). These surveys were specified as detailed investigations by a selected line separation of 5 to 10 m. The logging interval was set to 1 second. Assuming an average speed of 6 kn the point separation in survey line direction was about 3 m. The steep slopes in front of the river banks were surveyed with reduced speed to increase the quantity of data points.

The Site Surveys were chosen for investigations on the overall test structures area. During the monsoon 1995 the groyne field areas between groyne G-1 and groyne G-3 were of most interest (Fig. 5.3-1 to 5.3-16). A frame box defines the area of a Site Survey in Fig. 1.3-3.

The Main Channel Surveys were intended to monitor the morphological changes in a more global pattern. They had been carried out up to the opposite char of the Kamarjani main channel. Since the river loads on the test structures had been reduced in 1997 the monitoring was concentrating more on the main channel development over a total length of 10 km including the fast developing Kundarapara channel (Fig. 1.3-3). The Main Channel Surveys are mapped in Annex 1 (Morphological Investigations).

In conjunction with the bathymetric surveys of the site area and the main channel area float tracks were carried out. They were selected in that way to get a representative surface flow pattern of the survey area. Since 1996 the Site Surveys included current point measurements in the groyne fields as well. With respect to similar river conditions the monitoring team paid attention to carrying out the different types of surveys within the same survey period, i.e. bathymetric and flow data could be charted together to present the actual hydrographic river conditions.

The areas of monitoring were depending on the prevailing river conditions. Therefore, the selection of the respective areas had to be altered dynamically according to the aim of the project.

1.4.4 Definition of Survey Intervals

The test structures were continuously monitored from June 1995 to December 2000. The intensity of surveys was depending on the prevailing river conditions and the aims of the Project. In general, the bathymetry and flow data collection was intensified during the monsoon seasons (June to September) each year at the time of strong hydraulic loads on the structures.

Groyne Surveys were carried out on demand, especially in 1995, when the structures were endangered. Site Surveys were done at least once a month during the dry season and up to four times a month during the monsoon season (June to September). Main Channel Surveys were performed at least once a month, but during the monsoon season twice a month.

Attention was paid to keep at least one monitoring engineer always on site to carry out the daily routine work like site inspections, entries in the logbook etc.

1.4.5 Dhaka Office Tasks

Final quality control of site data, final processing, presentation and evaluation was done in the Project office in Dhaka. The tasks were the following:

- quality / completeness control of field monitoring;
- archiving of monitoring data, actualisation of data bases;
- final processing / presentation of survey results;
- determination / confirmation of priority / critical situations;
- initiation of emergency measures;
- evaluation of differential DTMs (Digital Terrain Models)
- statistical evaluation of wind / wave records;
- evaluation of water level recordings;
- evaluation of current point measurements;
- evaluation of discharge measurements;
- evaluation of flow directions and velocities from float tracks;
- comparison of results with applied design criteria, and
- comprehensive annual report on results of field monitoring.

2 ORGANIZATION / IMPLEMENTATION

2.1 ORGANIZATION OF THE MONITORING TEAM

The personnel of the monitoring team were as follows:

- 1 Expatriate Monitoring Expert (temporary);
- 2 Hydrographic Engineers;
- 1 Database / Processing Engineer;
- 1 Surveyor;
- 1 Assistant Hydrographic Technician (temporary);
- 1 Assistant Surveyor;
- 1 Database / Report Secretary (temporary);
- 3 Boat Drivers, and
- 4 Helpers

The monitoring personnel were responsible for the monitoring of the Test Sites at Kamarjani and Bahadurabad as well as for monitoring for FAP 22 activities. During the monsoon periods (June to September) the team was guided and trained by the expatriate Monitoring Expert. He organised the monitoring team and defined their duties in monitoring programmes. He further defined and improved the survey procedures and installed and maintained the survey equipment to fulfil the objectives of the monitoring.

In general, one hydrographic engineer was in charge of monitoring on each test site. He was responsible for all monitoring field tasks on site as they are listed in Subsection 1.4.3. The surveyor carried out all land survey tasks at both test sites, but could also take over monitoring tasks on site, if one hydrographic engineer was absent.

The database and processing engineer was in charge from 1996 onward in the Dhaka project office and was responsible for all monitoring office tasks as listed in Subsection 1.4.5.

For a well operating monitoring team communication between the team members and with the project management was of utmost importance. Job experiences and progress of works had to be exchanged and problems had to be recognised and solved in the team. Important events had to be reported to the project management. On the other hand the project management had to follow up and analyse the monitoring results to instruct the monitoring team, if the monitoring investigations had to be specialised and / or intensified to comply with the scope of the Project.

2.2 LOGISTICS

During the Test and Implementation Phase of the Project a permanent base camp was established downstream from the Test Site. Due to severe bank erosion during the monsoon season 1995 the camp location had to be shifted about 1 km southwest (see Fig. 1.3-4).

The camp consisted of five 40 feet containers and seven 20 feet containers to provide accommodation, office and storage facilities. One pickup and two off-the-road motor bikes were supplied for the monitoring team. The pickup was used for transport of personnel and survey equipment. The bikes were mainly used for river inspections surrounding the test site. The bikes were appropriate for driving on the embankments and to get quick access to almost any location on land. Equipped with DGPS they could also be used to easily survey roads and embankments to provide charts with topographic information of the hinterland of the test structures.

To carry out the monitoring field surveys the Project had two survey boats and three speed boats to its disposal, which were used for monitoring the second test site at Bahadurabad and the FAP 22 activities as well.

The monitoring office was provided with 2 personnel computers, a plotter and the necessary software for the preprocessing and preliminary charting of the collected monitoring data.

Communication between the base camp and the field survey teams was provided by VHF radio, to Dhaka head office by HF radio respectively. The radio communication allowed a proper planning and organisation of the monitoring activities. Critical situations, monitoring results or the necessity of adaptation works could be discussed with Dhaka head office.

2.3 GEODESY

2.3.1 Horizontal Reference

The Project chose the BTM projection (Bangladesh Transverse Mercator) as a reference system for horizontal co-ordinates; i.e. all monitoring results refer to the BTM co-ordinate system. Finmap under the FAP 18 project recommended this system, which should be used as a common horizontal reference system in Bangladesh for direct compatibility with measurements by other projects or agencies (Consulting Consortium FAP 21/22, 1994). Information from the projects FAP 22 and FAP 24 are based on that system as well as measurements by BWDB and EGIS.

The Landsat Images were adjusted for distortions by control points. These control points were of less accuracy and have not been checked for long time. Therefore, discrepancies of about 100 m were found between the Landsat Images and the BTM system. The images are scaled by 1:200 000; i.e. an error of 100 m is equivalent to 0.5 mm in the image.

FAP 21 was confronted with problems due to the difference between the transverse Mercator projections BTM and SPOT TM. Both projections are based on the same spheroid, but the scale factor of BTM is 0.9996 whereas the scale factor of SPOT TM is 0.9998. This difference caused a shift of 560 m for the area of Kamarjani lying 2800 km North of the equator ($(0.9998-0.9996) \times 2\,800\text{ km} = 0.56\text{ km}$).

There exist different spheroids called Everest. The BTM projection is based on the spheroid Everest modified from 1830. GPS receivers offer a local datum selection. GARMIN handheld GPS receivers offer the datum 'Indian Bngldsh', which is not conform to the Everest modified from 1830. User defined datum can be entered in GPS receivers. The needed parameters to shift from WGS'84 to Everest mod. 1830 are as follows:

da	=	-838.476 m
df * 10 ⁴	=	-0.283616
dx	=	-288 m
dy	=	-735 m
dz	=	-255 m

Different co-ordinate systems lead often to confusion, especially if co-ordinates derived from GPS receivers have to be converted into a local co-ordinate system. It is therefore of utmost importance to check co-ordinates for the spheroid and projection parameters on which they are based.

The parameters of the spheroid, the BTM projection and the datum shifts from WGS'84 used by the Project are given in Table 2.3-1.

BTM Projection		
Scale factor	:	0.9996
Central meridian	:	90°E
False easting	:	500 000 m
False northing	:	-2 000 000 m
Latitude of origin	:	0° (Equator)
Everest Modified Spheroid		
Semi-major axis a	:	6 377 298.524 m
Semi-minor b	:	6 356 097.518 m
Inverse flattening 1/f	:	300.8017
Spheroid datum shifts from WGS'84		
Translation x	:	-288 m
Translation y	:	-735 m
Translation z	:	-255 m
Rotation x	:	0
Rotation y	:	0
Rotation z	:	0
Scale	:	0 ppm

Table 2.3-1: Horizontal reference applied by FAP 21

2.3.2 Vertical Reference

The reference for the vertical co-ordinates is PWD datum (Public Works Department). The PWD datum is relative to the geoid, i.e. it depends on the local gravity field and is the most commonly used datum in Bangladesh. Its zero level is located around 46 cm below an estimated Mean Sea Level (River Survey Project, FAP 24, 1996).

All monitoring results of the land surveys and the bathymetric surveys are presented directly relative to the vertical datum PWD. Hence, they present heights above or below the zero level PWD. The land surveys were connected to benchmarks, which provided PWD heights in the hinterland (see Subsection 2.3.3). Using the water level readings from the water level gauge located downstream from the groyne G-A (the gauge was connected to a benchmark, see Section 2.6) the measured depths were converted to PWD heights. The water level difference between the water level gauge and the depth measurement locations was not considered in the conversion. Prevailing water level gradients between 10^{-5} (dry season) up to 10^{-4} (monsoon season) would mean an error of PWD heights of 1 to 10 cm per 1 km distance from the water level gauge. Assuming similar water level gradients of consequent bathymetric surveys the monitoring team neglected this error, because the error is irrelevant for changes of the riverbed morphology.

The decision to present heights instead of depths was made for better comparison between construction levels and the riverbed level. Therefore, bathymetry charts evaluated by the monitoring team and shown in this report present heights above or below the zero level PWD. The survey areas of the Project are

focused on the investigated test structures and therefore limited. For more global river survey investigations it is recommended to present bathymetric charts with depths referring to a water level datum, for instance Standard Low Water (River Survey Project, FAP 24, 1996).

For the design of bank protection structures the maximum and the minimum water levels are most important. Therefore, SLW (Standard Low Water), SHW (Standard High Water) and DHW (Design High Water) were defined for the location of the test site area. The definition of SLW and SHW in Bangladesh is the 5 % non-exceedance level and 5 % exceedance level respectively for non-tidal rivers. The DHW was defined as the maximum water level with a return period of 25 years for the purpose of the test structure. These values were determined from the FAP 25/GM model, which covers 25 hydrological years (Consulting Consortium FAP 21/22, 1993 a).

Location	SLW	SHW	DHW
Kamarjani Test Site	15.2 m+PWD	20.7 m+PWD	22.9 m+PWD

Table 2.3-2: Definition of water levels at Kamarjani

2.3.3 Benchmarks

At the beginning of the monitoring period only three benchmarks existed in the area of the test site. They were used as an origin to establish during the complete monitoring period a global net of benchmarks covering the area from Kamarjani Market (808 000 N) to Balashi Ghat (790 000 N) including the chars Batkamari, Kundarapara and Kharjani. An overview of the benchmarks first order is shown in Fig. 1.3-3. They were controlled between each other by a closed traverse or a traverse surveyed in two sections. All points located on the mainland are provided with elevations. The relative accuracy of the points is estimated as $S_{x,y} = S_z = 2$ cm. The absolute net accuracy relative to the BTM projection is estimated below 5 m.

Concrete pillars or steel pipes were used for the benchmarks. Descriptions of all existing benchmarks at the end of 1999 are given in Attachment 3. These benchmark descriptions shall serve future surveys in that area.

2.4 SURVEY EQUIPMENT

For the realisation of the monitoring survey (Section 1.4) the Project provided appropriate survey equipment. The equipment used by the monitoring team is listed and described in Table 2.4-1. The two survey boats (Section 2.5) were equipped with a DGPS system and a single beam echo sounder to perform hydrographic surveys. On both survey boats the same equipment set was installed (2nd set since 1996). That means that the equipment could be exchanged on the boats. The setup on board for bathymetric surveys is shown in Section 3.2.

Because of the humid climate during the monsoon and the continuous and intensive use of the equipment over a period of 5 years the monitoring team suffered from several equipment breakdowns. The problems resulted mainly from corrosion of electronic boards. The failures could mostly be repaired on site. If not, the defected part was immediately sent to Dhaka or to Europe for repair. If one survey boat was not operational due to equipment breakdown, the equipment was exchanged by the second set from the other survey boat. In case of failure of one DGPS set, the electronic total station could be used for positioning the survey boat carrying out current point measurements.

Survey Application	Type of Instrument	System Description
Position Bathymetry Float Tracking Long Distance Measurements	Ashtech X11, Ashtech DNS-12 GPS Base and Remote Receiver (12 channel, L1 C/A code)	Real-Time-DGPS Positioning, performed by MDL UHF data telemetry system (450-470 MHz). Standard deviation: ± 2.0 m*
Position Advanced Float Tracking	Trimble Pathfinder GPS receiver (10 channel, L1 C/A code) Operation only during monsoon seasons 1996-1998	DGPS Positioning Performed by post processing Continuous tracking of multiple floats Standard deviation: ± 4.1 m*
Position Single point positioning of topographic objects	Garmin GPS III Handhold GPS receiver Since 1998	GPS Positioning Stand-alone mode, no differential correction Standard deviation: ± 5 to 20 m**
Position Geodesy Topography Bankline Charline	Wild TC 1600 Electronic Total Station Incl. Wild GIF 10 REC-module reader	High accurate electronic theodolite built-in electronic distance measuring (EDM) unit EDM accuracy: 3 mm + 2 ppm Maximum archived distance range: ~3 km (triple reflector)
Depth Bathymetry	E-Sea Sound 103 (2 sets)	Hydrographic Echo Sounder Digital and graphic recording Transducer: 200 kHz Beam angle: 6° conical Accuracy: ± 0.5 % of depth (estimated)
Depth Bathymetry	Atlas Deso 22	Hydrographic Echo Sounder Digital and graphic recording Transducer: 33, 210 kHz Accuracy (210 kHz): 1.5 cm ± 0.12 % of depth Operational only in 1996 and partly in 1997
Navigation Computer Bathymetry Float Tracking Current Point Measurements	Roda computer Rocky I and Rocky II	Outdoor Notebook (Pentium processor) 2 serial ports 12V power supply
Flow Current Point Measurements	ADM Current meter	Electromagnetic Current meter Unpractical for currents > 1 m/s
Level Height Determination of Benchmarks Topography Water Level (Gauge Control)	Leica Wild NA2 & Wild Heerbrugg NA20	Precise leveling Accuracy: ± 1 mm/km
Flow Current Point Measurements Discharge	Valeport Current meter BFM 108/308 2 sets since 1996	Propeller Current meter Magnetic compass, Pressure sensor (1st set) practical, winch support for lowering the unit to selected depth Accuracy: $\pm 1-2$ % of current velocity ± 2 degree in current direction

* The project performed an accuracy test of the Ashtech GPS receiver in comparison to the Trimble receiver in August 1997. The test was scheduled on 12 hours logging the position by 20 seconds interval on one point. The test showed that the standard deviation of both DGPS systems is higher than given by the manufacturer.

** Since SA (Selective Availability) has been switched off in 2000, GPS offers a position accuracy of about 5 m (Stand-alone mode).

Table 2.4-1: Instrumentation Specifications

The monitoring team had to be flexible on the job concerning the use of the survey equipment, manpower and the survey procedures. By this flexibility the monitoring team was always able to carry out the surveys needed by the Project. The team was trained in installation, operation and maintenance of the equipment. An electronic engineer skilled in maintenance and simple repairs of survey equipment was often missing in the team (see Section 8.3). Regular maintenance and proper installation of the equipment on board is important to keep the survey boats operational.

In general, all equipment as listed in Table 2.4-1 was appropriate for the monitoring tasks. An electromagnetic current meter was tested in 1995 by the monitoring team. The model used in the Project was, however, found not to be practicable for current point measurements in high currents. Main problems were faced lowering the instrument, because the instrument inclined by the current and showed incorrect results. Another operation problem resulted by floating debris, which endangered the sensitive sensors of the instrument and finally damaged it. Therefore, the Project provided Valeport propeller-type current meter for both test sites in 1996, which was suitable for current measurements (see Subsection 3.3.3) under local conditions.

In June 1996 the dual frequency echo sounder Deso 22 was installed on the survey boat Obelix. The echo sounder operated with two different frequencies (33 kHz, 210 kHz). The pulse generated by the lower frequency penetrates through inhomogeneous layers and is reflected at the first homogeneous reflector of the riverbed. In general, the monitoring team found no significant depth differences between the two frequencies. This is obvious, because a mainly homogeneous sandy riverbed characterises the Jamuna river. The monitoring team faced different electronic problems with the Deso 22. Finally it could not be repaired in 1998. Therefore, it was replaced by a second E-Sea Sound echo sounder in 1998.

The E-Sea Sound echo sounder was easy to operate and only minor problems occurred. The Deso 22 has a better accuracy (see Table 2.4-1) due to its higher performance in electronics and acoustics, but on the other hand it is more difficult to operate and it is more expensive than the E-Sea Sound. The E-Sea Sound can be upgraded to a dual frequency echo sounder as well.

2.5 SURVEY BOATS

Two survey boats - called Obelix and Asterix - were mobilised for hydrographic surveys. They are shown in Fig. 2.5-1 and Fig. 2.5-2. The boat Obelix became operational in June 1996.

The advantages of Obelix in comparison with Asterix were a better stability and a closed cabin. Therefore, Obelix could be used for Valeport operations as well as for bathymetric surveys at bad weather conditions. On the other hand the survey boat Asterix was more favourable concerning the speed and the fuel consumption.

The closed cabin of Obelix protected the operating crew as well as the equipment against rain and sun. The cabin offered enough space for the helmsman, the survey operator and for a proper equipment installation. The transducer of the echo sounder was mounted at the hull of the boat. The placement of the transducer was well chosen to avoid disturbances by the engines and by floating debris. The GPS antenna was mounted above the transducer; i.e. no offset corrections had to be considered (see Fig. 2.5-3).

The installed survey equipment is listed in Table 2.5-1 and the specifications of the boats are given in Table 2.5-2. For detailed drawings see Fig. 2.5-3.

In addition, three speed boats were used for site inspection, visual observations, advanced float tracking, transport, etc. It is noticed that all boats were used for FAP 22 activities as well.

Equipment	Obelix	Asterix
DGPS	x	x
Echo Sounder	x	x
Navigation computer	x	x
Helmsman monitor	x	x
Navigation software	x	x
Current meter and winch	x	
Anchor winch	x	
VHF radio	x	x

Table 2.5-1: Instrumentation of the Survey Boats

Features	Obelix	Asterix
Length overall	7.10 m	5.70 m
Breadth	2.30 m	1.80 m
Draft	1.00 m	0.80 m
Maximum speed	15 knots	20 Knots

Table 2.5-2: Specifications of Survey Boats



Fig. 2.5-1: Survey boat Obelix during Valeport operation



Fig. 2.5-2: Survey boat Asterix

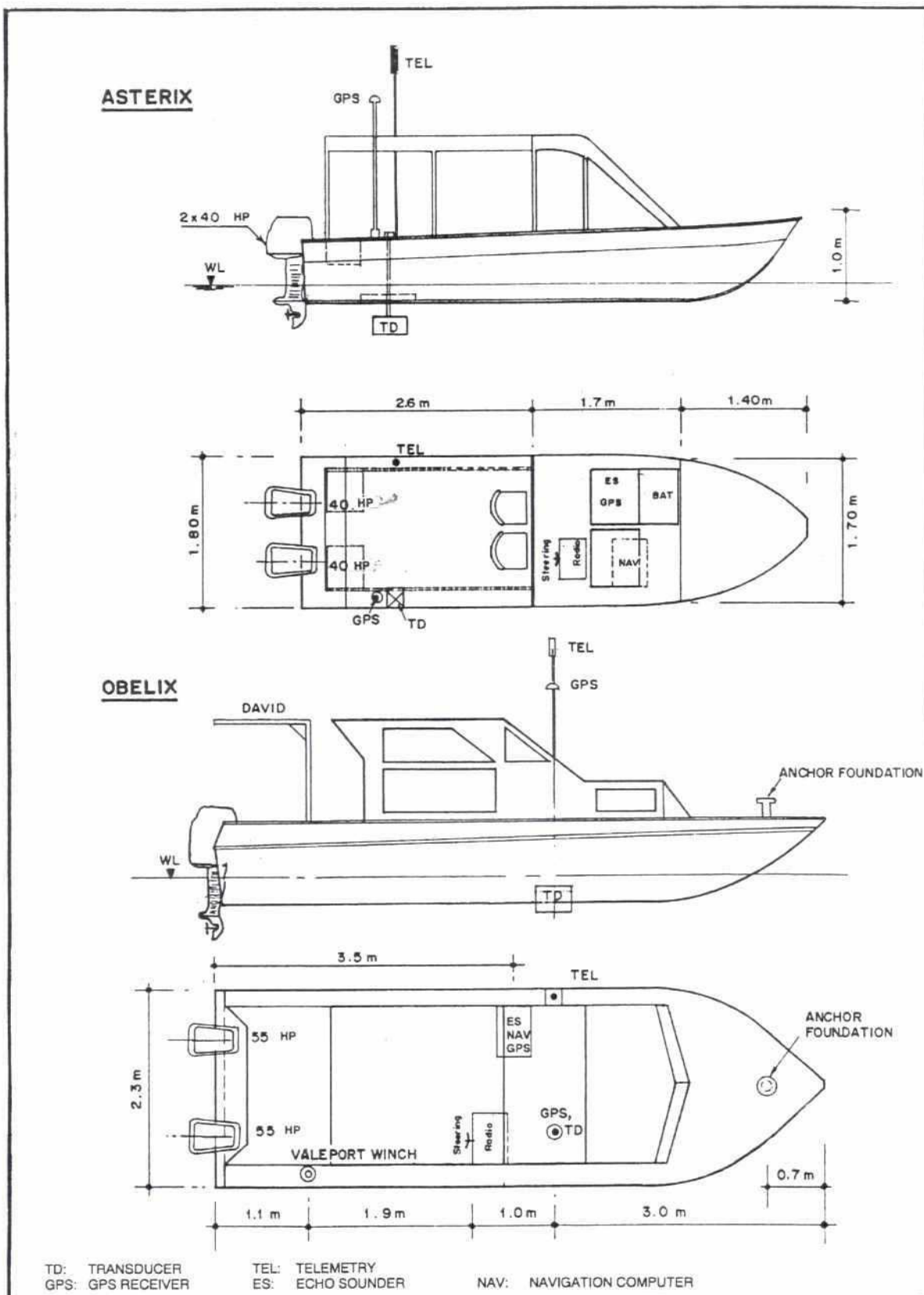


Fig. 2.5-3: Details of survey boats

2.6 WATER LEVEL GAUGES

Water level readings were taken from two staff gauges connected to zero PWD. They were located downstream from groyne G-A (gauge A) and upstream from groyne G-1 (gauge B). The readings were scheduled at 8, 13 and 17 hours daily.

The downstream gauge was shifted about 460 m towards upstream in January 06, 1997 because of permanent erosion at the original place. This should be considered for comparison before and after its displacement due to the water level slope. The original location is called A1, the latter A2. Besides the staff gauges a third auto gauge (gauge C) of the monitoring station was located at groyne G-2.

The exact location and the operating period of the gauges are given in Table 2.6-1. All water level readings refer to PWD. As to the definition of water levels see Subsection 2.3.2.

Gauge No.	Location	E	N	Operation Period
A1	Downstream from Manos confluence in front of FAP camp location in 1995.	461557	802841	Dec. '94 – Dec. '96
A2	Downstream from head of impermeable part of G-A.	461783	803239	Jan. '97 – Nov. '99
B	Between G-1 and G-B/1.	462167	804233	Jul. '96 – Nov. '99
C	1m upstream from G-2 between test pile and last pile.	462125	803916	Jun. '95 – Dec. '98

Table 2.6-1: Water Level Gauges

3 FIELD SURVEYS

3.1 HYDROGRAPHIC SOFTWARE

To achieve a good performance of hydrographic surveys, especially of bathymetric surveys, it was unavoidable to use appropriate software. The hydrographic survey software package Masterchart, Marimatech was used in the Project. This software offered the user a wide range of hydrographic survey applications as well as post processing utilities. It ensured the monitoring engineer to cover the survey area and to avoid any data gaps. It also helped the helmsman to follow the defined survey line or to approach to a certain point. An example of an online Masterchart survey display is shown in Fig. 3.1-1.

The top window shows a chart of the survey area, the survey boat and the selected trackline. Objects, like the structure upstream from groyne G-A, could be defined for better orientation. Above that window an arrow indicated the distance off-line to the selected trackline (here 2 m off to starboard side).

The bottom window showed the depth profile along the trackline and the right window provides navigation information. From this display the operator could start and stop the bathymetric data collection.

Besides the on-line collection of hydrographic data the software Masterchart was used for the off-line processing as well. The post processing of data is described in Chapter 4.

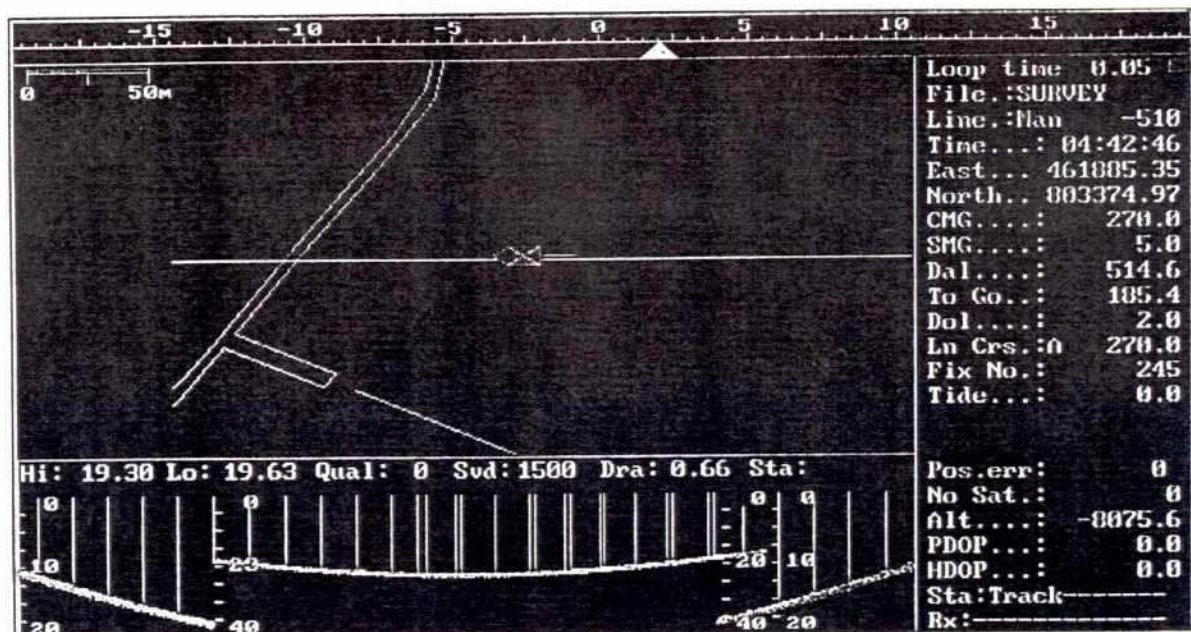


Fig. 3.1-1: Masterchart on-line survey display

3.2 BATHYMETRY

The procedure of a bathymetric survey is shown in Fig. 3.2-1. The survey boat was equipped with a GPS remote receiver, telemetry receiver, echo sounder and a navigation computer. The GPS remote receiver tracked all GPS satellites in view to calculate the present position, which was corrected by the differential correction received from the GPS reference station.

The transducer transmitted an acoustic pulse generated by the echo sounder, which was reflected at the riverbed and received by the echo sounder to derive the actual water depth by the travel time of the pulse.

Both data, the DGPS position and the water depth, were interfaced to the navigation computer. The data were recorded in by the hydrographic software. Before starting the survey the transducer depth, the speed of sound, the position offset between GPS antenna and transducer and the time delays for synchronization of position and depth had to be determined. Such parameters were the inputs to the echo sounder and the hydrographic software respectively.

After the definition of tracklines covering the specified area (see Subsection 1.4.3), the survey setup was completed. To follow straight lines by the survey boat the selected trackline was displayed on an external monitor. The display provided the helmsman with all navigation data to maintain the track.

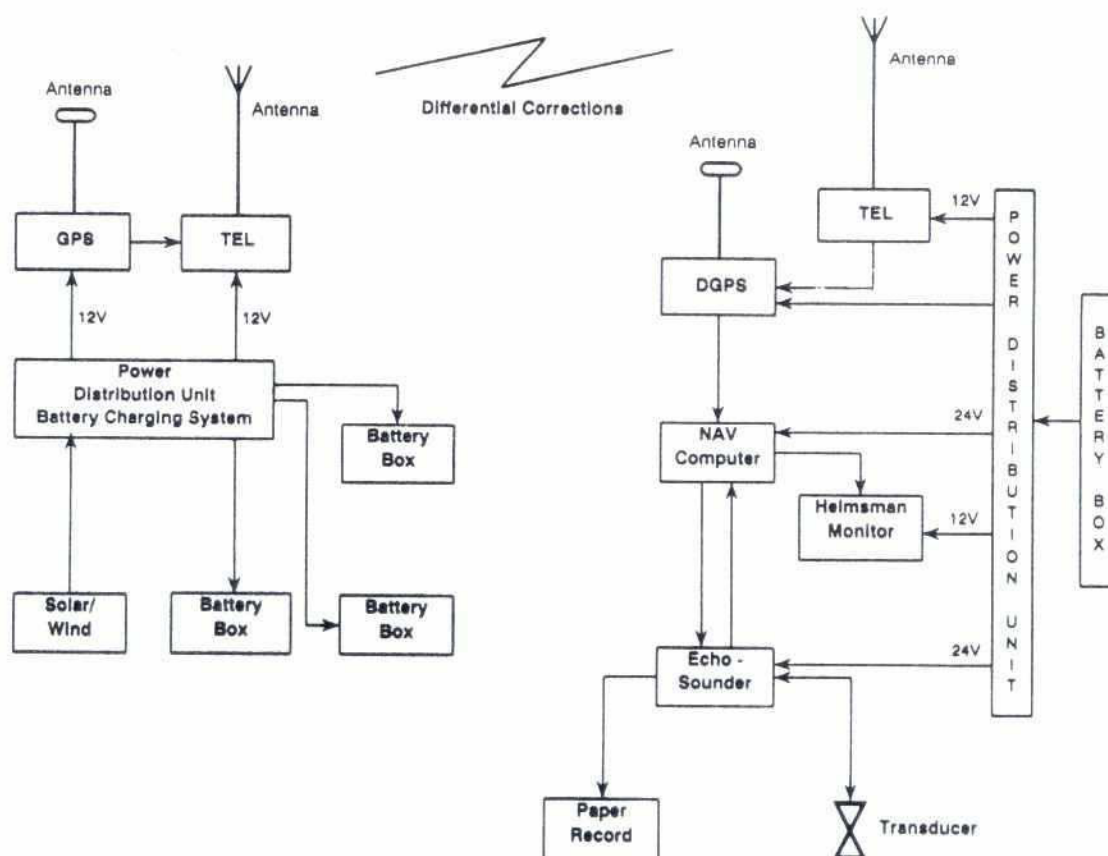


Fig. 3.2-1: GPS - reference station and survey boat setup for bathymetric surveys

3.3 FLOW MEASUREMENTS

3.3.1 DGPS Float Tracking

The DGPS positioning set up aboard the survey boats as shown in Fig. 3.2-1 was used for float tracking as well, which was an appropriate method to collect flow direction and velocity. A drogue (cross sheet metal) could be hung to the float with a rope at the required depth. The drag of the drogue was relatively high compared to that of the immersed float which allowed an interpretation of the flow conditions in the chosen depth. The monitoring team performed measurements mainly at 1 m depth. The Labor für Wasserbau, Bremen performed more intensive float tracking (see Subsection 3.3.2). They carried out float tracks in depth from 1 to 5 m.

The float tracking was practised by repeated approaches of the survey boat to the float. In between the approaches the survey boat kept a certain distance from the float to avoid interference with waves and flows created by the survey boat. In the moment of the closest approach a navigation fix was released. Those navigation fixes contained time and position. The flow velocity and the flow direction (average between two fixes) could be derived from these data.

The monitoring team carried out float tracks in the groyne fields and in the main channel. In general float tracking was done in combination with the bathymetric surveys (see Attachment 3, Inventory of Monitoring Data).

The disadvantage of the float tracking method was the gap of flow information between the navigation fixes. Between the groynes it was difficult to carry out float tracking in 1995. The reasons for the difficulty were the volume of floating debris, high turbulence and the insufficient fixed positions of the float. Therefore, instead of tracking the float, the flow lines were sketched to describe the flow pattern in the groyne fields.

3.3.2 Advanced DGPS Float Tracking

An improved method of float tracking was used during the monsoon seasons in 1996 to 1998 (Labor für Wasserbau, Bremen). The improvement was to set a GPS receiver (Trimble Pathfinder) in a waterproof float (Fig. 3.2-1).

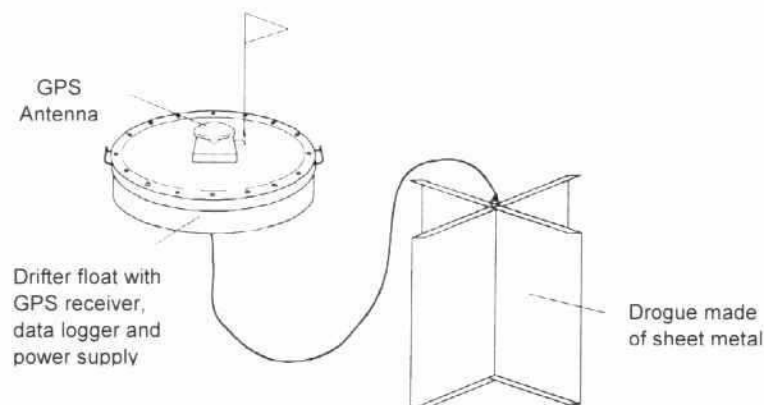


Fig. 3.3-1: GPS drifter float with Drogue

Logging the GPS position of the float every 2 seconds represented a more or less continuous flow line.

Parallel running of a GPS reference station provided DGPS accuracy by post processing the data. Surveys were taken by using a speed boat. Another advantage of this method was that multiple floats could be tracked at the same time.

Tracking of multiple floats could indicate parallel, diverging or converging flow lines and the data were well suited for validation of morphological and hydrological investigations.

Obviously, the computed velocities represented an average velocity over the depth level interval of the drogue. The drogue must be rather big in order to reduce the effect of wind drift (which becomes excessive if the wind drag force is significant as compared to the current drag force). Therefore, the method is not well suited for describing the vertical variation of the current, and in general it cannot provide detailed information about time and space variations.

3.3.3 Current Point Measurements

Vertical flow velocity profiles were measured by a Valeport propeller-type current meter while anchoring the survey boat Obelix. Since high flow velocities in the groyne field occurred, a proper anchoring of the boat was not practicable. Therefore, capstans (welded at an outer and a middle pile of each groyne) were provided for mooring the boat downstream from the groynes G-1, G-2 and G-3 at different locations by varying the rope length. This method was suitable to carry out Valeport measurements in the groyne fields.

Measurements were taken at 0.2, 0.5 and 0.8 multiples of the water depth. The average of these 3 current measurements along the water column represented roughly the depth-averaged flow velocity. The probe could be lowered by a winch. Besides the flow velocity the flow direction was measured by a magnetic compass of the Valeport current meter.

3.4 DISCHARGE MEASUREMENTS

Discharge measurements were derived from Valeport current measurements and bathymetric surveys. After a depth profiling across the channel the Valeport locations were selected to get representative flow velocities at the defined cross-section. Obviously, the cross-section had to be defined perpendicular to the river channel axis, which could be taken from the previous bathymetry chart.

The monitoring team carried out discharge measurements since 1997 to follow up the development of the Kundarapara channel in comparison with the Kamarjani channel. The results are shown in Section 7.3.

3.5 LAND SURVEYS

The land survey activities of the monitoring can be separated into the following tasks:

- horizontal and vertical control;
- bankline surveys;
- char waterlines, and
- topography (structure, embankment, objects, etc.).

Topographic, bank and char surveys were carried out to serve as a supplement to the bathymetry charts. Hence, these were taken in the same time period, if weather conditions allowed. Horizontal and vertical control measurements were the basis of the monitoring because all surveys referred to the fixpoints (see Section 2.3).

3.6 MONITORING STATION

To collect water level, wave height, wind data and test pile information a self-recording monitoring station had been designed and installed on the platform at groyne G-2.

The station consisted of the following units:

- gauge (ultra sound sensor) for measurements of water level, wave height and wave period;
- anemometer for measurement of wind velocity and direction;
- inclination and acceleration sensors for the test pile No 30;
- control unit for controlling data flow and timing parameters;
- data logger for storing measured data on removable memory-card;
- telemetry for sending data to the remote display unit;
- solar power supply with two batteries, and
- remote display unit.

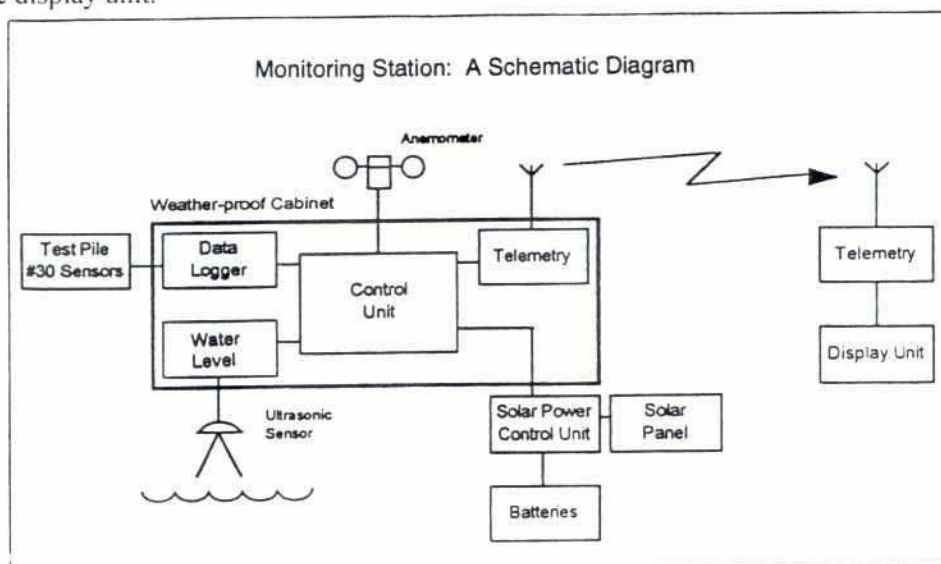


Fig. 3.6-1: Schematic diagram of monitoring station located at groyne G-2, Test Site I

The system did not work continuously. The reasons for data collection interruptions were:

- electronical failure;
- floating debris below the water level sensor;
- insufficient solar battery charging especially during monsoon;
- wrong operation, and
- no immediate maintenance after failure.

However, due to the 3.5 years operation of the system from June 1995 to December 1998 sufficient data for statistical analysis are available (see Inventory of Monitoring Data, Attachment 3).

The statistical evaluations of the data are presented in Section 6.2.

4 POST PROCESSING

4.1 GENERAL

The monitoring team processed all kind of data at site. Preliminary charts and presentations were carried out as well. Twice a month all digital raw data, processed data, logsheets, reports and the logbook were sent to the Project Office in Dhaka. Results of emergency measurements were transferred immediately to Dhaka by fax or courier.

The monitoring data collected in the field were stored on floppy disk and afterwards downloaded to the site office computer. Before processing, the data were checked for completeness, validation and quality. The main time investigation was spent in the processing of bathymetric data. Due to the repetition of surveys in the same areas standard layouts, chart limits, headers, scales, etc. were defined. This resulted in reduced processing time more or less equal to the time of surveying.

The monitoring team processed digital hydrographic, hydrodynamic and topographic data from five different sources. They were:

- bathymetry (position and depth);
- topography (position and height);
- float tracks (position with corresponding time);
- current point measurements (flow direction and velocity), and
- monitoring station (wind, water level, wave height, test pile inclination and acceleration).

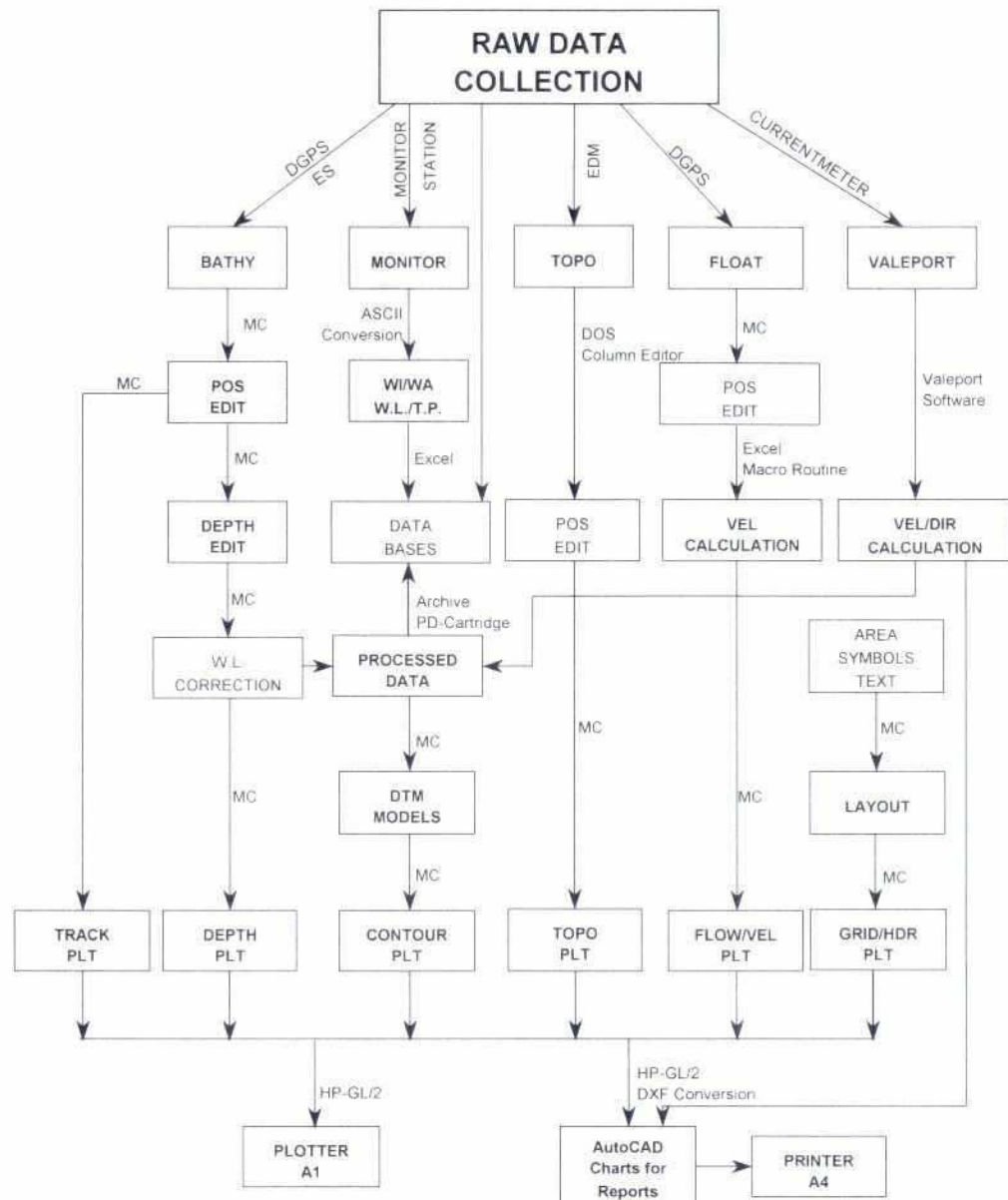
The Fig. 4.1-1 illustrates the flow of digital data processing from the collection to the final charts and to the archiving in the database. The processing steps are described for each data source in the following Sections 4.2 to 4.6.

The raw data was archived as well as the processed data in the database at Dhaka office (see Attachment 2). The bathymetric data could be processed by the hydrographic software Masterchart (see Section 3.1).

The topographic data and the float tracks were integrated in Masterchart for charting. The monitoring team defined the chart grid and the header information by Masterchart as well. Plot-files (HP-GL/2 Format) containing different information were created as follows:

- tracks of survey run lines (Track.plt);
- depth presented in meter with subscript decimeter (Depth.plt);
- contours of heights with a chosen contour interval (Contour.plt);
- topography including banklines, lines of actual water level, roads, embankments, structures, etc. (Topo.plt);
- flow lines from the float tracks (Flow.plt);
- averaged flow velocities along the float track (Vel.plt);
- co-ordinate grid (Grid.plt), and
- header and chart text including names, survey dates, datum, scale, etc. (Head.plt).

The plot-files could be combined as needed for the A1-size charting. The combination of a depth plot with a contour plot was helpful for the validation of the contours derived from the DTM. The advantage of separating different types of data in single files was, that each file could have a chosen print layout, for instance a bankline could be printed thicker than a contour line. In general, bathymetric, topographic and float track data of one survey period were plotted in one chart (see Subsection 1.4.3).



MC	Masterchart	Topo	Topography data	W.L.	Water level
ES	Echo sounder	Bathy	Bathymetry data	DTM	Digital Terrain Model
Float	Float track data	WA	Wave Height	WI	Wind direction/speed
T.P.	Test Pile	EDM	Electronic Distance Measurement unit	HP-GL/2	Hewlett-Packard Graphics Language

Fig. 4.1-1: Flowchart – Processing of digital monitoring data

The plot-files (HP-GL/2 format) could be converted by utility software to the AutoCAD compatible format DXF. The AutoCAD 14 software was appropriate for finalizing report presentations (A4-size). The coloring of bathymetry iso-patches was enabled by AutoCAD and the general layout of the charts could be improved as well. The Valeport current point measurements could be presented as velocity vectors by AutoCAD (for example see Fig. 5.3-23).

The data from the monitoring station were processed by Excel (for results see Section 6.2).

4.2 PROCESSING OF BATHYMETRIC DATA

The processing steps of a bathymetric survey were in the following order:

- position correction for spikes, jumps and noise;
- plotting surveyed tracks for completeness control;
- depth editing by comparison of digital data with echo sounder paper roll recordings;
- water level correction by time correlated converting measured depth into PWD-heights;
- evaluation of Digital Terrain Models (DTMs);
- derivation of contour lines of same heights from the DTM;
- plotting depths and contours to verify the validation of the model, and
- final charting with header, grid, topographic objects and flow information;

The monitoring team carried out further evaluations like differential DTMs, cross section plots, bathymetry charts of colored iso patches, etc.

4.3 PROCESSING OF FLOAT TRACKS

The float track data files contained time and position. From these data the average flow velocity and flow direction between two navigation fixes could be easily derived by Excel (see Subsection 3.3.1).

Although the high position resolution of the advanced DGPS float tracking (see Subsection 3.3.2) provided high accurate flow lines, the flow velocities should be calculated by a bigger distance between two float positions. Considering the accuracy of the Trimble Pathfinder GPS receiver (standard deviation = ± 4.1 m, see footnote of Table 2.4-1) the average flow velocities were derived over the way the float passed within 20 seconds. The monitoring team developed a software routine for the flow velocity calculation. This routine provided a flow velocity for each float track position by a moving average method. For instance, if a float track file contained every 2 seconds the positions $P_1, P_2, P_3 \dots P_n$, the velocity for position P_1 was calculated over a chosen time period of 20 seconds between P_1 and P_{10} ; the velocity for position P_2 was calculated between P_2 and P_{11} and so on. The last calculated velocity would correspond to the position P_{n-9} . That means the velocity given to the corresponding position represented the average velocity the float will pass downstream by a chosen time interval.

4.4 PROCESSING OF CURRENT POINT MEASUREMENTS

The measurements carried out by the Valeport current meter were processed by the manufacturer's own window based software. The software provided the following utilities:

- downloading the data from the Valeport probe to the office computer;
- computing the average flow velocity and flow direction of the logging period, and
- evaluation of the flow velocity and flow direction standard deviation from the single measurements.

Thereby a single measurement represented the mean values of all flow velocities and flow directions measured by the probe within a 10-second time interval. The monitoring team logged data over a time period of at least 2 minutes, i.e. more than 12 single current measurements were logged on each location. The standard deviation described the prevailing flow conditions at the location, whether the flow was more or less stable or turbulent.

4.5 PROCESSING OF TOPOGRAPHIC DATA

The data collected by the electronic total station Wild TC 1600 were downloaded by the Wild GIF 10 REC-module reader to the office computer at site. This data contained a point number, easting, northing and the height. Sketches of the topographic surveys were made in the field indicating the point numbers of lines or objects for comparison with the point numbers of the data files. The data had to be ordered by a column editor in that way the banklines, waterlines or any topographic objects had to be presented. Therefore, the data files were added with a column indicating a plot code. These data could be plotted by Masterchart. After plotting the topographic data had to be checked for validation and completeness.

4.6 PROCESSING OF DATA FROM THE MONITORING STATION

The data was downloaded from a REC-module to the office computer at site. All data since the last initialisation of the REC-module was compressed in one data file. Data files of different formats could be extracted from this file (see Attachment 2). These data were checked, ordered and saved in Excel tables for statistical analysis (see Section 6.2).

5 THE GROUYNE TEST STRUCTURE

5.1 SUMMARY

The Groyne Test Structure was exposed to heavy hydraulic loads during the monsoon 1995. The loads concentrated on the groynes G-2 and G-3 and caused damages at the downstream side of the transition area between the impermeable and the permeable sections of the groynes including the loss of the first 16 piles of groyne G-2. In the dry seasons of the following years the structures were adapted (see Fig. 1.3-1 and Fig. 1.3-2). In March 1996 groyne G-A came under attack, which resulted in the loss of 5 piles. During the following monsoon season 1996 the structures were a second time subject to heavy loads, but no significant damages occurred. From 1997 the loads on the structures decreased whereas bank erosion was monitored downstream from the structures in the areas of Syedpur, Rasulpur and Balashi Ghat (see Fig. 1.3-4).

Important events and interesting observations recorded in the logbook are listed in Section 5.2. Charts, cross-sections evaluated from selected bathymetric surveys and flow measurements at the test structures are presented in Section 5.3. Since not all survey results can be included in this annex, for further available data reference is made to Attachment 3, Inventory of Monitoring Data. The monitoring results are presented mainly from 1995 and 1996, since the structures have been well tested during that period.

5.2 LOGBOOK OBSERVATIONS

5.2.1 Chronology of Events

The monitoring team inspected the test site daily. Important observations made during the inspections were reported in the logbook. The logbook form sheet is shown in Attachment 1. Reported events with notable effect on the test structures are listed in chronological order in Table 5.2-1. Events of main interest are shown in bold letters.

Date	Groyne	Reported Logbook Event
15-16/05/95	G-B/2	Severe bank erosion downstream from groyne.
17/05/95	G-2	Crack developed on top of impermeable head.
20/05/95	G-2	Erosion at the downstream bank.
21/05/95	G-2	Boulders slid at the downstream side of the impermeable head due to heavy flow
04/06/95	G-1	Some cc-blocks slid at the downstream head of the impermeable groyne due to heavy rainfall.
04/06/95	G-2	Crack on the impermeable head reopened although it was repaired on 20/05/95 by compaction.
10-23/06/95	G-2	Erosion at the upstream and downstream bank.
17/06/95	G-1	Slides at the downstream side of the impermeable head.
19/06/95	G-2	Larger slide at the downstream side of the impermeable part and immediate wash out of the debris.
22-30/06/95	G-1	Return flow and eddies observed between G-1 and G-2.
24/06/95	G-2	Erosion of the toe of the main embankment started downstream from the groyne.
25/06/95	G-1	Erosion at the downstream bank.
25/06/95	G-2	Further slides and erosion at downstream embankment.

Table 5.2-1: Chronology of events reported in the logbook

Date	Groyne	Reported Logbook Event
01/07/95	G-3	First slide at the downstream side of the impermeable head. A crack formed across the impermeable part near head.
01-08/07/95	G-2	Strong return flow and eddies downstream from groyne.
03-06/07/95	G-2	Severe erosion at the downstream embankment.
04-05/07/95	G-3	Return flow at downstream from groyne.
08/07/95	G-1	Further slides of impermeable groyne.
09/07/95	G-2	Destruction of the impermeable groyne head in conjunction with loss of the first four piles of the permeable part.
11/07/95	G-2	Breach of the main embankment about 80 m downstream from G-2.
09-15/07/95	G-2	Settlement/deformation of first 16 piles of permeable part.
16/07/95	G-1	Return flow passing the permeable part of the groyne.
18/07/95	G-1	Erosion at the embankment downstream from the groyne.
22/07/95	G-2	Embankment erosion between G-2 and G-3.
22-23/07/95	G-1	Embankment erosion between G-1 and G-2 due to wind and wave. Wave height: 0.5 m, wind speed: 8-9 Bft from East
03-04/08/95 + 08/08/95	G-1	Severe erosion at the downstream embankment. Wave height: 0.4 m, wind speed: 6-7 Bft from East
06/08/95	G-2	Pile No 15 of permeable part lost.
13/08/95	G-2	Another pile of permeable part damaged. Erosion of the embankment downstream from the groyne.
19/08/95	G-3	Major slide at the downstream side of impermeable head, opening a gap between permeable pile structure and the impermeable part: 09.00 am cover layer of boulders at the downstream slope of the impermeable groyne head starts sliding, a crack appears along the centre line of the earth dam; 11.00 am erosion along the downstream side of the groyne continued, deformation of brick matting downstream starts; 12.00 am collapsing of the impermeable part of the groyne at the downstream side; 02.00 pm situation stabilised.
19/08/95	G-1	Embankment erosion between G-1 and G-2 continues. Wave height: 0.3 m
26/08/95	G-2	Displacement of Pile No 7.
22/09/95	G-3	Erosion of embankment 40 m upstream from G-3.
27/09/95	G-2	Pile No 11 lost. Erosion at downstream continued.
29/09/95	G-2	Embankment erosion continued.
24/10/95	G-3	Longitudinal crack developed in the embankment just downstream from the groyne.
25/10/95	G-A	Bank erosion started downstream from G-A.
27/10/95	G-3	Longitudinal crack of the downstream embankment became larger.
25/03/96	G-A	Bank erosion extended further downstream from G-A up to Rasulpur. Pile No 19 lost.
31.03.96	G-A	Pile No 14 lost.
05.04.96	G-A	Erosion just downstream from falling apron, return flow.
19.04.96	G-A	Bank erosion downstream from the groyne continued.
10.05.96	G-A	Bank erosion at downstream continued.
24.06.96	G-A	One of the piles became inclined.

Table 5.2-1 (continued): Chronology of events reported in the logbook

5.2.2 Floating Debris

Floating debris transported by the river were dominated by clusters of water hyacinths and banana trunks. The thickness and the area of the piled-up debris at the upstream side of each groyne was estimated from visual observations and reported in the logbook. After the first up-pilings it was decided to remove floating debris from the groyne field by hand as recommended in the Planning Study Report. Significant volume of floating debris observed during the monsoon seasons 1995, 1996 and 1997 are listed in Table 5.2-2.

Groyne	Date	Maximum Area (m ²)	Maximum Thickness (m)
G-1	1995, June 13	600	1.0
G-2	1995, June 07	300	1.4
G-3	1995, May 28/29	300	1.0
G-3	1995, June 06	200	1.5
G-1	1996, August 14/15	240	1.0
G-2	1996, July 01	300	1.0
G-2	1996, August 19	60	2.0
G-3	1996, September 03	225	0.7
G-3	1996, July 01	120	1.0
G-A	1996, September 04	320	0.7
G-1	1997, June 14 to 18	1,600	0.8
G-2	1997, June 19	10,000	2.0
G-3	1997, June 19/22	10,000	2.0
G-A	1997, June 18	1,200	1.0

Table 5.2-2: Observations on floating debris

5.3 BATHYMETRY AND FLOW CONDITIONS

5.3.1 Site Surveys

The bathymetry and the float tracks of selected site surveys from 1995 to 1997 are shown in Fig. 5.3-1 to Fig. 5.3-22. In 1995 the monitoring team could not always carry out float tracks in combination with the bathymetric surveys (see Subsection 3.3.1). Sketched flow lines from the logbook have been copied in the charts by AutoCAD. The presented charts are scaled by 1: 5000. The crest of the embankment, the impermeable part of the groynes and the groyne axes present the layout of the test structures in the charts. Thick lines present the bankline surveys. Two consequent surveys of 1995 can be compared in one page. A description of significant changes of the morphology of the riverbed is given in chronological order in the Tables 5.3-1 and 5.3-2.

Date	Observations	Fig. No.
May 18	Bank erosion of 40 m over a length of 100 m d/s from impermeable head of G-2. Bed level of channel in front of groynes reduced by about 5 m. Scour holes developed at about 70 m d/s from the heads of the groynes G-1 and G-2.	5.3-1
June 10		5.3-2
June 10	Bank erosion between G-1 and G-3 continued. Slope inclination from groyne axis of G-2 towards downstream was 1:2.5 on June 24.	5.3-2
June 24		5.3-3
June 24	Further deepening of scour holes downstream from G-1 and G-2. Surface flow velocity in front of groynes was measured as 3.0 m/s on June 26. The flow direction was parallel to the alignment of the test structures.	5.3-3
June 26		5.3-4
June 29	On June 29 the scour hole d/s from G-2 was below -8 m+PWD, which was equivalent to a water depth of 29 m. The deepest point of the scour hole d/s from G-2 shifted about 25 m towards the bank. The slope inclination d/s from G-2 was 1:2.	5.3-5
June 29	Bank erosion between G-1 and G-2 as well as between G-2 and G-3 continued. Embankment erosion started. The head of the impermeable groyne and the first piles of G-2 collapsed resulting in a wide opening between the impermeable and the permeable part. In the area of the opening a slope parallel to the bank characterised the morphology. A hill up to 12 m+PWD developed just u/s from the remained permeable part of G-2.	5.3-5
July 9/10		5.3-6
July 11	Embankment erosion d/s from G-2 continued. Bank erosion d/s from G-3 at the head of impermeable part.	5.3-7
July 17	Surface flow of 1.3 to 1.4 m/s parallel to the of test structures. Float track started at the riverside end of G-1 passing the middle part of the permeable groynes of G-2 and G-3. No significant further erosion in comparison to the survey from July 11, 1995.	5.3-8
July 31	Embankment erosion continued d/s from G-2. Significant bank erosion just d/s from the impermeable part of G-3.	5.3-9
July 31	Scour hole d/s from G-3 developed from below -8 m+PWD to -10 m+PWD on August 16. Significant siltation of the scour hole d/s from G-1 from August 5 to August 16. The contour lines show a slope d/s from G-3 parallel to the groyne axis at the first half of the permeable part. Slope inclination is 1:4.	5.3-9
August 5		5.3-10
August 16		5.3-11
August 16	Large scour area d/s from G-3. Slope d/s from G-3 extended further to the embankment. The slope inclination was 1:2. The scour hole d/s from G-1 eroded again. No further bank erosion d/s from G-1. Flow line of August 20 was passing the opening of G-2 ending in a rotating flow 75 m d/s.	5.3-11
August 20		5.3-12
August 20	Surface flow velocity between G-2 and G-3 was 1.7 m/s and 1.9 m/s between G-3 and G-A respectively. Slight siltation of scour holes.	5.3-13
August 27	Bankline from August 27 showed broken part of impermeable groyne G-3.	5.3-14
August 27	No further erosion between August 27 and September 11.	5.3-14
September 11	Bank erosion occurred u/s from G-3 and the scour hole eroded by 4 m between September 11 and September 24. On September 24 the scour hole d/s from G-3 was below -11 m+PWD, which was equivalent to a water depth of 32 m.	5.3-15
September 24		5.3-16

Table 5.3-1: Description of hydrographic conditions at Test Site I during monsoon 1995

Date	Observation	Fig. No.
June 11/12 1996	In comparison to September 1995 the channel in front of the test structures was narrower and its bed silted up by more than 5 m. The channel surface flow velocity was reduced by 50 % in comparison to June 1995. The flow was approaching the test structures u/s from G-1 in an angle of app. 30°. From G-2 towards d/s the flow was parallel to the alignment of the structures.	5.3-17
June 25-27	Slight erosion d/s from G-3.	5.3-18
July 13-16	Area from G-1 to d/s from G-3 was silted up by further 5 m since June 25 – 27.	5.3-19
July 27/28	No significant changes in the riverbed since July 13 - 16. Return flow close to the bank d/s from G-2 showed velocities of 0.5 to 0.6 m/s.	5.3-20
August 17-19	Flow approaches towards the head of G-3 in an angle of 30° to the alignment of the test structures. The area u/s from G-3 silted further up. A rotating flow d/s from the impermeable head of G-A.	5.3-21
July 24-25	Flow lines parallel to the alignment of the test structures. Further siltation, mainly d/s from G-3 since 1996.	5.3-22

Table 5.3-2: Description of hydrographic conditions at Test Site I during monsoons 1996 and 1997

5.3.2 Development of Scour Holes

Table 5.3-3 provides a list of the development of scour holes downstream from G-1, G-2 and G-3 from monsoon 1995 to the end of 1996. Downstream from G-A and G-A/2 no significant scour holes had developed. The table considers all site surveys carried out by the monitoring team.

Date	Groyne G-1						Groyne G-2						Groyne G-3						Fig No
	u_{cb} (m/s)	h_{cb} (m PWD)	h_{db} (m)	d_{db} (m)	d_{pb} (m)	d_{pb} (m)	u_{cb} (m/s)	h_{cb} (m PWD)	h_{db} (m)	d_{db} (m)	d_{pb} (m)	d_{pb} (m)	u_{cb} (m/s)	h_{cb} (m PWD)	h_{db} (m)	d_{db} (m)	d_{pb} (m)	d_{pb} (m)	
18/05/95	-	5	3	2	20	15	-	4	-2	6	45	0	-	0	-1	1	30	5	5.3-1
10/06/95	-	4	-2	6	70	0	-	1	-2	3	45	5	-	1	0	1	-	-	5.3-2
24/06/95	2.9	1	-5	6	80	0	3.0	-3	-6	3	65	-5	3.0	-1	0	-1	-	-	5.3-3
26/06/95	2.9	0	-6	6	85	-5	3.0	-3	-7	4	55	5	3.0	-2	-3	1	35	10	5.3-4
29/06/95	-	0	-7	7	80	0	-	-3	-8	5	70	-25	-	-1	-4	3	65	0	5.3-5
09-10/07-95	-	-1	-5	4	60	-10	-	0	-3	3	50	-20	-	-	-	-	-	-	5.3-6
11/07/95	-	-1	-4	3	60	-5	-	-3	-7	4	50	0	-	-5	0	-5	-	-	5.3-7
17/07/95	1.3	-1	-4	3	50	0	1.4	-1	-6	5	50	0	1.4	-5	0	-5	-	-	5.3-8
20/07/95	-	-	-	-	-	-	-	0	-7	7	45	0	-	-6	-8	2	60	0	
31/07/95	-	0	-7	7	60	-5	-	-1	-8	7	45	0	-	-5	0	-5	-	-	5.3-9
01-02/08/95	-	-2	-6	4	50	0	-	0	-7	7	60	0	-	-6	-9	3	40	5	
05/08/95	-	-2	-7	5	60	5	-	0	-8	8	50	0	-	-5	0	-5	-	-	5.3-10
10/08/95	-	-3	-8	5	65	5	-	0	-7	7	70	-10	-	-6	-9	3	55	5	
14/08/95	-	-4	-5	1	50	0	-	0	-8	8	60	0	-	-6	-10	4	40	0	
16/08/95	1.8	1	-1	2	35	-30	1.8	0	-8	8	65	10	2.5	-5	-10	5	55	5	5.3-11
20/08/95	1.7	0	-7	7	55	0	1.7	1	-9	10	60	0	1.9	-5	-9	4	40	0	5.3-12
24-25/08/95	1.5	-2	-8	6	55	0	1.3	0	-9	9	65	-5	1.2	-6	-9	3	75	0	
27/08/95	1.0	-2	-3	1	70	5	1.7	0	-8	8	95	-20	0.6	-5	-7	2	50	-5	5.3-14
03-04/09/95	-	-1	-4	3	65	-5	-	-2	-8	6	100	-60	-	-6	0	-6	-	-	
03-11/09/95	-	0	-4	4	70	-5	-	1	-8	9	100	-30	-	-7	-8	1	55	0	
07-08/09/95	-	1	0	1	60	5	-	1	-7	8	100	-30	-	-4	-6	2	70	-35	
11/09/95	-	-	-	-	-	-	1.2	0	-4	4	80	25	1.1	-3	-7	4	70	-15	5.3-15
15-16/09/95	-	1	-4	5	55	-5	-	1	-4	5	75	-30	-	-4	-9	5	55	-5	
19-20/09/95	-	-	-	-	-	-	-	0	-5	5	80	-30	-	-4	-10	6	65	0	
24/09/95	-	-2	-1	-1	65	-15	-	2	-5	7	80	-5	-	-3	-11	8	70	0	5.3-16
07/08/10/95	-	2	-2	4	55	-10	-	1	-5	6	85	-35	-	-4	-10	6	75	0	
13-14/10/95	1.0	3	-1	4	100	-25	1.0	1	-6	7	60	-15	1.1	-4	-10	6	100	5	

Table 5.3-3: Development of scour holes d/s from G-1, G-2 and G-3

Date	Groyne G-1					Groyne G-2					Groyne G-3					Fig No	
	u_{ch} (m/s)	h_{ch} (m PWD)	h_{sh} (m)	d_{sh} (m)	d_{gp} (m)	u_{ch} (m/s)	h_{ch} (m PWD)	h_{sh} (m)	d_{sh} (m)	d_{gp} (m)	d_{lp} (m)	u_{ch} (m/s)	h_{ch} (m PWD)	h_{sh} (m)	d_{sh} (m)		d_{gp} (m)
26-27/10/95	1,2	4	-1	5	135	-30	2	-7	9	70	-30	1,1	-4	-10	6	55	-5
14/11/95	1,1	5	0	5	150	-50	1,1	-3	4	65	-25	1,1	-4	-9	5	80	-20
13/12/95	-	6	0	6	115	-30	-	1	3	50	0	-	-5	-10	5	70	-35
22/12/95	0,8	5	0	5	115	-35	0,8	1	2	55	-60	0,8	-6	-10	4	60	-5
13/02/96	-	-	-	-	-	-	-	0	5	40	-50	-	-2	-5	3	60	-35
08/03/96	-	-	-	-	-	-	-	7	0	50	-60	-	2	-4	6	50	-25
26/03/96	-	4	0	4	50	-25	-	7	0	45	-70	-	2	-4	6	50	-40
06-08/06/96	1,3	12	7	5	55	-55	1,4	-1	5	95	-45	1,2	1	-3	4	40	-20
11-12/06/96	1,2	11	7	4	50	-40	1,4	9	0	80	-55	1,4	2	-4	6	45	-25
14-16/06/96	1,3	10	7	3	55	-40	1,1	6	0	90	-20	1,1	1	-4	5	55	-30
25-27/06/96	1,4	11	7	4	55	-40	-	9	1	70	-65	1,3	1	-6	7	65	-40
03-05/07/96	1,7	10	8	2	55	-35	1,5	6	2	60	-70	1,9	0	-3	3	70	-40
13-15/07/96	1,9	12	10	2	55	-35	1,8	8	5	3	20	-45	2,1	0	-2	2	40
13-16/07/96	1,9	11	10	1	45	-35	2,2	11	5	6	25	-45	2,3	3	0	3	40
27-28/07/96	1,9	13	11	2	45	-40	1,9	11	5	6	10	-40	2,1	0	-2	2	55
01-04/08/96	1,6	13	11	2	55	-50	1,6	9	6	3	20	-40	1,2	0	-1	1	55
17-19/08/96	-	13	12	1	55	-50	1,8	10	7	3	15	-35	1,4	0	-2	2	60
03-05/09/96	1,3	15	13	2	45	-50	1,2	12	10	2	30	-35	1,0	9	1	8	40
17-23/09/96	1,2	13	11	2	30	-15	1,5	12	12	0	5	-70	1,1	8	1	7	20
05-07/10/96	1,4	12	10	2	20	-20	1,2	14	13	1	10	-40	1,0	13	10	3	35
23-24/10/96	1,5	13	11	2	20	-20	1,6	14	12	2	35	-35	1,5	13	12	1	30
24-29/07-97	1,5	10	4	6	50	-25	1,4	10	9	1	10	-10	1,7	11	12	-1	5
																	5 3-22

Notes:

u_{ch} = cross sectionally averaged surface flow velocity of channel (m/s)

h_{ch} = height of channel bed (PWD) just u/s from groyne

h_{sh} = height of centre scour hole (PWD)

d_{sh} = $h_{ch} - h_{sh}$

d_{lp} = distance of centre scour hole perpendicular to groyne axis

d_{ga} = distance parallel to groyne axis from last pile of groyne to centre scour hole

('+' = towards river, '-' = towards bank)

Table 5.3-3 (continued): Development of scour holes d/s from G-1, G-2 and G-3

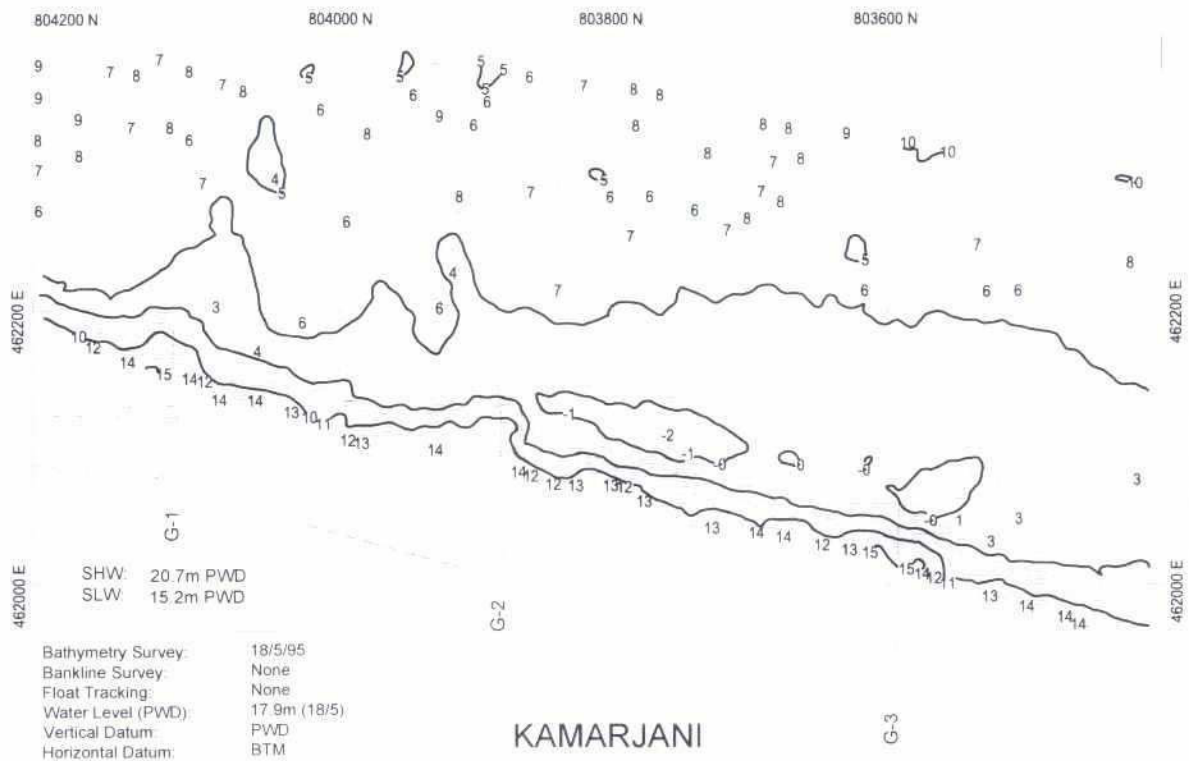


Fig. 5.3-1: Bathymetry at the test site area on May 18, 1995

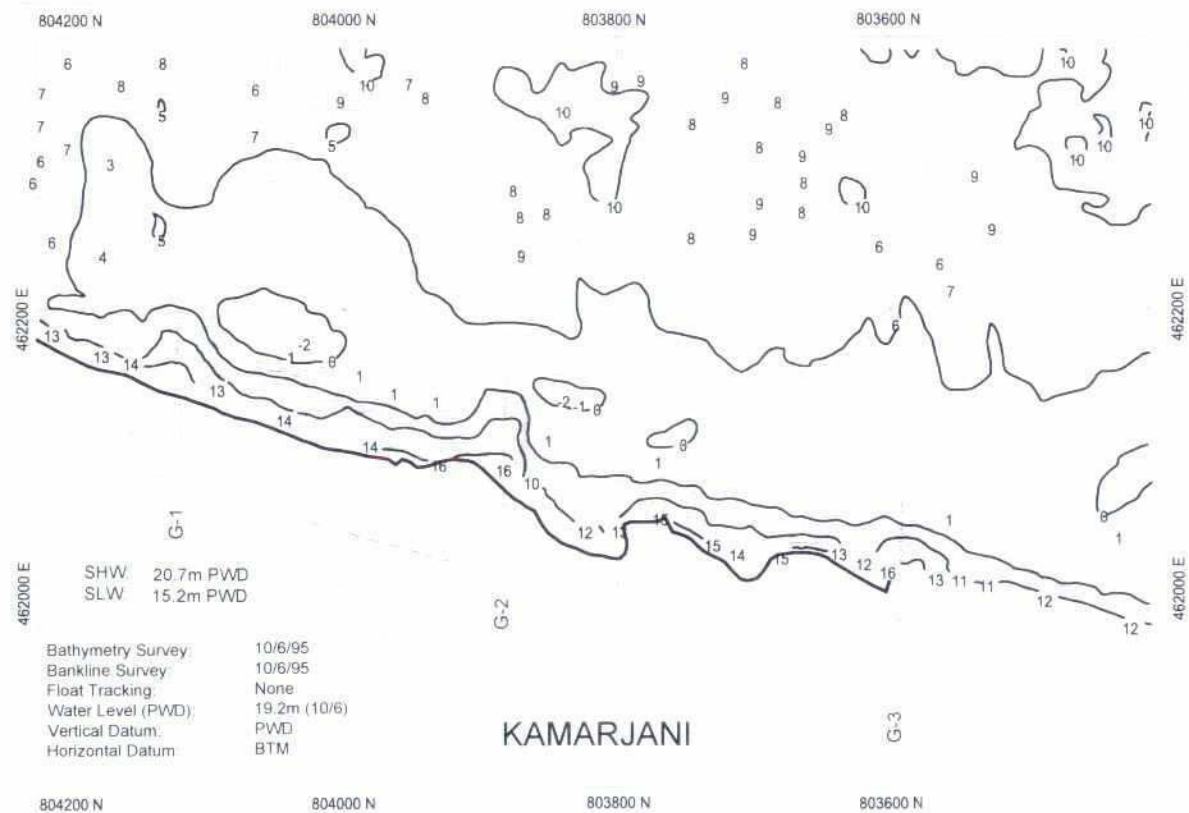


Fig. 5.3-2: Bathymetry at the test site area on June 10, 1995

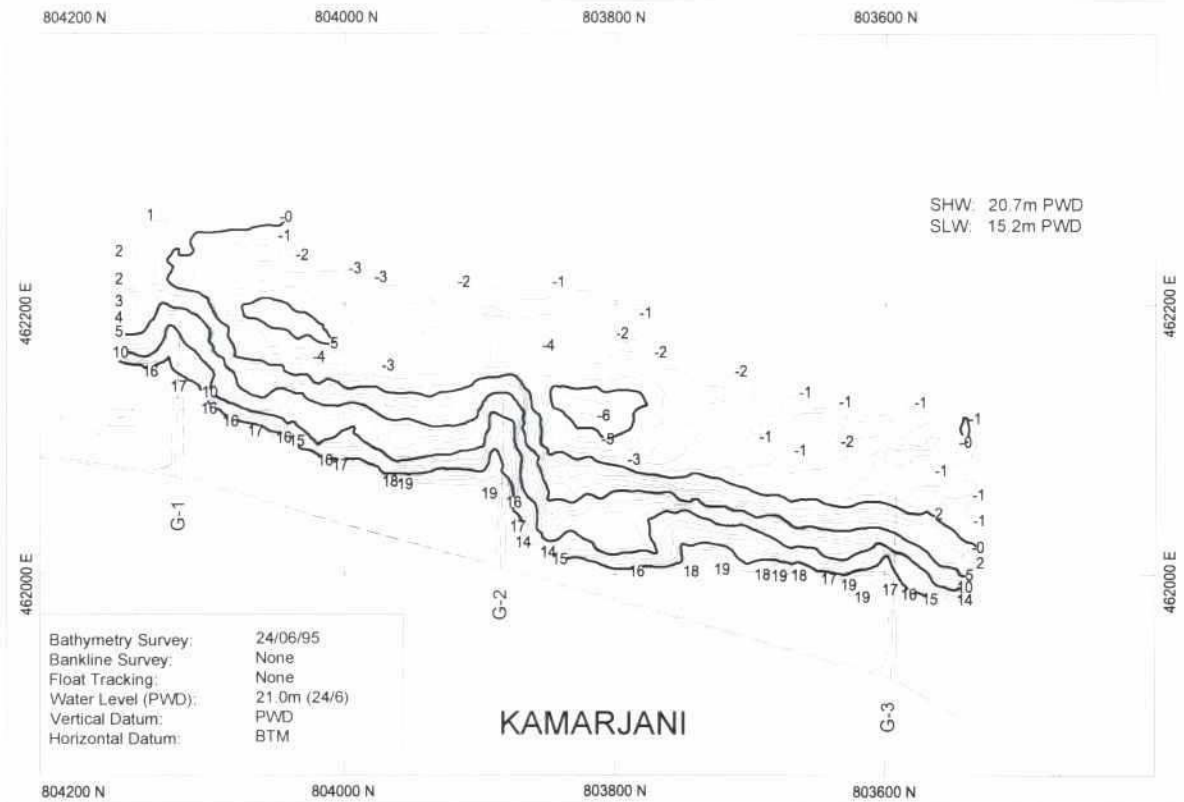


Fig. 5.3-3: Bathymetry at the test site area on June 24, 1995

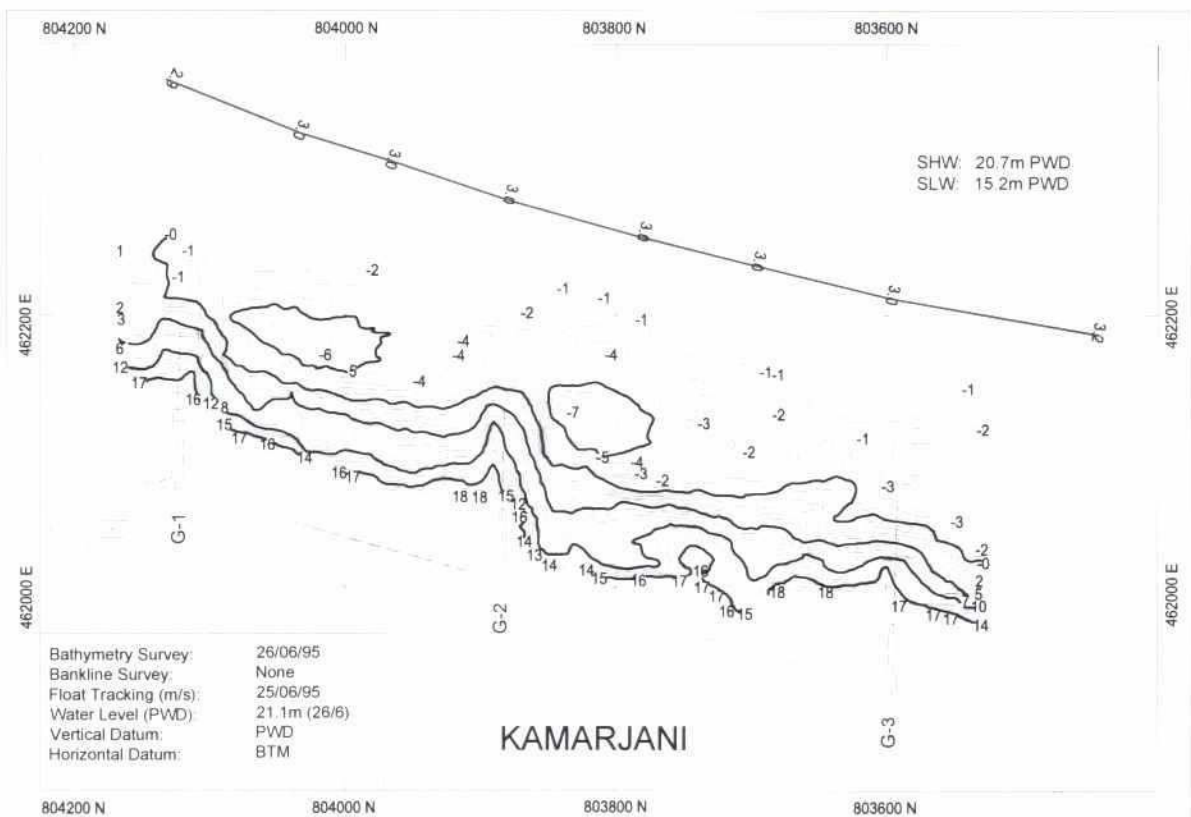


Fig. 5.3-4: Bathymetry and flow at the test site area on June 26, 1995

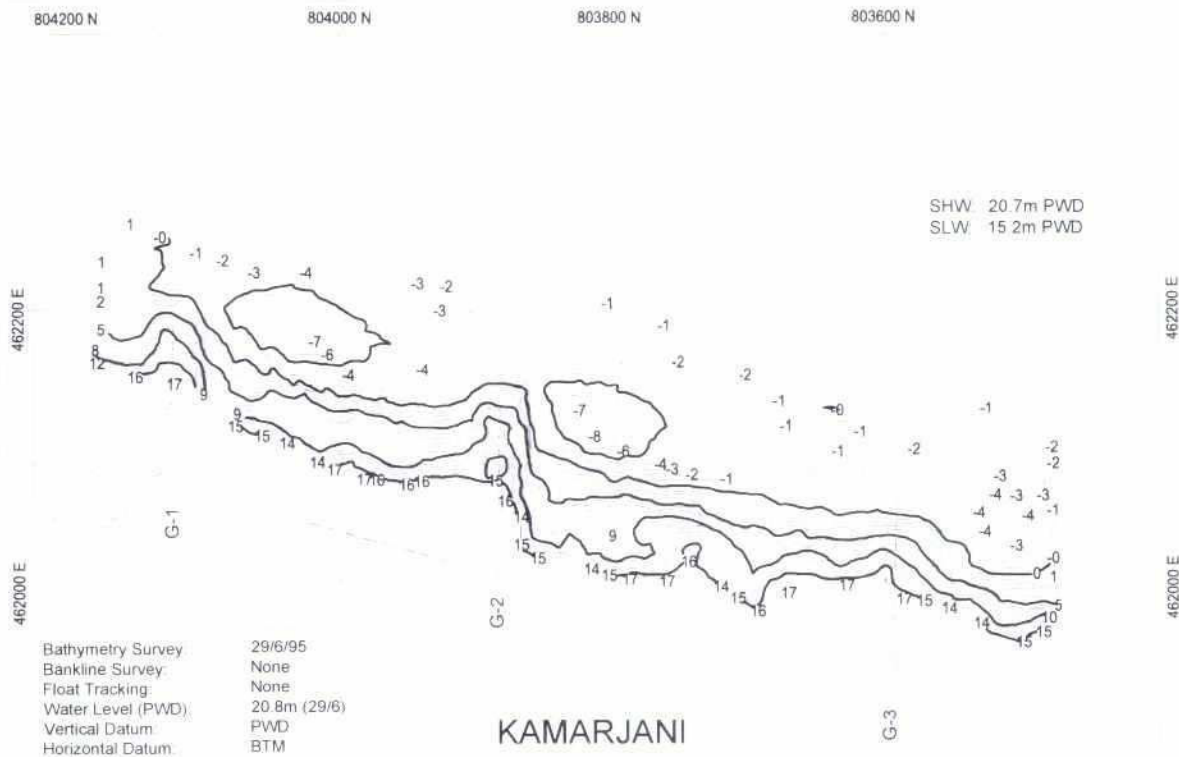


Fig. 5.3-5: Bathymetry at the test site area on June 29, 1995

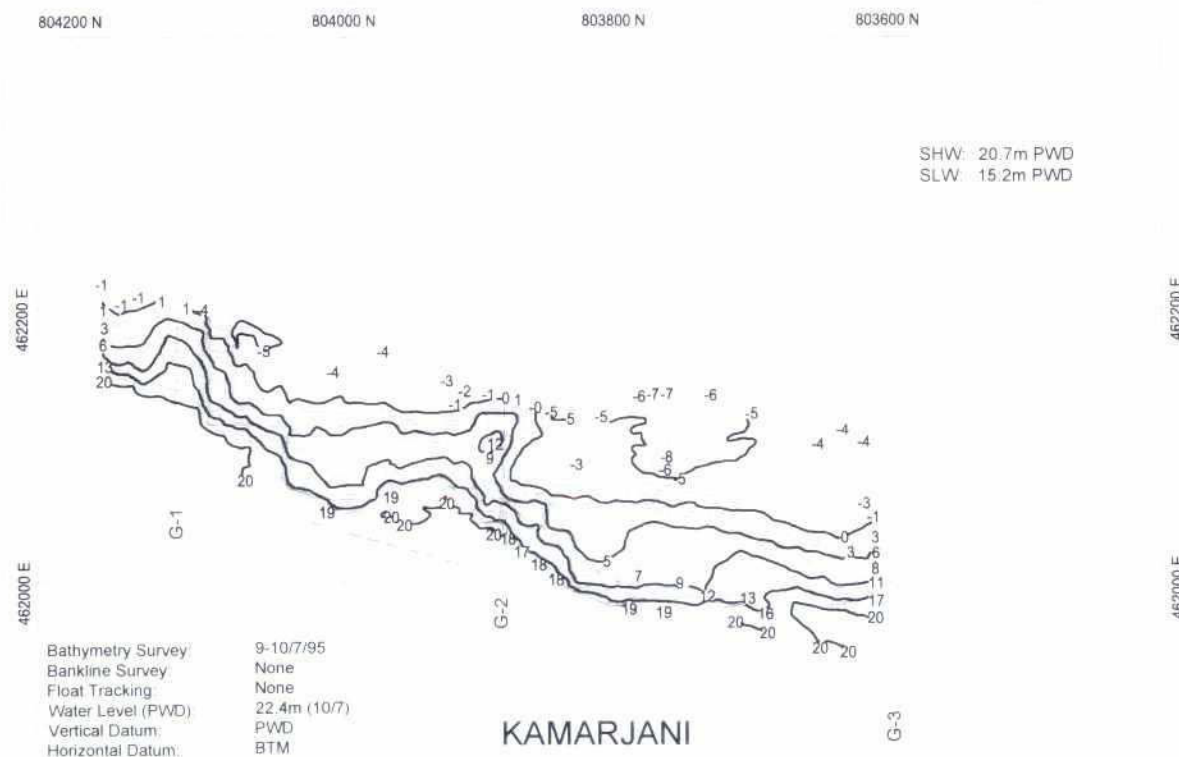


Fig. 5.3-6: Bathymetry at the test site area on July 09-10, 1995

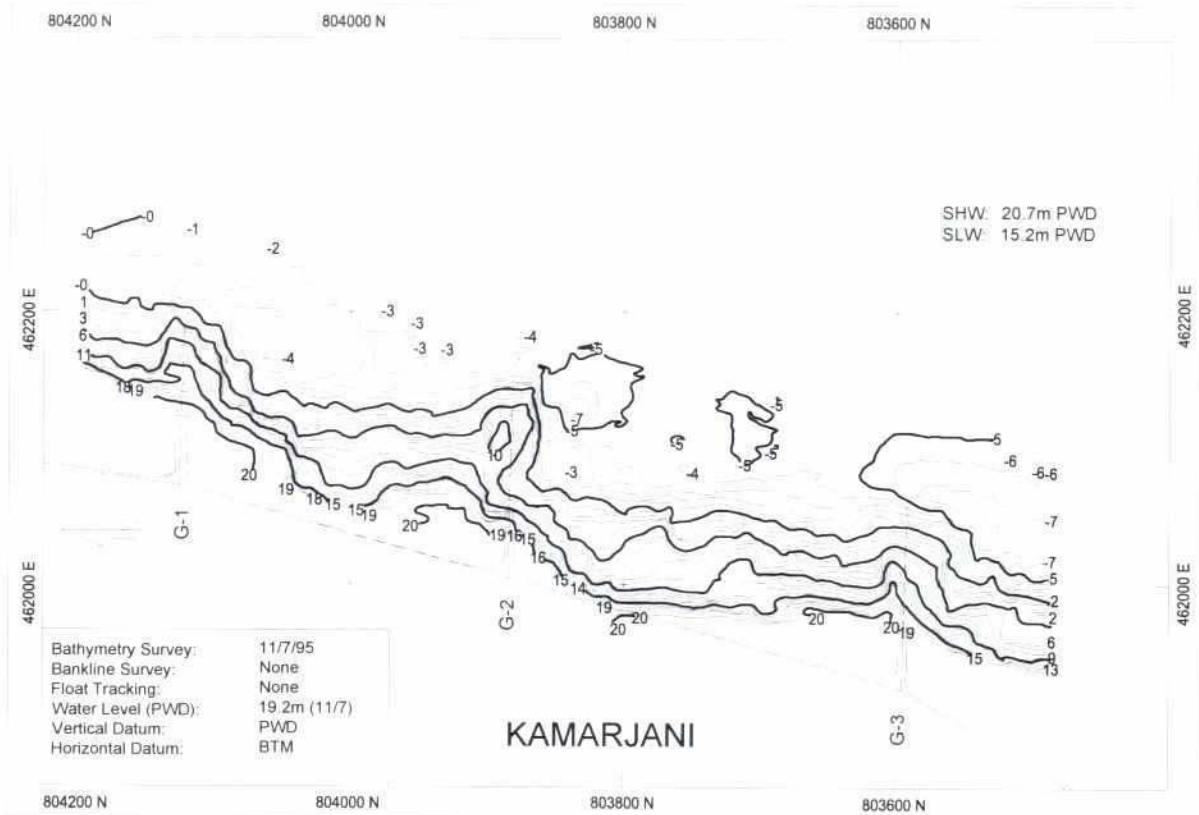


Fig. 5.3-7: Bathymetry at the test site area on July 11, 1995

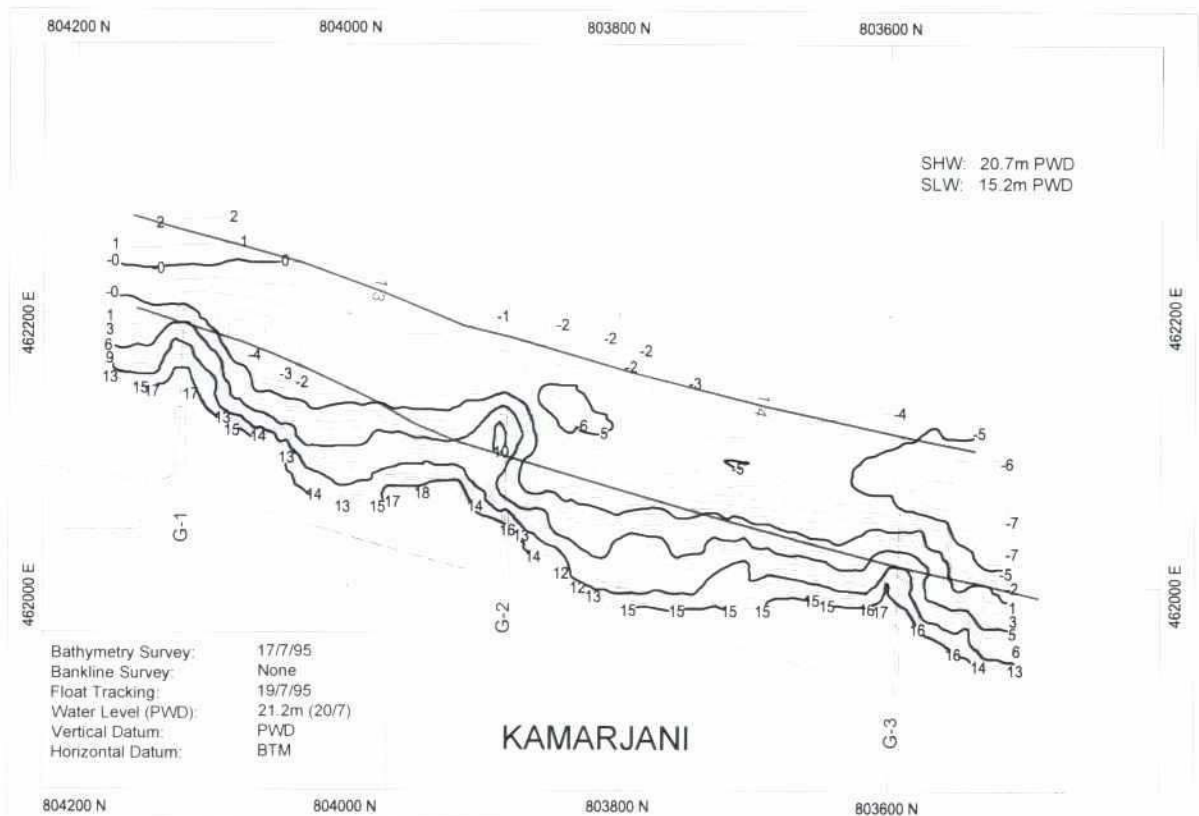


Fig. 5.3-8: Bathymetry and flow at the test site area on July 17, 1995

32

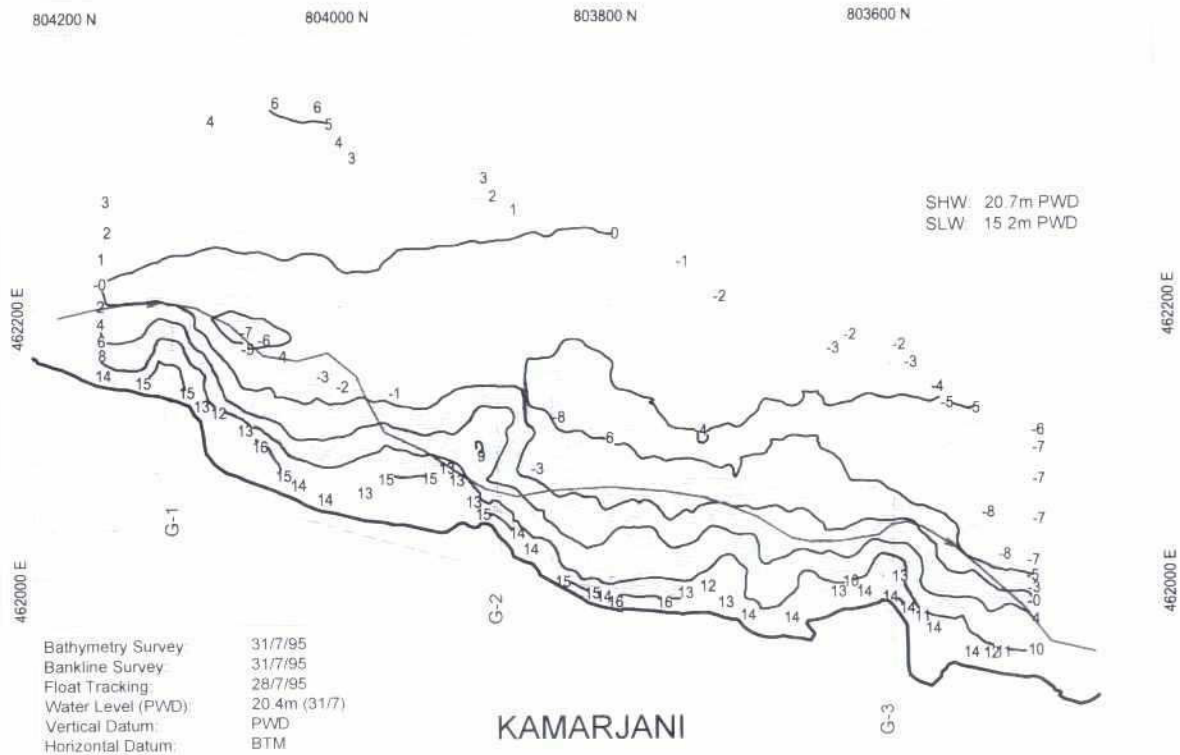


Fig. 5.3-9: Bathymetry and flow at the test site area on July 31, 1995

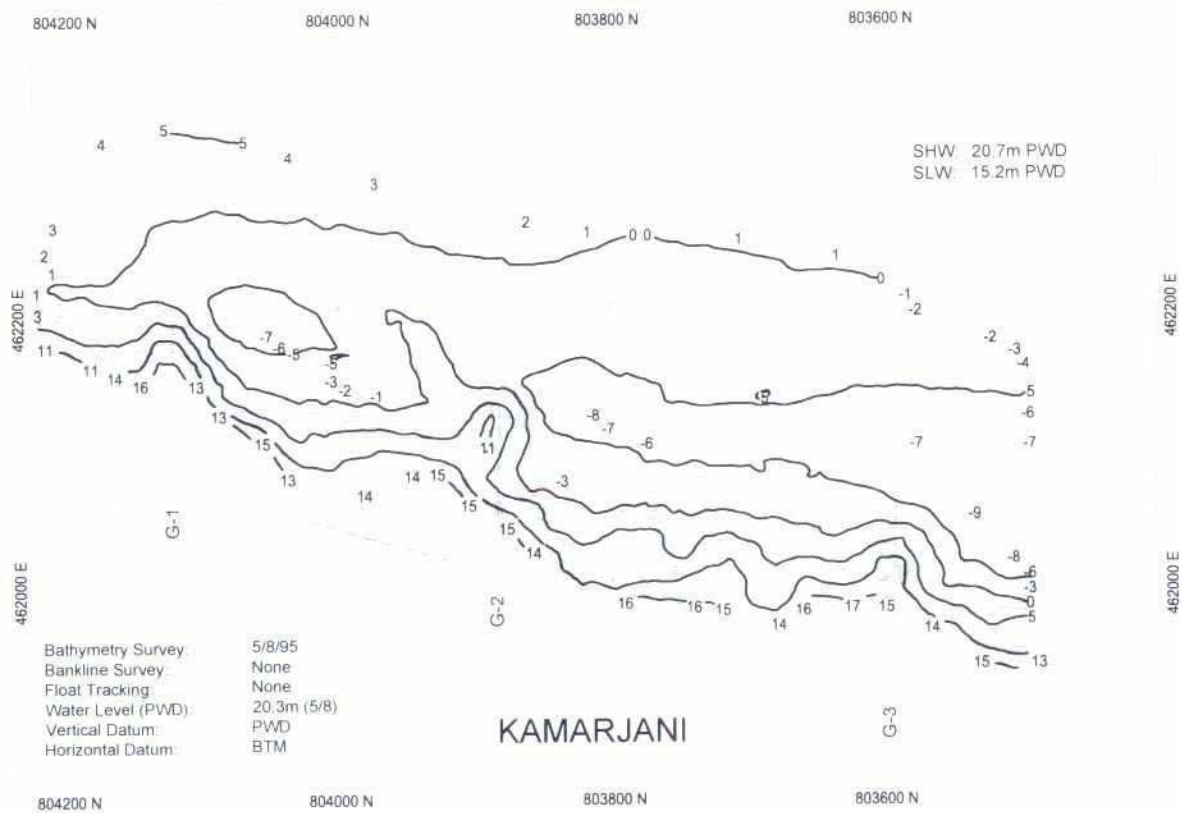


Fig. 5.3-10: Bathymetry at the test site area on August 05, 1995

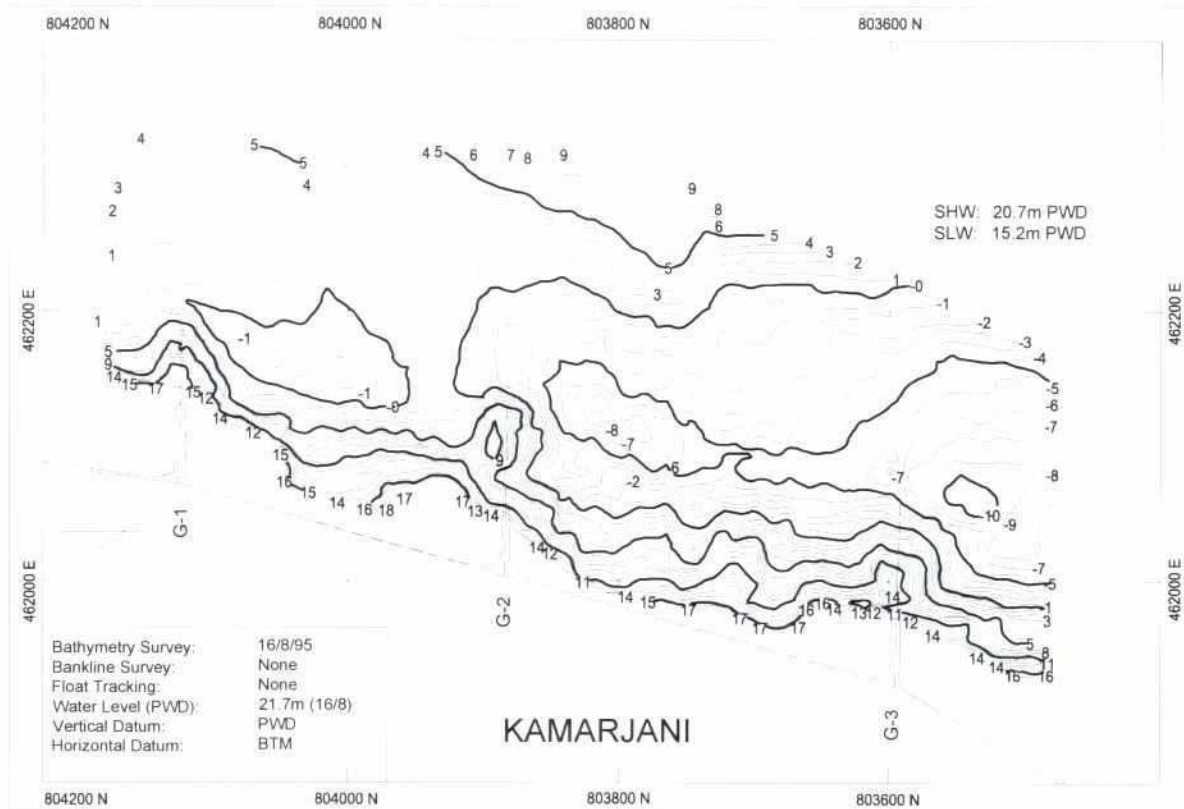


Fig. 5.3-11: Bathymetry at the test site area on August 16, 1995

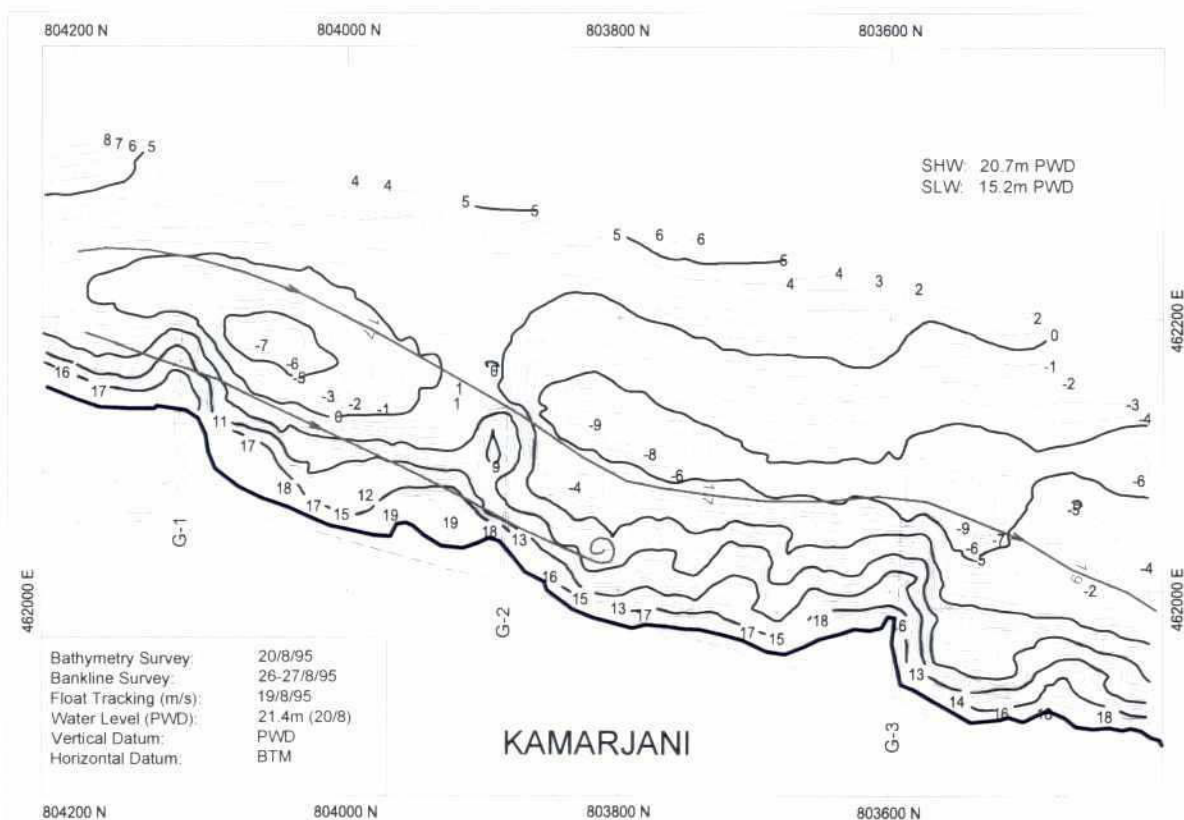


Fig. 5.3-12: Bathymetry and flow at the test site area on August 20, 1995

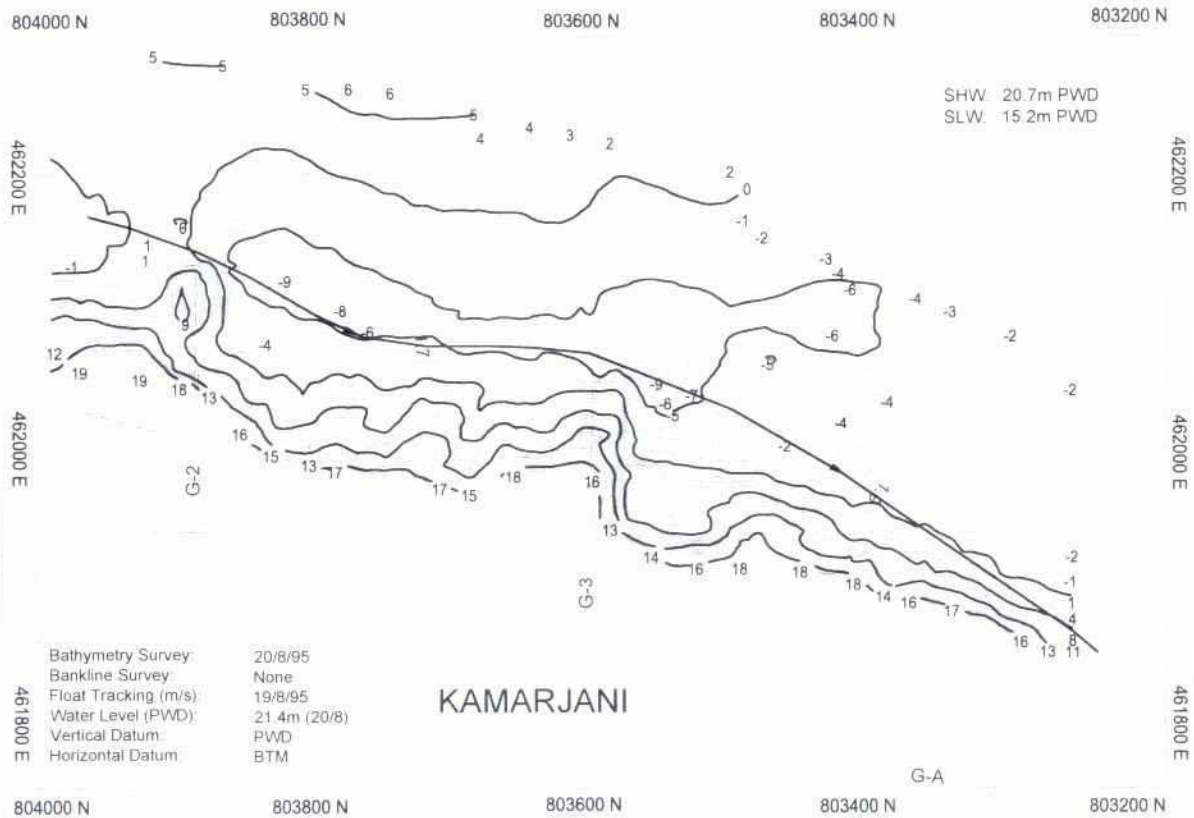


Fig. 5.3-13: Bathymetry and flow at the test site area on August 20, 1995

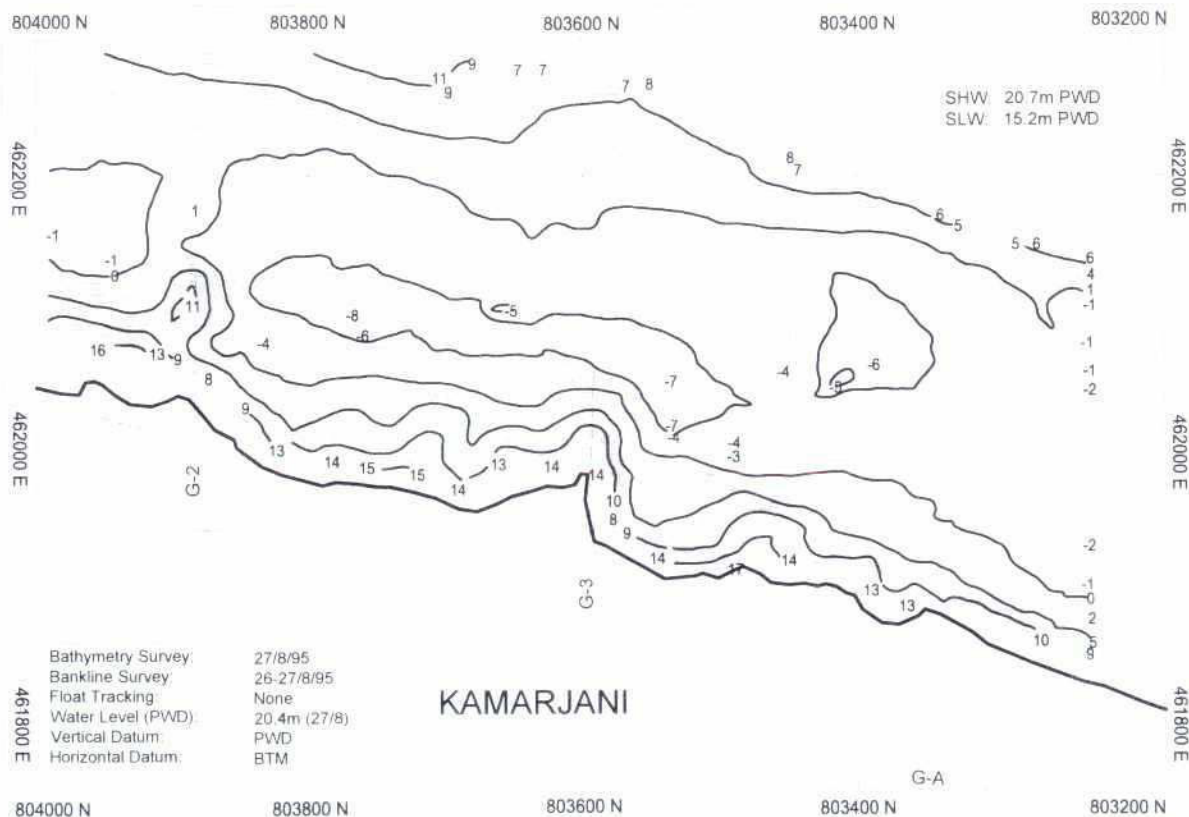


Fig. 5.3-14: Bathymetry at the test site area on August 27, 1995

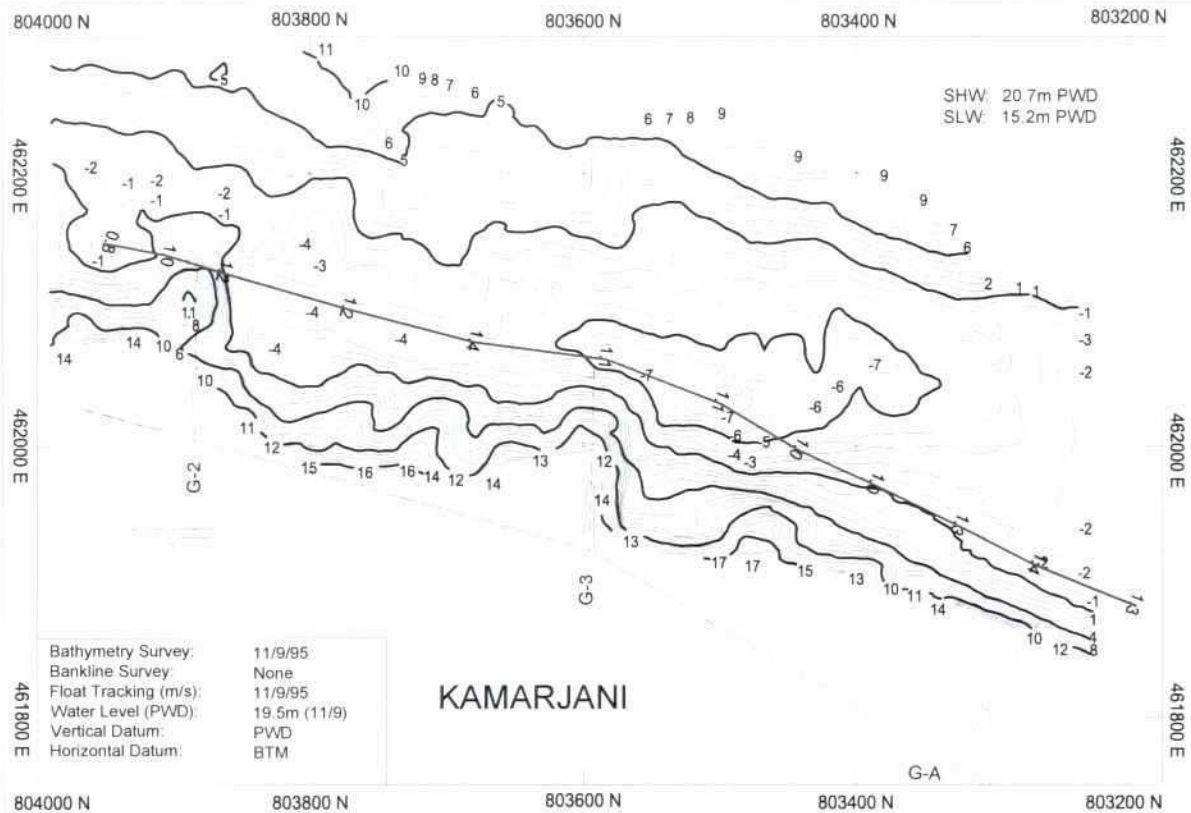


Fig. 5.3-15: Bathymetry and flow at the test site area on September 11, 1995

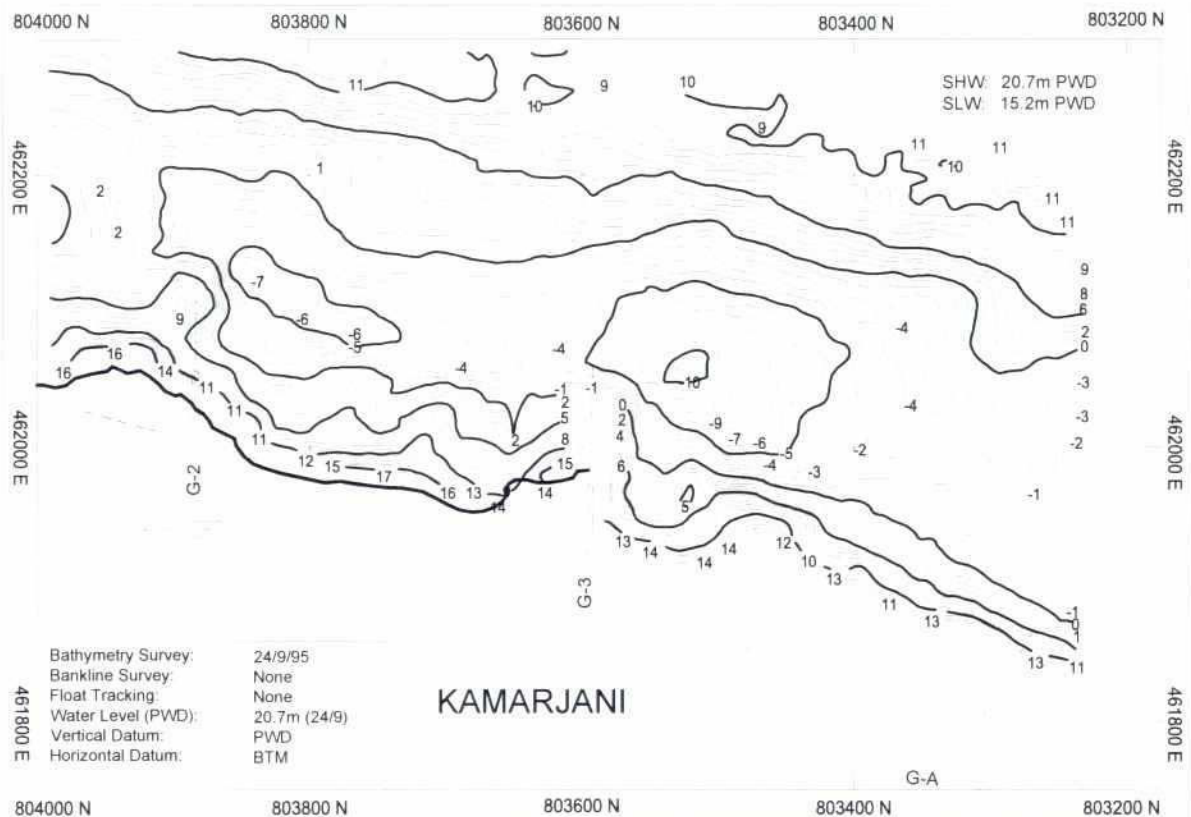
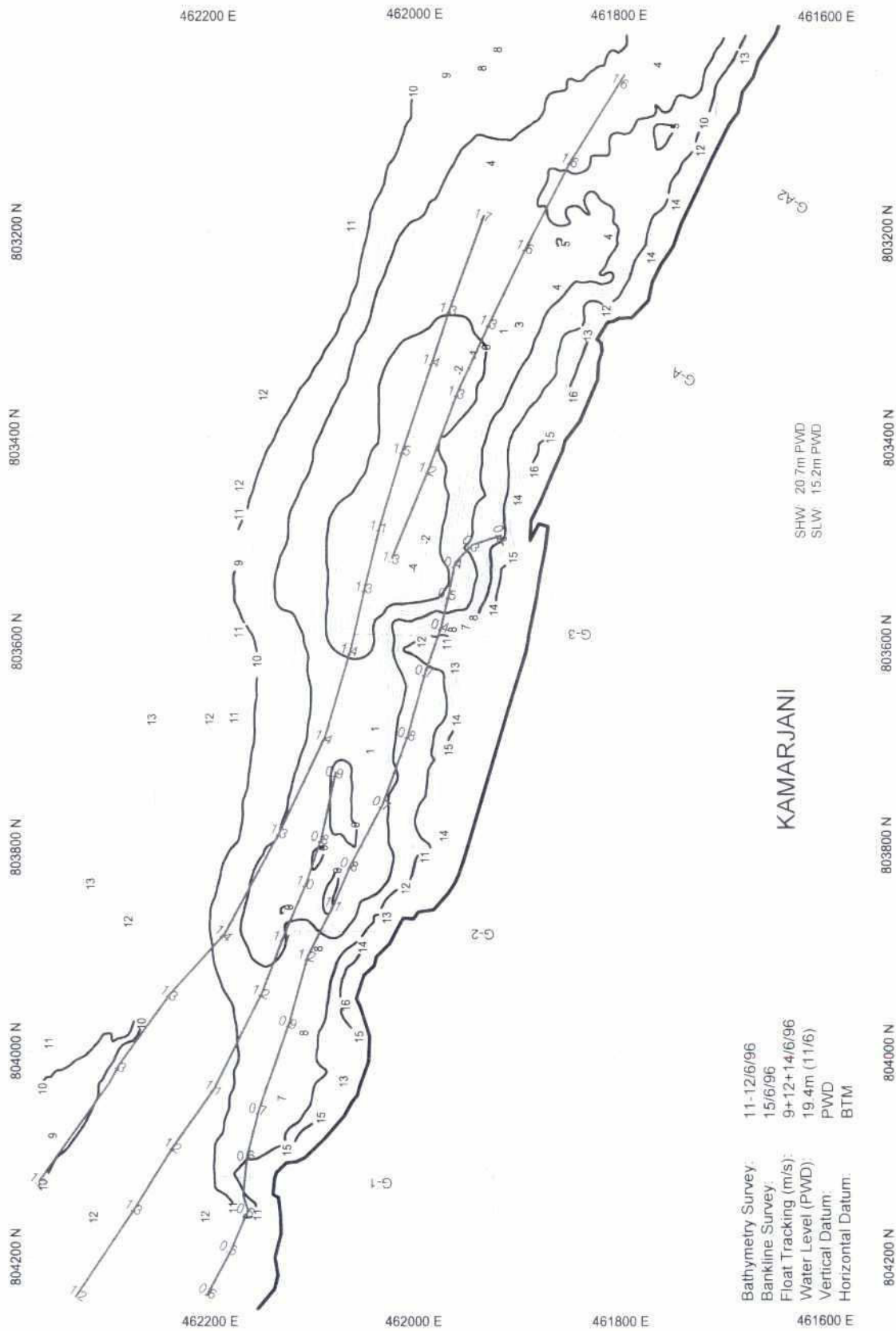


Fig. 5.3-16: Bathymetry at the test site area on September 24, 1995



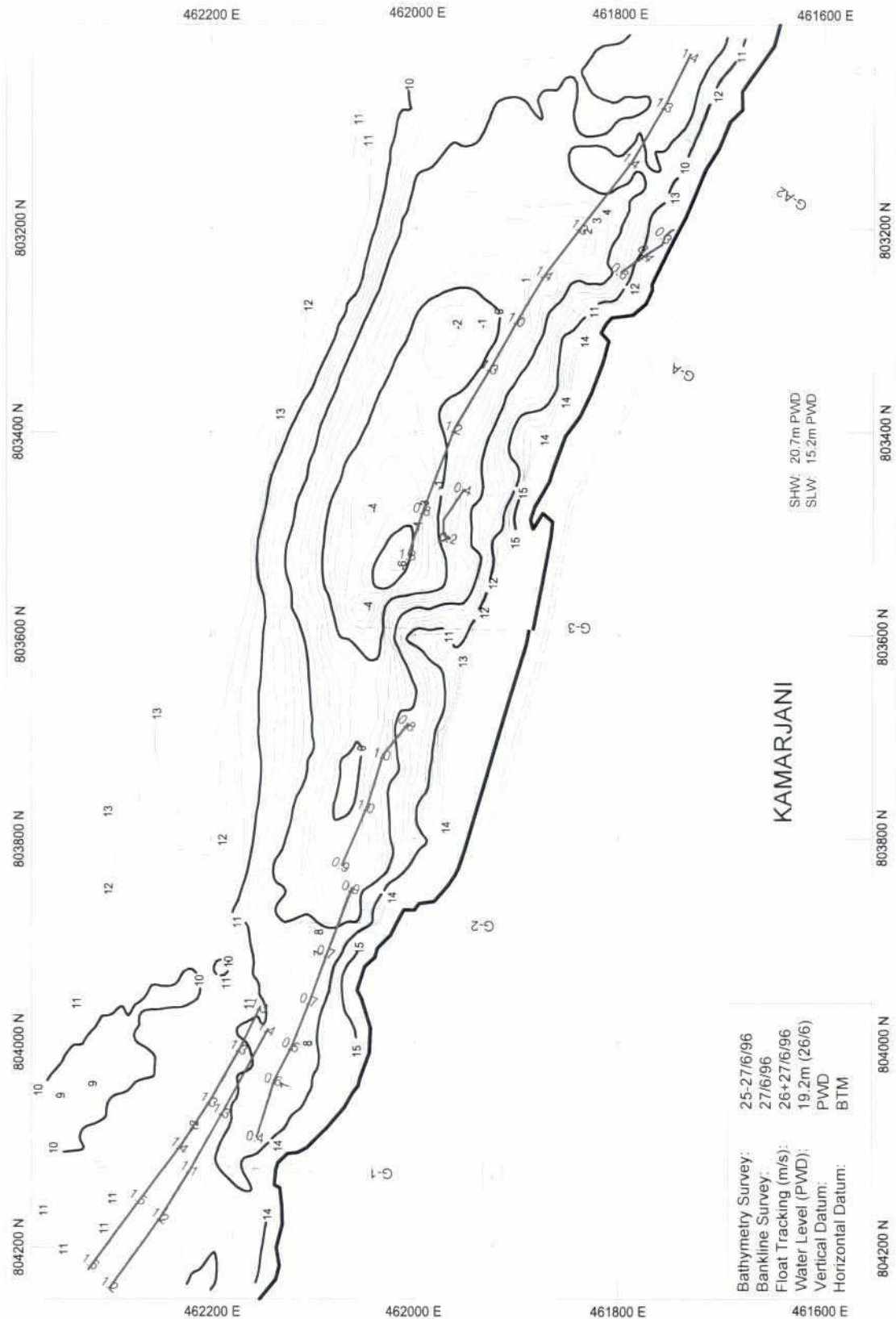


Fig.5.3-18: Bathymetry and flow at the test site area on June 25-27, 1996

29

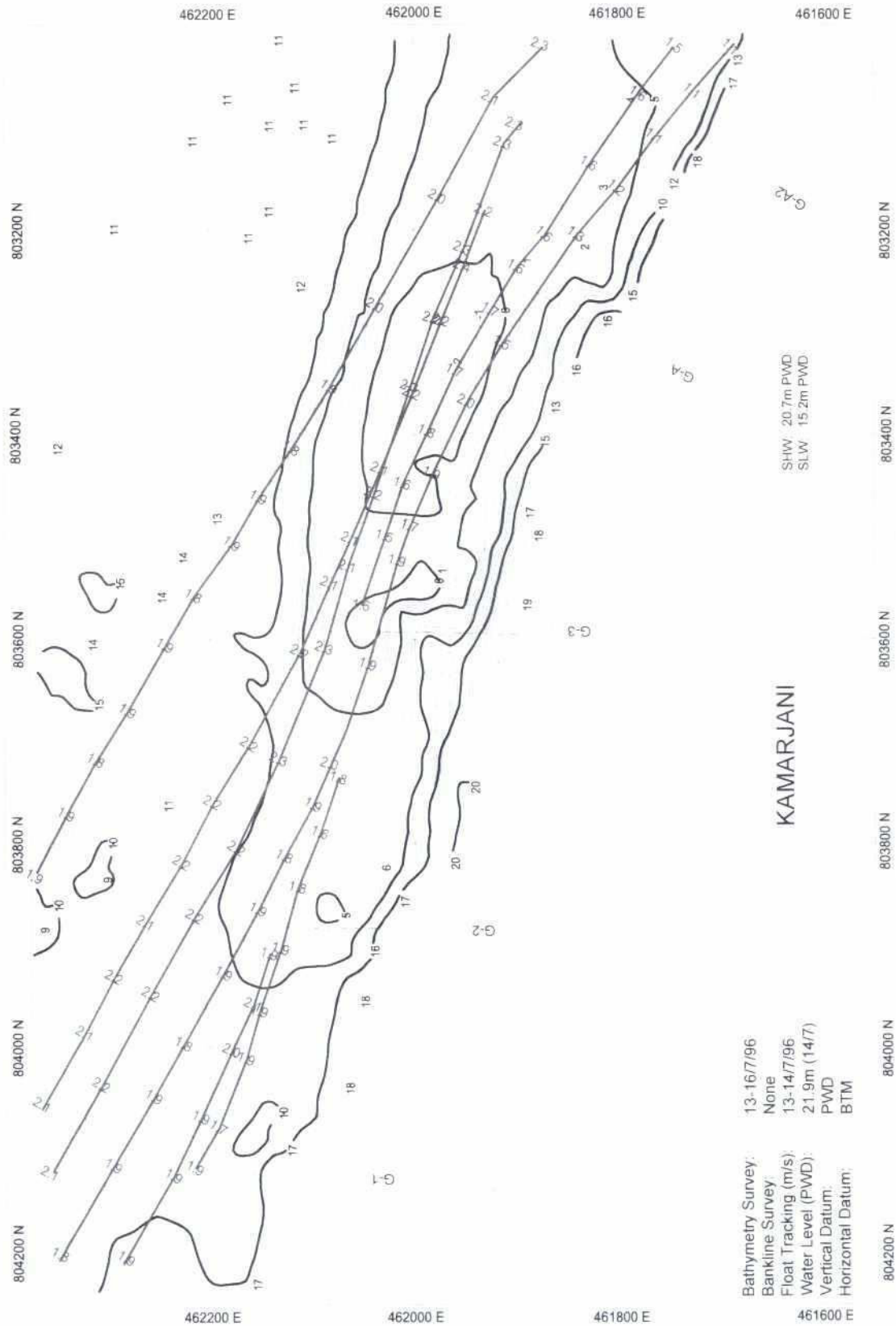


Fig.5.3-19: Bathymetry and flow at the test site area on July 13-16, 1996

5-19

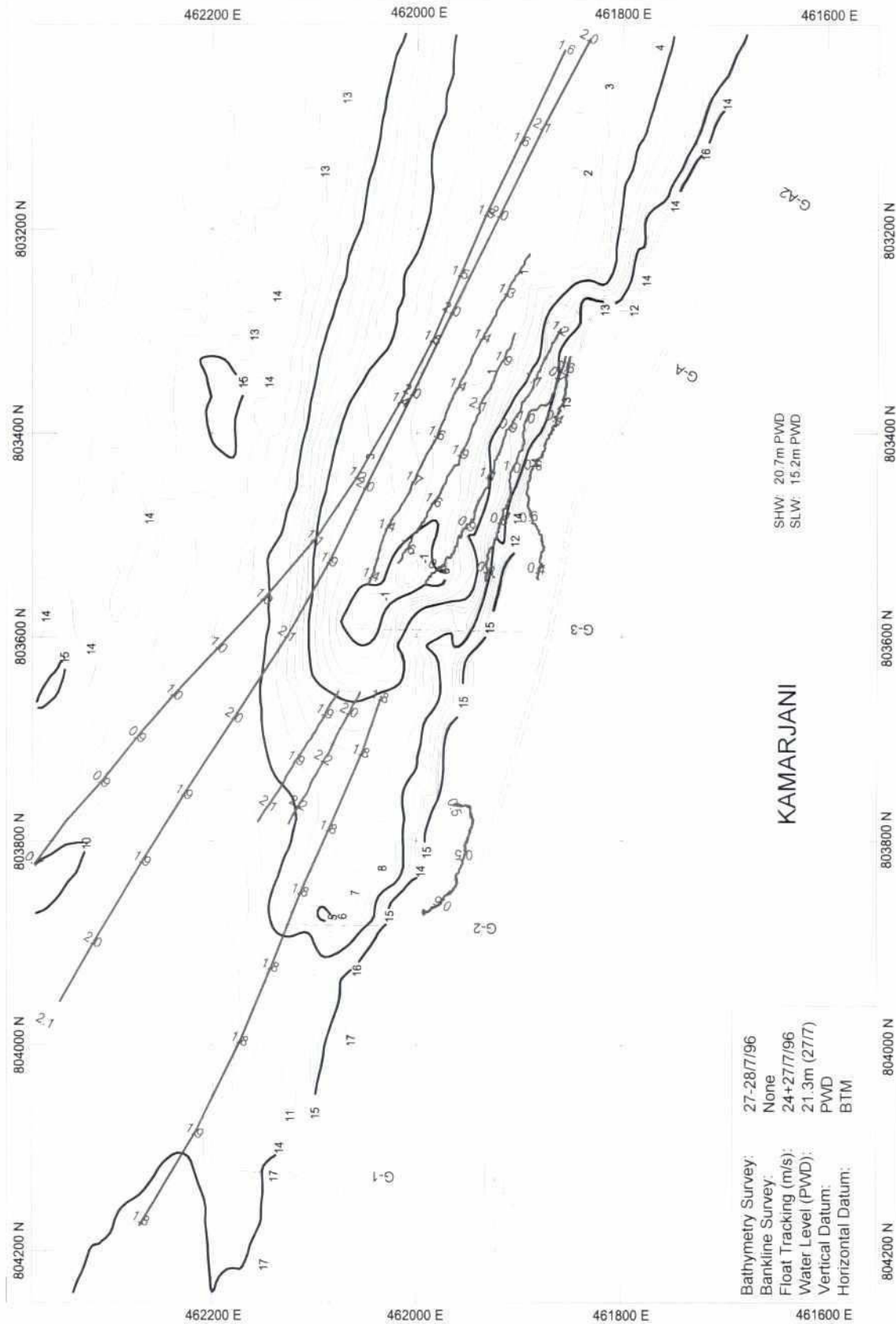




Fig.5.3-21: Bathymetry and flow at the test site area on August 17-19, 1996

5-21

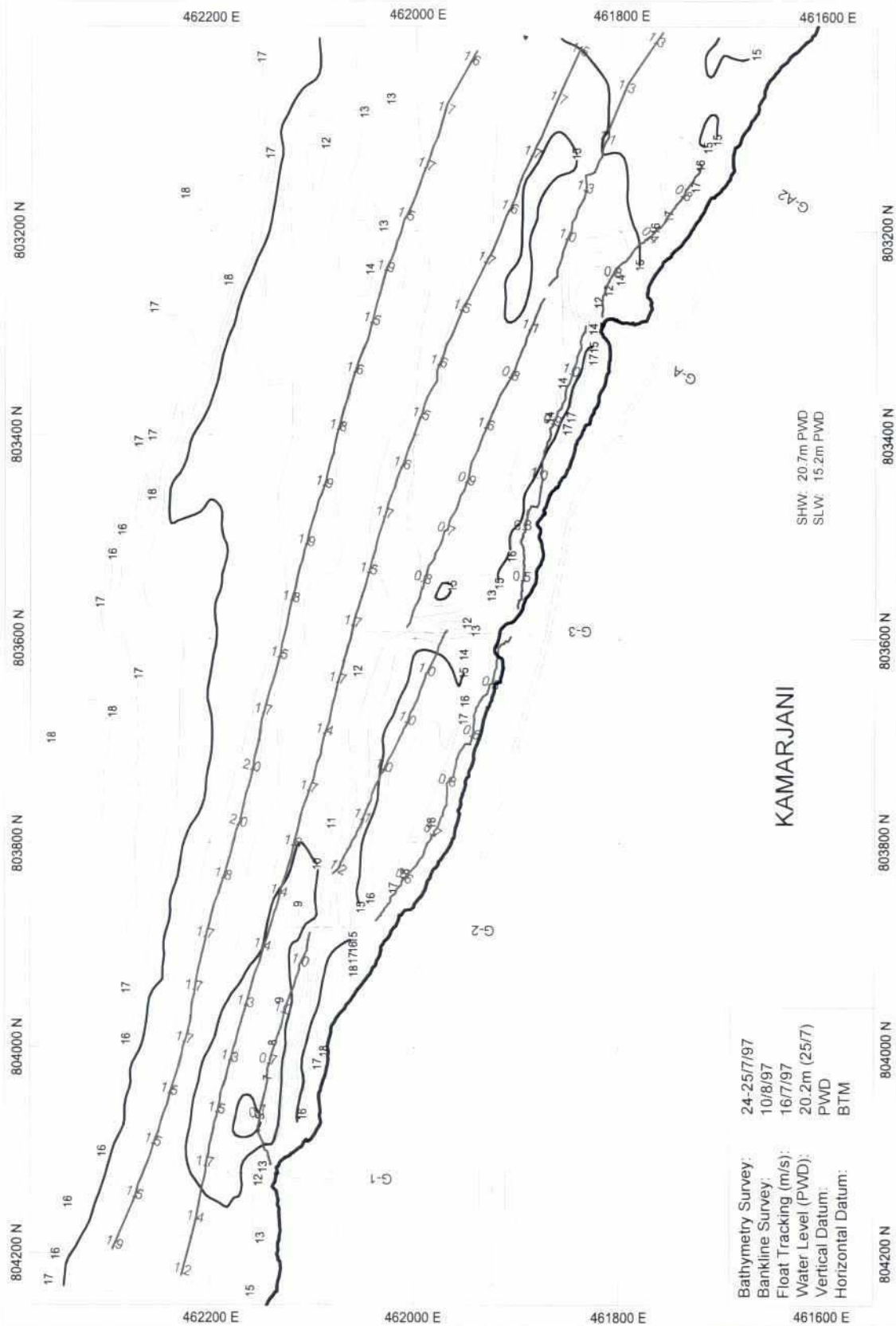


Fig.5.3-22: Bathymetry and flow at the test site area on July 24-25, 1997

5.3.3 Flow Pattern in the Groyne Field

The databases for this detailed investigation were the advanced float tracking and the current point measurements. These survey methods were not available in 1995 (see Section 3.3). In 1996 the flow velocities upstream from G-3 were lower than further downstream. For that reason the groyne fields between G-3 and G-A and between G-A and G-A/2 have been selected to describe their flow pattern as detailed below.

Figure 5.3-23 shows the surface flow pattern downstream from G-3 at the end of July 1996 at decreasing water level stage after a water level peak on July 19, 1996 had been recorded at 22.07 m+PWD. The flow information is overlaid on the actual riverbed morphology presented as iso-patches. Highest velocities are recorded between 2.0 and 2.6 m/s on the float track of July 23 (outer track). Velocities up to 2.1 m/s were recorded on July 27 (outer tracks). Only 20 m from these tracks the flow velocity decreased by 50 % to about 1 m/s. Along the bank velocities between 0.3 and 0.7 m/s were measured. Of special interest is the track along the bank, which accelerated twice. The accelerations occurred where the track converged with the upper track. After diverging from the upper track the velocity was reduced from 0.7 m/s to 0.4 m/s. In front of G-A it was accelerated again by 100 %. The current point measurements were carried out downstream from G-3 at multiples of 0.2, 0.6 and 0.8 of the water depth. The current vectors show a reduction of the velocities with increasing depth. The bottom flows changed their directions towards east i.e. away from the bank.

Another surface flow pattern of this groyne field is presented in Fig. 5.3-24. It has been surveyed on August 15, 1996. The flow tracks and the current point measurements were collected at the same day at rising water level stage three days before the water level reached its peak of 21.1 m+PWD. The velocities measured in the channel are lower in comparison to the survey of July. Maximum velocities of 1.7 m/s had occurred on the outer track. On the other hand a converging of flow lines was observed in front of G-A close to the bank where maximum velocities of 0.8 m/s occurred. The current point measurements showed again a diverging of the bottom flow to the east.

From all surface flow tracks carried out on August 15 iso-velocities were derived. The result is presented in Fig. 5.3-26. Such evaluations should be done only, if sufficient float tracks are covering the investigated area. If such dense flow information is available, this method provides a good impression of the flow pattern. Highest surface velocities occurred around the scour hole (see bathymetry in Fig. 5.3-24), whereas the mean velocity (v_m) along the water column at the scour hole is less than at the two further downstream locations. In general, the flow velocities decreased towards the bank but upstream from G-A higher velocities existed near the bank. For comparison the original flow track data is shown in Fig. 5.3-25.

The flow pattern in the groyne field between G-A and G-A/2 on August 18, 1996 is described in Fig. 5.3-27 and Fig. 5.3-28. Current points measurements were not carried out at that time. Therefore, a comparison of flow tracks taken at 1.5 m depth and at 3.0 m depth are presented here.

Interesting is the rotation of flow downstream from the groyne G-A. The flow direction near the bank was opposite to the general river flow direction (return flow) before it is turning in front of the head of the impermeable groyne to its regular direction. The circle described by the track at 3 m depth is smaller than at 1.5 m depth. The velocity is measured as 0.3 m/s in 3 m depth and 0.4 to 0.5 m/s in 1.5 m depth.

The return flow near the bank was visually observed by the monitoring team downstream from the impermeable parts of the main groynes in 1995 too.



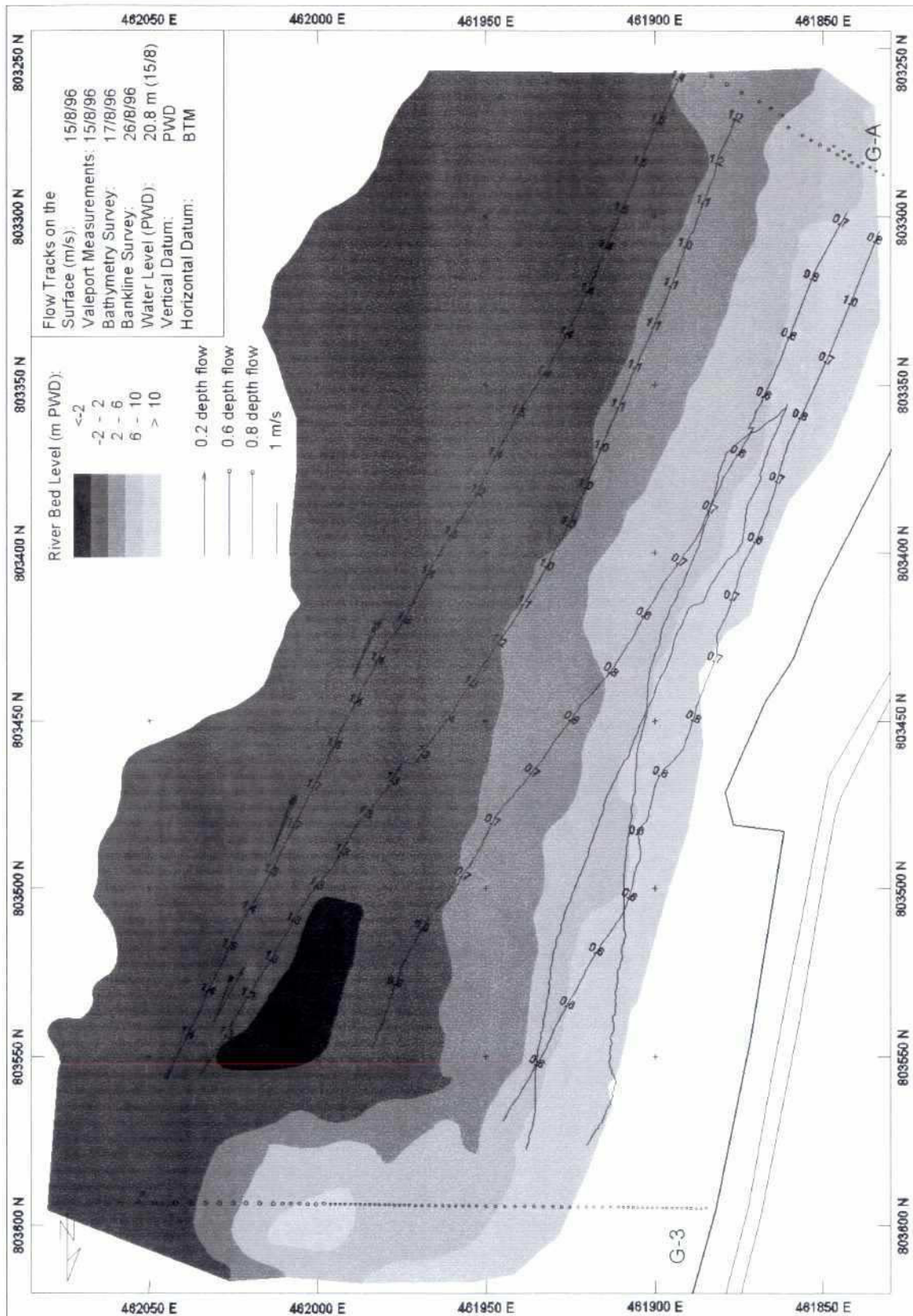


Fig.5.3-24: Flow pattern d/s from G-3 in July 1996

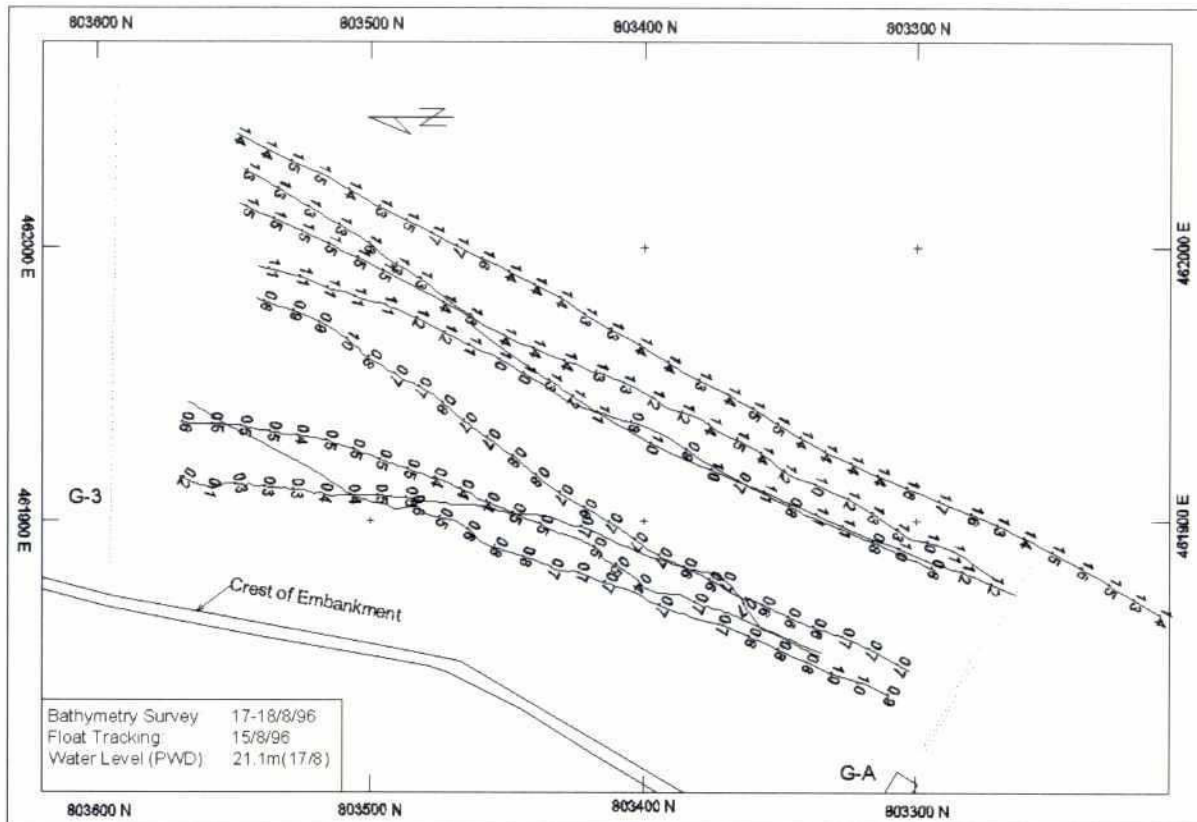


Fig. 5.3-25: Float tracking d/s of G-3 in August 1996

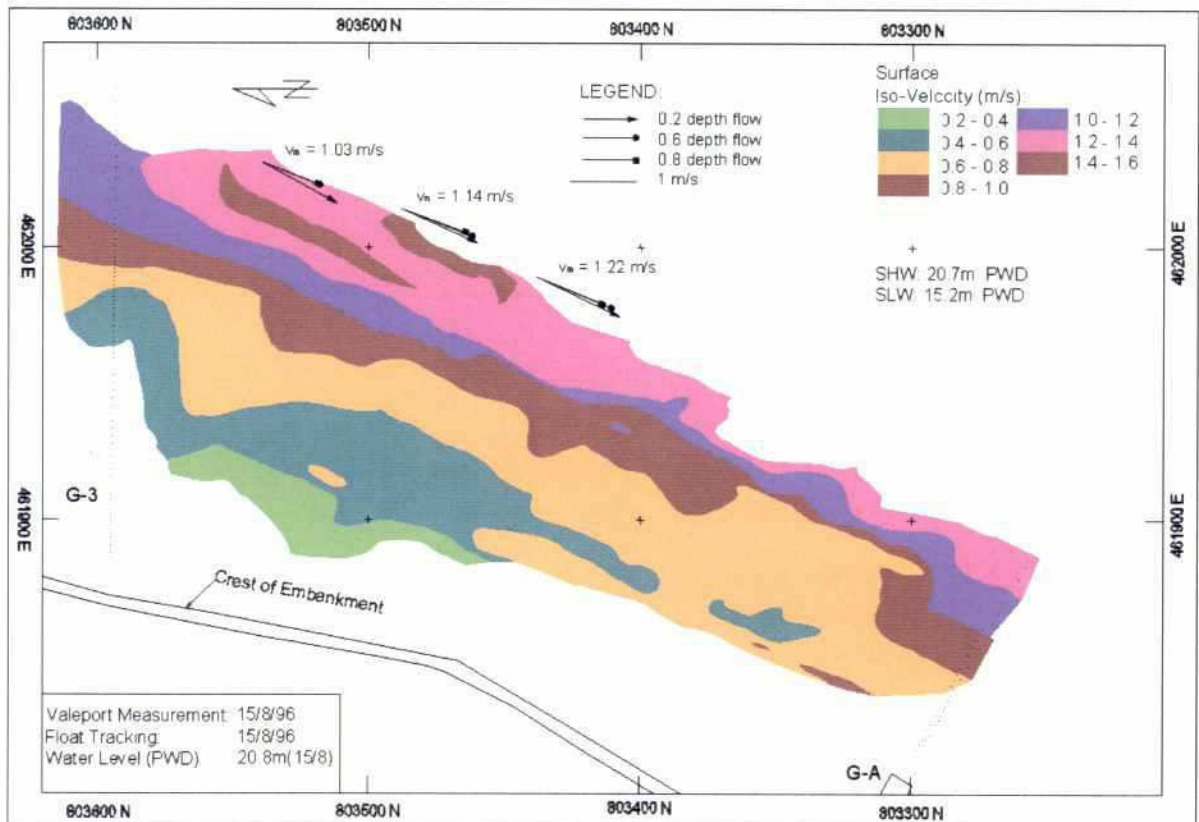


Fig. 5.3-26: Iso-velocities evaluated from float tracks in August 1996

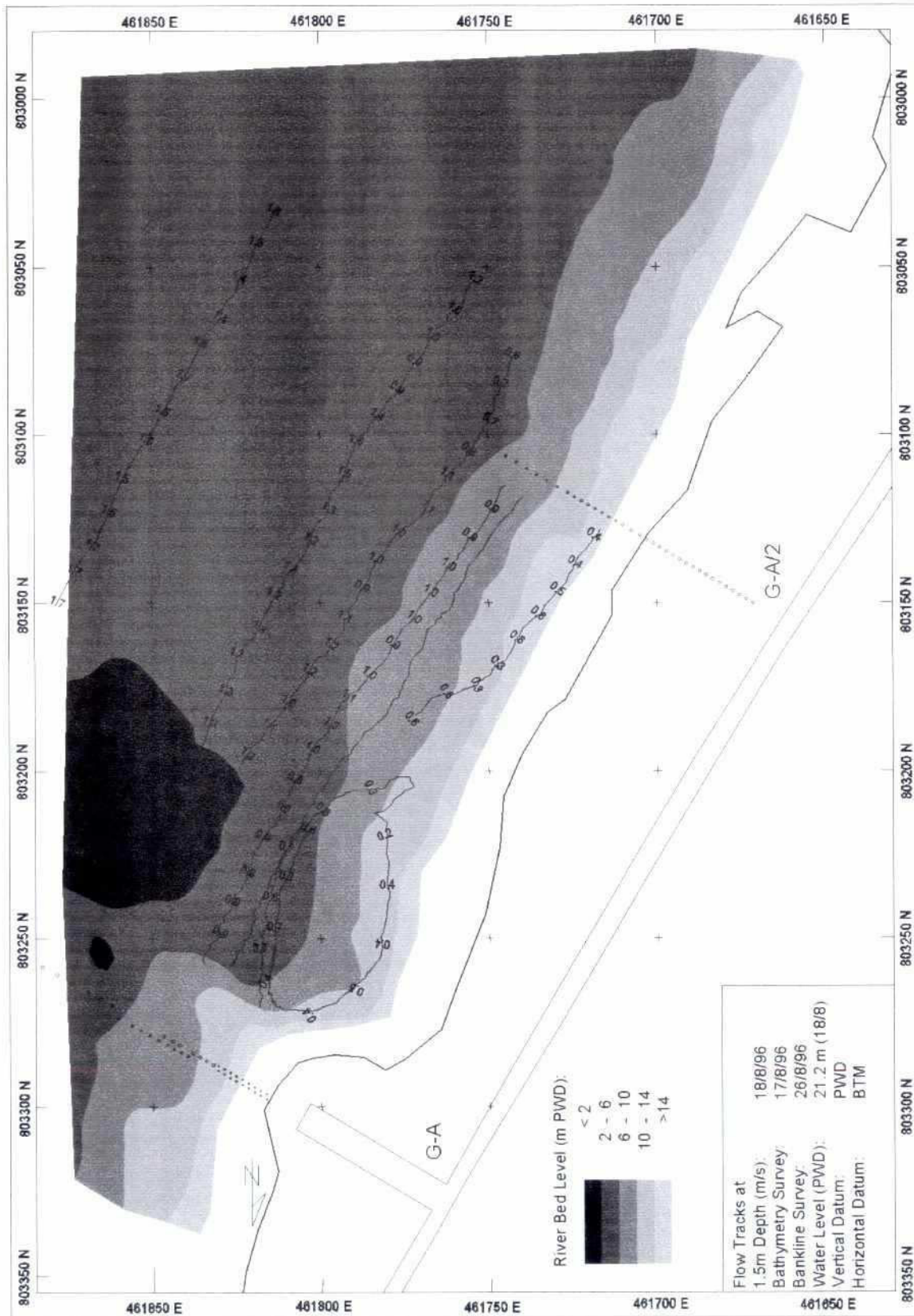


Fig. 5.3-27: Flow pattern d/s from G-A in August 1996

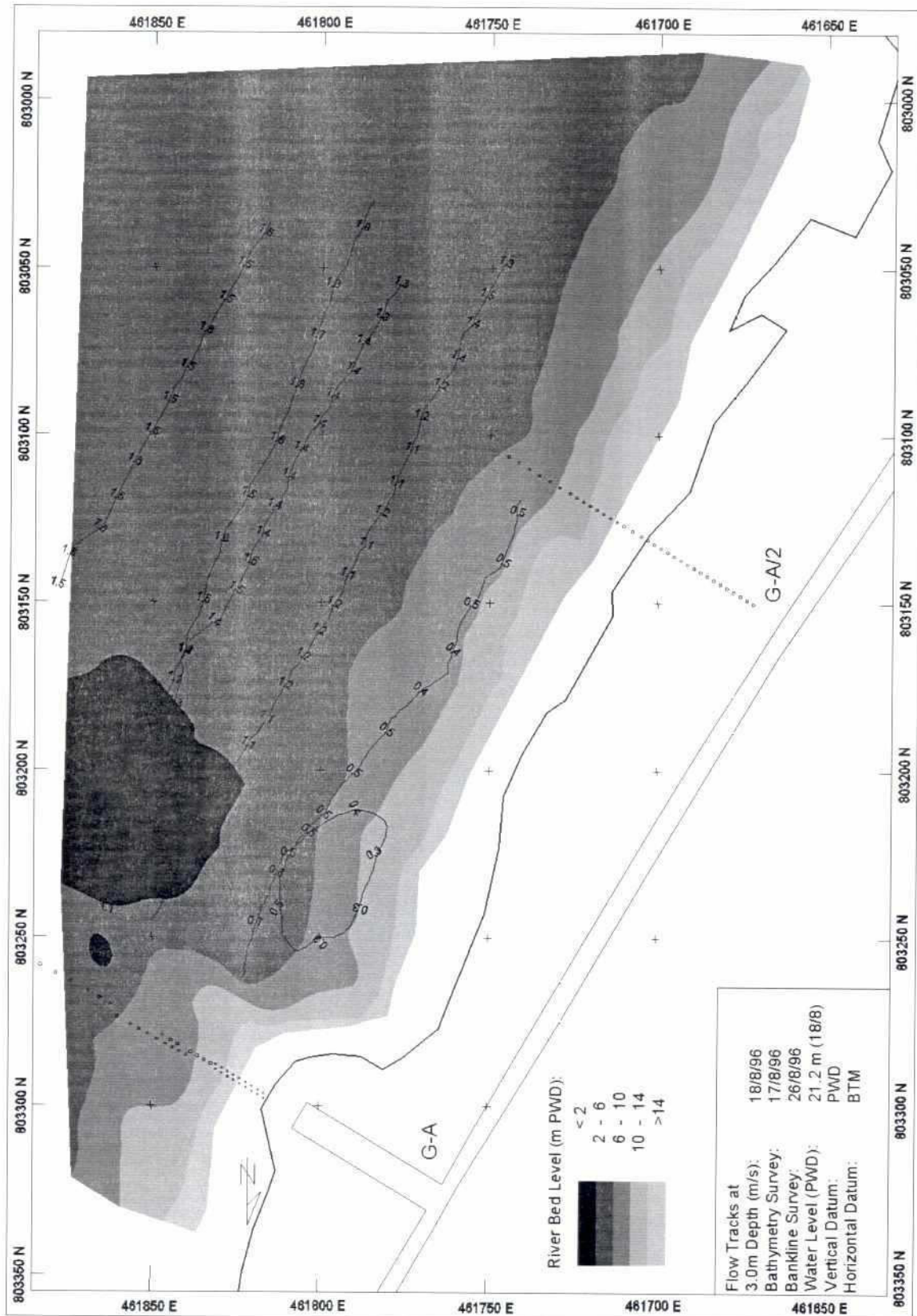


Fig. 5.3-28: Flow pattern d/s from G-A in August 1996

5.3.4 Groyne Surveys

The bathymetric development downstream from the groynes G-1, G-2, G-3, G-A and G-A/2 is described in the following charts (Fig. 5.3-29 to Fig. 5.3-60). The selected results derived from bathymetric surveys concentrate on that time period, when the river has mostly endangered the individual groynes. Five cross sections evaluated at 10 m downstream from each groyne axis are presented. The cross sections charts show how far the scouring has endangered the piles. Detailed bathymetric contour charts scaled 1:1250 follow the cross section charts. The scouring process and the slides downstream from the groynes can be recognised from these contour charts. Table 5.3-4 shows the investigated time period of the individual groynes, the chart observations and the corresponding figure numbers.

Time Period	Cross Sections G-1 Observations	Fig.- No	Time Period	Contour Charts G-1 Observations	Fig.- No
1995 18/05 to 11/07	The scouring did not endanger the pile row.	5.3-29	1995 08/06 to 11/07	Several slides towards the scour hole are indicated. Significant slide on Jun 8 at 70 m downstream from groyne axis. Further slides on Jun 20 at 10 m, 60 m and 90 m d/s as well as at 10 m u/s.	5.3-30 to 5.3-33
Time Period	Cross Sections G-2 Observations	Fig.- No	Time Period	Contour Charts G-2 Observations	Fig.- No
1995 10/06 to 11/07	On Jul 9 cross section carried out 2 hrs before collapsing started. It was below critical scour profile of first 6 piles. Until next day about 12 m eroded up to pile 24 caused by the opening. Piles 19 to 24 not collapsed even they had got exposed far below the critical scour profile. Following day on Jul 11 the wide opening silted up by 4 m.	5.3-34	1995 08/07 to 14/07	Immense scour area d/s on Jul 8-9. Scour hole on Jul 9: -11 m+PWD. Embankment erosion shown on Jul 8 at 80 m d/s; erosion had deteriorated the next days. Breach on Jul 11, although the scour hole silted up. After collapsing no significant changes around the groyne.	5.3-35 to 5.3-40
Time Period	Cross Sections G-3 Observations	Fig.- No	Time Period	Contour Charts G-3 Observations	Fig.- No
1995 24/06 to 19/08	First piles of G-3 endangered. Between Jul 11 and Sep 9 last pile close to critical profile. Only 30 % of the pile length had been buried during 3 months but the pile did not collapse.	5.3-41	10/08 to 24/08	Large deep scour hole area d/s from head of groyne on Aug 10, 14 and 16 (3000 m ² below -8 m+PWD). Slide 50 m d/s on Aug 10 towards scour hole. Several slides shown on Aug 16. Major slide between Aug 16 and Aug 20 (partly collapse of impermeable head on Aug 19). Scour hole filled up by slides from bank. Steep slopes generated parallel d/s from groyne and at the bank. Area remained critical as shown on Sep 24 (scour hole below -11 m+PWD).	5.3-42 to 5.3-47

Table 5.3-4: Observations of groyne surveys

Time Period	Cross Sections G-A (before adaptation) Observations	Fig.- No	Time Period	Contour Charts G-A Observations	Fig.- No
1995 24/09 to 1996 24/03	Continuous erosion from Sep 95 to Mar 96. Loss of piles: No 19 on Mar 25; No 14 on Mar 31; No 18, 20 and 21 on Apr 1 to 10. Piles No 22 to 24 have been re-driven and extended on Feb 10.	5.3-48	1996 15/01 to 08/03	No significant scour hole developed. Area in front of groyne 0 m+PWD.	5.3-49 to 5.3-50
Time Period	Cross Sections G-A (after adaptation) Observations	Fig.- No	Time Period	Contour Charts G-A Observations	Fig.- No
1996 11/04 to 23/09	Slight siltation from Apr 11. After adaptation piles not endangered during monsoon 1996.	5.3-51	1996 19/04 to 23/09	Small scour hole about 50 m d/s since Apr 19. Significant slides 10 m d/s from groyne axis on all 4 figures. The direction of the slides is always in line with the d/s head from the impermeable groyne. Enlargement of scour area began 30 m d/s from groyne.	5.3-52 to 5.3-55
Time Period	Cross Sections G-A/2 Observations	Fig.- No	Time Period	Contour Charts G-A/2 Observations	Fig.- No
1996 23/02 to 06/04	Slight erosion from Feb 23 to Mar 26; riverbed eroded not below 4. m+PWD; then slight siltation until Apr 6.	5.3-56	1996 23/02 to 26/03	Slight erosion from Feb 23 to Mar 6. From Mar 13 mid of channel passing outer piles parallel to alignment of embankment, but no scour holes developed.	5.3-57 to 5.3-60

Table 5.3-4 (continued): Observations of groyne surveys

5.3.5 Cross Sections at Eroded Embankments

Cross sections have been evaluated perpendicular to the alignment of the embankment at the center points of damages in 1995. The zero stations of the cross sections intersect with the crest of the embankment defined at 70 m downstream from G-1 (Fig. 5.3-61), 80 m downstream from G-2 (Fig. 5.3-62) and 30 m downstream from G-3 (Fig. 5.3-63). The calculated rates of bank erosion are listed in Table 5.3-5.

Groyne	From	To	No. of days	Total erosion (m)	Erosion per day (m)
G-1	May 18	Jun 08	21	10.4	0.5
G-1	Jun 08	Jun 29	21	9.6	0.5
G-1	Jun 29	Jul 11	12	9.6	0.8
G-2	May 18	Jun 10	23	44.0	1.9
G-2	Jun 10	Jun 26	16	20.8	1.3
G-2	Jun 26	Jul 07	11	20.8	1.9
G-3	May 18	Jun 29	42	16.0	0.4
G-3	Jun 29	Aug 05	37	20.0	0.5
G-3	Aug 05	Aug 23	18	34.4	1.9

Table 5.3-5 Bank erosion rates d/s from G-1, G-2 and G-3

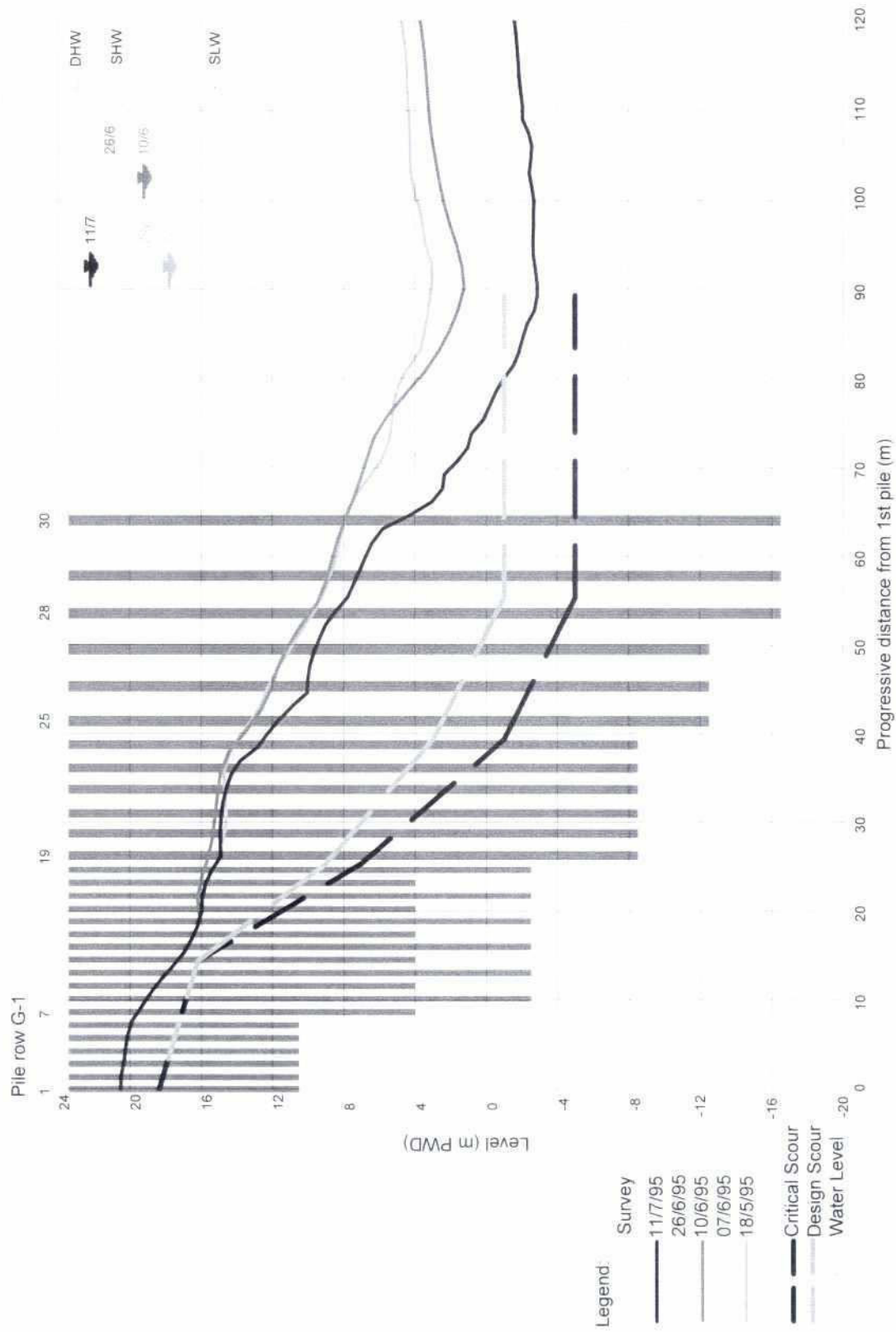


Fig. 5.3-29: Cross-section at 10 m d/s from groyne G-1

32

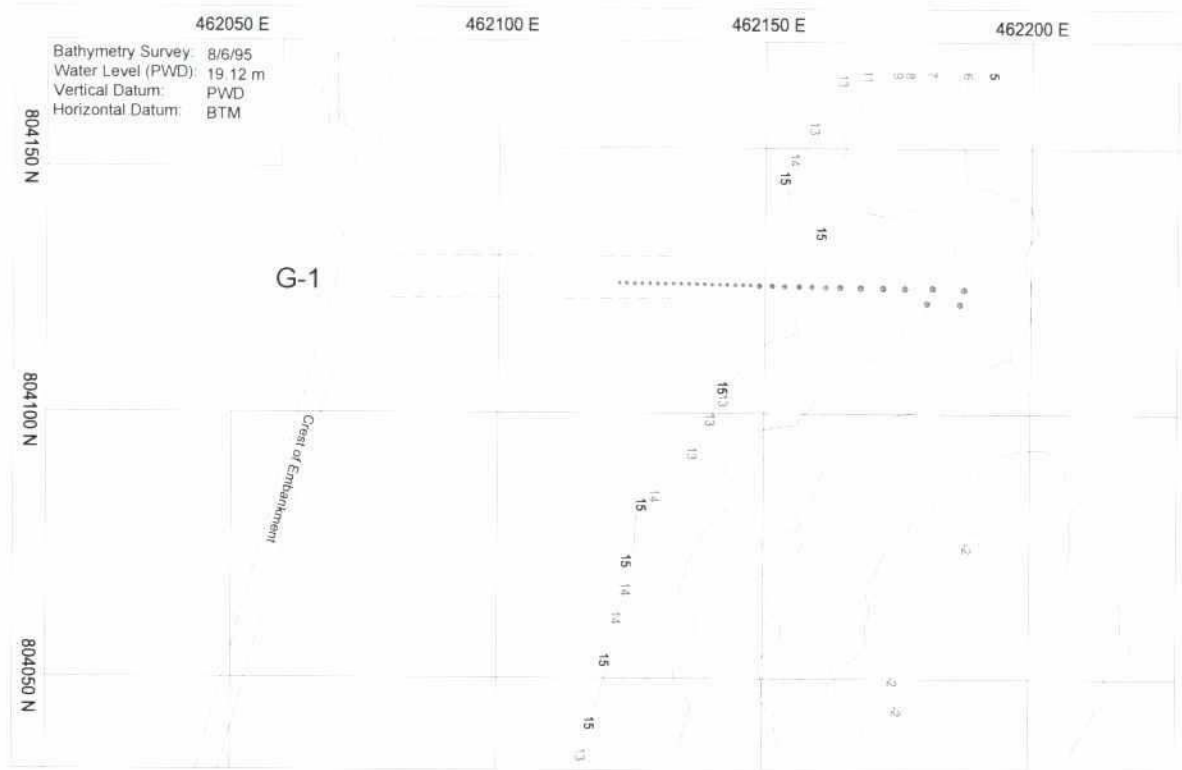


Fig. 5.3-30: Bathymetry at groyne G-1 on June 08, 1995

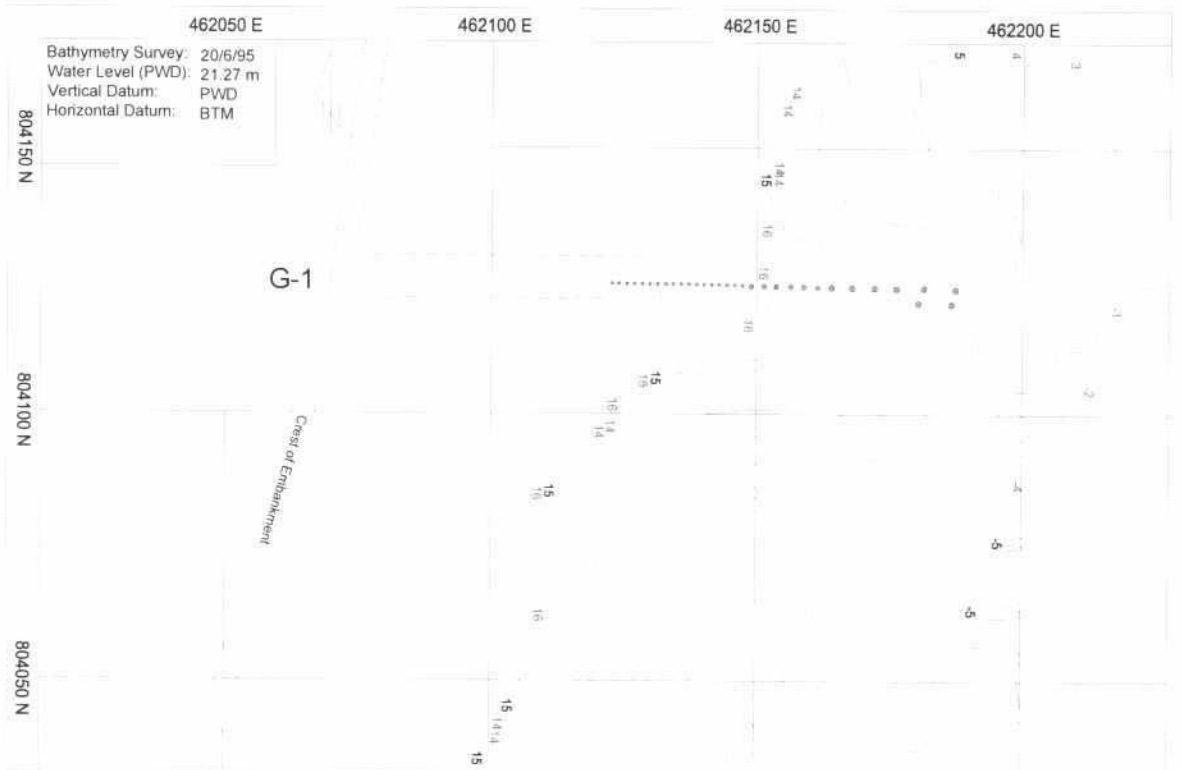


Fig. 5.3-31: Bathymetry at groyne G-1 on June 20, 1995

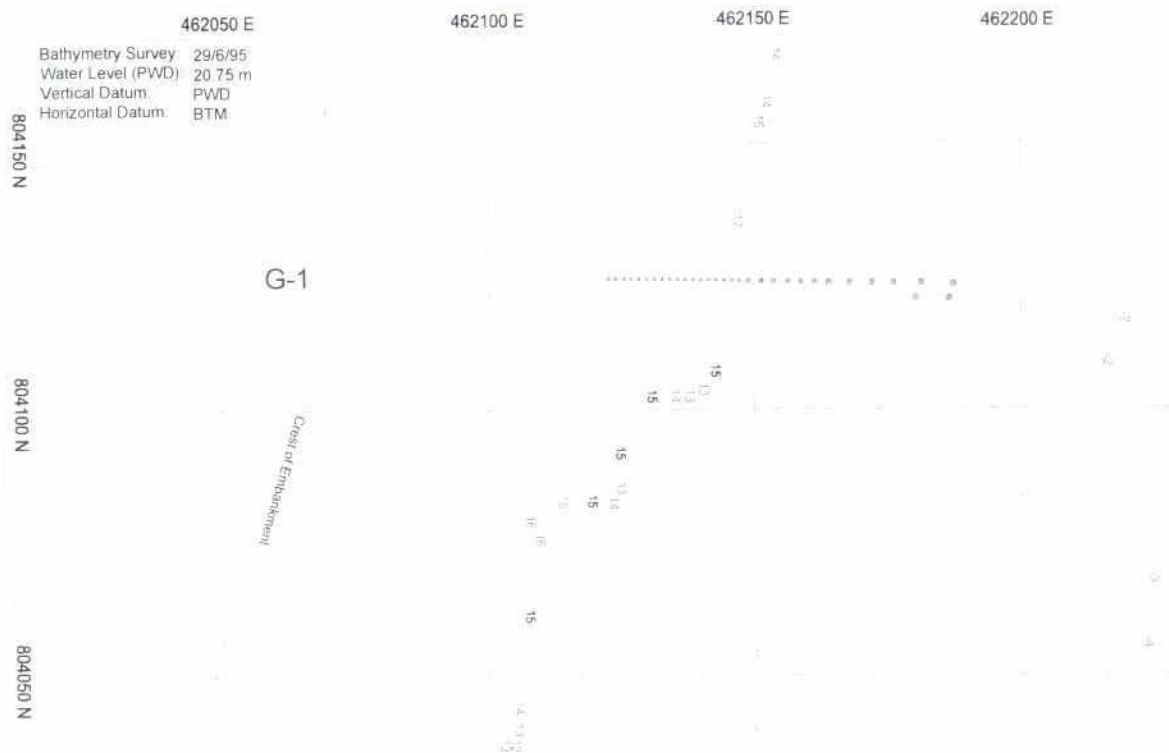


Fig. 5.3-32: Bathymetry at groyne G-1 on June 29, 1995

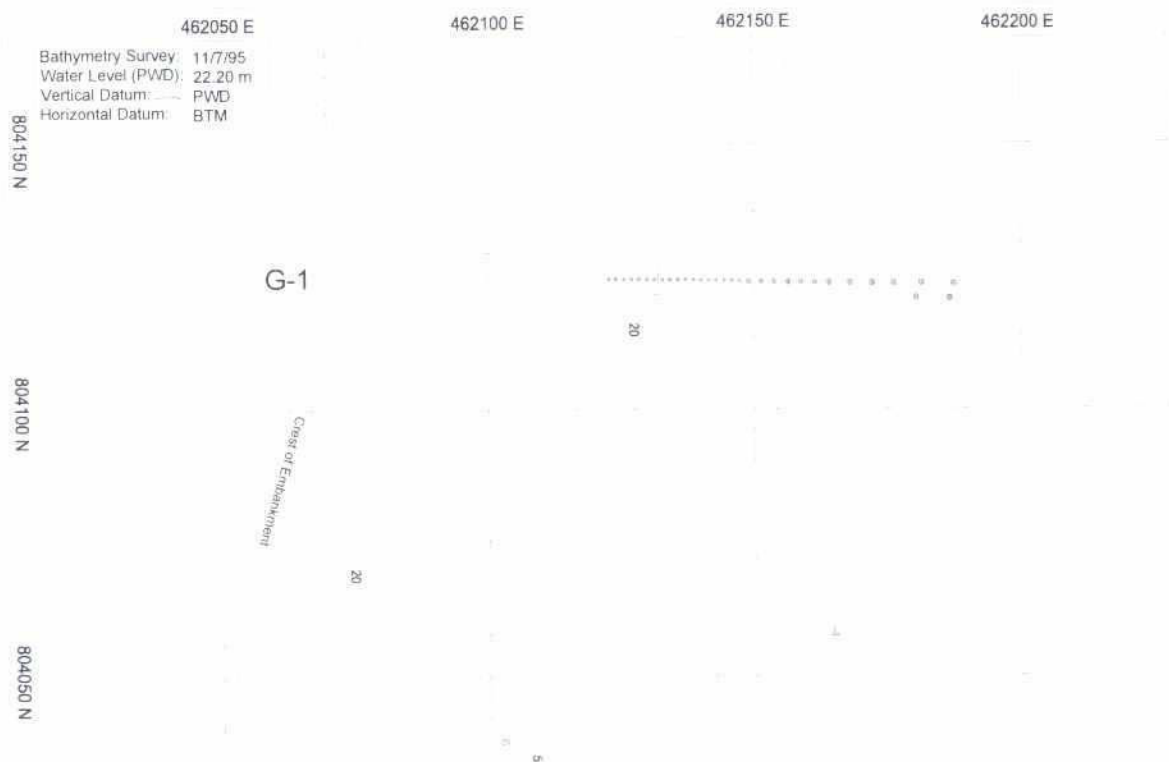


Fig. 5.3-33: Bathymetry at groyne G-1 on July 11, 1995

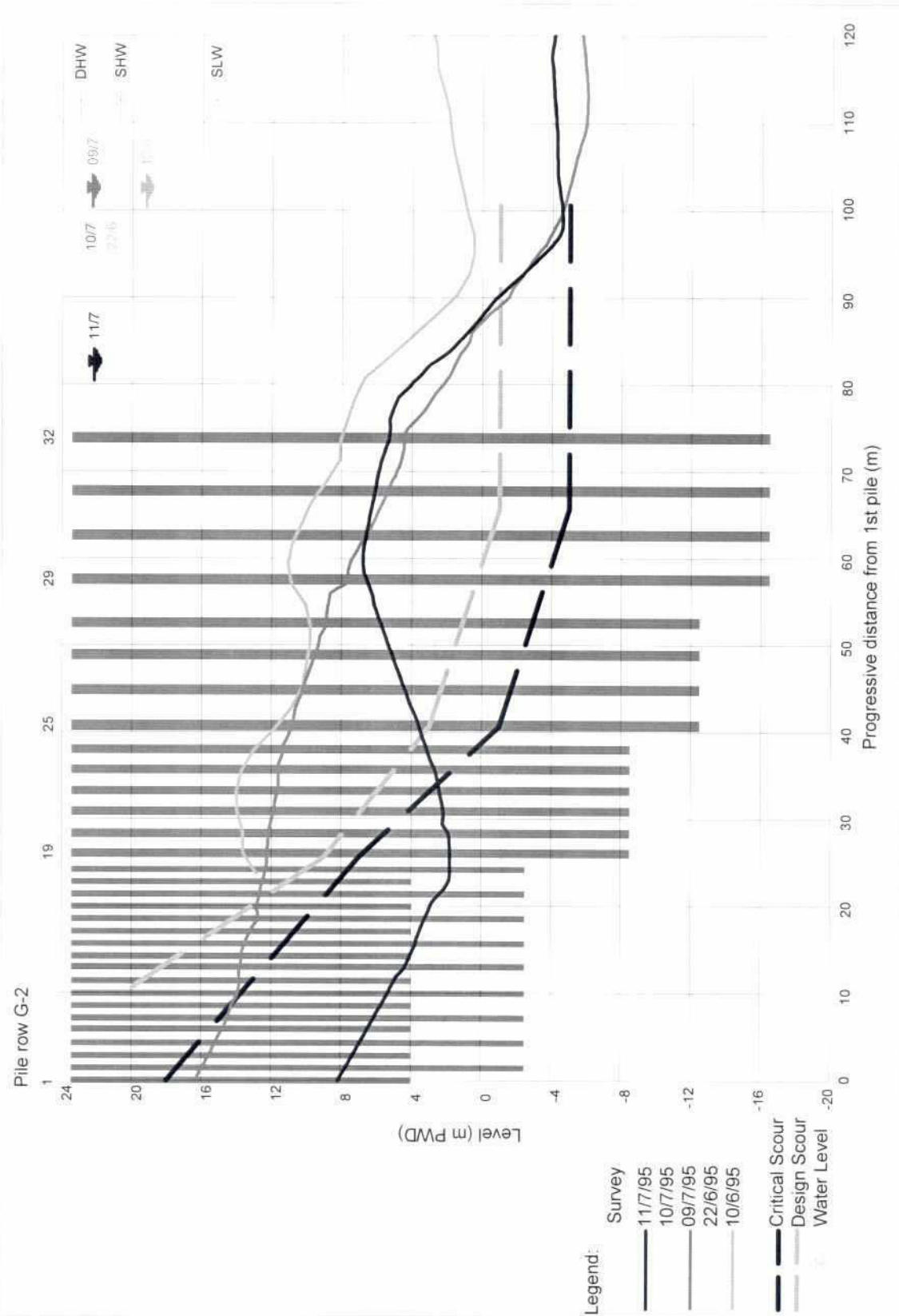


Fig. 5.3-34: Cross-section at 10 m d/s from groyne G-2

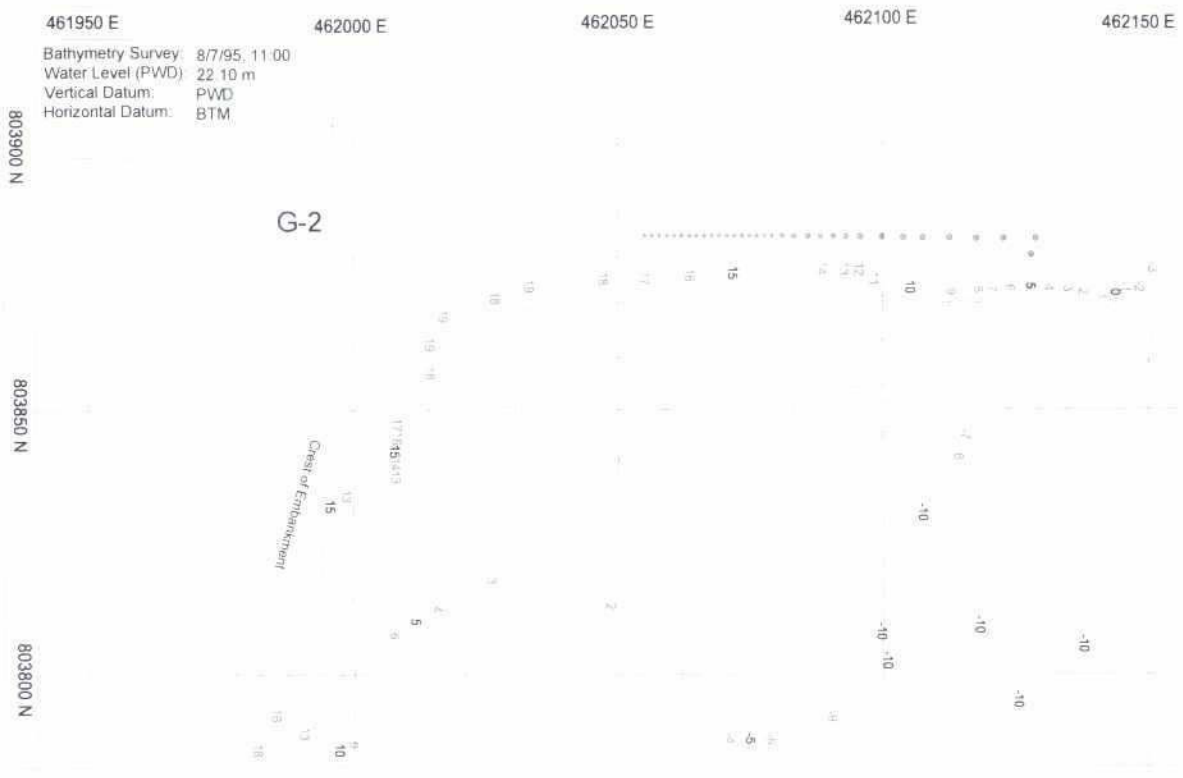


Fig. 5.3-35: Bathymetry at groyne G-2 on July 08, 1995

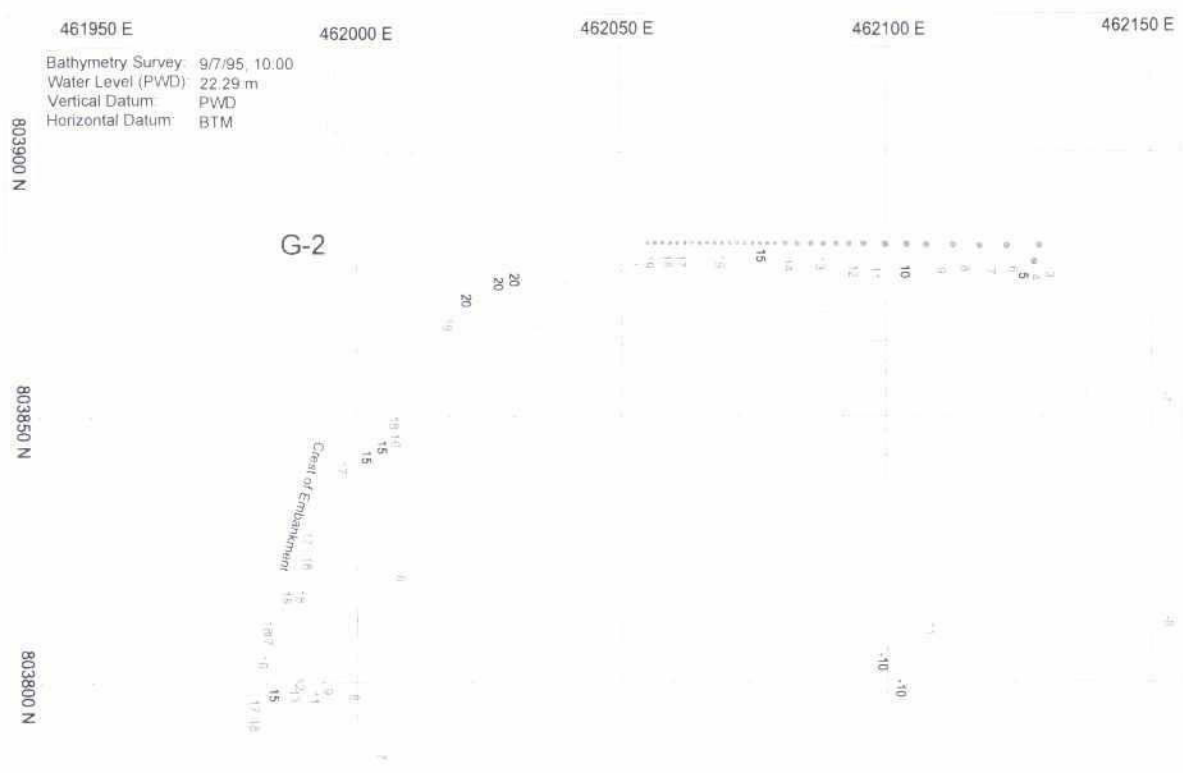


Fig. 5.3-36: Bathymetry at groyne G-2 on July 09, 1995

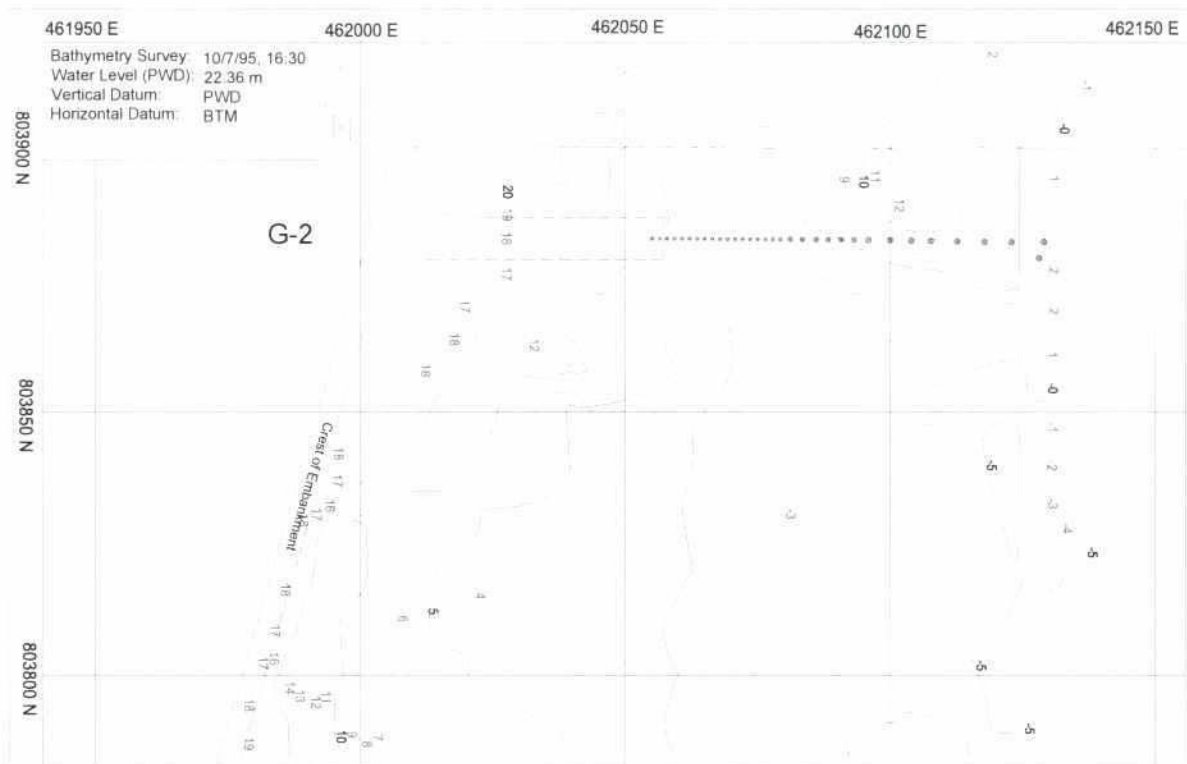


Fig. 5.3-37: Bathymetry at groyne G-2 on July 10, 1995

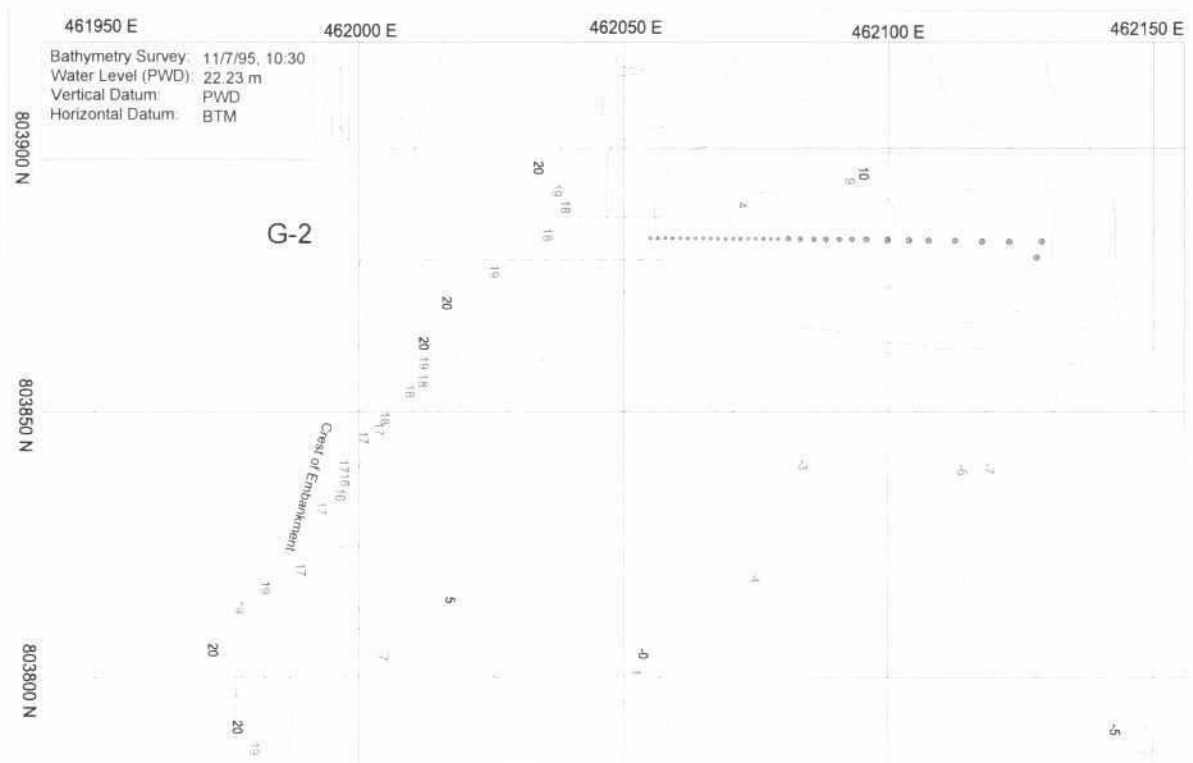


Fig. 5.3-38: Bathymetry at groyne G-2 on July 11, 1995

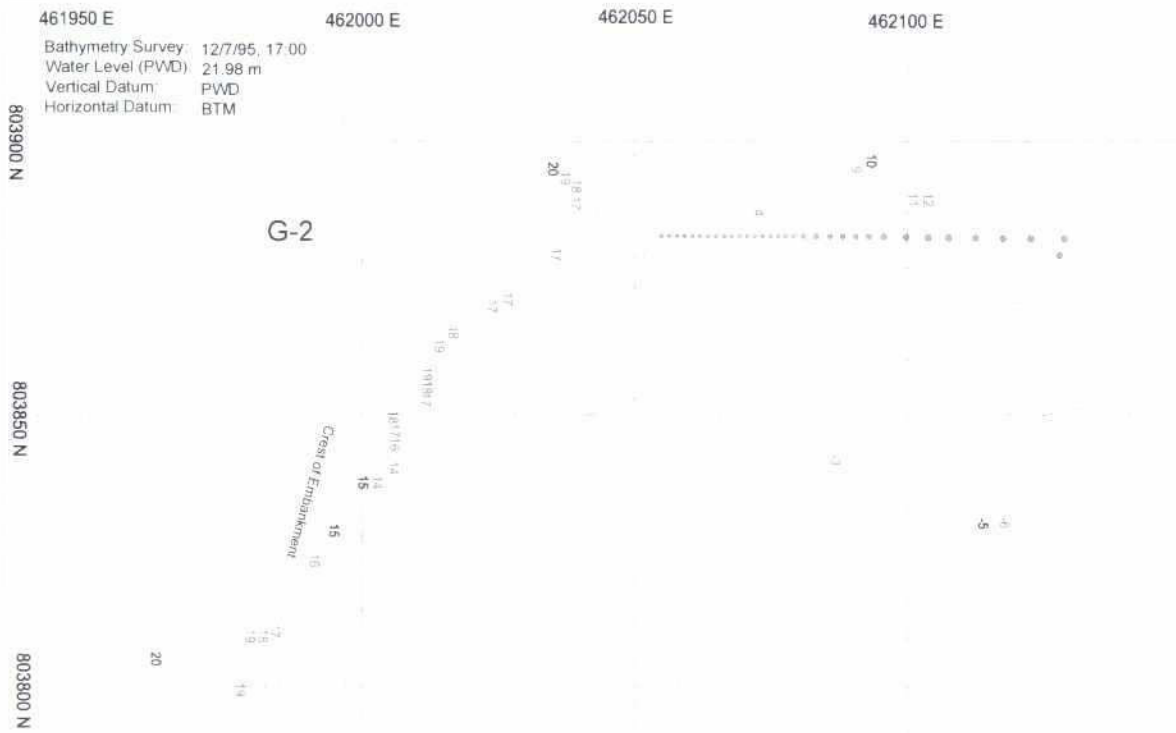


Fig. 5.3-39: Bathymetry at groyne G-2 on July 12, 1995

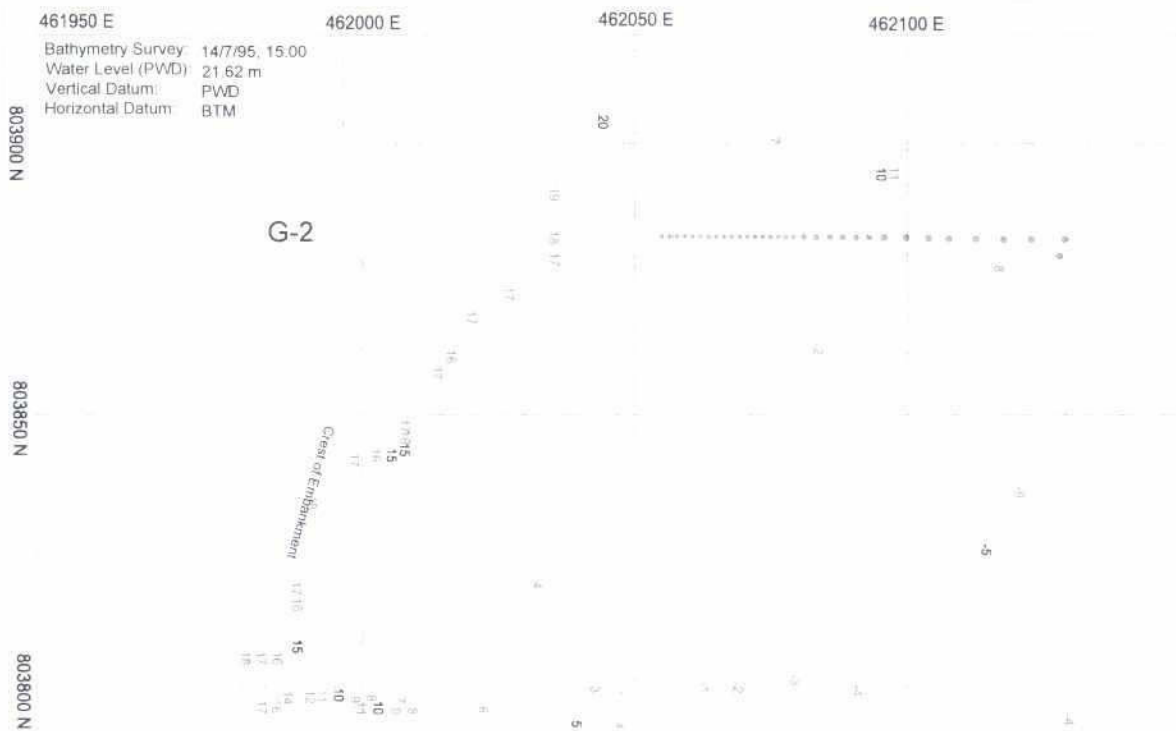


Fig. 5.3-40: Bathymetry at groyne G-2 on July 14, 1995

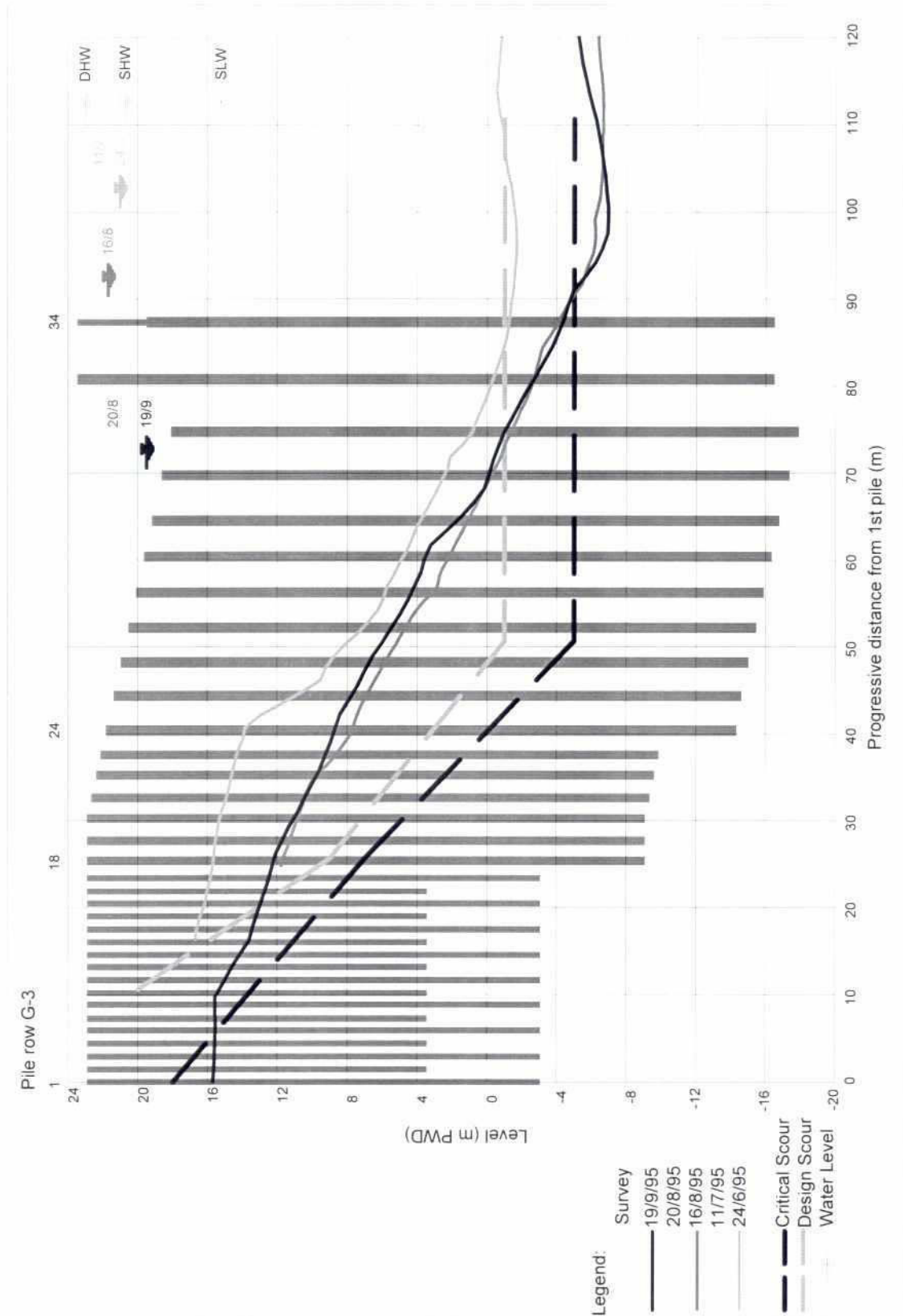


Fig. 5.3-41: Cross-section at 10 m d/s from groyne G-3

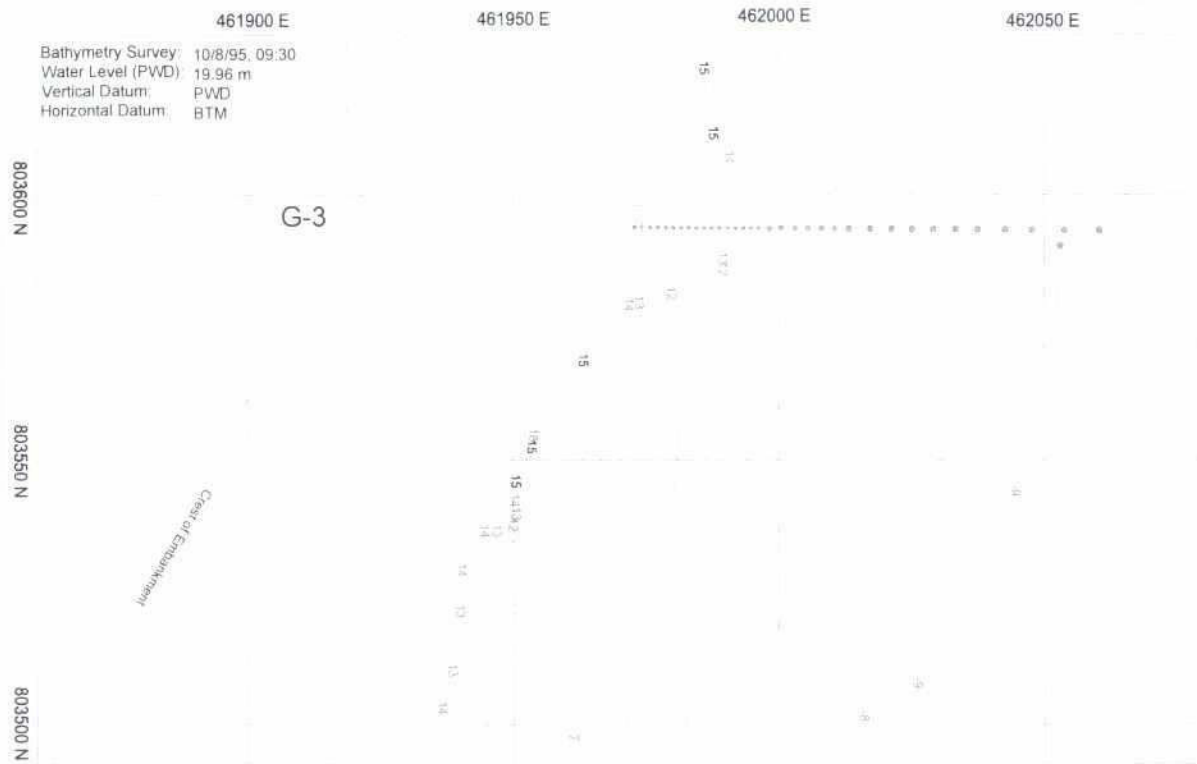


Fig. 5.3-42: Bathymetry at groyne G-3 on August 10, 1995

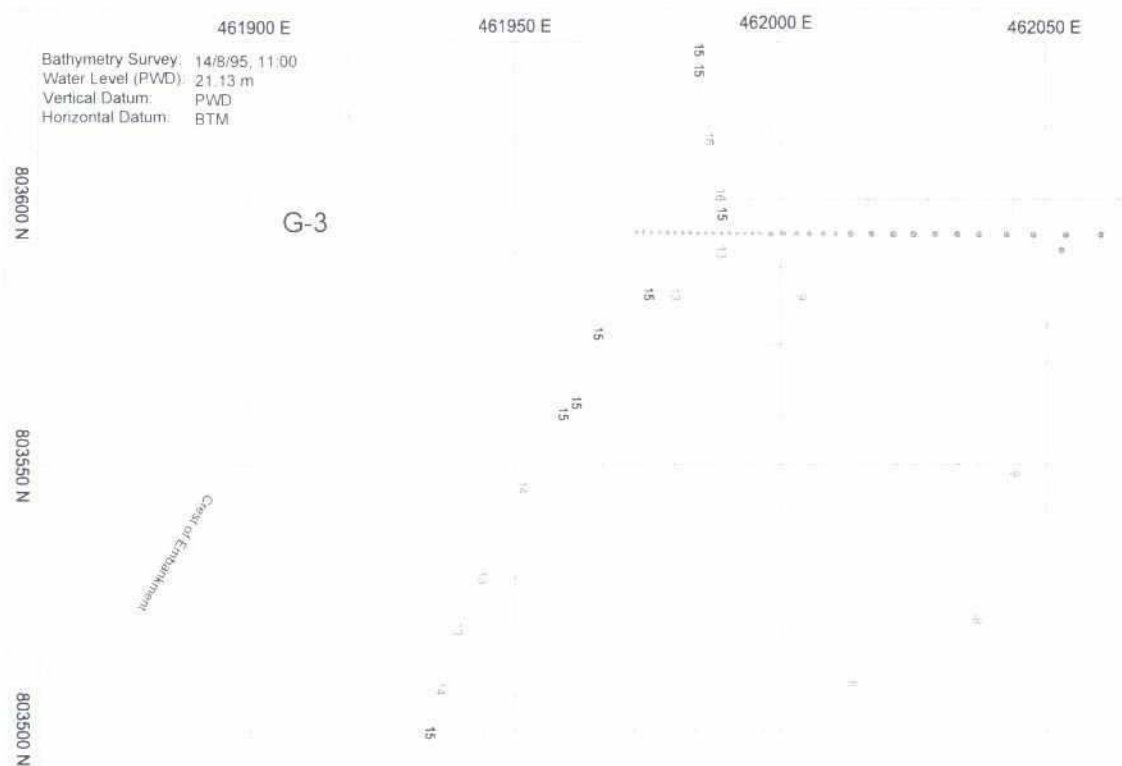


Fig. 5.3-43: Bathymetry at groyne G-3 on August 14, 1995

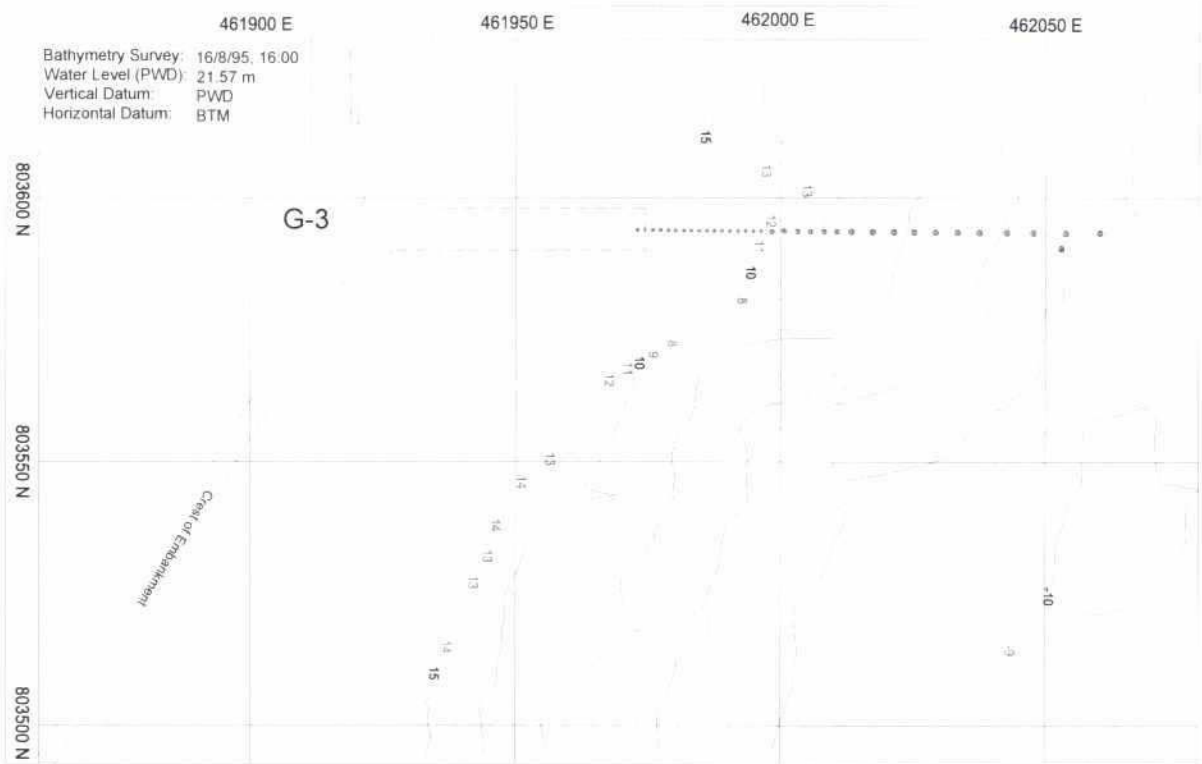


Fig. 5.3-44: Bathymetry at groyne G-3 on August 16, 1995

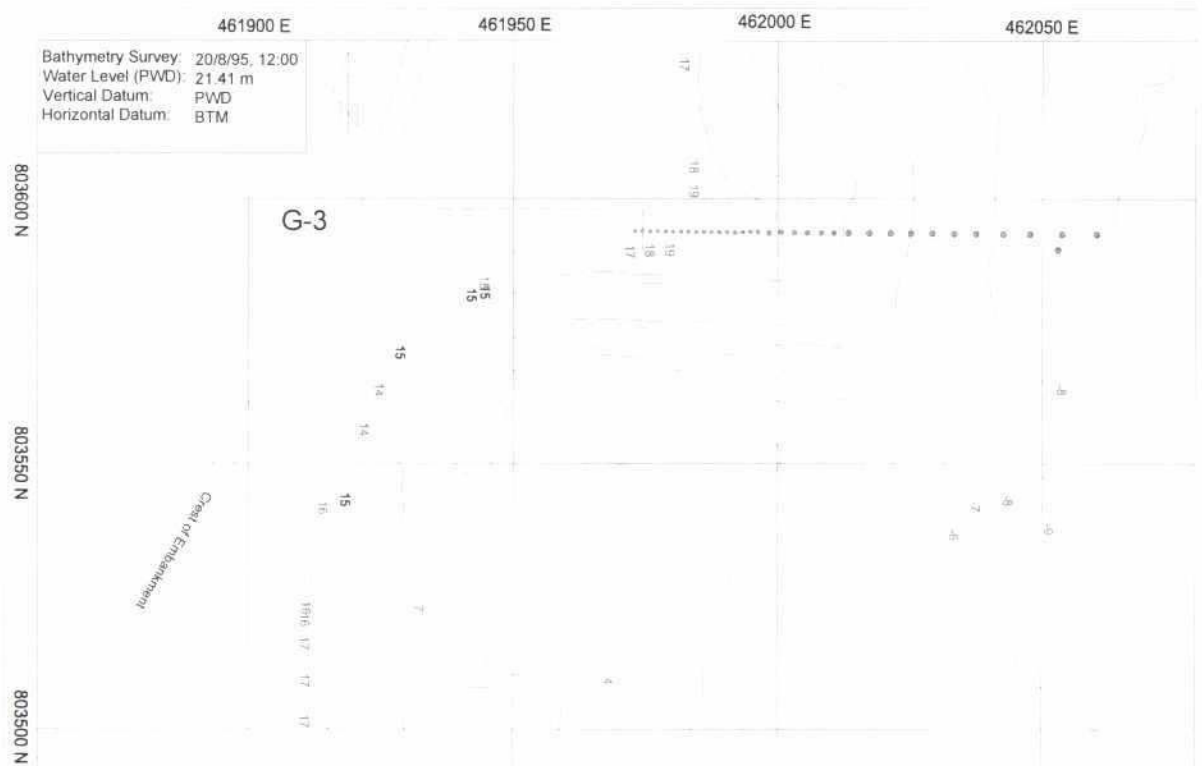


Fig. 5.3-45: Bathymetry at groyne G-3 on August 20, 1995

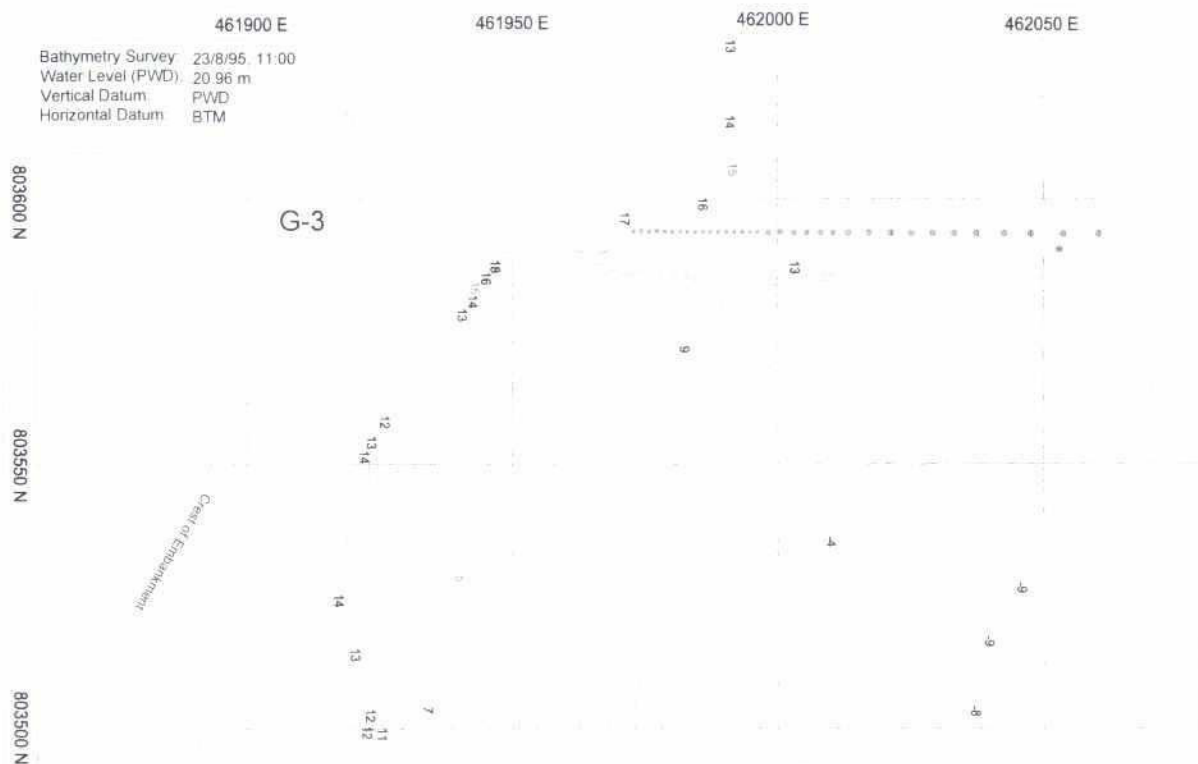


Fig. 5.3-46: Bathymetry at groyne G-3 on August 23, 1995

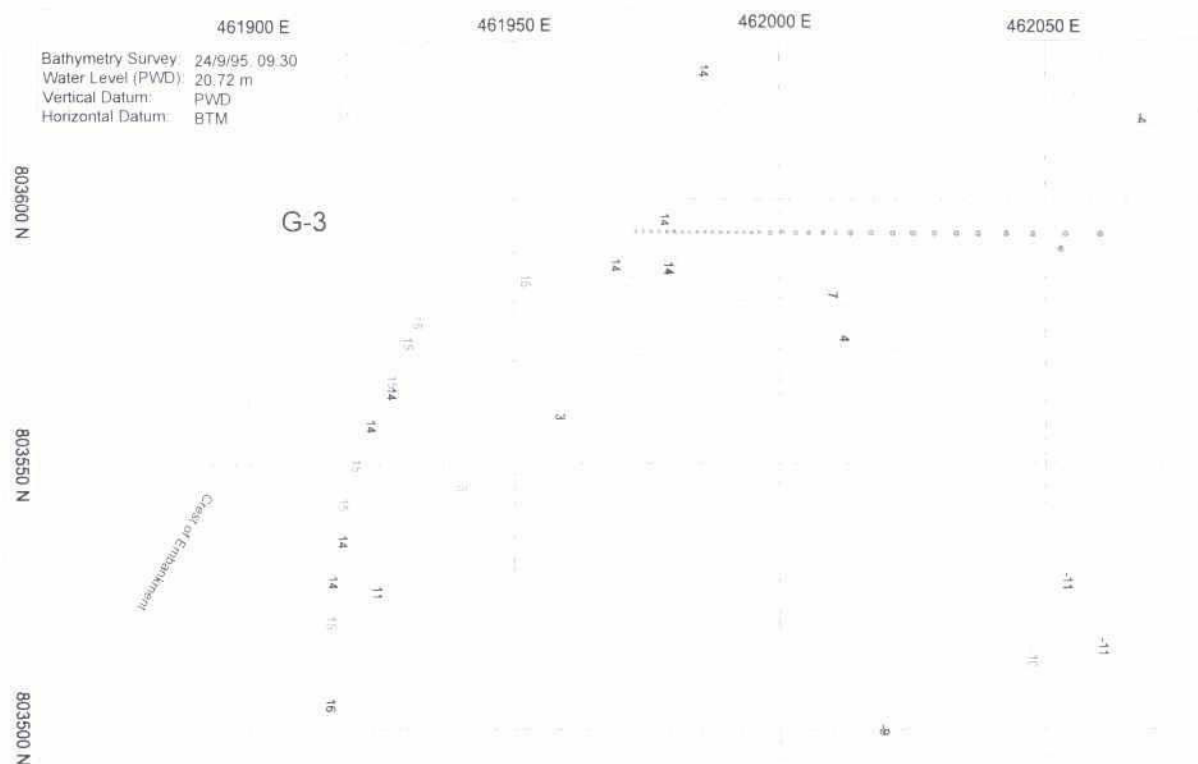


Fig. 5.3-47: Bathymetry at groyne G-3 on September 24, 1995

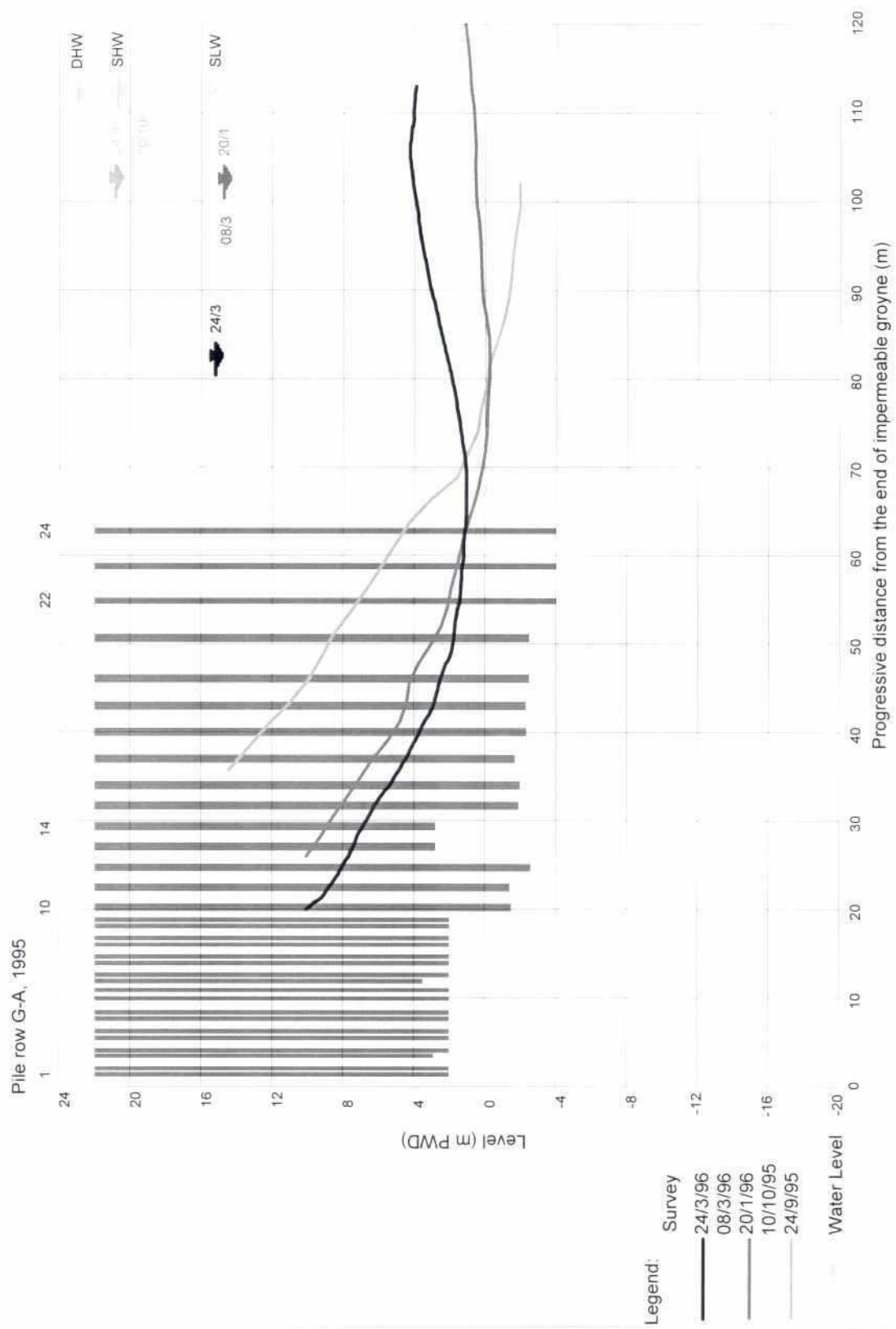


Fig. 5.3-48: Cross-section at 10 m d/s from groyne G-A (before adaptation)

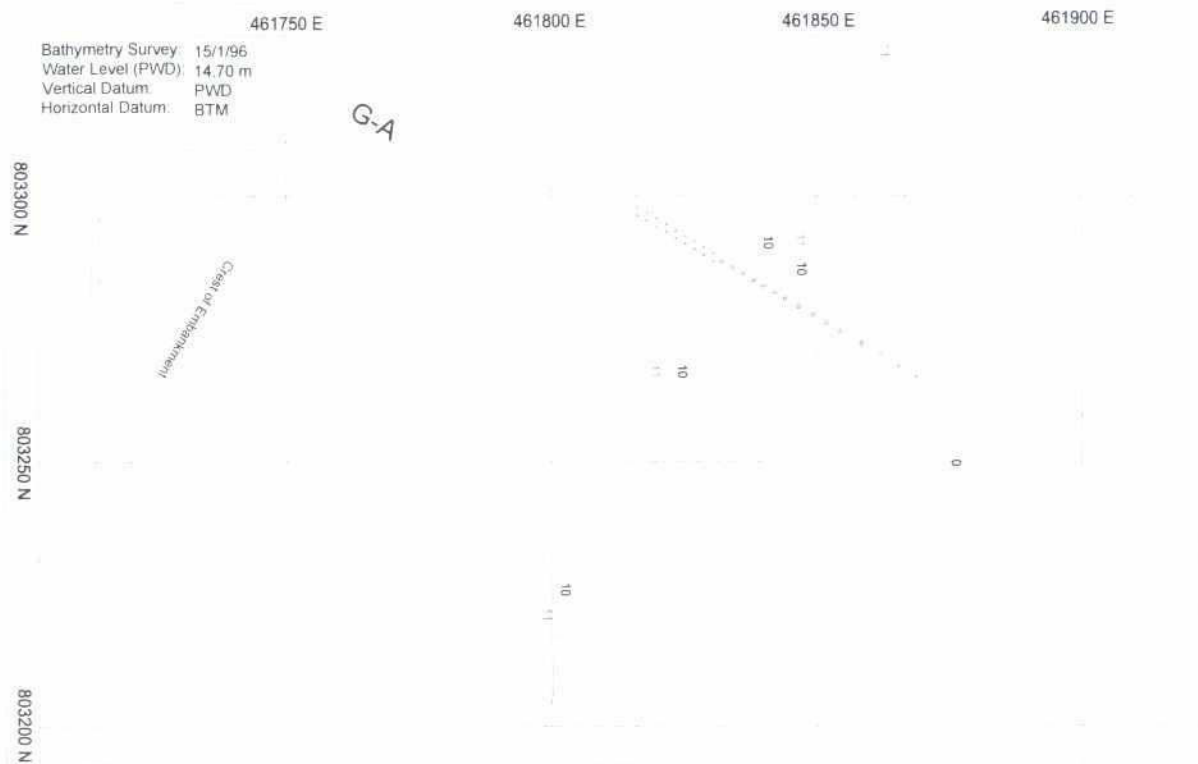


Fig. 5.3-49: Bathymetry at groyne G-A on January 15, 1996

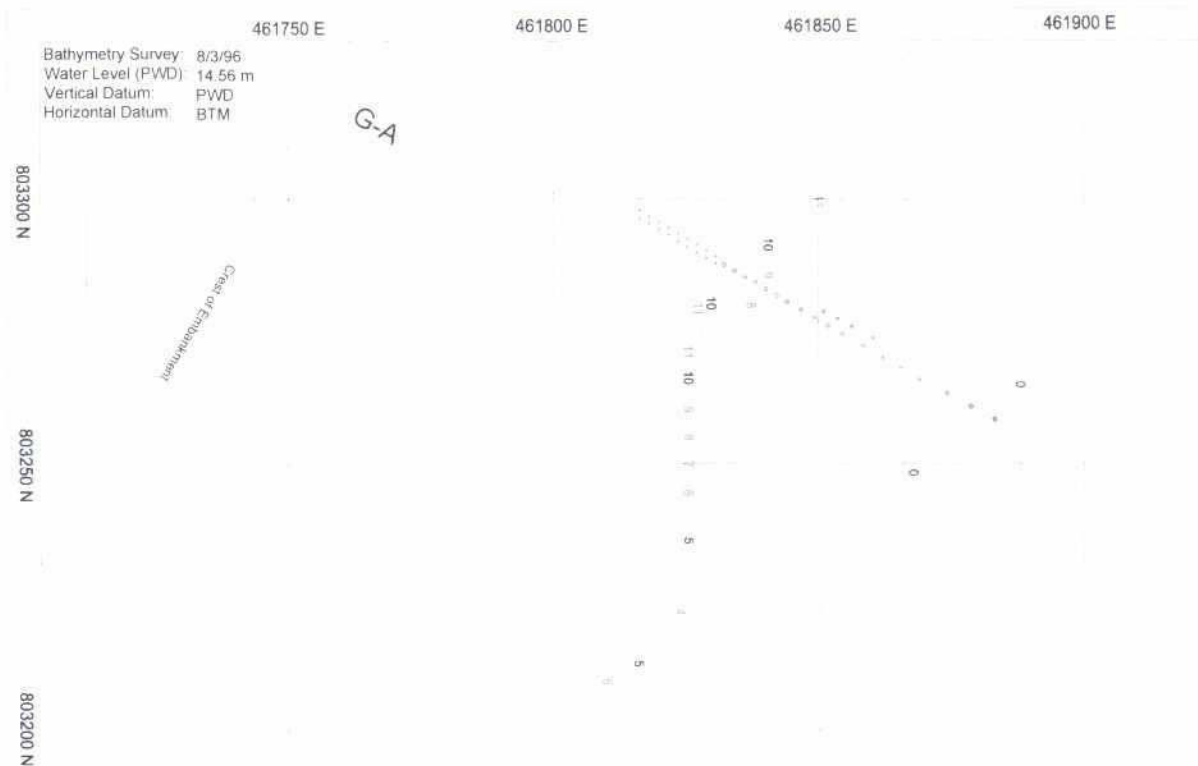


Fig. 5.3-50: Bathymetry at groyne G-A on March 08, 1996

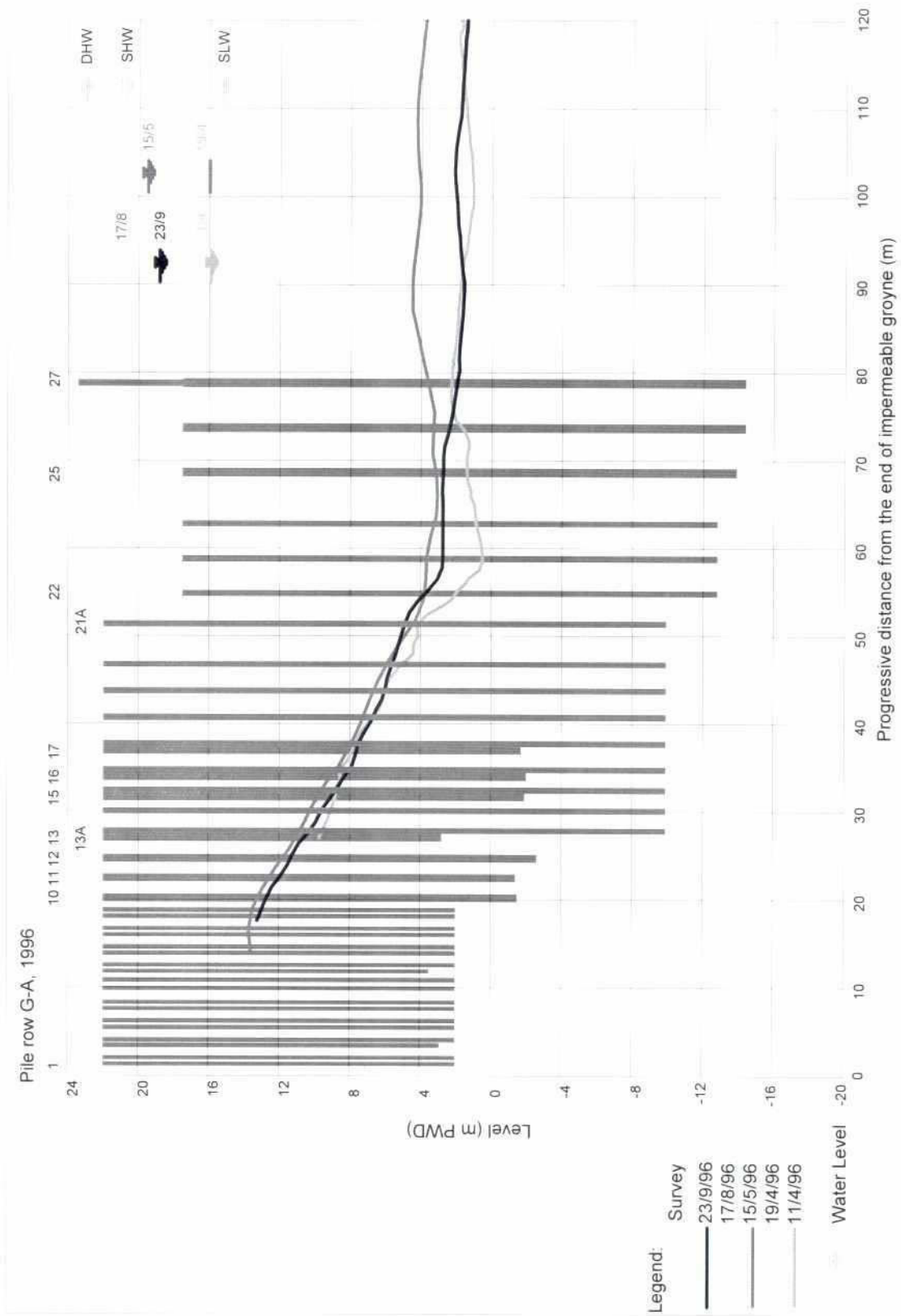


Fig. 5.3-51: Cross-section at 10 m d/s from groyne G-A (after adaptation)

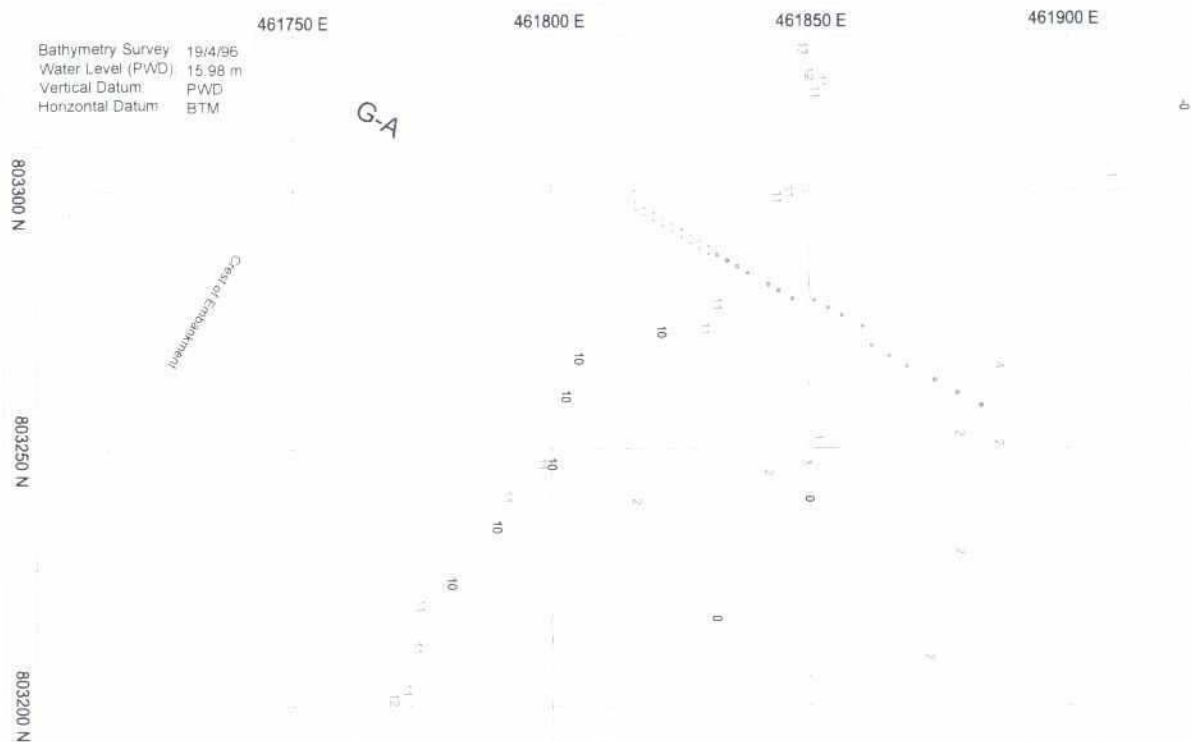


Fig. 5.3-52: Bathymetry at groyne G-A on April 19, 1996

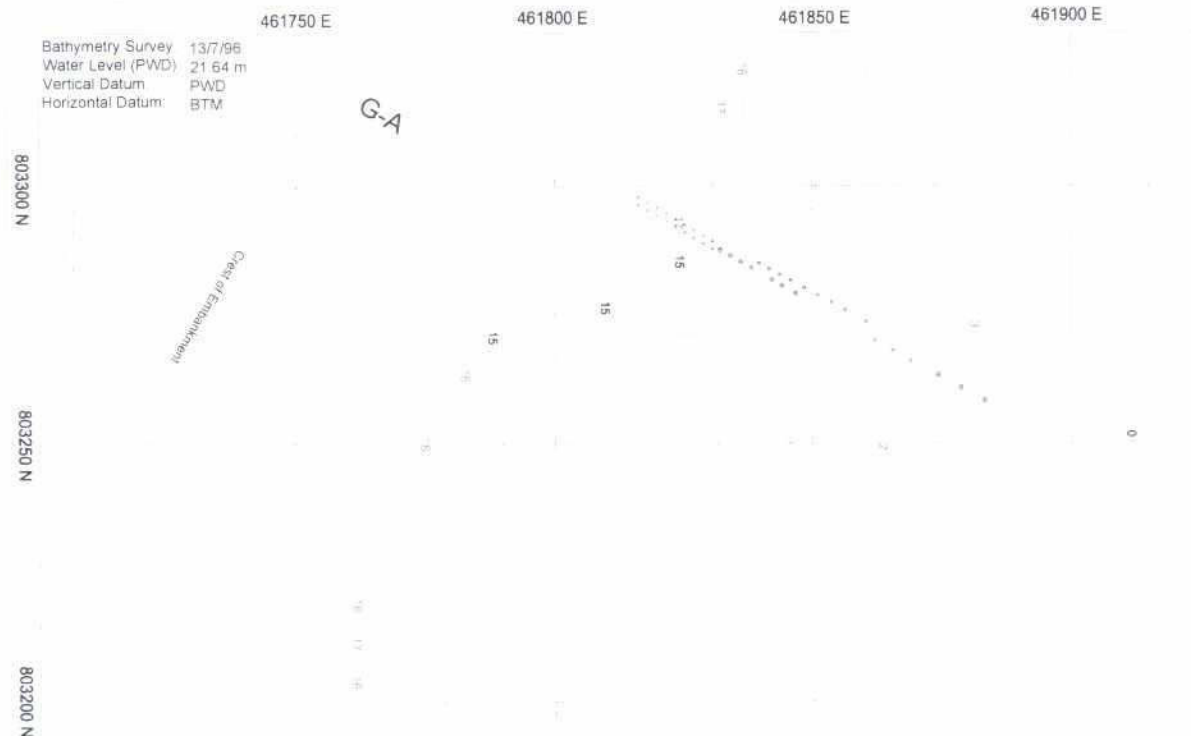


Fig. 5.3-53: Bathymetry at groyne G-A on July 13, 1996

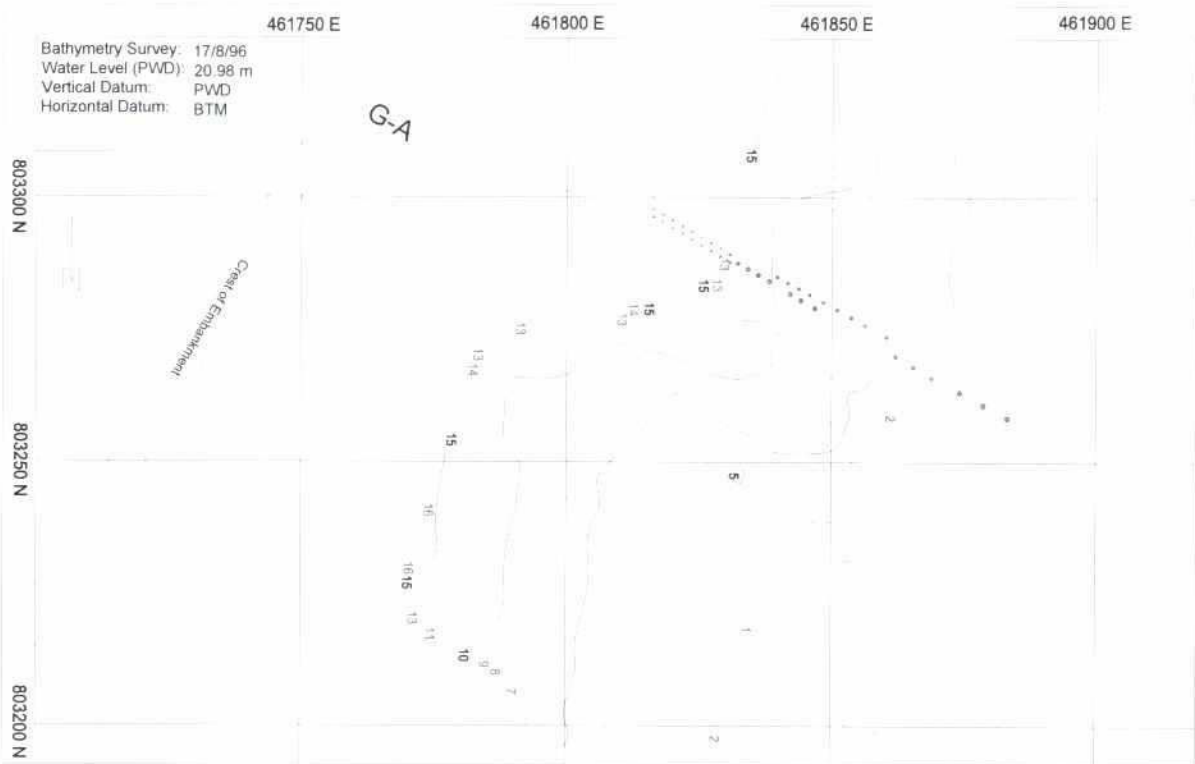


Fig. 5.3-54: Bathymetry at groyne G-A on August 17, 1996

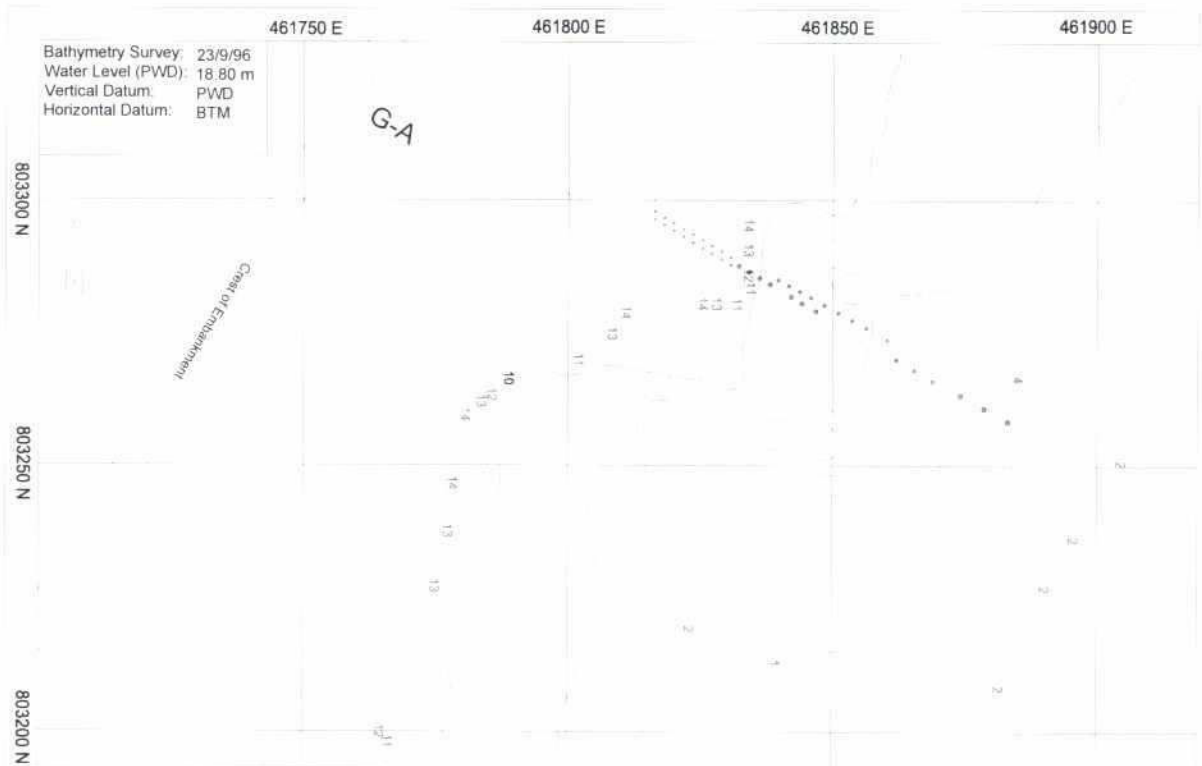


Fig. 5.3-55: Bathymetry at groyne G-A on September 23, 1996

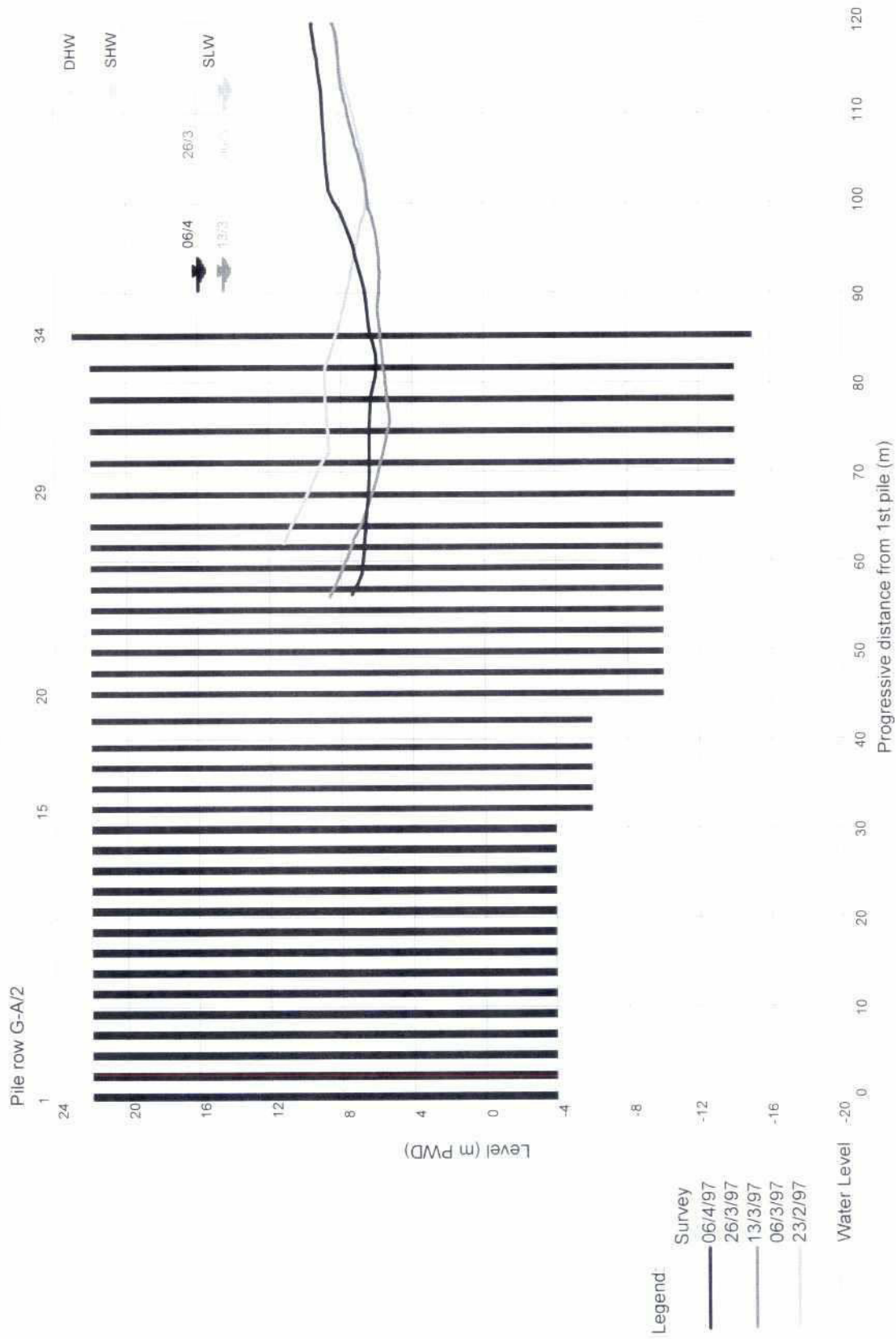


Fig. 5.3-56: Cross-section at 10 m d/s from groyne G-A/2

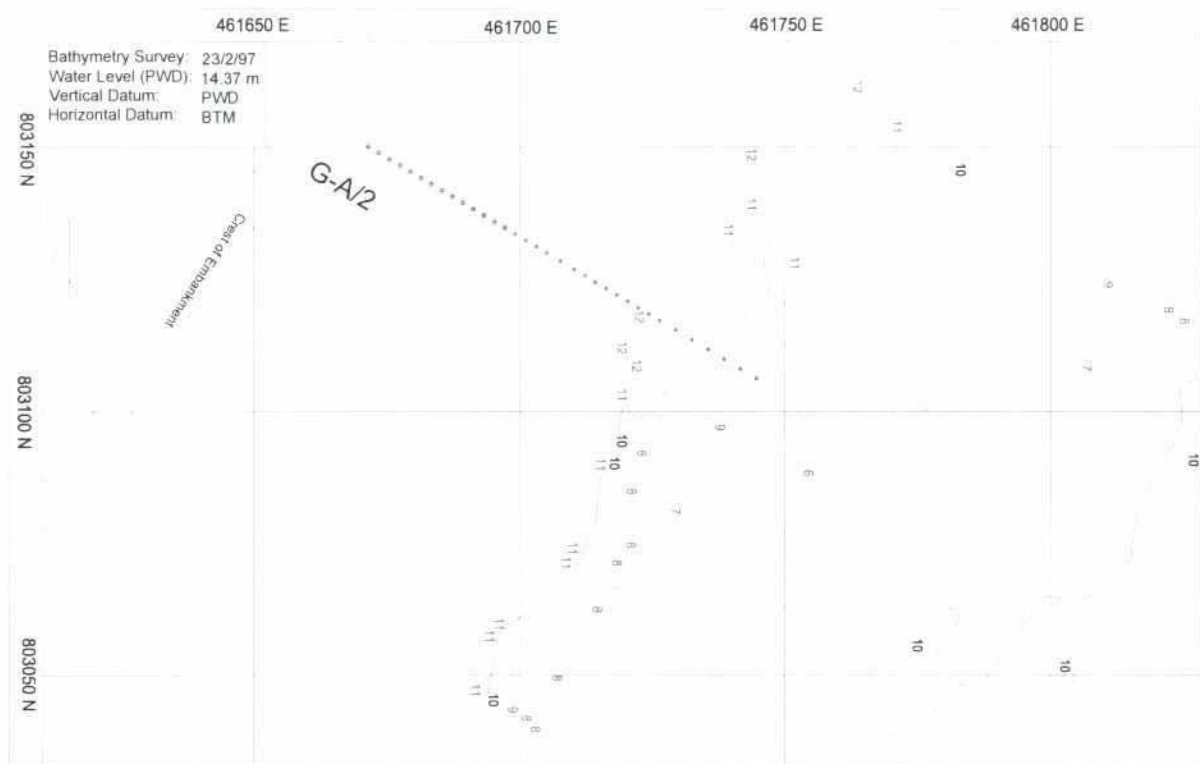


Fig. 5.3-57: Bathymetry at groyne G-A/2 on February 23, 1997

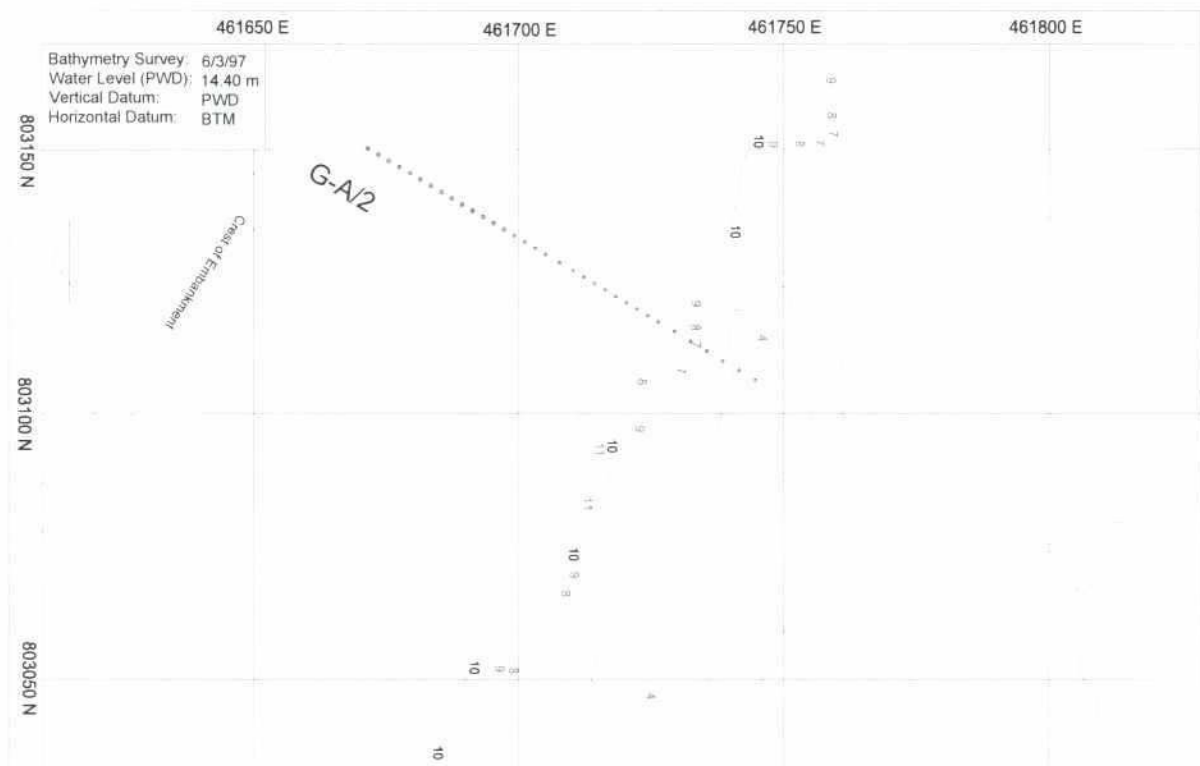


Fig. 5.3-58: Bathymetry at groyne G-A/2 on March 06, 1997

67

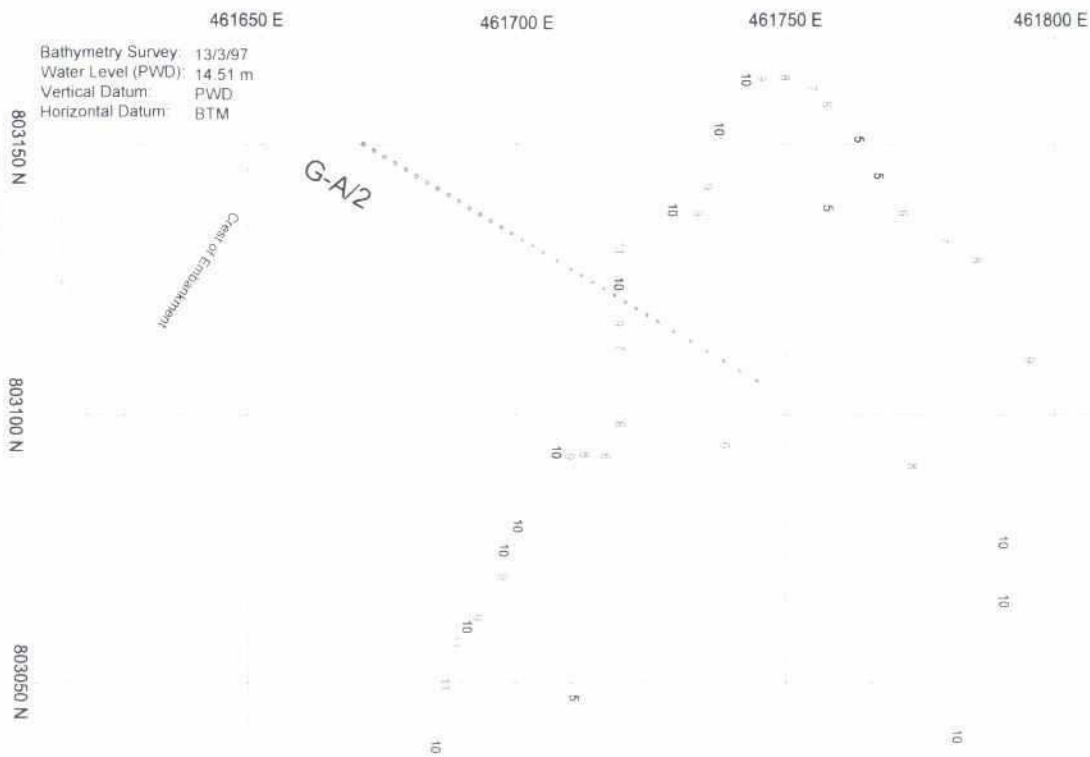


Fig. 5.3-59: Bathymetry at groyne G-A/2 on March 13, 1997

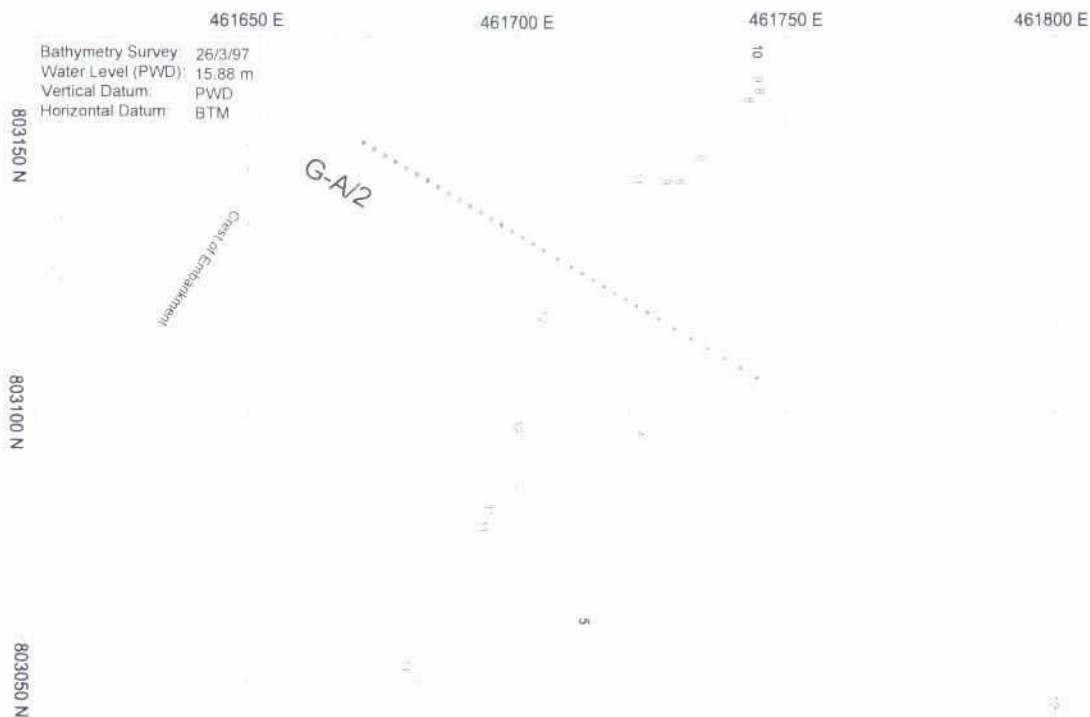


Fig. 5.3-60: Bathymetry at groyne G-A/2 on March 26, 1997

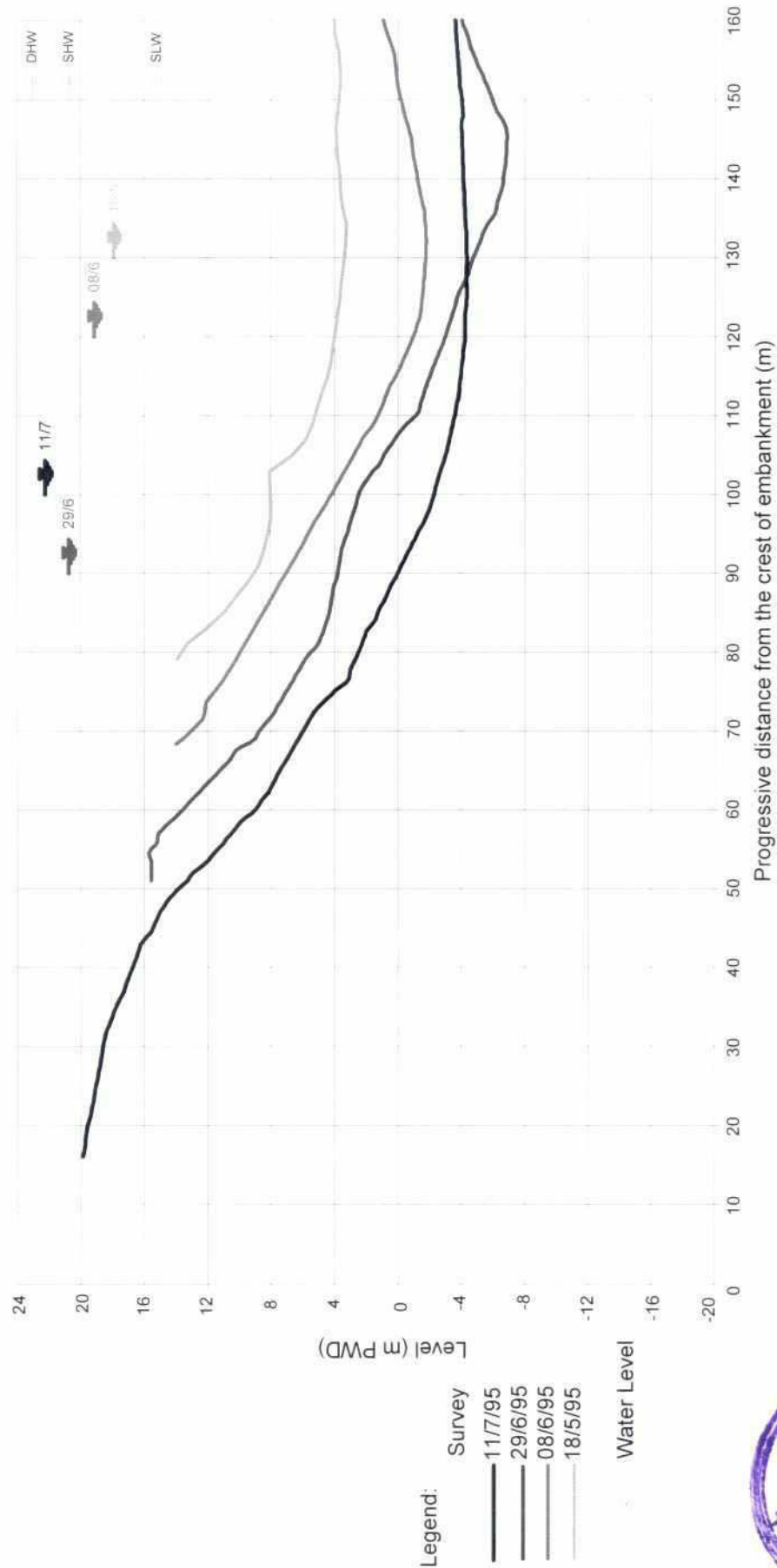


Fig. 5.3-61: Cross-section at 70 m d/s from groyne G-1



68

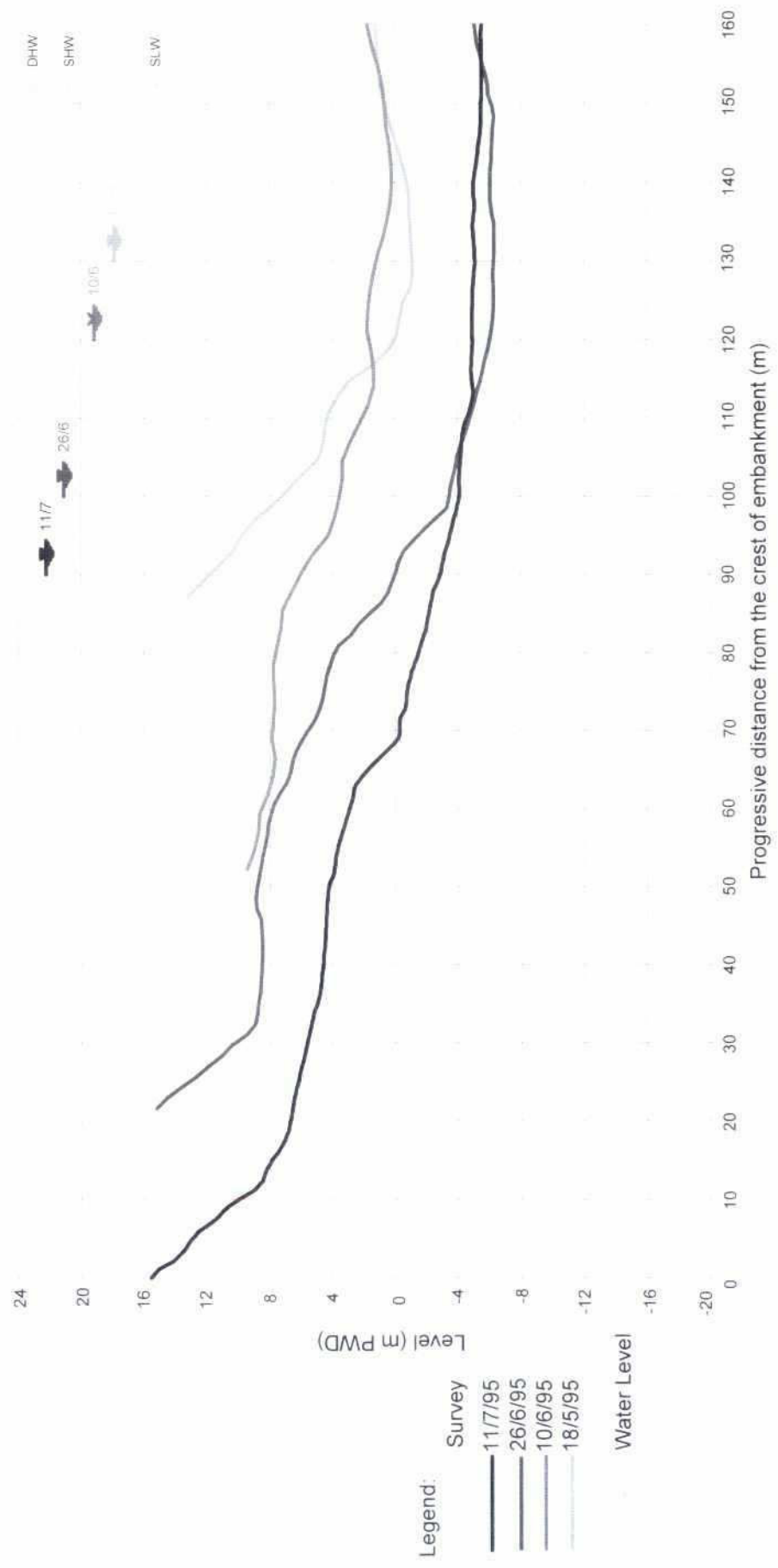


Fig. 5.3-62: Cross-section at 80 m d/s from groyne G-2

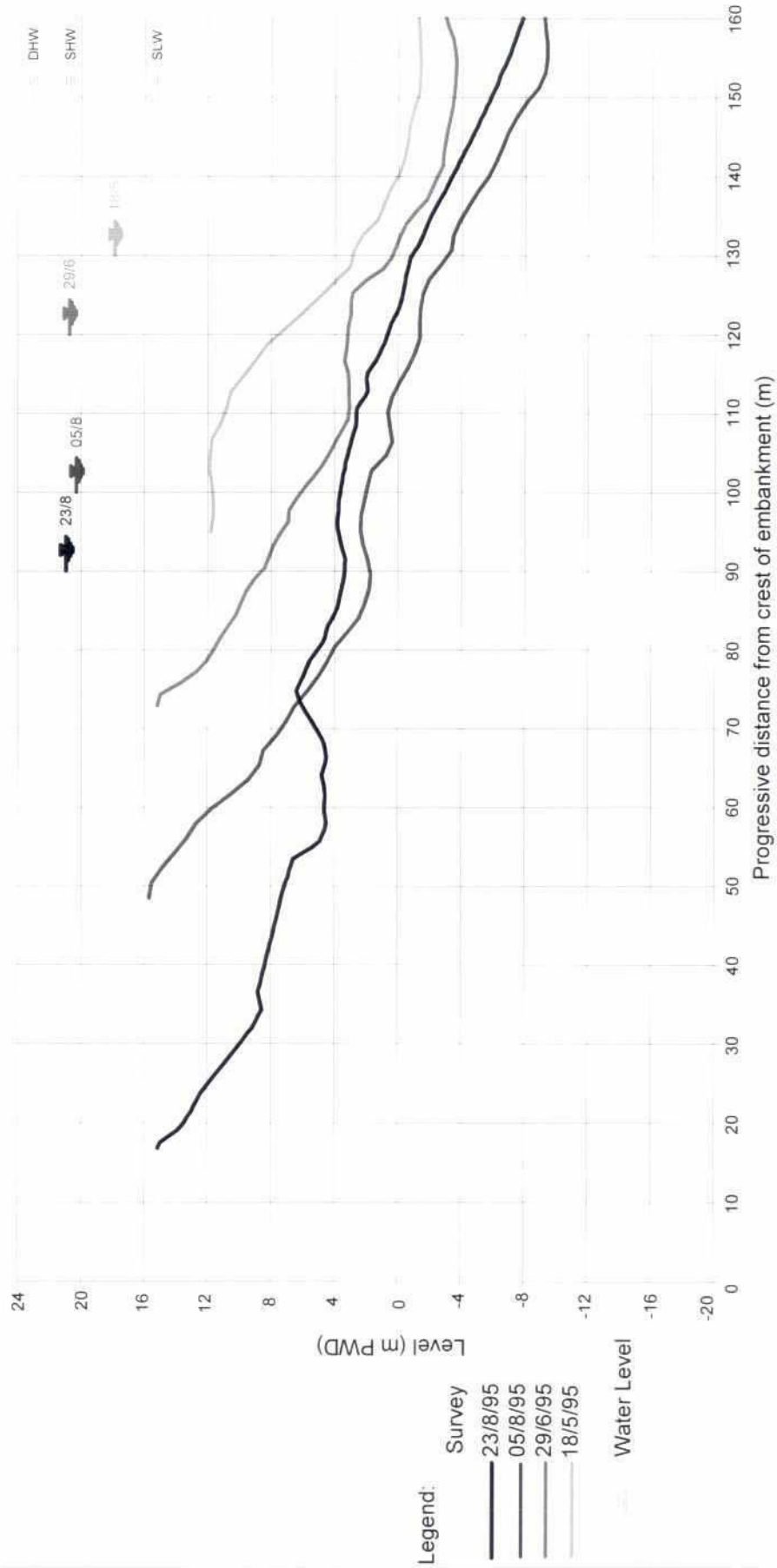


Fig. 5.3-63: Cross-section at 30 m d/s from groyne G-3

6 STATISTICAL EVALUATIONS

6.1 WATER LEVEL RECORDS

6.1.1 Staff Gauges

The hydrographs of the monsoon seasons from 1995 to 1999 are compared in Fig. 6.1-1. The presented water levels refer to the G-A location at the test structures, whereas the readings from the gauge A1 in 1995 and 1996 are corrected for the water level slope to the A2 location (see Section 2.6). The listed recordings refer to the water level readings at 8:00 hrs. The yearly maximum-recorded peak levels are listed in Table 6.1-1.

	1995	1996	1997	1998	1999
Water Level (m+PWD)	22.42	22.18	22.19	22.46	21.75
Date	10/7	15/7	14/7	7/9	27/8
Time (hrs.)	8:00	13:00	8:00	13:00	13:00

Table 6.1-1: Maximum recorded water levels from 1995 to 1999

The water level slope has been calculated between the gauges B and A1/A2 over a distance of 1060/1520 m). The variations of the water level slope in comparison to the rise and fall of the water levels are shown in Fig.6.1-2 and Fig.6.1-3. A water level slope of 9 to 12 cm over 1 km waterway is calculated between the gauge A1 and the gauge B before the July peak level in 1996 (Fig. 6.1-2). After the August peak level the slope reduced to a minimum of 4×10^{-5} .

The high water level slope of 9 to 10×10^{-5} at the beginning of the graph in Fig. 6.1-3 follows the water level peak on July 14, 1997. After that peak the water level falls continuously by almost 3 m until August 4; in the same time period the water slope is reduced by 50 %.

6.1.2 Water Level Auto Gauge

The rise of the water level over a period of $5 \frac{1}{2}$ days to the peak flow on July 13, 1997 is shown in Fig. 6.1-4. The data have been taken from the auto gauge C of the monitoring station, which has recorded the water level every 10 minutes. The water level does not gradually rise to its peak. A fast rise is recorded on July 12 after midnight, when the water level rises by 14 cm in 3 hours. On the other hand the water level is almost constant for 8 hours on July 10, 1997.

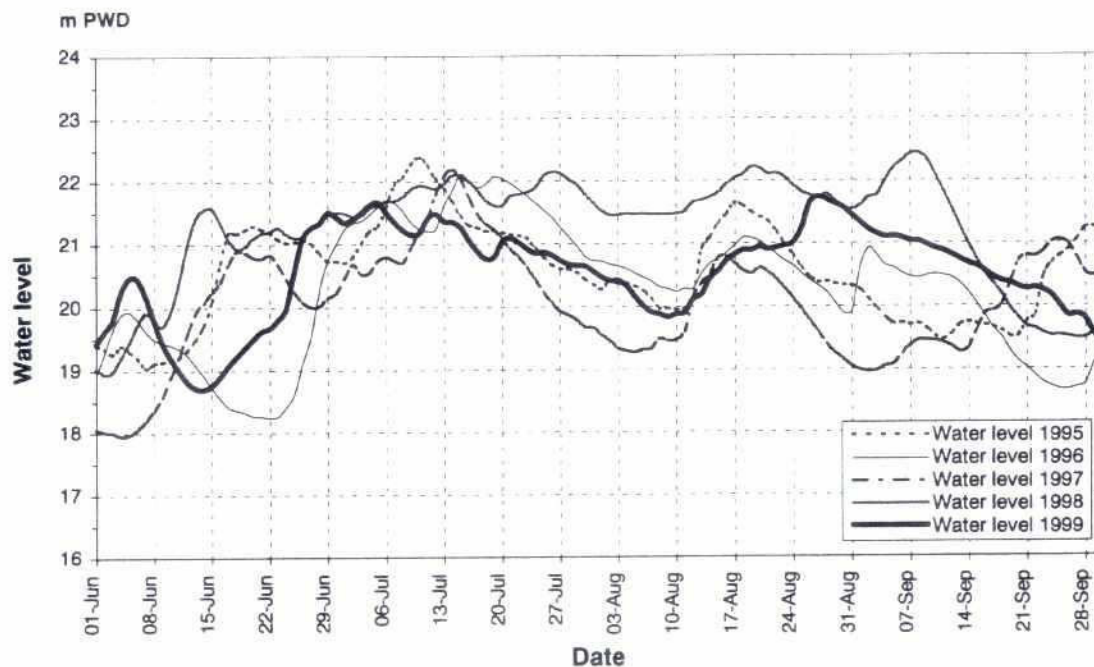


Fig. 6.1-1: Hydrographs from June to September in 1995 to 1999

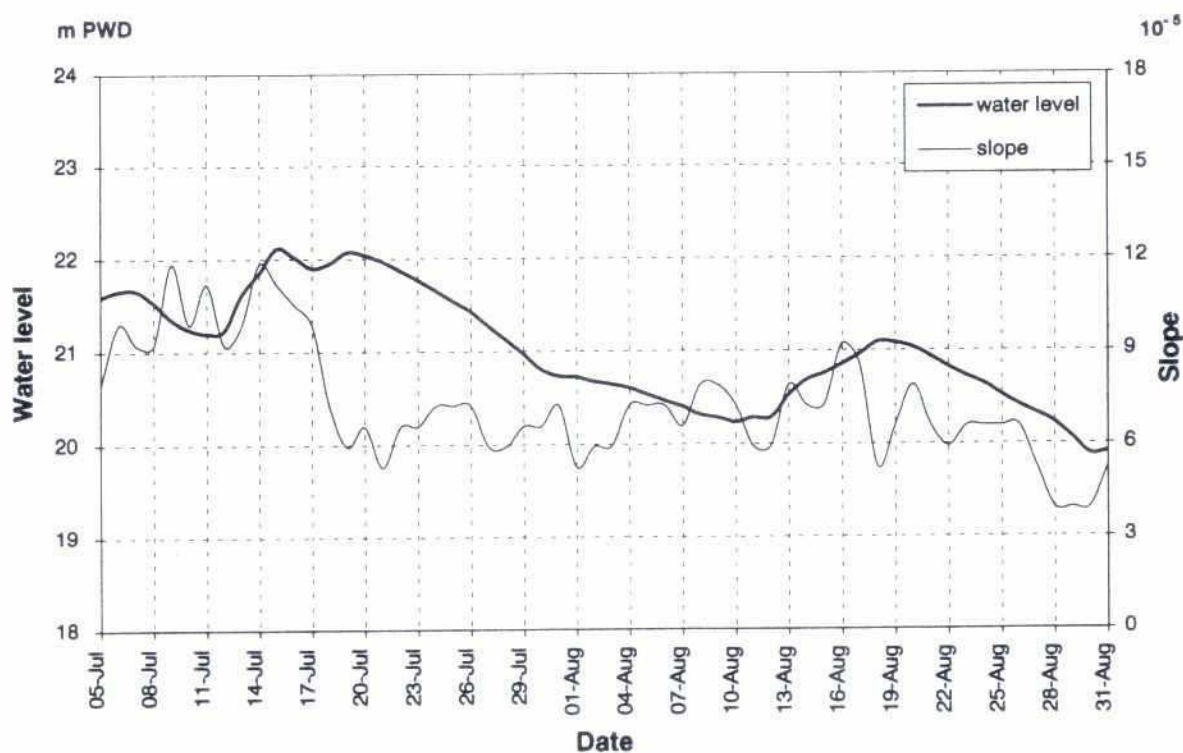


Fig. 6.1-2: Water level at G-A during two peak levels in 1996
vs water level slope between G-B/1 and downstream from Manos river

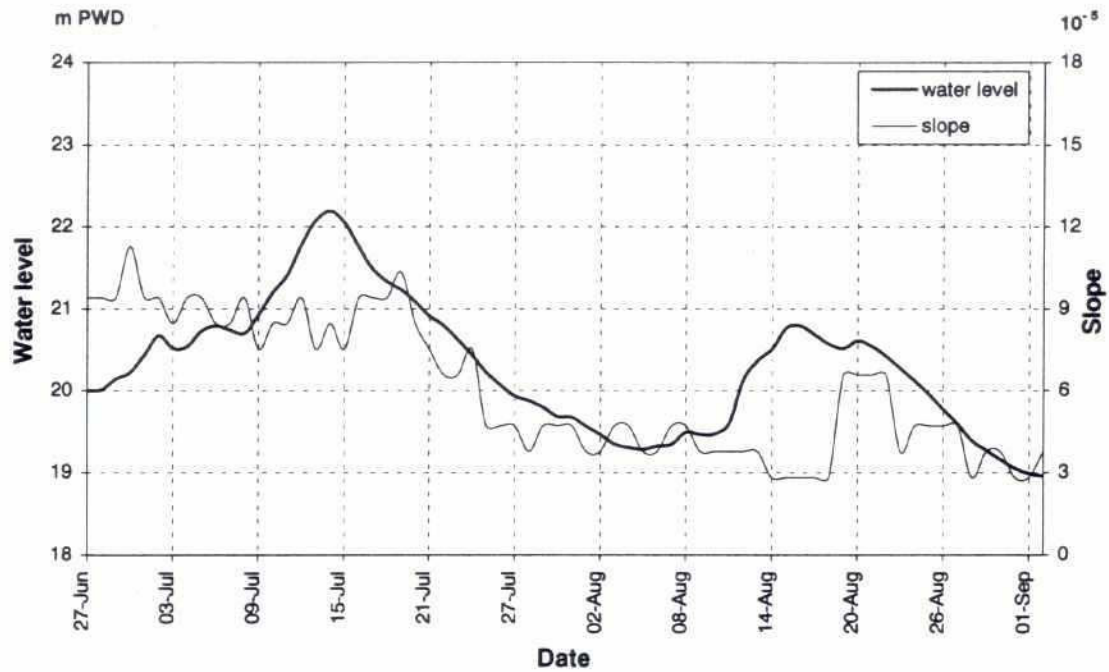


Fig. 6.1-3: Water level at G-A during two peak levels in 1997
vs water level slope between G-B/1 and G-A

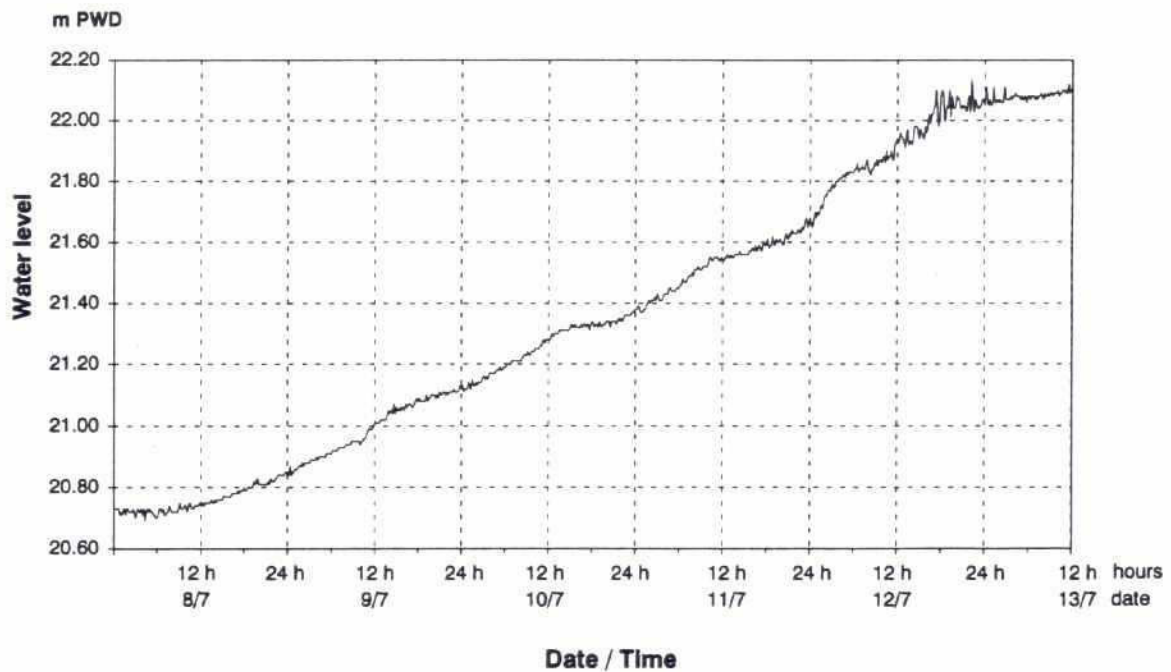


Fig. 6.1-4: Rise to water level peak in July 1997
10 minutes interval recordings of auto gauge at G-2

6.2 DATA COLLECTED BY MONITORING STATION

6.2.1 Wind and Waves Statistics

The monitoring station (see Section 3.6) recorded wind and wave data every 10 minutes. The monthly mean wind speed is presented in Fig. 6.2-1. If sufficient data has been available, the monthly average wind has been calculated for this analysis. During the monsoon seasons from 1995 to 1998 higher wind speed has been recorded than during the other months.

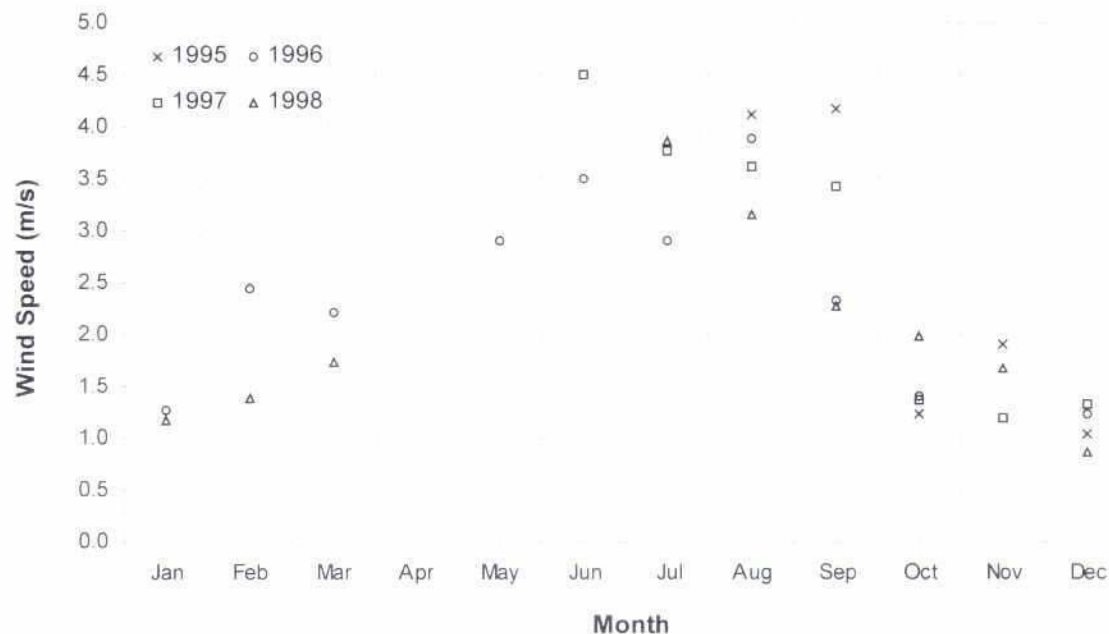


Fig. 6.2-1: The Groyne Test Structure
Monthly mean wind speed measured at G-2

The monitoring team observed maximum wave heights of 0.4 to 0.5 m in the groyne fields, especially in monsoon 1995 and 1996. The records of the water level auto gauge of the monitoring station confirmed such observations. During storm conditions (exceeding of user defined wind speed) a storm measurement mode was released by the system; i.e. every 30 seconds data were recorded over a period of 10 minutes. After a 10 minutes break of data collection the system checked, whether storm condition remained. If yes, the storm measurement continued for further 10 minutes. If not, the system switched back to normal mode; i.e. every 10 minutes data were recorded.

The monitoring station determined the wave heights as the difference of maximum and minimum water level recordings (46 water level measurements in 30 seconds). Wave analyses of 3 selected storm measurements are presented in Fig. 6.2-2 to Fig. 6.2-4. The wave heights collected during the storm measurement are summarised in groups of 5 cm. From the histogram a curve of non-exceedance is evaluated. The significant wave height $H_{1/3}$ of the measurement period is defined as the average of one third of all values containing the highest records.

Wave heights in relation to wind speed and wind direction are shown in Fig. 6.2-5. All data recorded from the monitoring station of 1996 have been taken for this analysis. Data of wind speed below 3 m/s and water levels below 19.5 m+PWD have not been considered. Wave heights are averaged for the

same wind speed and the same wind direction within 5 degrees. The analysis shows, that higher waves occur if the wind blows from southern direction; i.e. the wind blows against the current direction.

At extreme storm conditions from southern directions, which the monitoring team did not observe or record, wave heights of more than 0.5 m can be expected in the groyne field area.

An observation of higher waves was made 2 km downstream from Balashi Ghat on August 25, 1997 (see Jamuna overview in Fig. 1.3-3). During a sudden storm (10 Bft, SE) wave heights of about 1.5 m and a wave period of 5 seconds were estimated.

6.2.2 Test Pile Inclination and Acceleration

The maximum inclination and acceleration measured in two axes of the test pile are derived from two storm measurements. The graphs are presented in Fig. 6.2-6 and Fig. 6.2-7. The maximum-recorded inclination is 1.5° and the maximum acceleration is 0.5 m/s^2 .

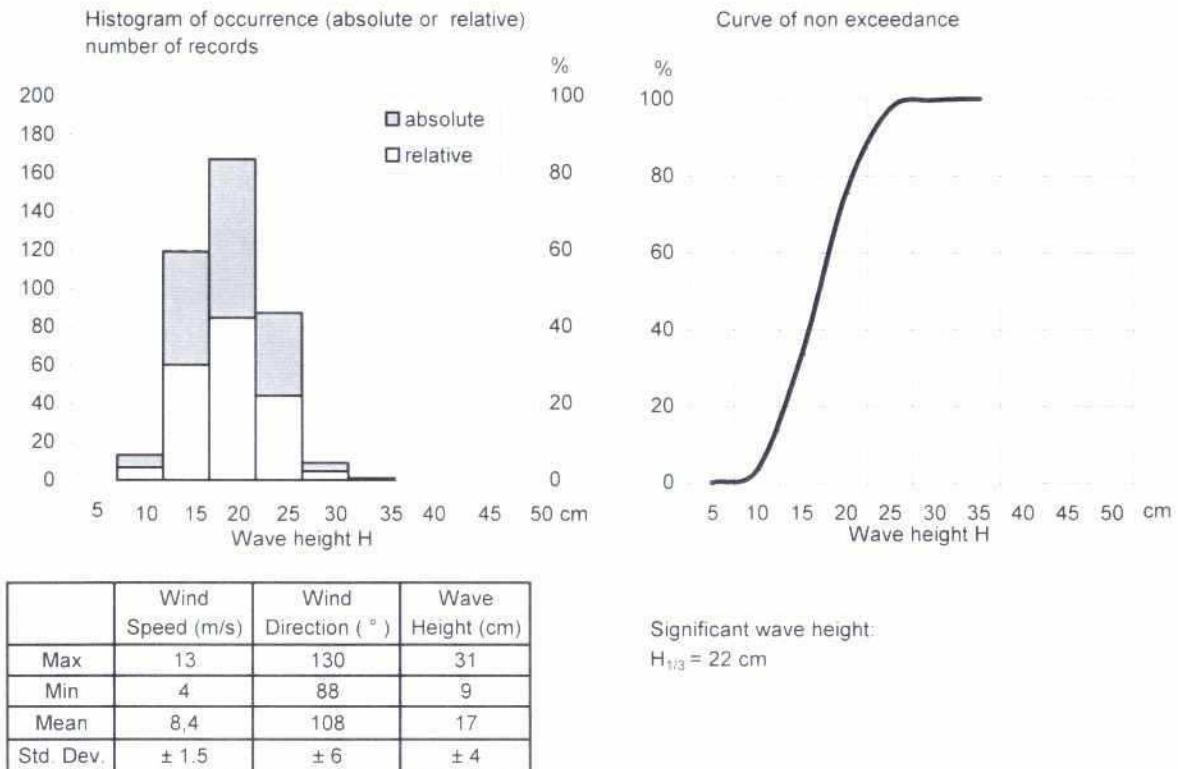


Fig. 6.2-2: Wave height during storm measurement 02/09/95 (4:46 - 11:11)

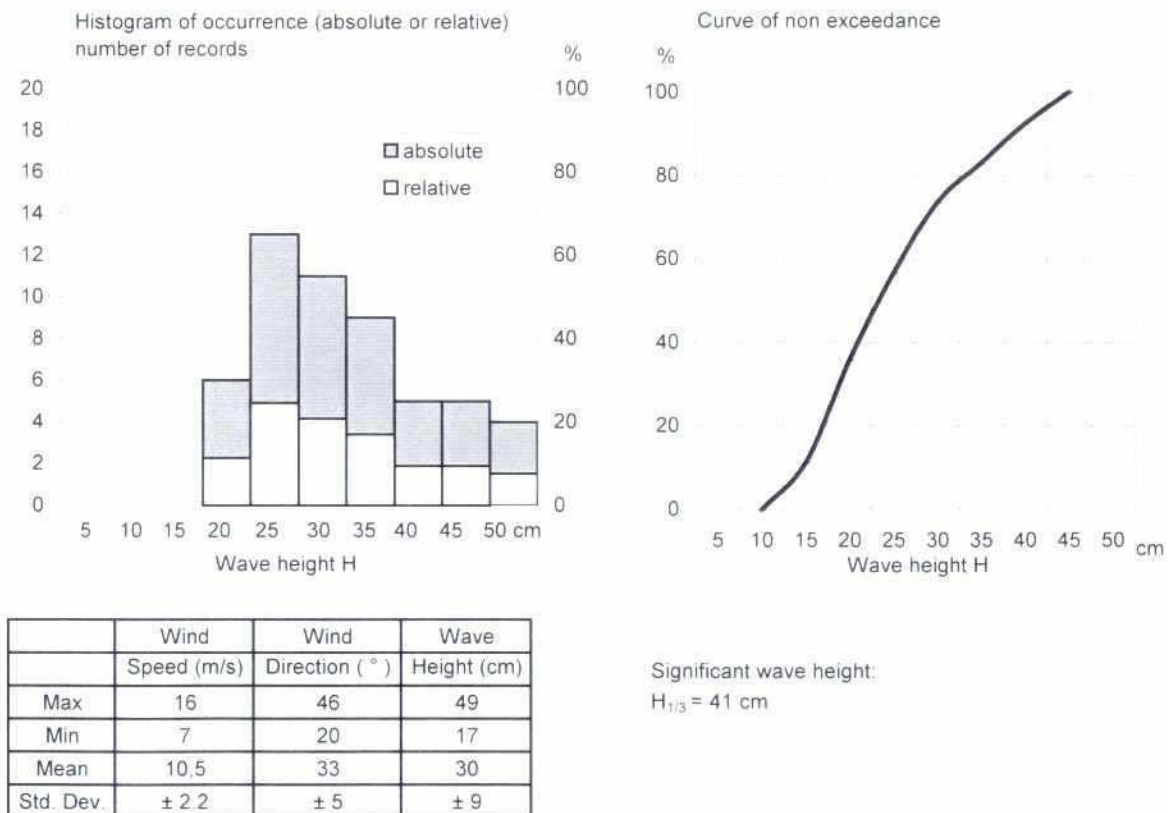


Fig. 6.2-3: Wave height during storm measurement 14/09/96 (15:40 - 16:07)

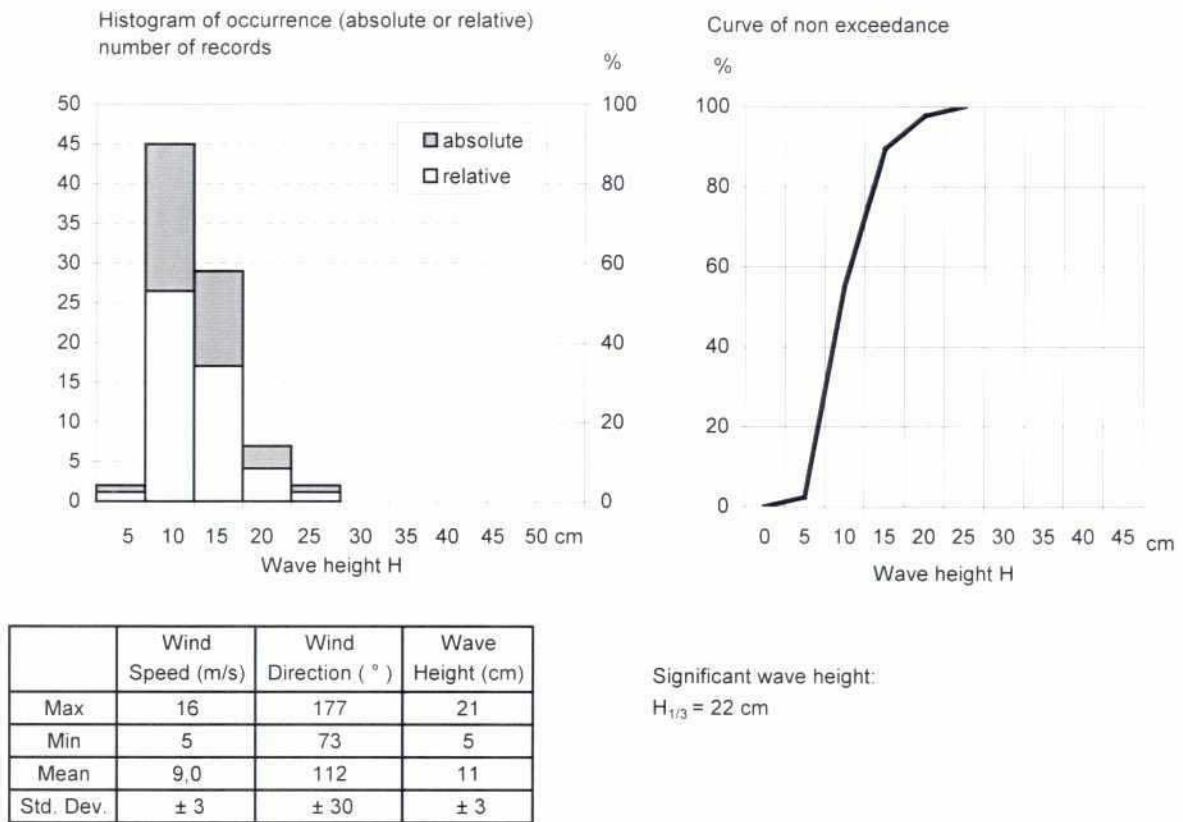


Fig. 6.2-4: Wave height during storm measurement 25/08/97 (18:25 - 19:53)

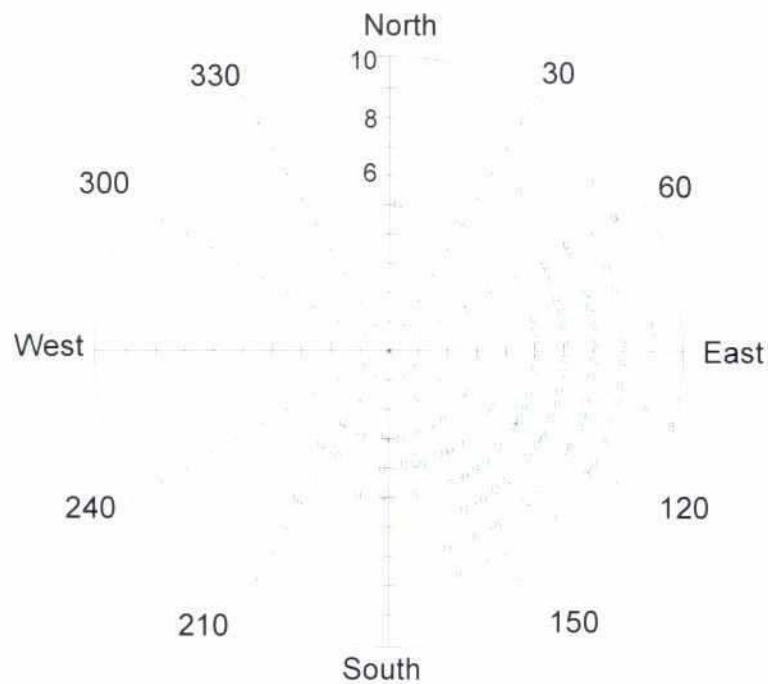
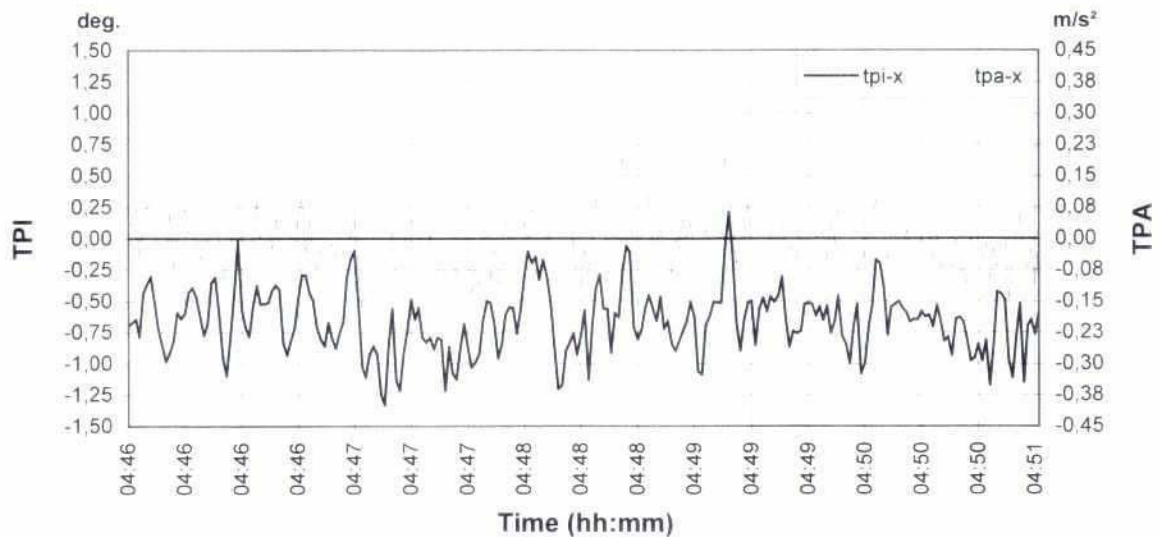
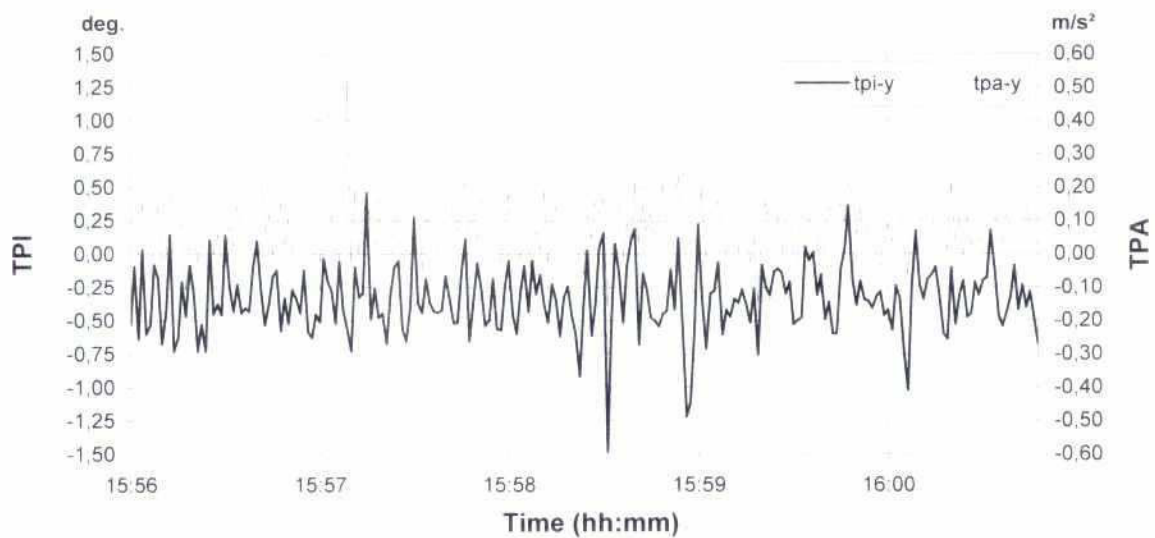


Fig. 6.2-5: Average wave heights in relation to wind speed and wind direction (1996)



Wind speed:	9 m/s \pm 1 m/s
Wind direction:	110° \pm 6°
Wave height:	19 cm \pm 2 cm
Water depth:	4 m PWD



Wind speed:	9 m/s \pm 1 m/s
Wind direction:	110° \pm 6°
Wave height:	19 cm \pm 2 cm
Water depth:	4 m PWD

Fig. 6.2-6: Movements of Test Pile # 30 at G-2 (02/09/95)

6.3 PRECIPITATION

The monitoring team reported the rainfall, which was collected by a rainfall gauge at the Consultants Camp, in the logbook. The measurements were scheduled at 8:00 hrs daily; i.e. a record represented the rainfall from 8:00 hrs in the morning to 8:00 hrs at the next morning. The data were archived in Excel tables for further evaluations. A comparison of the monthly rainfalls in the years 1995 to 1999 is shown in Fig. 6.3-1. Extraordinary daily rainfalls are listed in Table 6.3-1.

Date	Rainfall (mm)	Date	Rainfall (mm)
1995, June 18	212	1996, August 31	250
1995, July 6-7	280	1996, August 31-September 01	353
1995, August 12	187	1998, October 20	169
1995, September 21-22	260	1998, October 20-21	313
1996, June 25-27	340	1999, July 19	167

Table 6.3-1: Maximum daily rainfalls

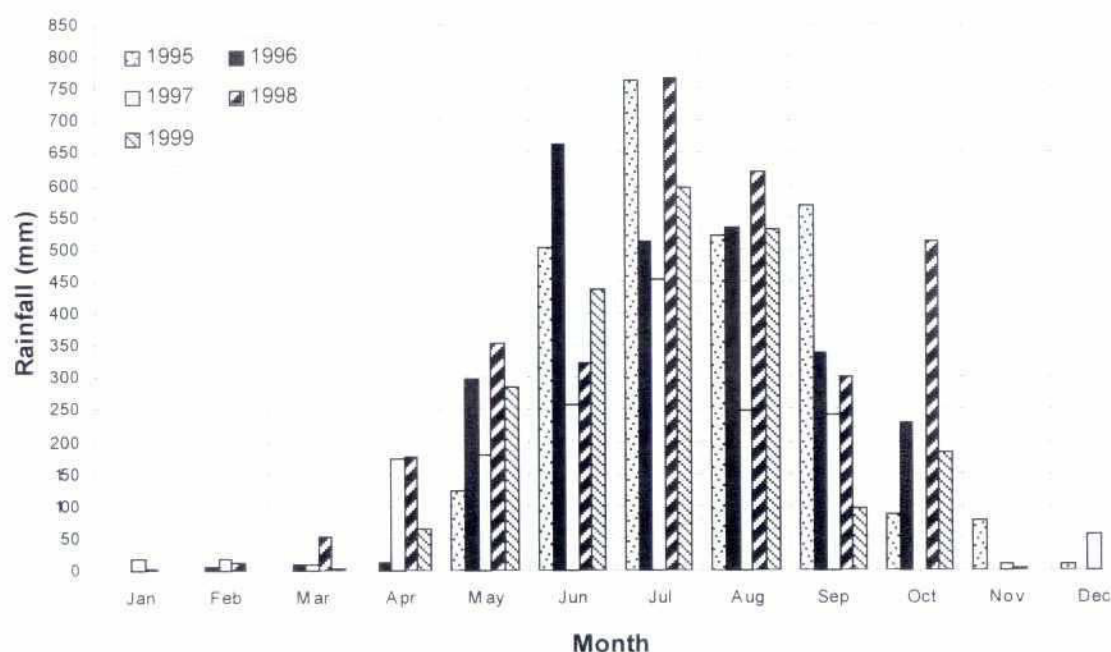


Fig. 6.3-1: The Groyne Test Structure
Comparison of monthly rainfall

6.4 TEMPERATURE AND RELATIVE HUMIDITY

Statistics of collected temperature and relative humidity data are shown in Fig. 6.4-1.

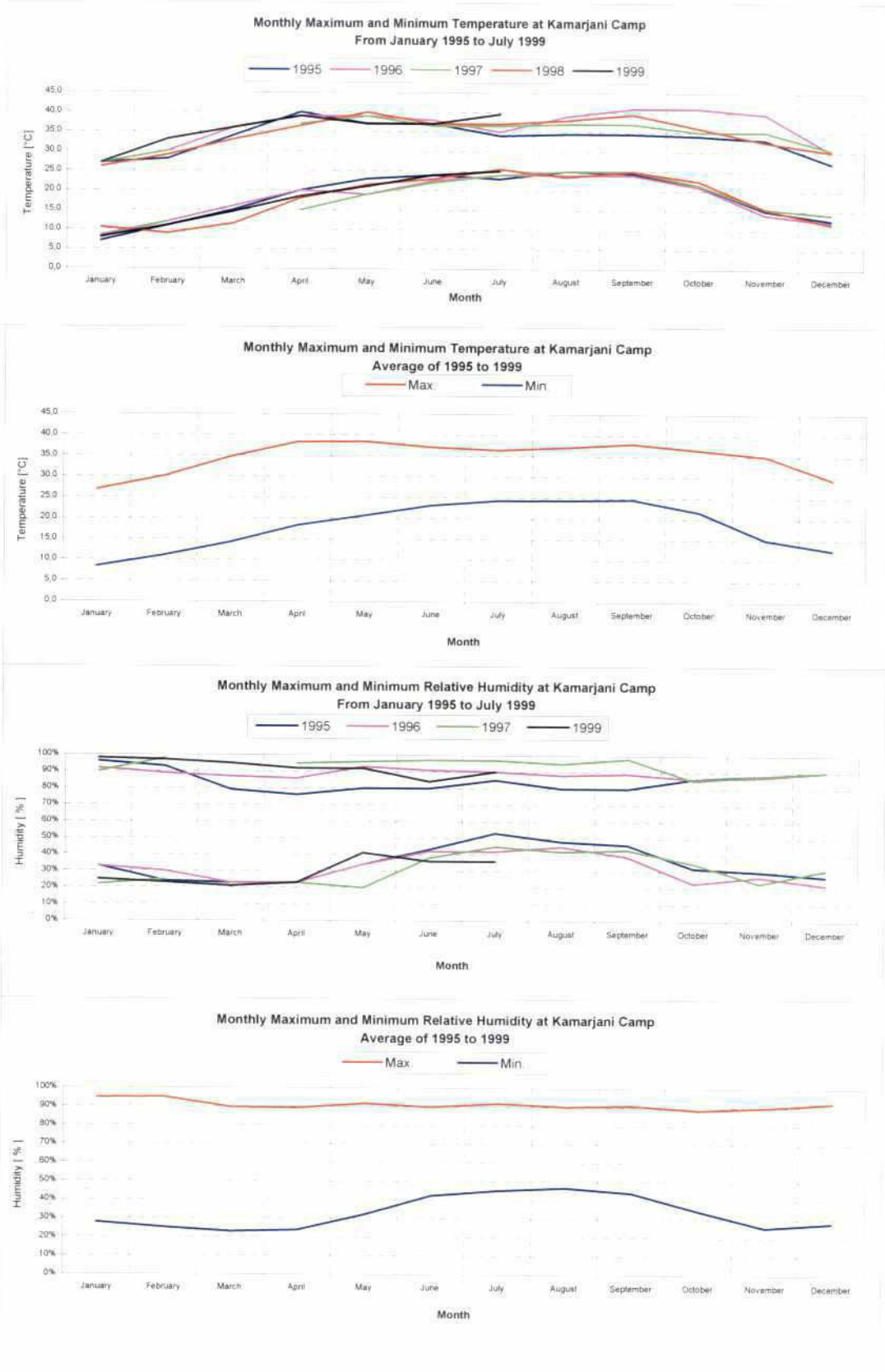


Fig. 6.4-1: Temperature and relative humidity

6.5 PIEZOMETER MEASUREMENTS

6.5.1 Water Level Difference at G-2

Piezometer tubes were installed directly upstream and downstream from groyne G-2 to measure the water level difference caused by the pile row. Measurements were taken by an electronic plumb at pile No 29 of the groyne in 1995. A maximum water level difference of 30 cm was measured on September 26, 1995.

Date	Difference (cm)	Date	Difference (cm)	Date	Difference (cm)
24/06	20	25/06	19	18/08	10
21/08	12	23/08	12	25/08	6
27/08	14	31/08	8	04/09	4
06/09	8	08/09	6	09/09	10
10/09	8	11/09	6	12/09	7
13/09	8	15/09	8	26/09	30
29/09	17	01/10	15	02/10	20
03/10	14	04/10	14	13/10	5

Table 6.5-1: Water level differences at G-2

6.5.2 Embankment at G-A

Piezometer tubes were installed surrounding the embankment at G-A. Measurements were made from July 1996 onwards. A comparison of the groundwater level with the surface water level of June to July 1997 is given in Fig. 6.5-1.

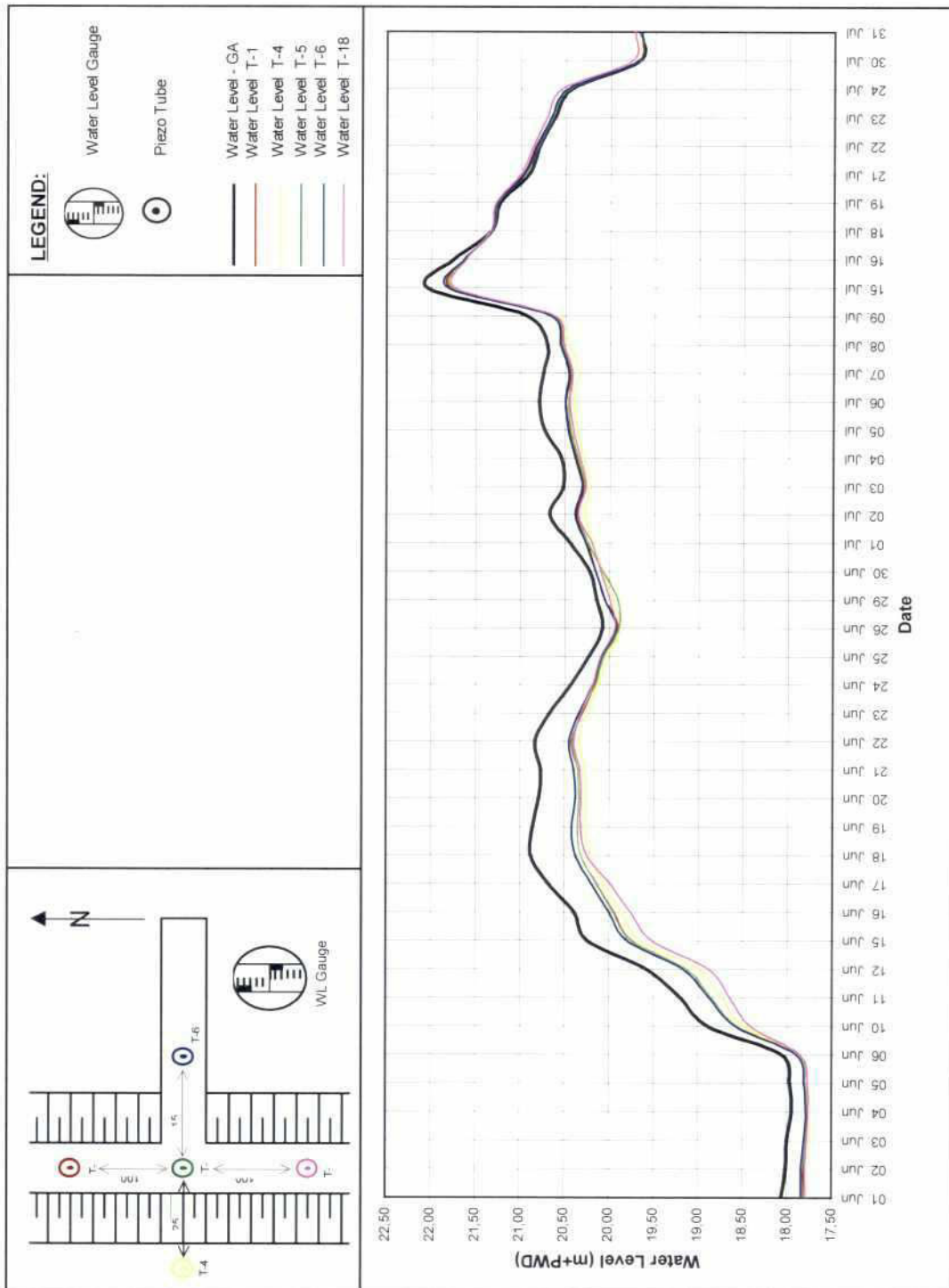


Fig. 6.5-1: Ground water and surface water level at G-A, June to July 1997

7 THE KAMARJANI MAIN CHANNEL

7.1 MAIN SURVEYS

The bathymetry and the float tracks of all Kamarjani main channel surveys carried out by the monitoring team from 1995 to 1999 are presented in Annex 1 (Morphological Investigations). In this annex, only three bathymetry charts and one differential DTM (Fig. 7.1-1 to Fig. 7.1-4) are selected to describe briefly the bathymetry and flow situation of the Kamarjani Main Channel during the monsoon 1995.

Fig. 7.1-1 presents the bathymetry of June 1995. It shows patches of bed contour levels when the stage of the river was in the rising limb of the hydrograph prior to the maximum flood of that monsoon. The approaching deeper channel (below 8 m+PWD) continued up to the downstream end of the test site, which was intercepting the groyne fields tangentially (also confirmed by the overlaid float track). The channel near the test site was deeper (below 4 m+PWD) and narrower comparing to the main river.

The bathymetry of July 1995 (Fig 7.1-2), after the maximum flood of the monsoon, shows that the upstream approach channel had become shallower and wider but the channel near the test site had become deeper (below 0 m+PWD). The shallower part (above 16 m+PWD) of main river had been shifted further to the south.

Fig. 7.1-3 illustrates the channel bed condition in September 1995 after the recession of the maximum flood. The erosion deposition pattern during two months (comparing the bathymetry of Fig. 7.1-2 and Fig. 7.1-3) is presented in the differential DTM of Fig. 7.1-4.

In September the western part of the upstream approach channel had become shallower, which is confirmed from the differential DTM showing contour shades in that region greater than 0 m deposition. The deeper (below 0 m+PWD) channel was approaching from further east directing to the area downstream from G-2. Erosion in the upstream eastern part of the river (Fig. 7.1-4) and reduction of the eastern shallower (above 16 m+PWD) part of the channel (Fig. 7.1-3) also confirmed this situation. The main approaching flow channel was more oblique and towards south-western direction. The thalweg had shifted westward approaching the Manos.

In general, it can be stated from the differential model (Fig. 7.1-4) that deposition had occurred in the main channel (in the period mid July to mid September) except near the bank of the Test Site where erosion (-6 m to -2 m) had been observed. Near the bank severe erosion (-14 m to -10 m) is seen further d/s from the Manos river.

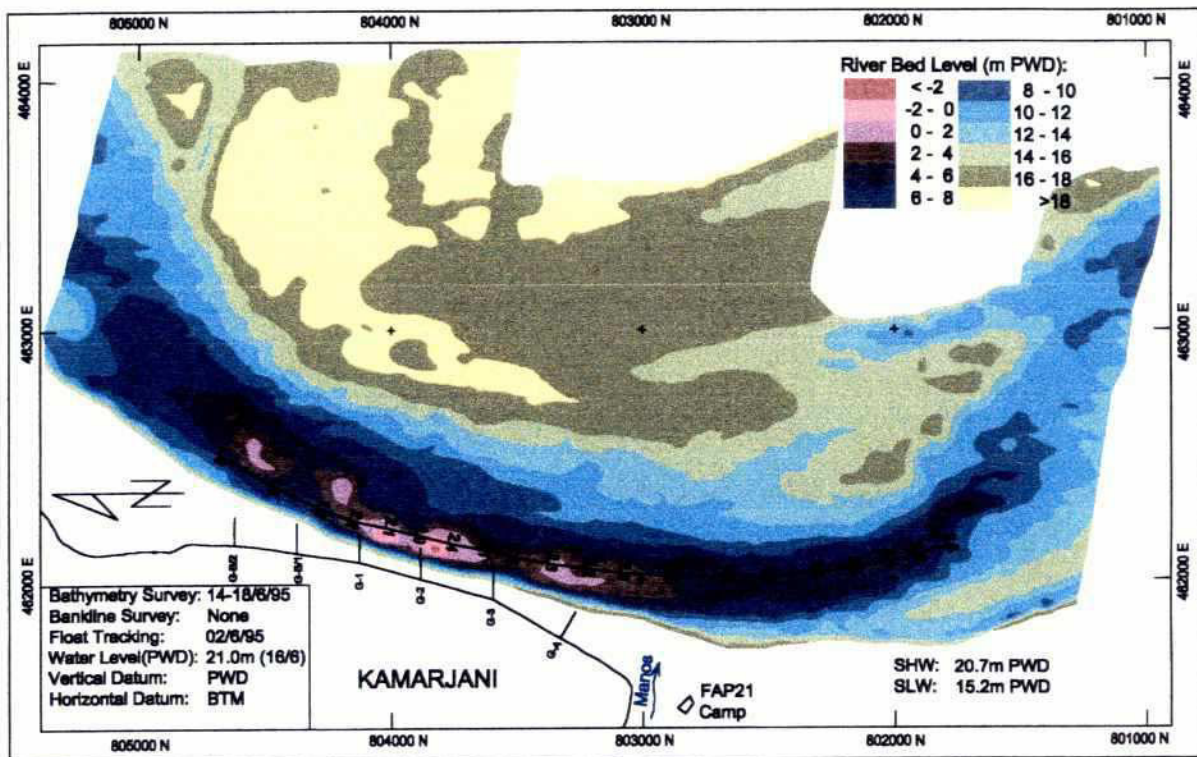


Fig. 7.1-1: Bathymetry and flow at main channel in June 1995

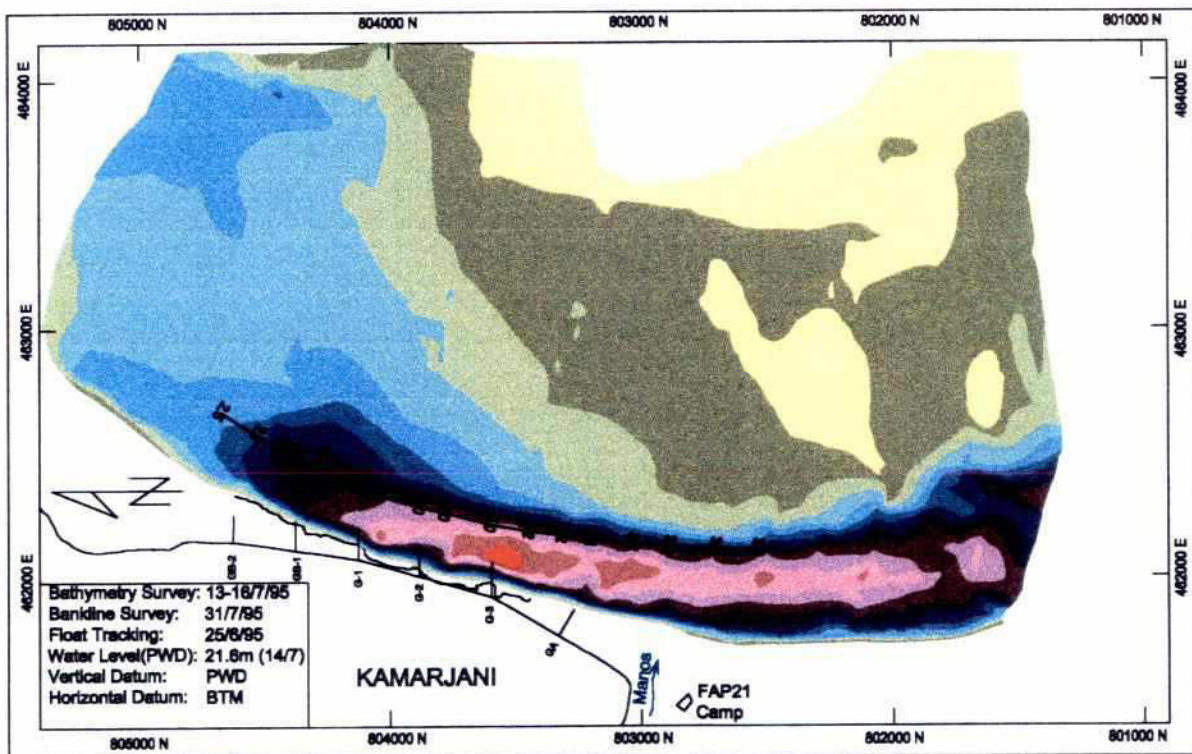


Fig. 7.1-2: Bathymetry and flow at main channel in July 1995

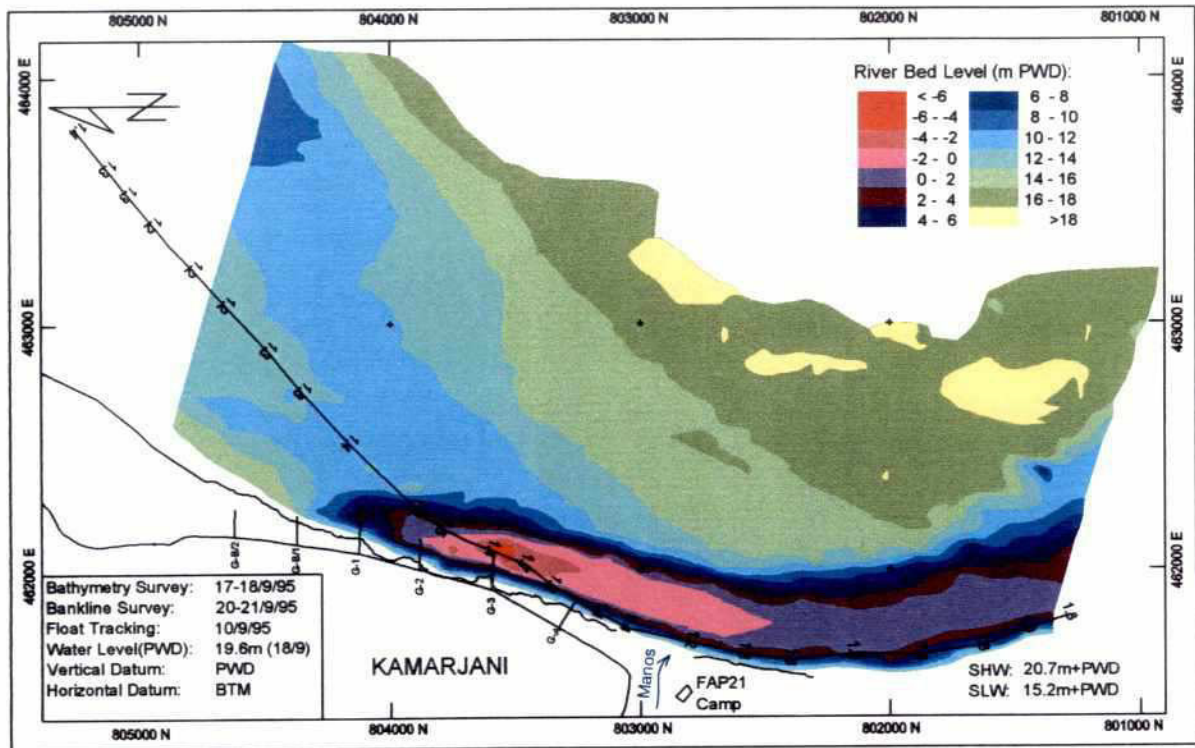


Fig. 7.1-3: Bathymetry and flow at main channel in September 1995

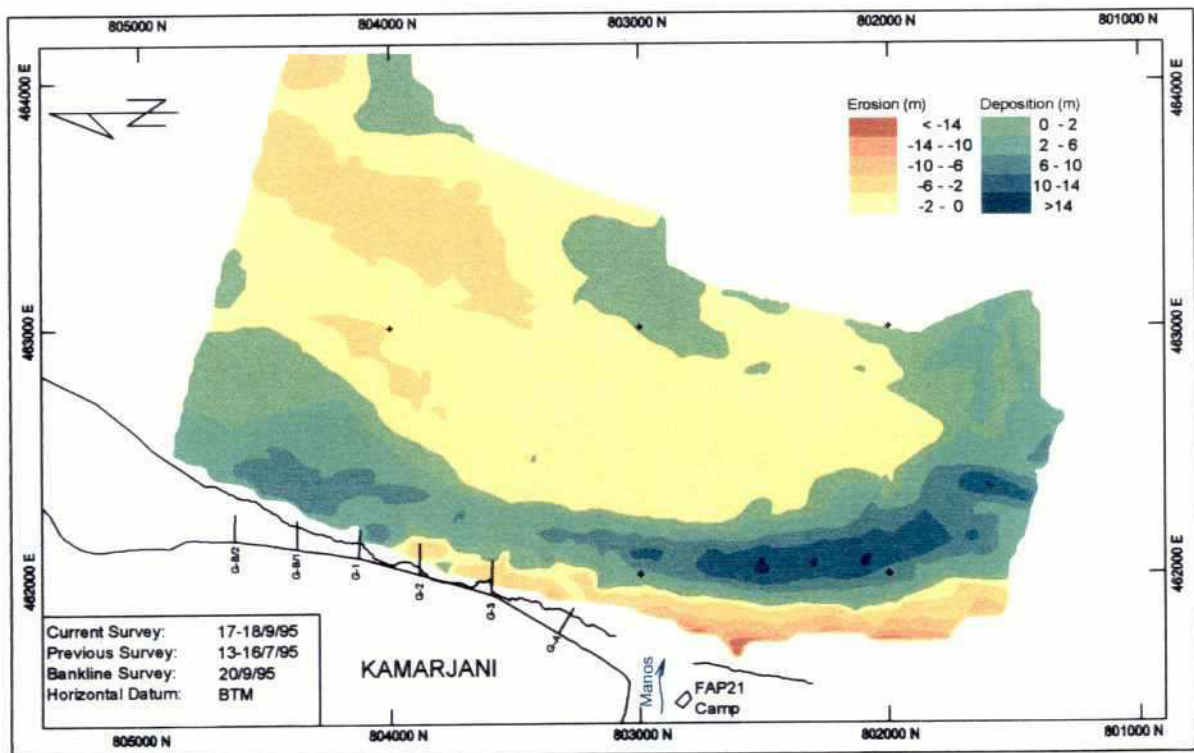


Fig. 7.1-4: Differential DGM model July 1995 – September 1995

7.2 CROSS SECTIONS AT MAIN RIVER

To get an idea about the channel dimensions and its shifting, cross sections at 4 locations, which are calculated from the main river bathymetry DTMs are presented here. The locations are:

- at 150 m upstream from groyne G-B/2 (Fig. 7.2-1)
- at groyne G-2 (Fig. 7.2-2)
- at the area of Syedpur, about 2 km downstream from G-2 (Fig. 7.2-3)
- at the area of Rasulpur, about 4 km downstream from G-2 (Fig. 7.2-4)

The cross sections start from the right bank perpendicular to the general channel direction over a length of 2000 m. The section comparison is done over 5 years showing a survey at the beginning and at the end of each monsoon season. At Rasulpur surveys have been carried out from monsoon 1997 onwards.

The bank erosion progress downstream from the structure can be derived from the section plots as well. Strongest bank erosion happened in the area of Syedpur (Fig. 7.2-3). From 1995 to 1997 the channel shifted its bed about 1 km to the main land. That means 1 km bank erosion had taken place. After the monsoon season in 1997 the bank erosion process had stopped, but it had continued 2 km further downstream in the area of Rasulpur, where about 300 m bank had been eroded from 1997 to 1999 (Fig. 7.2-4). The deepest point of the channel had been created in 1996 in front of Syedpur (21 m water depth at SHW), which confirm the strong bank erosion process at that time. Downstream from the structure the channel had become very narrow during the erosion process that led to high flow velocities as well.

The cross sections at G-2 (Fig. 7.2-2) show the continuous sedimentation of the channel in front of the structure since 1995. A char created 200 m in front of the structure in 1997 had divided the channel. The survey of September 1999 shows a distance of the main channel to the test structures of about 1 km. At the place of the main channel a char has been found in 1995.

The cross sections upstream from G-B/2 (Fig. 7.2-1) show a similar channel development as at groyne G-2. No bank erosion has taken place at this place.

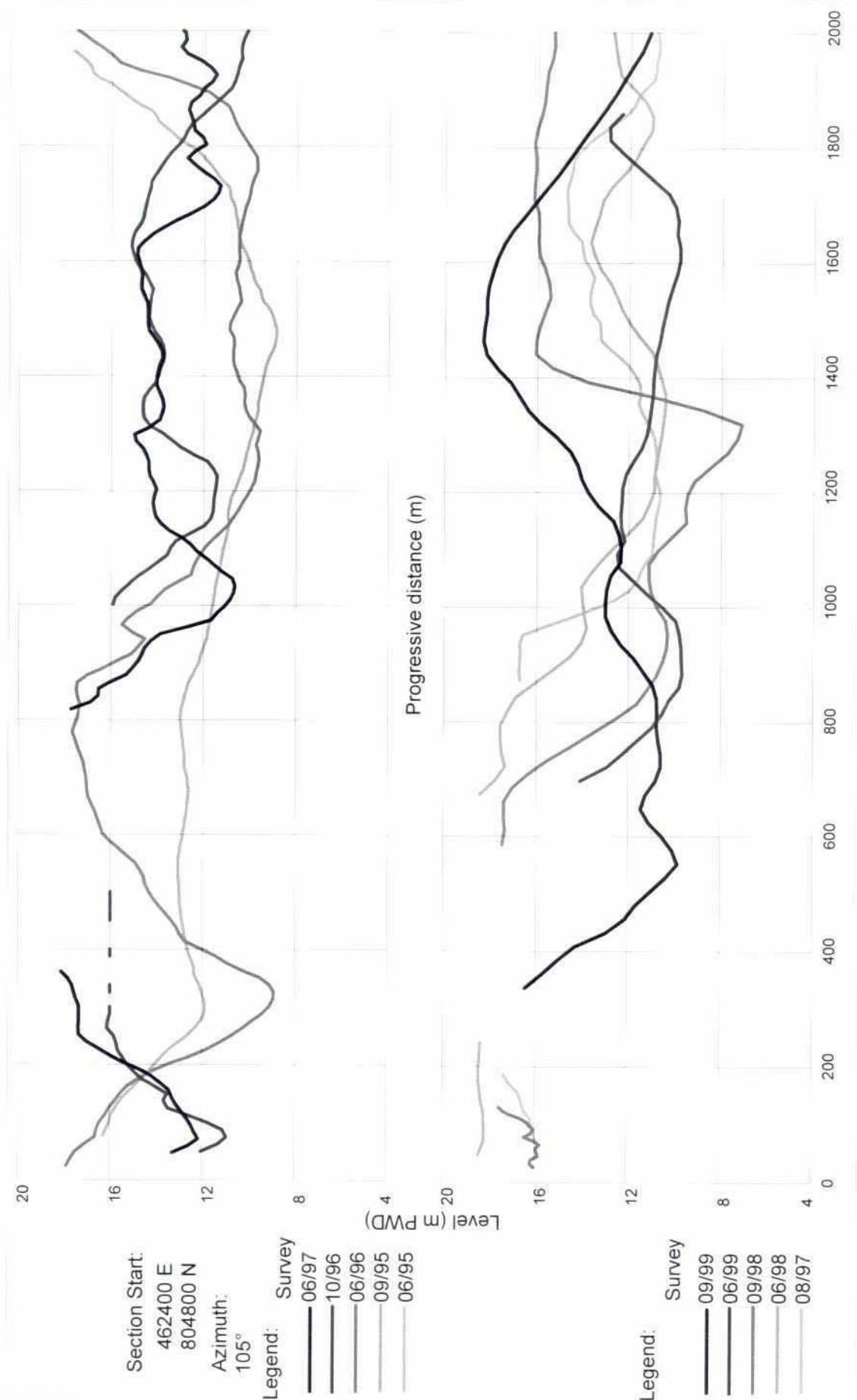


Fig. 7.2-1: Cross-section Kamarjani channel starting from 150 m upstream of G-B/2

204

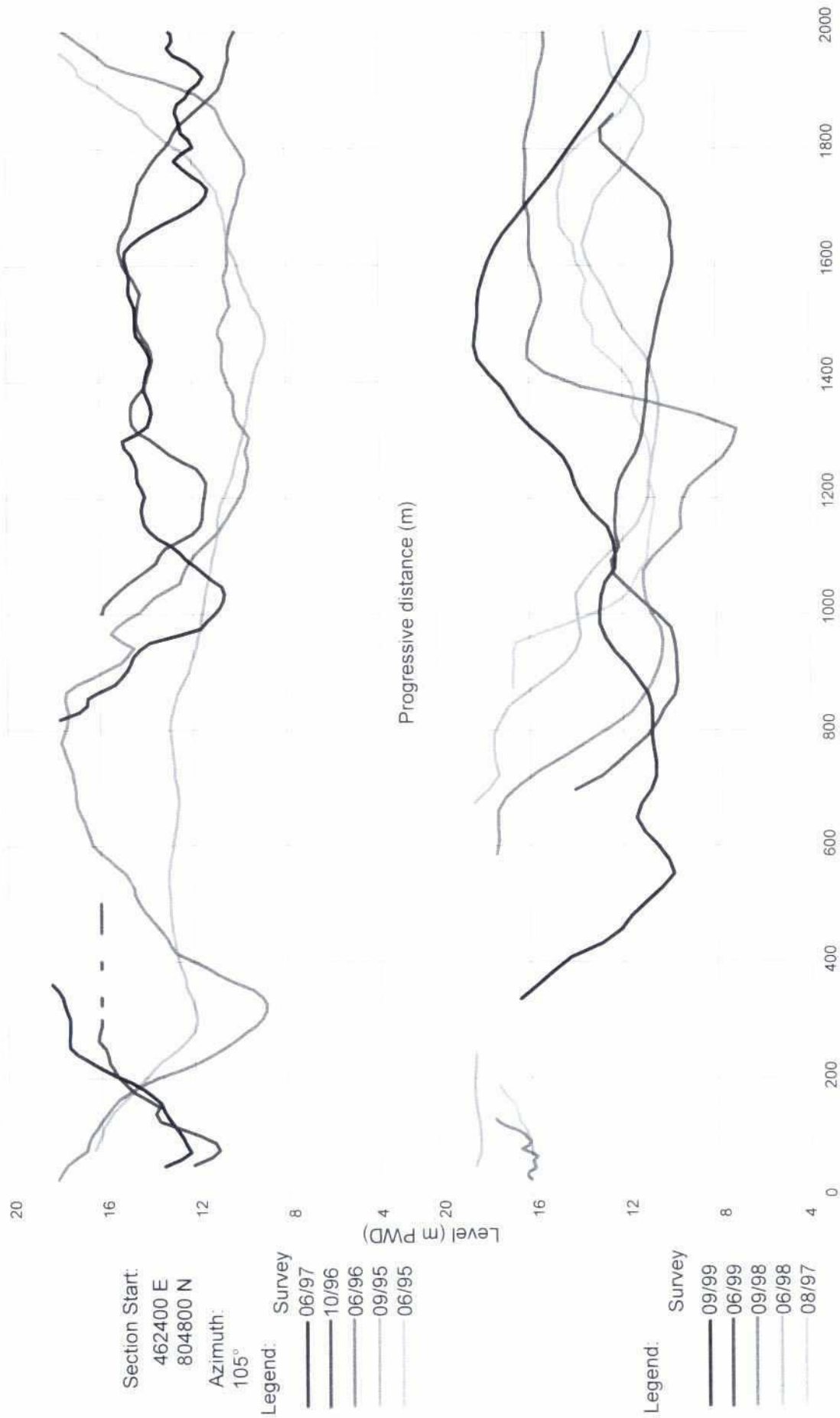


Fig. 7.2-2: Cross-section Kamarjani channel starting from G-2

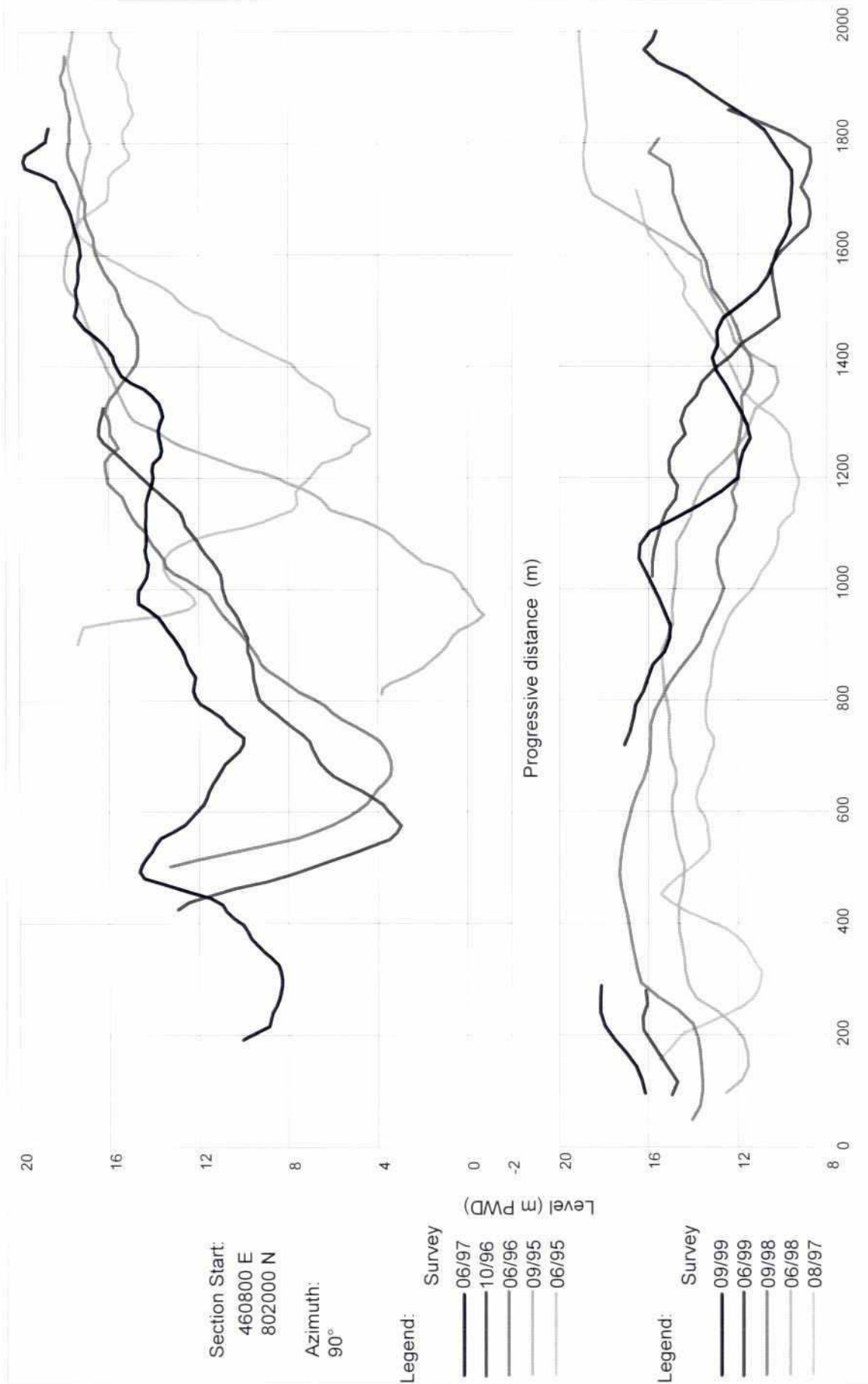


Fig. 7.2-3: Cross-section Kamarjani channel starting from Syedpur

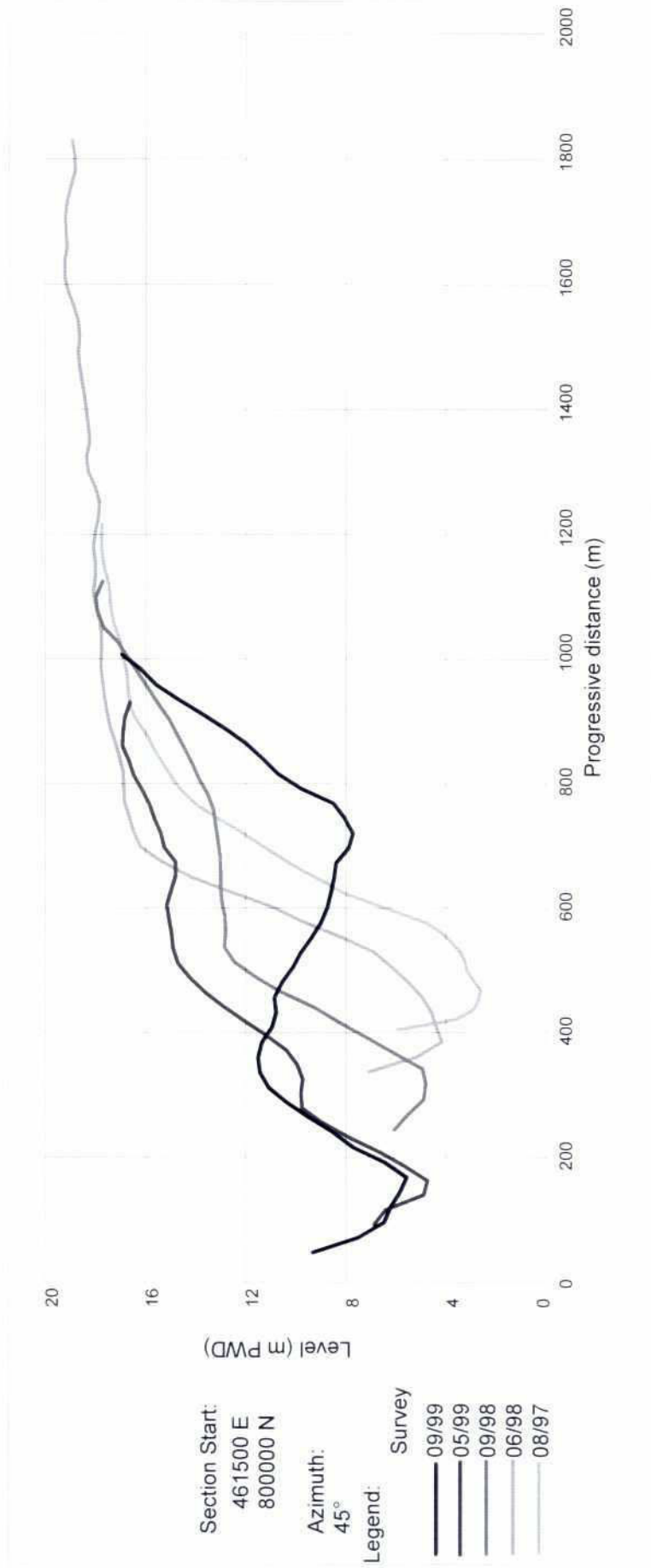


Fig. 7.2-4: Cross-section Kamarjani channel starting from Rasulpur

7.3 DISCHARGE

Discharge measurements were taken in the Kamarjani channel in front of the test site and at the entrance of the Kundarapara channel (see Fig. 1.3-3).

A discharge comparison of these channels is given in Table 7.3-1. For better comparison all figures are converted to SHW level conditions. It shows the fast developing Kundarapara channel, which discharge has increased from 1997 to 1999 by more than 300 %. The Kundarapara channel developed during the monsoon season in 1997. To get an idea of the Kamarjani discharge in 1995 and 1996 the measured cross sections at G-2 are combined with an estimated average flow. The estimation of flow velocity is based on float track data in these years.

The table shows a continuous decreasing of the Kamarjani channel discharge whereas the discharge of the Kundarapara channel is increasing fast. The corresponding discharge measurements of 1997 to 1999 are presented in Fig. 7.3-1 to Fig. 7.3-5.

Date	Kamarjani Channel				Kundarapara Channel			
	W (m)	A (m ²)	u (m/s)	Q (m ³ /s)	W (m)	A (m ²)	u (m/s)	Q (m ³ /s)
06/95	1600	11500	1.50*	17200	-	-	-	-
06/96	1600	13900	1.20*	16700	-	-	-	-
08/97	2000	12800	1.03	13200	560	3600	0.96	3400
07/98	1270	8100	1.29	10500	660	4300	1.75	7500
08/99	1470	8200	1.26	10300	1040	6900	1.63	11300

W: Channel Width

A: Cross Section Area

u: Average Flow Velocity

Q: Discharge

* Estimated from flow track data

Table 7.3-1: Discharge Kamarjani channel vs Kundarapara channel relative to SHW

222

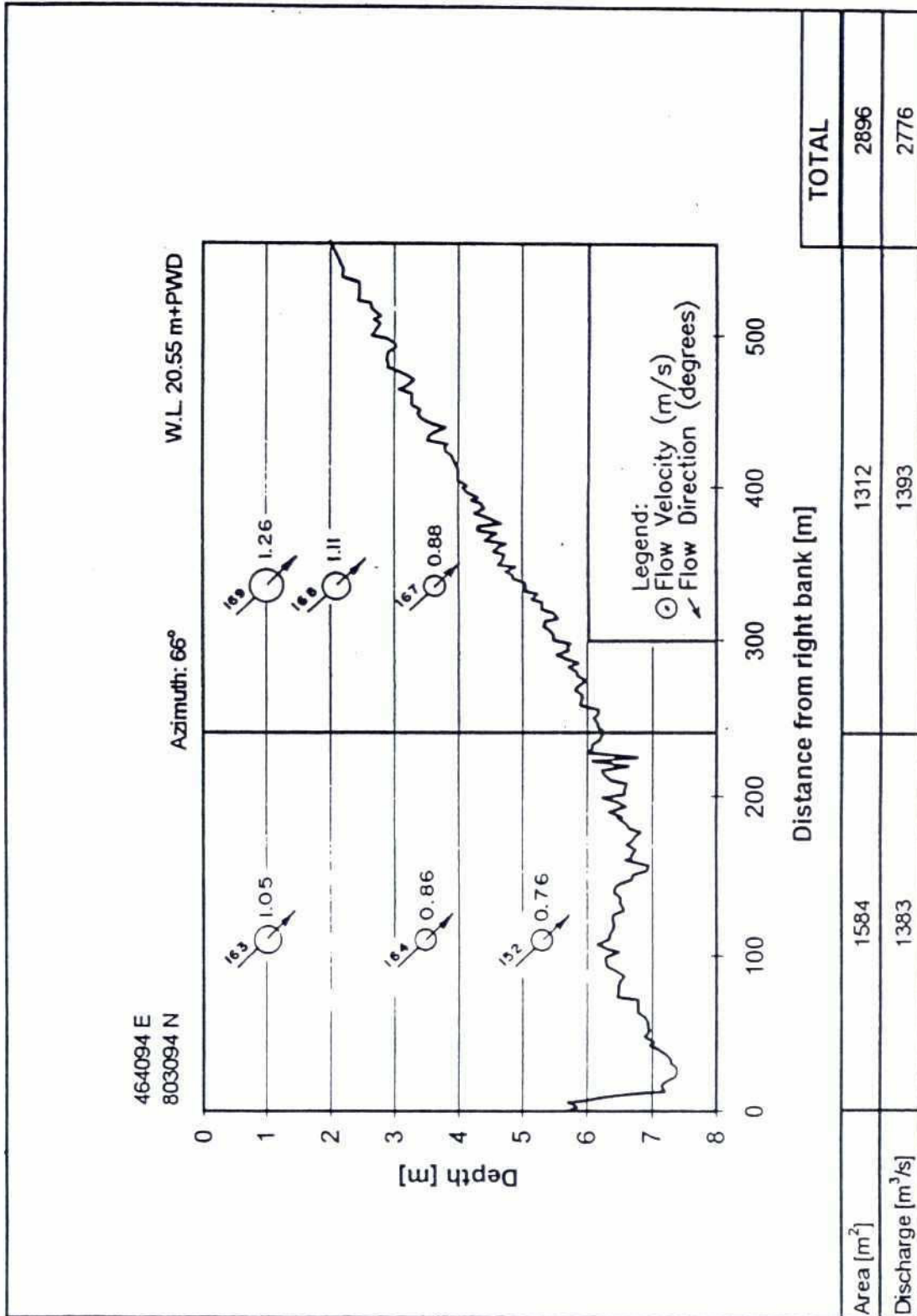


Fig. 7.3-1: Discharge measurement Kundarapara channel on August 19, 1997

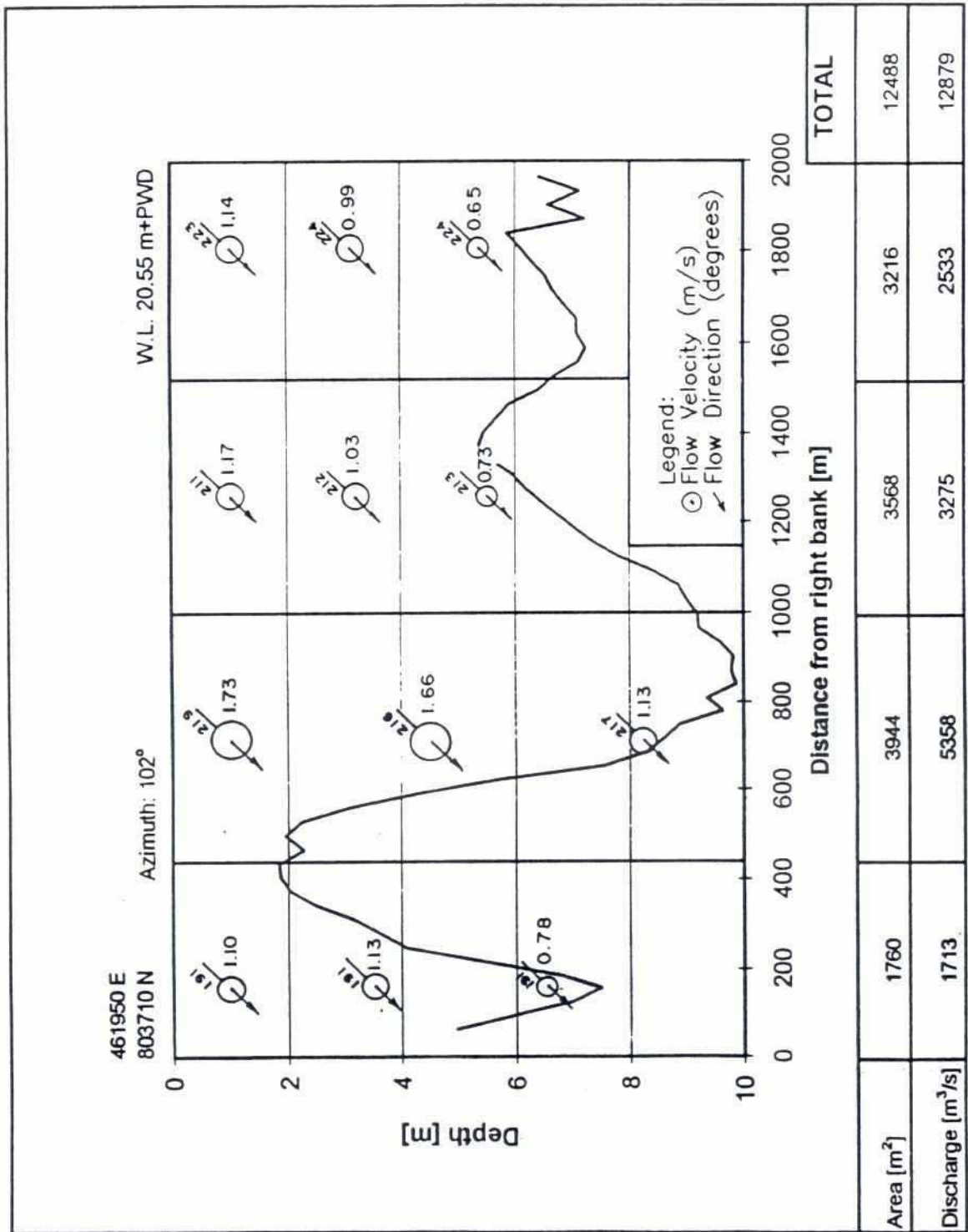


Fig. 7.3-2: Discharge measurement Kamarjani channel on August 19, 1997



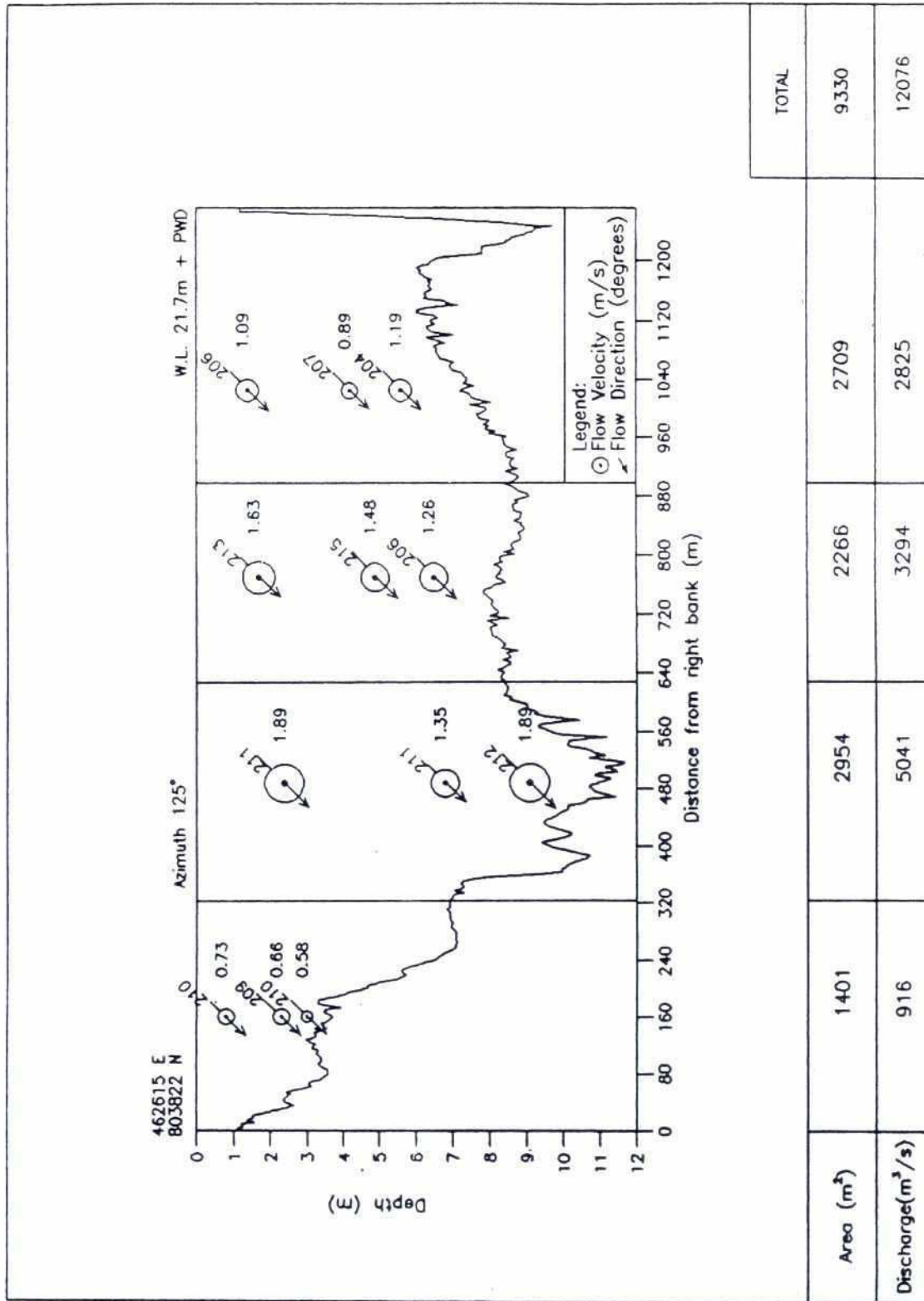


Fig. 7.3-3: Discharge measurement Kamarjani channel on July 31, 1998

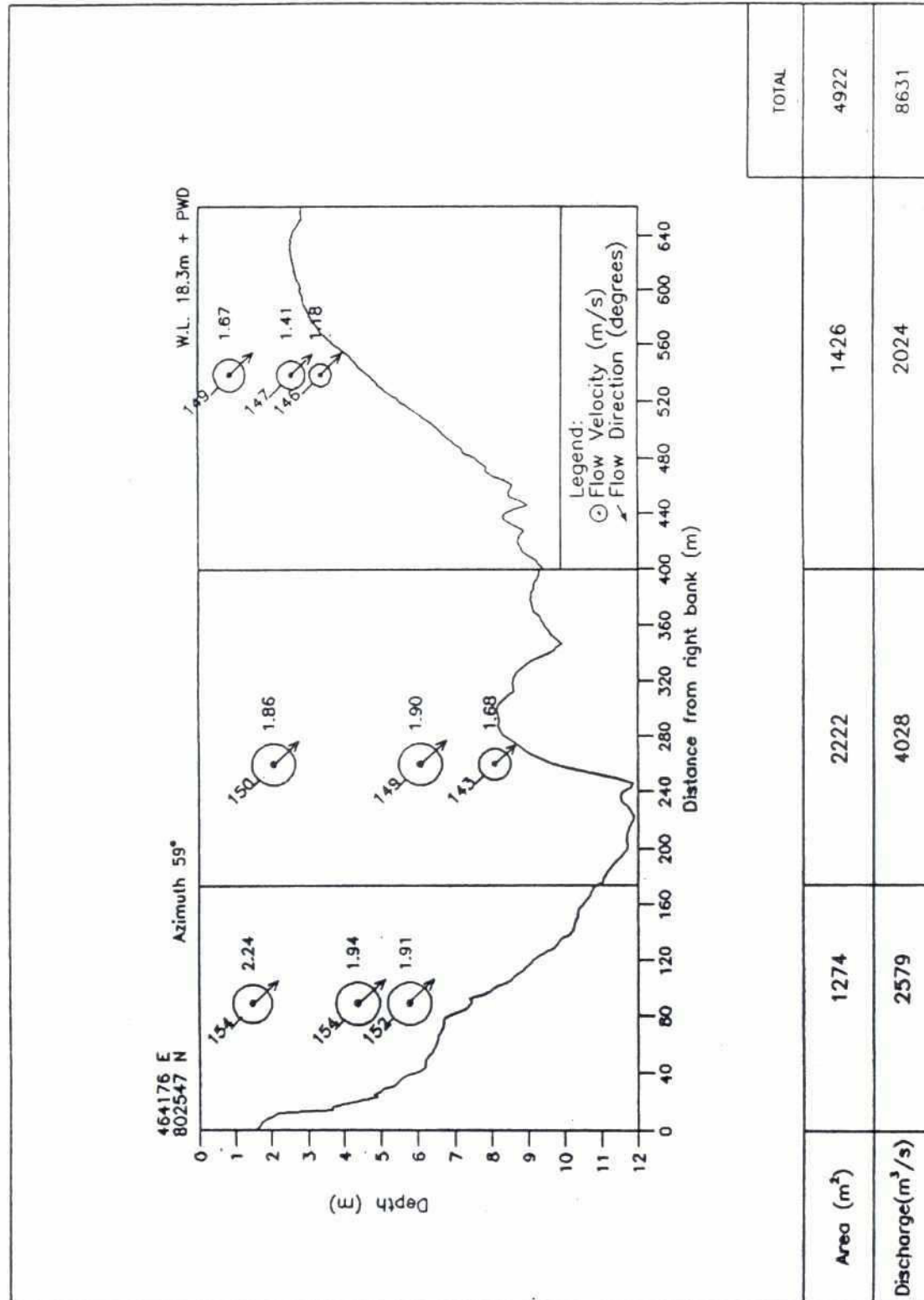


Fig. 7.3-4: Discharge measurement Kundarapara channel on July 31, 1998

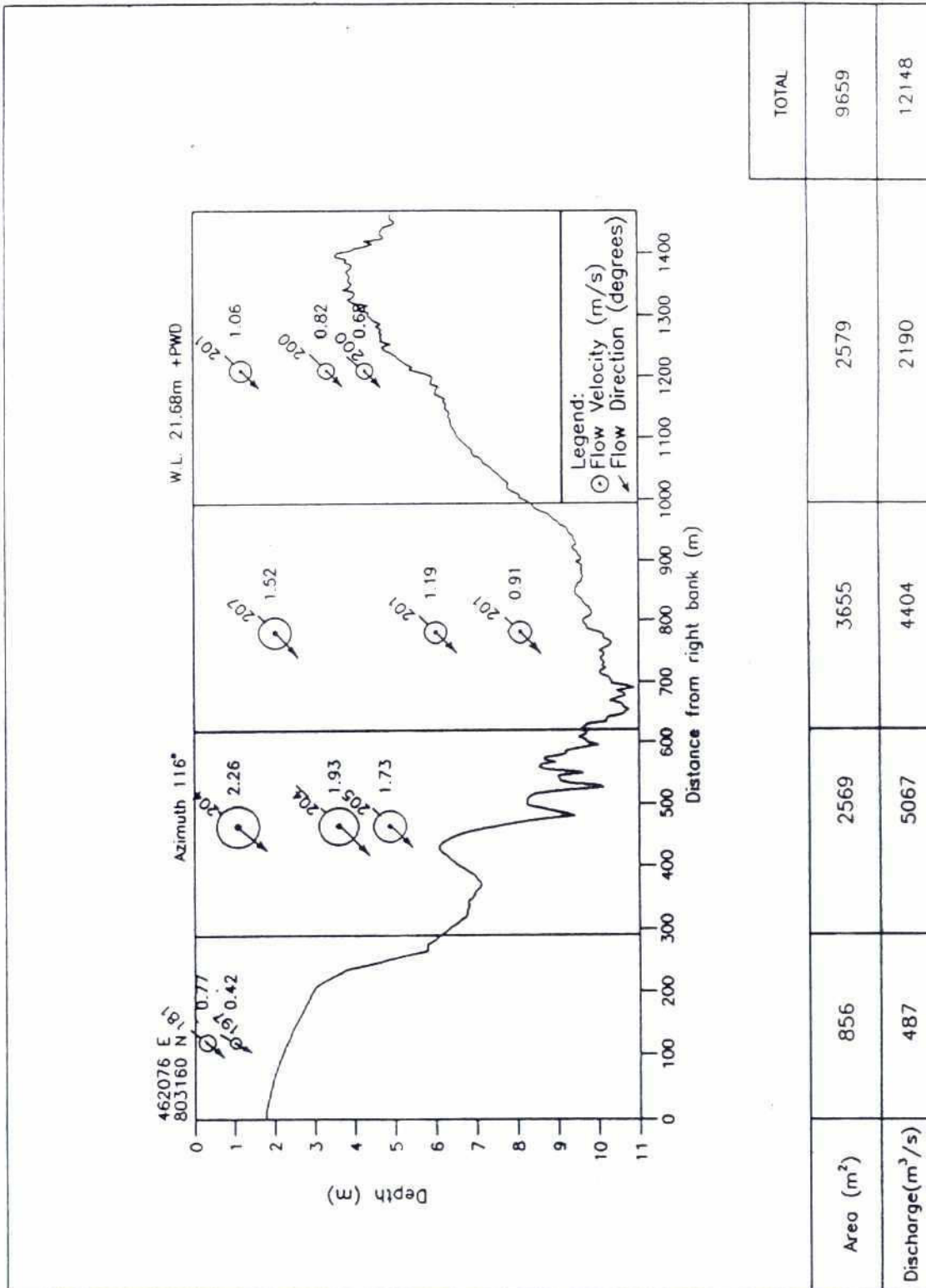


Fig. 7.3-5: Discharge measurement Kamarjani channel on August 26, 1999

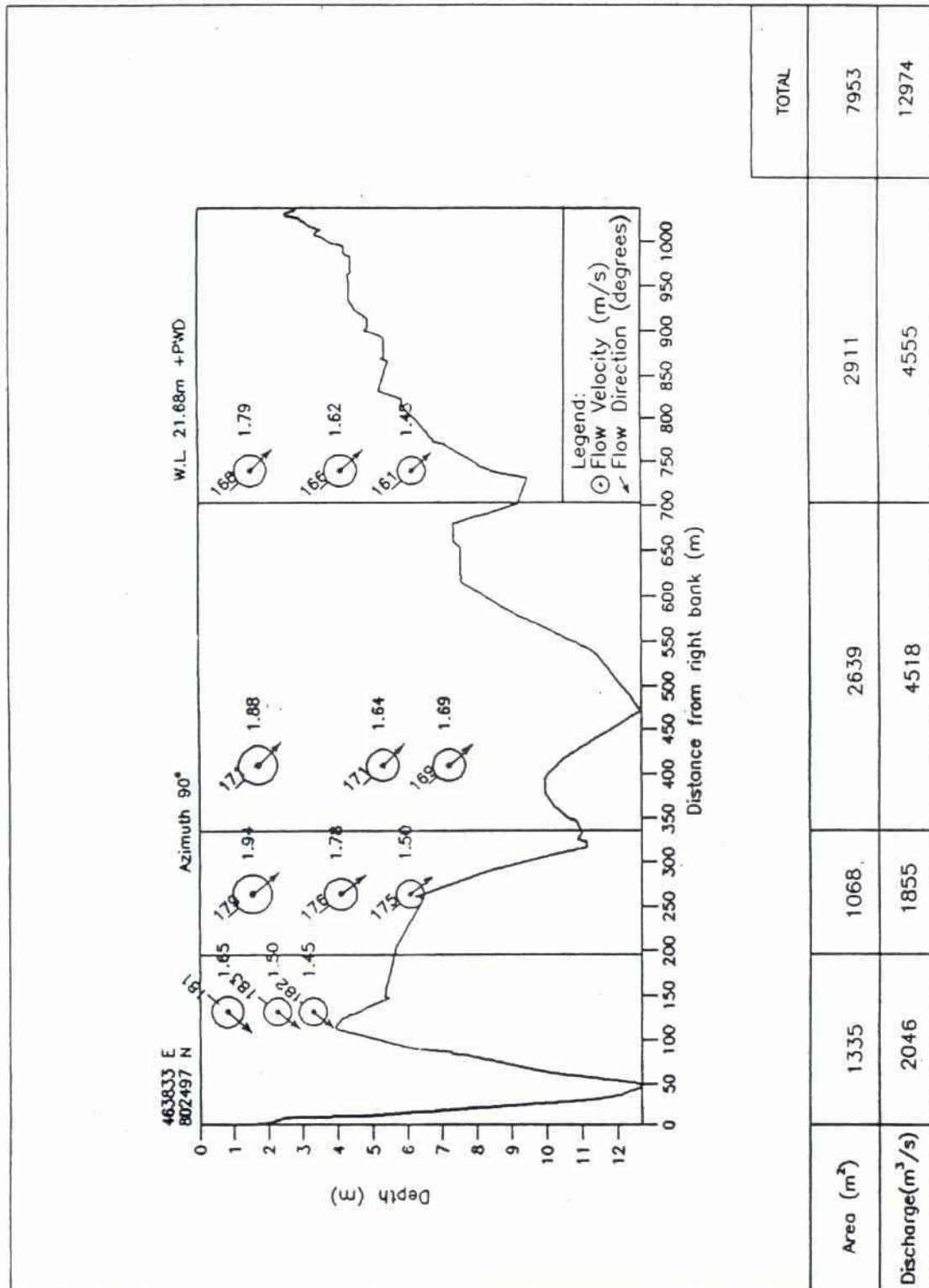


Fig. 7.3-6: Discharge measurement Kunderapara channel on August 26, 1999

8 RECOMMENDATION FOR FUTURE MONITORING OF RIVER BANK PROTECTION WORKS

8.1 NECESSITY

The monitoring of river bank protection works after their completion should be considered as a basic element of preventive maintenance and future design and must be included in the planning. Several large dimensioned structures exist along the main rivers of Bangladesh and more will be constructed. All of them are limited to a designed safety level, but there is no guarantee of permanent resistance of a structure against the river forces. The recent extreme flood conditions in Bangladesh during the monsoons 1988, 1989, 1995 and 1998 have shown the difficulty to do bank protection resistant against the river forces.

The rapid changes of the Jamuna riverbed morphology allow only short-term predictions. Therefore the planning of bank protection is difficult. Maintenance and possibly adaptation works must already be considered in the planning and the design of bank protection works.

After construction of a bank protection structure monitoring is needed to recognise at an early stage whether the structure becomes endangered and up to which extent. From the monitoring information it must be decided, whether a deterioration of the situation can be avoided or at least restricted by timely action or whether damages will occur anyhow and cannot be avoided. A decision to wait with preventive investigations until the erosion process will save at least money of unnecessary and ineffective operations. If for instance serious damages have occurred during the monsoon, there is enough time until the coming dry season to do the necessary planning and design of repair and/or adaptation works. The repair of damages or the adaptation of a structure's part must be done to keep the structure as functional as it has been designed. Moreover, The results of the monitoring activities will serve the future planning of bank protection works.

8.2 INTENSITY

Due to the test status of this project the monitoring has been carried out by high frequent and intensive measurements. Obviously such an intensity of monitoring is not needed for the purpose of controlling a regular bank protection structure.

Generally, more information is needed during monsoon. The necessary measurements are depending on the prevailing hydraulic conditions facing the structure. The conditions can be subdivided in 4 monitoring levels described as follows:

Level 0: The structure is not attacked by the river. Only shallow water and low flow velocities are in front of the structure. No erosion takes place.

A fortnightly inspection report of the site is sufficient. The inspection should concentrate on possible damages by human or animal action. It must be reported if the monitoring level has to be changed.

Level 1: The structure is slightly attacked by the river. Places of erosion and sedimentation are found in the area of the site. Flow velocities of more than 1.5 m/s are observed.

Besides a weekly inspection report 2 bathymetry surveys in combination with float tracking should be carried out during the monsoon and another survey to be done during the dry season. Possible bank erosion processes upstream, along and downstream from the structure should be quantified and reported in the weekly inspection report.

Level 2: The structure is attacked by the river. Erosion and scouring processes or water depth of more than 20 m below SHW are predominant in the channel in front of the structure. Flow velocities of more than 2 m/s are measured in the channel during the monsoon.

Bathymetry and float tracking should be carried out once during each of the monsoon months June, July, August and September. Another two surveys are to be done during the dry season. In the weekly inspection report should be mentioned which parts of the structure are particularly exposed to the river attack. Occurrences of importance like rotation flows, back flows, bank erosion should be reported as well.

Level 3: The structure is strongly attacked by the river. A critical situation exists. Probability of damages at the structure is high. Riverbed levels are close to critical design values.

If a structure reaches the monitoring level 3, preparations should be done for immediate action in case intervention is needed to prevent damages. Inspection reports should be done daily. A survey boat should be permanently placed at site to enable surveys at any required time.

Besides the described activities above according to the monitoring level status, the water level should be recorded daily.

A report form sheet (see for example the logbook form of this Project in Attachment 1) must be prepared for each site. Water level staff gauges should be installed upstream and downstream from the structure. The readings scheduled in the morning (8:00 hrs.) and in the evening (17:00 hrs) should be noted in the inspection reports. The reports should mention whether the gauges need to be shifted. Shifting of gauges has to be done perpendicular to the channel. The position has to be defined clearly and the level must be measured relative to PWD. Two gauges are needed for data validation.

8.3 LOGISTICS

Bathymetric surveys and float tracking measurements are the most appropriate survey techniques to describe the prevailing river conditions. To carry out these surveys sufficient operational survey boats are needed provided with hydrographic survey equipment and skilled personnel.

The boats should fulfil the following specifications:

- powerful and stable enough to resist strong currents and turbulence;
- easy manoeuvrable to follow straight survey lines;
- well protected against monsoon rain for equipment and personnel, cabin preferable, and
- good visibility for operator and driver.

The catamaran type of survey boat as it is used by BWDB seems to be suitable for survey operations on the Jamuna. Maintenance of the boats and the equipment must be considered.

The hydrographic equipment aboard should include the following minimum requirements:

- DGPS system^{1, 2};
- hydrographic echo sounder with digital and graphical recording;
- floats with drogues;
- hydrographic software for data collection, and
- notebook preferable like it was used in this Project (see Survey Equipment, Section 2.4).

The personnel must be skilled in hydrographic surveying and should be trained on general knowledge about monitoring of bank protection works.

The following personnel should be aboard of each survey boat:

- Surveyor, preferable with hydrographic experience (chief)

Duties:

- operating hydrographic software, DGPS, echo sounder;
- planning of survey;
- responsible for data quality and completeness;
- calibration of survey systems, and
- reporting, logsheets and delivery of data

- Electronic Engineer

Duties:

- setup of survey equipment;
- maintenance of equipment, and
- operating hydrographic software, DGPS, echo sounder.

- Boat Driver, preferable with hydrographic experience

Duties:

- boat operating;
- maintenance of boat engines, and
- responsible for safety aboard.

- Helper

It is stressed that from the experience of this Project an electronic engineer is of utmost importance.

¹ New Positioning Service by BIWTA Bangladesh Inland Water Transport Authority

The service of BIWTA shall be operational from the monsoon 2000 and will offer GPS differential corrections for all users.

The differential GPS beacon system of BIWTA consists of three reference stations at the previous Decca chain transmitter stations in Dhazari, Monirampur and Rupchandrapur, which will broadcast permanently (24 hours per day) DGPS corrections via beacon transmitters within a frequency range of 283.5-325.0 kHz (low frequency). The range of each beacon transmitter will be 500 km, guaranteeing the coverage of the whole territory of Bangladesh. The system will deliver a positioning accuracy of 1-5 m for GPS users. The correction information will be encoded in RTCM-104 data format.

To guarantee this permanently high accuracy positioning service, the system is supervised by a Central Control Station at the BIWTA office as well as a Universal Reference Station and has back-up reference stations, which will be switched on automatically in case of reference station failure. With the Universal Reference Station BIWTA is able to deliver post-processed correction data with sub-decimetres accuracy to users on request.

Leica Geosystems Inc., USA has supplied the differential GPS beacon system.

To use the BIWTA DGPS positioning service, the user has to link his GPS receiver with a telemetry receiver, which is able to receive RTCM GPS differential correction data.

² SA OFF

Since SA (Selective Availability) has been switched off in 2000, GPS offers a position accuracy of about 2m (Stand-alone mode). As long as SA is off, DGPS positioning systems are not absolutely necessary for monitoring of bank protection works.

Electronical equipment is needed for the monitoring purpose. Any failure of that equipment will interfere with the hydrographic operation.

Due to the high humid conditions a regular maintenance and service of the equipment is necessary to avoid corrosion and keep the equipment operational.

8.4 ORGANISATION

The organisation of monitoring the bank protection works should be under the authority of Bangladesh Water Development Board. A proper organisation of the monitoring is required. The logistic places must be defined for:

- Field troop bases;
- Operation and maintenance departments (O&M), and
- Dhaka Monitoring & Evaluation Centre.

The field troop bases have to be located close to the structures. It is the base of survey boats, survey equipment and the field personnel. At least two field troops should be at one base. The base should offer facilities for maintenance and repair works to keep the field troops operational. Communication to the operation and maintenance department should be provided.

The monitoring results from the surveys and the site inspections are collected and archived at the operation and maintenance departments, which are also responsible for the data processing and the evaluation. Based on these results decision have to be taken for the monitoring level of a structure and for necessary action.

The operation of the field troops is coordinated by this department. Therefore, the department should maintain contact to the field troop bases. It has to be guaranteed that important measurements can be processed within 2 days after the decision is made to carry out a survey.

The Dhaka Monitoring & Evaluation Centre should maintain and serve a database for all monitoring data. All processed data from the O&M departments shall be collected in that organisation. A suitable graphic information system (GIS) has to be defined for a quick access to all data.

Besides the surveyed monitoring data information from satellite images should be collected as well. These images will provide information about the global channel development at the structures. These information should be passed to the O&M departments to help them in their monitoring planning.

REFERENCES

- Bangladesh University of Engineering and Technology, Dhaka (1982), A Text Book of Surveying
- Consulting Consortium FAP 21/22 (1993 a), Final Planning Study Report, Vol. IA
- Consulting Consortium FAP 21/22 (1993 b), Final Planning Study Report
Vol. V, Annex 12: Surveys
- Consulting Consortium FAP 21/22 (Dec. 1994), Update of Morphological Predictions for Test Areas,
Annexes
- Consulting Consortium FAP 21/22 (Jun. 1995 - 1999), Monthly Monitoring Reports
- Consulting Consortium FAP 21/22 (Jun. 1995 - 1999), Monthly Monitoring Logbooks
- Consulting Consortium FAP 21/22 (Mar. 1996), Monitoring and Adaptation Report 1995
Kamarjani Test Site, Interim Report, Main Report
- Consulting Consortium FAP 21/22 (Mar. 1996), Monitoring and Adaptation Report 1995
Kamarjani Test Site, Interim Report, Annexes
- Consulting Consortium FAP 21/22 (Sep. 1996), Monitoring and Adaptation Report
Kamarjani Test Site, Monsoon 1995 , Main Report
- Consulting Consortium FAP 21/22 (Sep. 1996), Monitoring and Adaptation Report
Kamarjani Test Site, Monsoon 1995, Annexes
- Consulting Consortium FAP 21/22 (Sep. 1998), Monitoring and Adaptation Report
Kamarjani Test Site, Monsoon 1996
- Consulting Consortium FAP 21/22 (Mar. 1999), Monitoring and Adaptation Report
Kamarjani Test Site, Monsoon 1997
- River Survey Project FAP 24 (Nov. 1996), Final Report, Annex 1: Surveys

Attachment 1
Logbook Form Sheet

Date: / /		Radio contact with/at [hrs.]		Emergency message reported	
Page 1		Dhaka CSE		To: at: hrs.	
METEOROLOGICAL DATA recorded at: hrs.					
Temperature [°C]	Rainfall [mm]	Wind Direction	Wind Speed [m/s]		
WATER LEVEL DATA - Gauge readings [m PWD]					
Gauge at G-A			Gauge at G-B/1		
8.00 hrs.	13.00 hrs.	17.00 hrs.	8.00 hrs.	13.00 hrs.	17.00 hrs.
WAVE OBSERVATIONS (gauge readings at G-2)					
Time	Duration	Wave height [m]	Wave [s]	Wave Direction	Wind Direction Speed [m/s]
VISUAL CONTROL OF TEST STRUCTURES (add Special Damage Report, if required)				Time of Inspection: hrs.	
Location	Impermeable Groyne	Permeable Groyne	Floating Debris		
			Area [m x m]	Thickness	
G - B/1					
G - B/2					
G - 1					
G - 2					
G - 3					
G - A					
G - A/2					
BANKLINE OBSERVATIONS (changes, location, progress / use page 2 for sketch, measurements)					
MONITORING SURVEYS CARRIED OUT					
Bathymetry from:		to:		Rolls. No.	
Current Measurements	Location:			Float Trackings:	
	Cross-section:				
Bankline Survey:			Char Survey:		
Reported by:		Checked:		Seen CSE:	

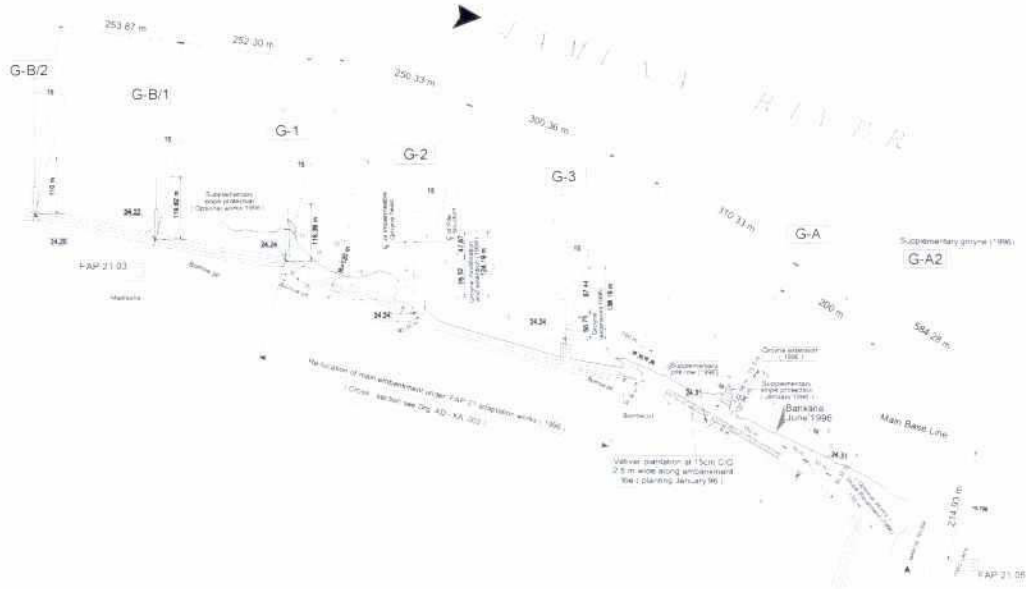
(to be used for sketches, measurements, special notes, etc. to support
the daily observations and activities)

Date: / /
Page 2

Photos taken Film No.: Picture Nos.:

Location Plan of Test Structures

(mark location of photos, measurements, special observations, etc.)



Reported by:

Checked:

CSE:

Attachment 2
Data Archive System FAP 21

DATA ARCHIVE SYSTEM

All kind of digital monitoring data is stored on PD-Cartridge (optical disk of 650 MB capacity) It will be available on CD-ROM as well.

The chosen data format is ASCII. A flow chart of the directory structure is given in Fig. 1. The storage is done monthly according to the source of data.

Besides the survey data report documentation and figure plots are stored as well.

The different types of data described in the flow chart by abbreviations are explained as follows:

- **Bankline:** All bankline surveys of the selected month.
 File convention: BLddmmyy.COA
 Format: Plot code, point No. Easting, Northing, Height
 Height measurements cannot be used.
- **Bathy:** All bathymetry surveys of the selected month subdivided by area (groyne, test site, main channel).
 Raw data (*.log) and
 processed data (*.geo).
 Each survey profile is stored in one file.
 Format: Time, Fix Number, Easting, Northing, PWD Height
- **Charline:** All waterline surveys of the selected month.
 File convention: WL ddmmyy.COA
 Format: like bankline
- **Current:** All current point measurements (Valeport).
 Raw data files: one file for each probe storage.
 Processed data files (word documents) of one day including corresponding position, time period of measurement, mean velocity and mean direction including standard deviation.
 File convention of processed data: VAddmmyy.DOC
- **Float:** All float track data of the selected month subdivided by conventional and advanced float track data.
 Raw data and processed data.
 File convention of processed data: ddmm-00a.FLT.
 00, 15, 30: selected depth of drogue in dm.
 a, b, c, d....: counting of tracks
- **Monitor:** All collected data from the monitoring station of the selected month subdivided by:
 STD: Standard Measurements
 Date, Time, Water Level, Wave Height, Wind Velocity, wind direction.
 Data interval of 10 minutes.
 STM: Storm Measurements
 Like STD, but data interval of 30 seconds.
 TP: Test Pile Recordings
 Inclination and acceleration of test pile during storm conditions
- **Tables:** Masterchart format files like definition of charts, tracklines, etc.
- **Topo:** All topographic surveys of the selected month
 File convention: TOddmmyy.GEO
 Format: Point Number, Easting, Northing, Height

224

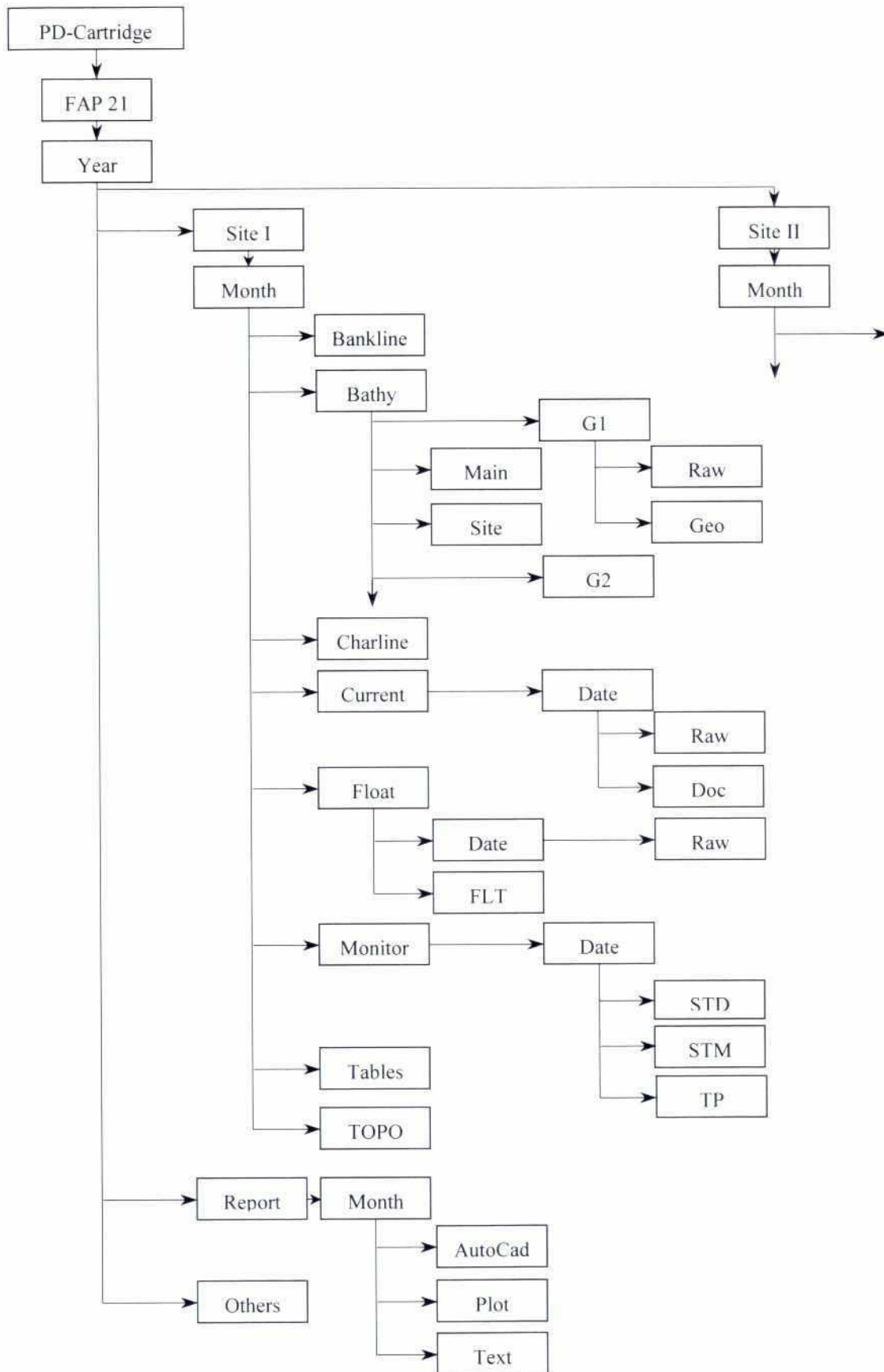


Fig. A.2-1: Flow chart of data archive system

Attachment 3

Inventory of Monitoring Data



1 INVENTORY OF MONITORING DATA

1.1 BATHYMETRY

Inventory of Bathymetry Survey Monsoon 1995 - 1999

Sl. No.	Survey Type*	Test Site-I, Kamarjani Area**	Date	Line Spacing (m)	Water Level (m+PWD)
1	G	G3	02/05/95	5	16.7
2	G	G1-G2	03/05/95	5	16.9
3	S	site (-350/500)	18-19/05/95	10	17.9-18
4	G	G1-G2	20/05/95	5	18.4
5	G	G2-G3	21/05/95	5	18.9
6	G	G2	22/05/95	5	19.4
7	M	main channel (-250/1750)	23/05/95	100	19.6
8	G	G2	28/05/95	5	20.0
9	G	G2	29/05/95	5	19.8
10	G	G2	01-02/06/95	5	19.4
11	G	G3	06/06/95	5	19.2
12	G	G1	07/06/95	5	19.0
13	G	G2	08/06/95	5	19.1
14	S	site (-350/500)	09-10/06/95	10	19.2
15	M	main channel (-1500/2200)	14/06/95	100	21.2
16	G	G1-G2	20/06/95	5	21.3
17	G	G1	21/06/95	5	21.3
18	S	site (-300/350)	22-24/06/95	5, 10	21.2
19	G	G2-G3	25/06/95	10	21.0
20	S	site (-300/350)	26-27/06/95	10	21.1-21.0
21	S	site (-300/400)	29/06/95	10	20.7
22	G	G3	01/07/95	10	20.7
23	G	G3	02/07/95	10	20.8
24	G	G1	03/07/95	10	21.0
25	G	G2	08/07/95	10	22.1
26	S	site (-300/400)	09-10/07/95	10	22.3-22.4
27	S	site (-330/400)	11/07/95	10	22.3
28	S	site (-50/400)	12/07/95	10	22.0
29	G	G2	14/07/95	10	21.6
30	M	main channel (-1100/2400)	13-16/07/95	200	21.9-21.3
31	G	G3	15/07/95	10	21.5
32	S	site (-300/370)	17/07/95	10	21.3
33	S	collapsed part of embankment	19/07/95	10	21.2
34	S	site (10/370)	20/07/95	10	21.2
35	G	site (-300/400)	31/07/95	10	20.4

Sl. No.	Survey Type*	Test Site-I, Kamarjani Area**	Date	Line Spacing (m)	Water Level (m+PWD)
36	S	site (-300/400)	01-02/08/95	10	20.4
37	S	site (-350/500)	05/08/95	10	20.3
38	G	GB1 + GA	06/08/95	10	20.3
39	S	site (-300/400)	10/08/95	10	20.0
40	S	site (-300/400)	14/08/95	10	21.1
41	G	GB1+ GA	15/08/95	10	21.3
42	S	site (-300/400)	16/08/95	10	21.5
43	M	main channel (-1100/2400)	17-18/08/95	10	21.7
44	S	site (-550/650)	20-21/08/95	10	21.4
45	G	G3	23/08/95	10	21.0
46	S	site (-310/650)	24-25/08/95	10	20.8
47	G	GB1	26/08/95	10	20.5
48	S	site (-550/650)	27-29/08/95	10	20.9-20.4
49	M	main channel (-1100/2400)	30-31/08/95	200	20.3
50	S	site (-300/400)	03-04/09/95	10	20.0-19.8
51	S	site (-540/400)	07-08/09/95	10	19.7
52	G	G3	09-10/09/95	10	19.7-19.5
53	S	site (-270/650)	11-12/09/95	10	19.5-19.6
54	S	site (-300/400)	15-16/09/95	10	19.7
55	M	main channel (-850/2400)	18/09/95	200	19.6
56	S	site (100/650)	19-20/09/95	10	19.5
57	S	site (-500/650)	24-25/09/95	10	20.7-20.8
58	M	main channel (-1850/2600)	02-04/10/95	100	20.9-20.6
59	S	site (-550/650)	07-08/10/95	10	20.2-19.9
60	S	site (-240/650)	10-11/10/95	10	19.4-19.2
61	S	site (-550/650)	13-14/10/95	10	18.9-18.8
62	S	site (550/1400)	16/10/95	10	18.6
63	M	main channel (-1800/2600)	18/10/95	100	18.4
64	S	site (550/1400)	23-24/10/95	10	17.9
65	S	site (-550/650)	26-27/10/95	10	18.1-18.0
66	M	main channel (-1800/2600)	09-13/11/95	100	16.6-17.1
67	S	site (-300/650)	14/11/95	10	16.9
68	S	site (550/1400)	15/11/95	10	16.7
69	S	site (-300/650)	13-15/12/95	10	15.4
70	M	main channel (-1800/2600)	16-17/12/95	100	15.3
71	S	site (550/1300)	17/12/95	10	15.3
72	S	site (-300/650)	22-23/12/95	10	15.2
73	M	main channel (-1800/2600)	26-27/12/95	100	15.2-15.1
74	S	site (800/1400)	01/01/96	10	15.1
75	S	site (-240/650)	05/01/96	10	15.0
76	M	main channel (-1600/2400)	09-11/01/96	100	14.8
77	S	site (-220/800)	15/01/96	10	14.7

A.3-3

Sl. No.	Survey Type*	Test Site-I, Kamarjani Area**	Date	Line Spacing (m)	Water Level (m+PWD)
78	S	site (550/1400)	18/01/96	10	14.7
79	S	site (-240/800)	20/01/96	10	14.7
80	M	main channel (-1600/2400)	25-26/01/96	100	14.6
81	S	site (-170/800)	01-02/02/96	10	14.5
82	S	site (550/1400)	05-06/02/96	10	14.4
83	M	main channel (-1900/1600)	08-10/02/96	100	14.4
84	S	site (-230/800)	13/02/96	10	14.3
85	M	main channel (-1600/2400)	28-29/02/96	100	14.2-14.3
86	S	site (-220/800)	08/03/96	10	14.5
87	M	main channel (-1100/2400)	13-14/03/96	100	14.5
88	G	GA	24/03/96	10	15.2
89	S	site (-290/800)	26/03/96	10	15.7
90	M	main channel (-1600/2400)	01-03/04/96	100	15.9
91	G	GA	05/04/96	10	15.6
92	G	GA	11/04/96	10	15.9
93	S	site (-300/800)	19/04/96	10	16.0
94	M	main channel (-1600/2400)	02-03/05/96	10	17.7
95	S	site (-120/800)	07-08/05/96	10	17.1-17.4
96	S	site (-300/750)	15-16/05/96	10	19.5-19.6
97	S	site (-300/780)	26/05/96	10	19.1
98	G	GA2	28/05/96	10	18.8
99	M	main channel (-1600/2400)	31/05 - 03/06/96	100	18.9-19.7
100	S	site (-300/900)	06-08/06/96	10	19.8-19.5
101	S	site (-290/1000)	11-12/06/96	10	19.4-19.3
102	S	site (240/1450)	14-15/06/96	10	18.9-18.7
103	G	G3	16/06/96	10	18.6
104	S	site (-500/800)	25-27/06/96	10	18.6-19.6
105	M	main channel (-2100/2400)	28-30/06/96	100	20.3-21.0
106	S	site (-800/850)	03-05/07/96	10, 20	21.4-21.6
107	S	site (-800/840)	13-15/07/96	10, 20	21.6-21.1
108	G	G3	16/07/96	10	22.0
109	S	site (-500/400)	19-20/07/96	10, 20	22.1-22.0
110	M	main channel (-2100/2400)	18, 21, 23, 24/07/96	100	22.0-21.7
111	S	site (-800/870)	27-28/07/96	10, 20	21.3-21.1
112	S	site (-850/600)	01-04/08/96	10, 20	20.7-20.6
113	M	main channel (-2100/2400)	11-15/08/96	100	20.3-20.8
114	S	site (-810/600)	17-19/08/96	10, 20	21.0-21.1
115	S	site (-860/870)	24-25/08/96	10, 20	20.6-20.5
116	M	main channel (-2100/2400)	26-28/08/96	100	20.1-20.2
117	S	site (-780/600)	03-05/09/96	10, 20	20.9-20.7
118	M	main channel (-2100/2400)	08-10/09/96	100	20.5-20.6
119	M	Rasulpur area	13/09/96	100	20.4

Sl. No.	Survey Type*	Test Site-I, Kamarjani Area**	Date	Line Spacing (m)	Water Level (m+PWD)
120	S	site (-500/650)	17. 23/09/96	10, 20	19.7-18.9
121	S	site (-850/1200)	05-07/10/96	10, 20	19.8
122	M	main channel (-2100/2400)	19-21/10/96	100	18.3-18.0
123	S	site (-850/1200)	23-24/10/96	20	17.7-17.6
124	S	site (-850/1200)	04/12/96	20	15.7
125	M	main channel (-2100/2400)	12-13/12/96	100	15.4-15.2
126	S	site (-600/1200)	26/12/96	20	15.0
127	S	site (-700/1200)	06-07/01/97	20	14.7
128	M	main channel (-1900/2600)	14-17/01/97	100	14.6
129	S	site (-700/1300)	26/01/97	20	14.4
130	S	site (-300/1300)	12-13/02/97	10, 20	14.6
131	M	main channel (-1900/2600)	14-15/02/97	100	14.4
132	G	GA2	23/02/97	10	14.5
133	S	site (-300/1300)	25/02/97	20	14.6
134	S	site (-250/1200)	06/03/97	10, 20	14.5
135	M	main channel (-1600/2400)	12-14/03/97	100	14.6
136	G	GA2	16/03/97	100	14.7
137	S	site (-850/1200)	26/03/97	20	16.0
138	S	site (-850/1200)	06-07/04/97	20	16.0
139	M	main channel (-1900/2600)	15-16/04/97	100	16.0
140	S	site (-850/1200)	28/04/97	20	16.2
141	S	site (-850/1200)	08-09/05/97	20	16.1-16.2
142	M	main channel (-1900/2600)	15-16/05/97	100	16.8-16.9
143	S	site (-850/1200)	24-25/05/97	20	17.4-17.6
144	S	site (-850/1200)	07-11/06/97	20	18.3-19.3
145	M	main channel (-1600/2400)	19-20/06/97	100	20.9-20.9
146	S	site (-850/1200)	28-30/06/97	20	20.1-20.3
147	M	main channel (-1600/2400)	02-18/07/97	100	20.8-20.6
148	M	main channel (-1100/3900)	13-18/07/97	100	22.1-21.4
149	S	site (-850/1200)	24-25/07/97	40	20.5-20.3
150	M	main channel (-1600/3900)	02-04/08/97	100	19.5-19.4
151	S	site (-850/1200)	17/08/97	40	20.7
152	M	main channel (-1600/3400)	21-24/08/97	100	20.6-20.2
153	S	site (-850/1200)	09/09/97	40	19.5
154	S	site (-850/1200)	28/09/97	40	20.6
155	M	main channel (-1600/2400)	25-26/10/97	100	17.3-17.2
156	S	site (-600/1200)	26/10/97	40	17.2
157	M	main channel (-1100/3200)	17-20/11/97	100	16.2
158	M	main channel (-1600/3200)	12-13/12/97	100	16.0
159	S	site (500/1100)	27/12/97	10	16.0
160	S	site (800/1200)	30/12/97	20	16.0
161	M	main channel (-1100/3200)	06-08/01/98	100	15.9

Sl. No.	Survey Type*	Test Site-I, Kamarjani Area**	Date	Line Spacing (m)	Water Level (m+PWD)
162	M	main channel (-1100/5900)	23-24/01/98	100	15.8
163	M	main channel (-1600/3400)	22-26/02/98	100	15.4-15.3
164	M	main channel (-1100/3800)	22-23/03/98	100	15.2
165	M	main channel (-1600/5900)	19-24/04/98	100	16.1-16.5
166	M	main channel (-1600/2800)	20-22/05/98	100	17.8-17.5
167	M	main channel (-4100/5900)	23-30/06/98	100	21.3-21.5
168	S	site (-800/1200)	08/07/98	40	21.1
169	M	main channel (-2100/5900)	22-26.30/07/98	100	22.0-22.2
170	S	site (-800/1200)	09/08/98	40	21.5
171	M	main channel (-5100/5900)	22-29/08/98	100	22.9-21.7
172	S	site (-800/1200)	17/09/98	40	20.3
173	M	main channel (-5100/6400)	23-28/09/98	100	19.6-19.5
174	M	main channel (-5100/2900)	26-30/10/98	100	19.7-19.3
175	M	main channel (-5100/4400)	23-27/11/98	100	16.6-16.5
176	M	main channel (-5100/4800)	23-29/12/98	100	15.7-15.5
177	M	main channel (-5100/6800)	24-28/01/99	100	15.05-14.95
178	M	main channel (-5100/6800)	21-24/02/99	100	14.7
179	M	main channel (-5100/6800)	17-21/03/99	100	14.6-14.8
180	M	main channel (-5100/6800)	21-28/04/99	100	15.5-15.9
181	M	main channel (-5100/4800)	28-30/05/99	100	17.8-18.7
182	M	main channel (-4600/4800)	01-06/07/99	100	21.3-21.5
183	M	main channel (-5100/4800)	18-23/08/99	100	20.9-21.0
184	M	main channel (-5100/4800)	23-28/09/99	100	20.2-19.8
185	M	main channel (-5100/4300)	17-20/10/99	100	19.0
186	M	main channel (-5100/6800)	19-21/11/99	100	16.8-16.7
187	M	main channel (-5100/6800)	16-18/12/99	100	15.7

*M = main channel; S = Test Site; G = Groyne

**Distances with respect to Groyne G2 (u/s negative, d/s positive)

Groynes		Other places	
GB-1	-500 m	Balashi Ghat	4800 m
GB-2	-750 m		
G1	-250 m	Kamarjani Market	-3800 m
G2	0 m	Manos river	1200 m
G3	300 m	Old Camp	1300 m
GA	600 m	Syedpur	2800 m
GA-2	800 m	Rasulpur	4300 m

1.2 RIVER BANK AND CHAR SURVEYS

Inventory of Bankline and Charline Survey
Monsoon 1995 - 1999

Sl. No.	Survey Type*	Test Site-I, Kamarjani Area**	Date	Water Level (m+PWD)
1	B	- 600/300	10/06/95	19.6
2	B	0/300	20/07/95	21.2
3	B	-750/600	28-31/07/95	20.4
4	B	1050/-750, 600/800	05-06/08/95	20.3
5	B	-250/300	16/08/95	21.5
6	B	-2500/1200	26-27/08/95	20.5-20.4
7	B	-800/1200	10-11/09/95	19.5
8	B	1000/1575	17/09/95	19.7
9	B	-800/1000	20-21/09/95	19.5-19.8
10	B	-850/1200	14-15/10/95	18.8-18.7
11	B	600/950	24/10/95	17.9
12	B	600/950	05-06/11/95	16.9
13	B	300/950	27/11/95	16.0
14	B	-850/700	19/12/95	15.3
15	B	-1600/2300	21-22/01/96	14.7
16	C	Kharjani char	24-25/01/96	14.6
17	C	Kharjani char	09/02/96	14.4
18	B	600/4300	10-11/02/96	14.4
19	B	-250/2800	06/03/96	14.4
20	B	600/2800	27-29/03/96	15.9-15.8
21	B	-750/4300	19/04/96	16.0
22	B	-750/4300	05-06/05/96	17.1
23	B	-750/1200	13-14/05/96	18.8-19.1
24	B	-1000/2800	20/05/96	19.5
25	B	-950/1200	03/06/96	19.7
26	B	-800/0	15-17/06/96	18.7-18.4
27	B	-750/1300	23-24/06/96	18.3-18.4
28	B	300/1300	27/06/96	19.6
29	B	-650/1200	04/08/96	20.6
30	B	2800/4300	25/08/96	20.5
31	B	1300/4300	26/08/96	20.4
32	C	Kharjani char	26/08/96	20.4
33	B	-950/1200	12-13/09/96	20.5-20.4
34	B	1200/4300	15-16/09/96	21.1-19.9
35	C	Kharjani char	22/09/96	19.0
36	B	-950/4300	25-26/09/96	18.8
37	B	-950/600	18/10/96	18.6
38	C	Kharjani char	19-20/10/96	18.3-18.1

Sl. No.	Survey Type*	Test Site-I, Kamarjani Area**	Date	Water Level (m+PWD)
39	B	-800/4300	24-25/11/96	16.1
40	B	-1000/300	14/12/96	15.3
41	B	-100/600	14/01/97	14.6
42	C	Kharjani char	15/01/97	14.6
43	B	600/2800	18/01/97	14.6
44	C	Kharjani char	25/01/97	14.6
45	B	-2250/4300	19-20/02/97	14.5
46	C	Kharjani char	23-24/02/97	14.5
47	B	-1600/3000	15/03/97	14.7
48	B	Kharjani char	15-16/03/97	14.7
49	B	-2500/4300	30-31/03/97	16.6-16.5
50	B	Kharjani char	31/03/97	16.5
51	B	600/2800	12/04/97	15.9
52	B	-1600/3000	29/04/97	16.2
53	C	Kharjani char	30/04/97	16.1
54	B	-1600/3000	10/05/97	16.3
55	C	Kamarjani char	11-12/05/97	16.3-16.4
56	B	-1600/3000	07/06/97	18.2
57	B	-1600/3000	27/06/97	20.1
58	B	-2300/2800	26/07/97	20.1
59	B	-2750/4800	10-11/08/97	19.5-19.6
60	B	-1700/2800	04/10/97	20.1
61	B	800/2800	11/10/97	18.9
62	B	300/2800	06-07/01/98	15.9
63	C	Kharjani char	09-10/01/98	15.9
64	C	Kharjani char	15-17/01/98	15.9
65	C	Kharjani char	23/01/98	15.8
66	B	1300/4800	27/02/98	15.3
67	B	1000/4800	21-22/03/98	15.2
68	C	Kharjani char	23/04/98	16.6
69	B	600/4300	25/04/98	16.4
70	B	900/3050	22/05/98	17.5
71	C	Kharjani char	23/05/98	17.4
72	C	Batkamari char	07/07/98	21.7
73	B	-3800/4800	27-29/9/98	19.5
74	B	600/4800	29-30/10/98	19.8-19.5
75	B	1200/4800	17/11/98	17.0
76	B	-3800/4800	23, 28/12/98	15.7-15.5
77	C	Batkamari, Kunderapara and Kharjani char	23-26, 29/12/98	15.7-15.5
78	B	1200/4800	23-25/01/99	15.1-15.0
79	C	Kunderapara & Kharjani char	23-25/01/99	15.1-15.0
80	B	2800/5800	26/02/99	14.7
81	C	Kunderapara & Kharjani char	27/02/99	14.7

Sl. No.	Survey Type*	Test Site-I, Kamarjani Area**	Date	Water Level (m+PWD)
82	C	Kundarapara char	16/03/99	14.6
83	C	Kharjani char	17/03/99	14.6
84	B	2800/4800	18/03/99	14.6
85	C	Kharjani char	18/03/99	14.6
86	B	2800/4800	26/04/99	15.9
87	B	2800/4800	28/05/99	17.8
88	C	Kharjani & Batkamari char	29/05/99	18.3
89	C	300/4800	29-30/09/99	19.6-19.4
90	B	-4800/-1600	02/10/99	19.2
91	B	-5800/-2800	24/10/99	19.6

*B = Bankline; C = Charline

**Distances with respect to Groyne G2 (u/s negative, d/s positive)

Groynes		Other places	
GB-1	-500 m	Balashi Ghat	4800 m
GB-2	-750 m		
G1	-250 m	Kamarjani Market	-3800 m
G2	0 m	Manos river	1200 m
G3	300 m	Old Camp	1300 m
GA	600 m	Syedpur	2800 m
GA-2	800 m	Rasulpur	4300 m

1.3 DGPS FLOW TRACKING

Inventory of DGPS Float Tracking
Monsoon 1995 - 1999

Sl. No.	Test Site-I, Kamarjani Area	Date	No. of Tracks	Water Level (m+PWD)
1	main channel	02/06/95	1	19.4
2	site	21. 25/06/95	1	21.2-21.0
3	G2-G3	03/07/95	1	21.0
4	G1-G3	19. 29/07/95	4	21.2-20.5
5	site	01-07/08/95	6	20.3-20.1
6	site	09-12/08/95	5	20.0-20.1
7	site	16-18/08/95	8	21.5-21.6
8	site	19-31/08/95	29	21.5-20.3
9	site	01-03/09/95	5	20.3-20.0
10	G1-G3	06-07/09/95	4	19.7
11	site	08/09/95	2	19.7
12	main channel	09-11/09/95	5	19.6-19.5
13	site	15-21/09/95	3	19.7-19.8
14	site	23/09/95	2	20.5
15	site	30/09/95	1	21.2
16	site	01-04/10/95	5	21.1-20.6
17	site	07-09/10/95	6	20.2-19.6
18	site	13/10/95	2	18.9
19	main channel	15-17/10/95	3	18.7-18.4
20	site	18/10/95	2	18.4
21	main channel	20/10/95	1	18.2
22	site	21-30/10/95	10	18.2-17.5
23	main channel	03-04/11/95	2	17.0-16.9
24	site	06-08/11/95	3	16.8-16.6
25	site	12-15/11/95	5	17.0-16.7
26	GA to Rasulpur	19/12/95	3	15.3
27	site	20-23/12/95	3	15.2
28	site	01-07/01/96	4	15.1-14.9
29	site	09.12.18/01/96	3	14.6-14.7
30	site	28/01/96	1	14.6
31	site	01-08/02/96	8	14.5-14.4
32	site	11-12/02/96	2	14.4-14.3
33	site	14. 16/02/96	2	14.3
34	site	24-25/02/96	2	14.2
35	site	8. 12. 23/03/96	3	14.5-14.9
36	site	29-30/03/96	2	15.8
37	main channel	24-25/04/96	2	15.9-16.0

Sl. No.	Test Site-I, Kamarjani Area	Date	No. of Tracks	Water Level (m+PWD)
38	main channel	05/05/96	1	17.2
39	main channel	07/05/96	1	17.1
40	site	13, 16, 21/05/96	3	18.9-19.5
41	main channel	22/05/96	1	19.5
42	main channel	03, 06, 07/06/96	3	19.7-19.6
43	site	09, 10, 12/06/96	9	19.5-19.3
44	site	14-19/06/96	19	18.9-18.3
45	site	25-27/06/96	13	18.6-19.6
46	G2-G3	28/06/96	1	20.3
47	site	01.04-07/07/96	21	21.2-21.7
48	site	13-20/07/96	17	21.6-21.9
49	site	24/07/96	3	21.7
50	main channel	25/07/96	3	21.5
51	site	28/07/96	4	21.1
52	site	04.09/08/96	5	20.6-20.3
53	main channel	15-16/08/96	4	20.8-20.9
54	site	19.25/08/96	7	21.1-20.5
55	main channel	29/08/96	8	20.1
56	site	05/09/96	7	20.7
57	main channel	07/09/96	4	20.5
58	site	12/09/96	6	20.5
59	main channel	25-26/09/96	5	18.8
60	site	26-27/09/96	4	18.9
61	site	07/10/96	3	19.8
62	main channel	21-22/10/96	2	17.9
63	site	24/10/96	3	17.6
64	main channel	20.26-27/11/96	6	16.4-16.0
65	site	28/11/96	4	16.0
66	site	05/12/96	2	15.7
67	main channel	18.25/12/96	2	15.2-15.0
68	site	27/12/96	3	14.9
69	main channel	28-31/12/96	6	14.9-14.8
70	site	08/01/97	4	14.7
71	main channel	23-25/01/97	6	14.6
72	main channel	03/02/97	2	14.6
73	main channel, site	06-07/02/97	4	14.6
74	site	13/02/97	3	-
75	site	25/02/97	4	14.6
76	site	05-06/03/97	5	14.6-14.5
77	GA2	13/03/97	2	14.6
78	site	16/03/97	7	14.7
79	main channel	17-18/03/97	4	14.7-14.8

Sl. No.	Test Site-I, Kamarjani Area	Date	No. of Tracks	Water Level (m+PWD)
80	site	19/03/97	3	14.8
81	main channel	20/03/97	2	14.8
82	site	27/03/97	3	14.2
83	main channel	28/03/97	2	16.5
84	site	07/04/97	3	16.0
85	main channel	16-17/04/97	4	16.0-15.9
86	site	29/04/97	4	16.2
87	site	11/05/97	1	16.3
88	main channel	20/05/97	3	17.0
89	site	26/05/97	3	17.8
90	main channel	28/05/97	1	18.4
91	main channel	24/06/97	2	20.5
92	main channel	19/07/97	1	21.3
93	site	09/09/97	4	19.5
94	main channel	27-28/10/97	8	17.2-17.1
95	main channel	19-20/11/97	7	16.2
96	main channel	14/12/97	3	16.0
97	site	30/12/97	2	16.0
98	Kundarapara channel	12/01/98	3	15.9
99	main channel	24/01/98	7	15.8
100	main channel, main channel	26/02/98	7	15.3
101	main channel	28/02/98	1	15.3
102	main channel, main channel	28/03/98	9	15.3
103	main channel	24-25/04/98	4	16.5-16.4
104	main channel	22/05/98	5	17.5
105	main channel	28/05/98	3	18.5
106	in front of Kamarjani bazar	29/08/98	2	22.0
107	Kundarapara channel	27/09/98	1	19.5
108	main channel, site	29/09/98	5	19.6
109	Kundarapara channel, main channel, site	29/10/98	4	19.5
110	main channel, Kundarapara channel	27/11/98	2	16.5
111	main channel, Kundarapara channel	30/12/98	3	15.5
112	main channel, Kundarapara channel	29/01/99	2	15.0
113	main channel, Kundarapara channel	24/02/99	4	14.7
114	main channel, Kundarapara channel	22/03/99	2	14.9
115	main channel, Kundarapara channel	29/04/99	2	16.0
116	main channel, Kundarapara channel	29-30/05/99	3	18.7
117	main channel	06-07/07/99	3	21.5-21.4
118	main channel	24/08/99	8	21.0
119	main channel	27/09/99	3	19.9
120	main channel	27-28/09/99	5	19.9-19.8
121	main channel	23/11/99	2	16.6

1.4 ADVANCED DGPS FLOW TRACKING

Inventory of Advanced DGPS Float Tracking Monsoon 1996 - 1998

Sl. No.	Test Site-I, Kamarjani Area	Date	Drogue Depth (m)	No. of Tracks	Water Level (m+PWD)
1	site	22-25/07/96	0.1.5.3	38,16,12	21.9-21.5
2	site	27/07/96	0.1.5	19,1	21.7
3	site	30-31/07/96	1.5.3	14,17	20.8-20.7
4	site	02-03/08/96	1.5.6	15,19	20.7
5	site	05/08/96	3	15	20.6
6	site	08/08/96	0	11	20.4
7	main channel	10/08/96	0.1.5.3.6	42	20.3
8	site	11-12/08/96	6	21	20.4
9	site	15/08/96	0.3	12,2	20.9
10	main channel	16/08/96	0.1.5.3	12,12,12	21.0
11	site	18/08/96	3	8	21.2
12	site	22/08/96	0	9	20.9
13	main channel	23/08/96	1.5.3	10,10	20.8
14	main channel	07-08/06/97	0.1.5	9,8	18.2-18.4
15	main channel	11/06/97	0.1.5.3	4,4,5	19.2
16	main channel	12/06/97	0.1.5.3	6,6,2	19.6
17	main channel	16/06/97	0.1.5.3	7,7,7	20.4
18	main channel	18/06/97	0.1.5.3	7,7,4	20.9
19	main channel	20-22/06/97	3	36	20.8
20	site	25/06/97	1.5	21	20.2
21	site	30/06/97	0	25	20.2
22	site	01/07/97	3	23	20.4
23	site	05-07/07/97	0.1.5.3	25,27,28	20.7
24	main channel	09/07/97	0.1.5.3	5,5,5	20.9
25	main channel	10/07/97	0.1.5.3	5,5,5	21.2
26	main channel	14-15/07/97	0.1.5.3	10,10,10	22.2
27	site	16/07/97	0	24	21.7
28	main channel	22-23/07/97	0.1.5.3	16,16,16	20.8-20.6
29	main channel	25/07/97	0.1.5.3	3,2,2	20.2
30	site	28-30/07/97	1.5.3	36,26	19.9-19.7
31	main channel	02/08/97	0.1.5.3	9,9,9	19.5
32	main channel	03/08/97	0.1.5.3	8,8,8	19.3
33	site	08-10/08/97	0.1.5.3	28,25,26	19.5
34	main channel	13-16/08/97	0.1.5.3	27,28,21	20.4-20.8
35	main channel	19/08/97	1.5	2	20.5
36	site	19-23/06/98	0.1.5.3	23,28,27	20.5-18.3
37	main channel	30/06/98	0.1.5.3	6,6,8	21.0
38	main channel	01-06/07/98	0.1.5.3	26,25,22	21.5-21.7

1.5 CURRENT POINT MEASUREMENTS

**Inventory of Valeport Measurement
Monsoon 1996 - 1998**

Sl. No.	Test Site-I, Kamarjani Area	Date	No. of Verticals	Water Level (m+PWD)
1	downstream of GA	29/05/96	-	18.7
2	downstream of G2	20/07/96	4	22.0
3	downstream of G2, G3	23/07/96	10	21.8
4	downstream of G2	25/07/96	10	21.5
5	downstream of G3	26/07/96	2	21.4
6	downstream of G3	04/08/96	4	20.6
7	downstream of G1, G3	05/08/96	7	20.5
8	downstream of G2	10/08/96	4	20.2
9	downstream of G3	15/08/96	3	20.8
10	downstream of G2, G3	17/08/96	8	21.0
11	downstream of G1	20/8/96	4	21.0
12	downstream of G1, G2, G3	21/08/96	15	20.9
13	downstream of G1& G2	31/08/96	12	19.9
14	downstream of G1, G2	04/09/96	12	20.7
15	downstream of G3	05/09/96	4	20.7
16	downstream of G3	08/09/96	8	20.6
17	downstream of G1, G2	09/09/96	9	20.6
18	downstream of G1, G2	20/09/96	7	19.2
19	downstream of G1, G2	29/09/96	8	19.2
20	downstream of G2	30/09/96	3	19.3
21	downstream of G3	11/10/96	4	19.4
22	downstream of G2	12/10/96	4	19.5
23	downstream of G1	26/10/96	4	17.4
24	downstream of G1, G2, G3	26/12/96	5	15.0
25	upstream of site	28/12/96	8	14.9
26	downstream of G1, G2	25/01/97	4	14.6
27	main channel (upstream of Kharjani char)	26/01/97	2	14.6
28	downstream of GA	22/02/97	1	14.5
29	downstream of G1, G2, G3	23/02/97	5	14.5
30	in front of GA	17/03/97	3	14.7
31	downstream of G2, GA, GA2	20/03/97	5	14.8
32	downstream of G1, G2, G3, GA	29/04/97	4	16.2
33	downstream of G2, G3	30/04/97	1	16.1
34	main channel (upstream of Kharjani char)	10/05/97	5	16.3
35	in front of groyne field	11/05/97	4	16.3
36	Kamarjani channel, Syedpur	12/05/97	7	16.4
37	Kamarjani channel (downstream of Manos river)	23/05/97	1	17.2
38	downstream of G1	24/05/97	3	17.4
39	downstream of G1, G2	25/05/97	8	17.6
40	downstream of G2, G3	15/06/97	4	20.3
41	downstream of G3	05/07/97	10	20.8
42	in front of Kamarjani bazar	29/08/98	3	21.7

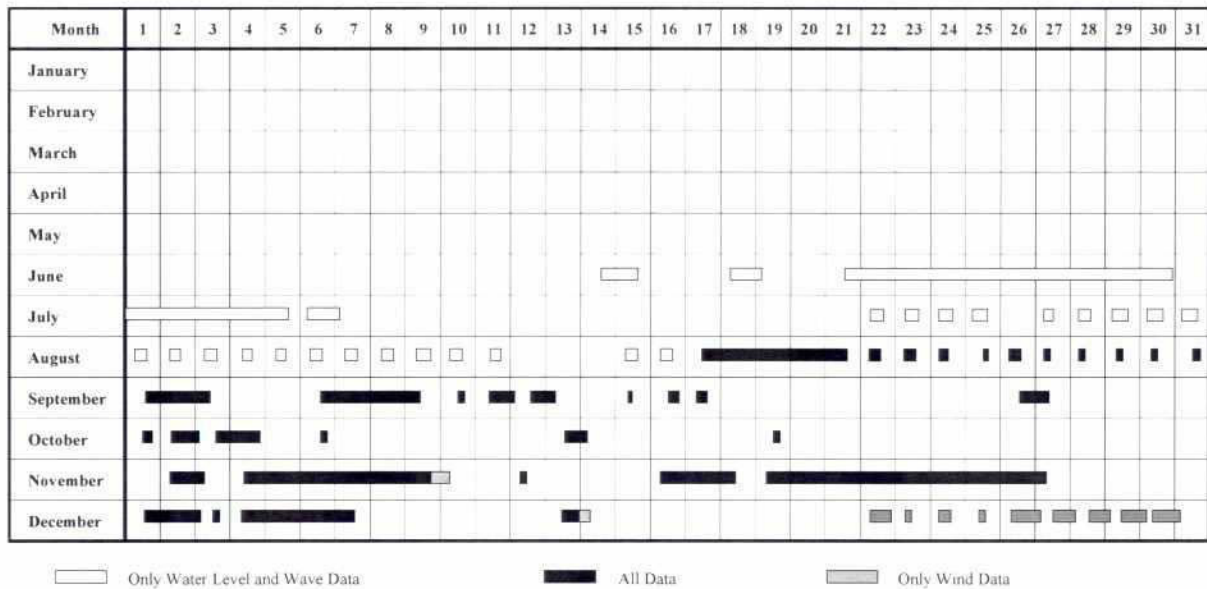
1.6 DISCHARGE MEASUREMENTS

**Inventory of Discharge Measurement
Monsoon 1997 - 1999**

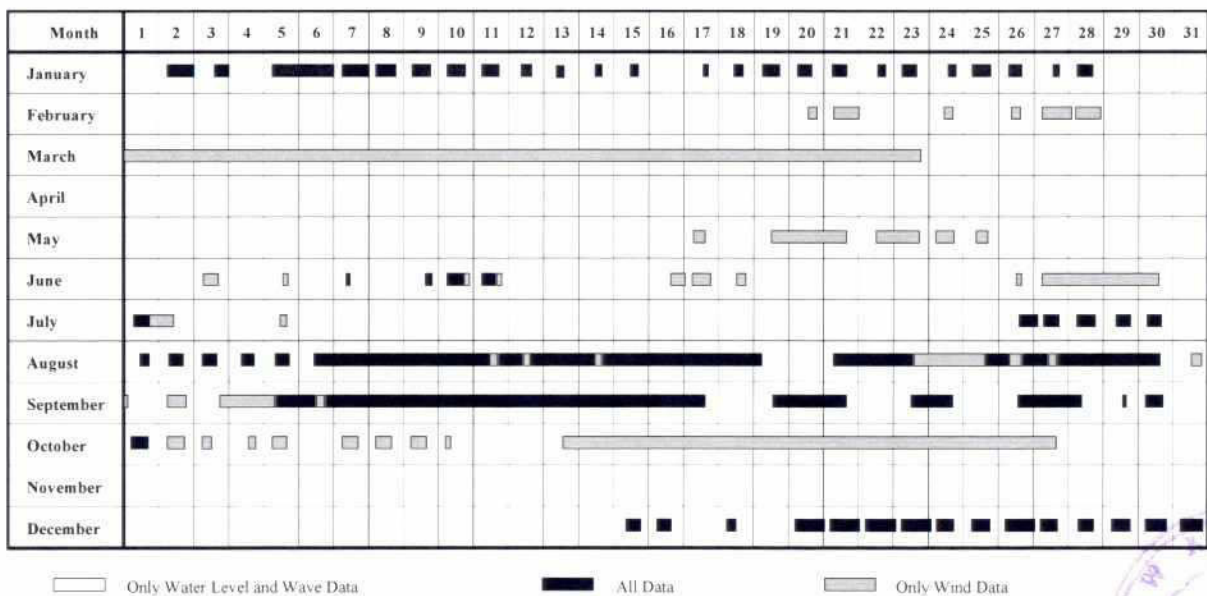
Sl. No.	Test Site-I, Kamarjani Location/Cross-section	Date	Area (m ²)	Q (m ³ /s)	Water Level (m+PWD)
1	Kamarjani channel	01/03/97	2200	2000	14.6
2	Kamarjani channel	15/03/97	1900	1800	14.6
3	Kamarjani channel	27/04/97	3200	3200	16.1
4	Kamarjani channel	20/05/97	3000	4000	16.9
5	Kamarjani channel	28/05/97	5100	6700	18.4
6	Kamarjani channel	19/08/97	12500	12900	20.6
7	Kundarapara channel	19/08/97	2900	2800	20.6
8	Kamarjani channel	16/02/98	2400	1600	14.7
9	Kundarapara channel	17/02/98	100	100	14.7
10	Kamarjani channel	16/03/98	2500	1900	14.9
11	Kundarapara channel	17/03/98	200	100	15.1
12	Kundarapara channel	02/04/98	900	500	16.5
13	Kundarapara channel	17/04/98	600	400	15.9
14	Kamarjani channel	17/04/98	3300	2500	15.9
15	Kamarjani channel	06/05/98	4600	3700	17.0
16	Kamarjani channel	17/05/98	4300	5200	18.2
17	Kundarapara channel	17/05/98	1400	1300	18.2
18	Kamarjani channel	05/06/98	10400	12600	19.5
19	Kundarapara channel	05/06/98	4400	6600	19.5
20	Kamarjani channel	31/07/98	9300	12100	21.7
21	Kundarapara channel	31/07/98	4900	8600	21.7
22	Kamarjani channel	19/09/98	7000	7900	20.0
23	Kundarapara channel	19/09/98	5000	6500	20.0
24	Kamarjani channel	25/10/98	7500	7200	19.2
25	Kundarapara channel	25/10/98	4200	5500	19.2
26	Kamarjani channel	29/11/98	2700	3100	16.4
27	Kundarapara channel	29/11/98	2000	1500	16.4
28	Kamarjani channel	31/12/98	2300	2300	15.4
29	Kundarapara channel	31/12/98	1600	900	15.4
30	Kamarjani channel	30/01/99	2000	2000	14.9
31	Kundarapara channel	30/01/99	1000	800	14.9
32	Kamarjani channel	23/03/99	1800	1800	14.9
33	Kundarapara channel	23/03/99	1000	700	14.9
34	Kamarjani channel	31/05/99	6200	7000	16.9
35	Kamarjani channel	26/08/99	9700	12100	21.7
36	Kundarapara channel	26/08/99	8000	13000	21.7
37	Kamarjani channel	28/09/99	7300	6600	19.7
38	Kundarapara channel	28/09/99	6900	7000	19.7
39	Kamarjani channel	20/12/99	1700	1700	15.6
40	Kundarapara channel	20/12/99	2500	2300	15.6

1.7 MONITORING STATION

Recorded Data from Auto Station at G-2 (1995)

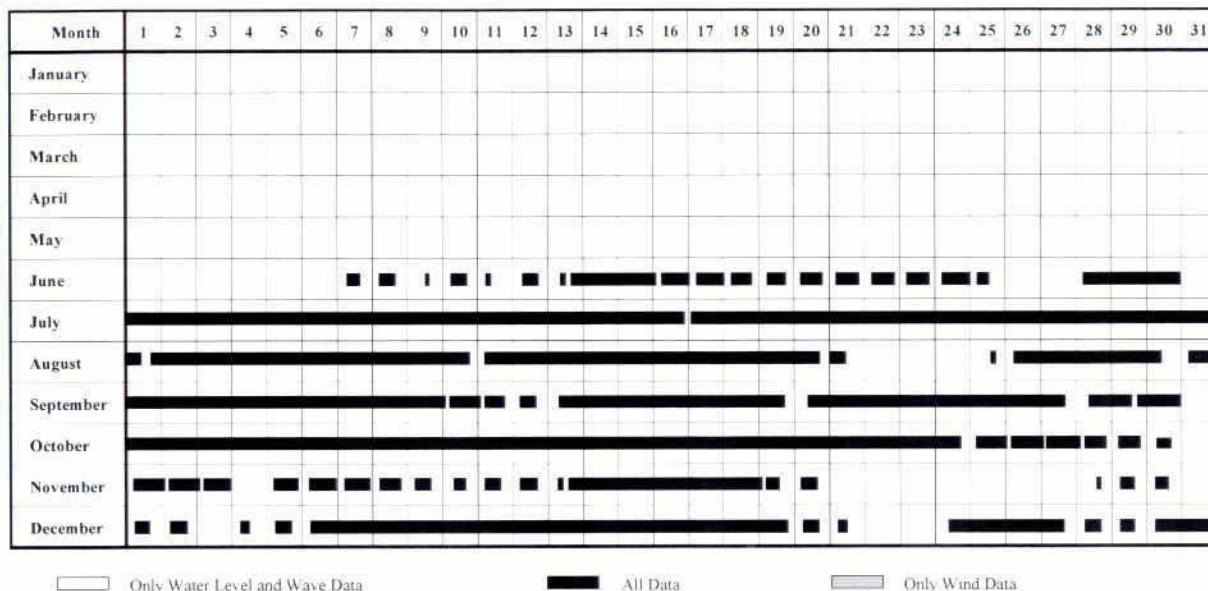


Recorded Data from Auto Station at G-2 (1996)

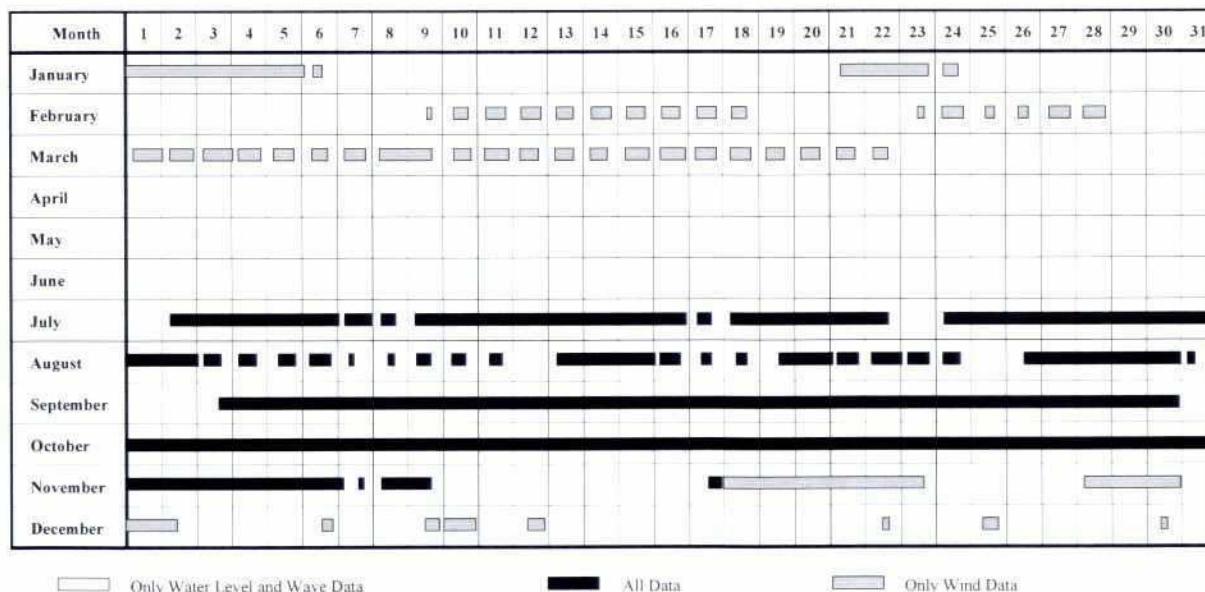


281

Recorded Data from Auto Station at G-2 (1997)



Recorded Data from Auto Station at G-2 (1998)



1.8 BM DESCRIPTION

BENCHMARK DESCRIPTION
FAP 21

Point No.	9802
Location	Test Site I, Dhutichhara S/E corner of Manos Regulator, North of Ghagot River
BM- Type	Drilling hole with screw, marked by red paint
Height above surface	- 0.05m
Instrument	EDM, Wild TC 1600
Surveyor	Osman Ghani
1st Installation	20/06/98
Access	By boat By car/motor bike starting from Gaibandha along left embankment of Ghagot River (20 min.)
Remarks	

Connecting Fixpoints

Location Point No.	Target Point No.	Horizontal Angle [gon]	Distance [m]
9802	9801	221.4243	1287.20
	2439	97.5684	1003.78

Coordinates

	Everest Modified	WGS '84
Easting (BTM), [m]	460842.54	
Northing (BTM), [m]	803428.03	
Height (PWD), [m]	23.480	
Latitude [°,'. ''''''']	25°20.94115' N	25°20.97190' N
Longitude [°,'. ''''''']	89°36.64787' E	89°36.47918' E

Sketch:

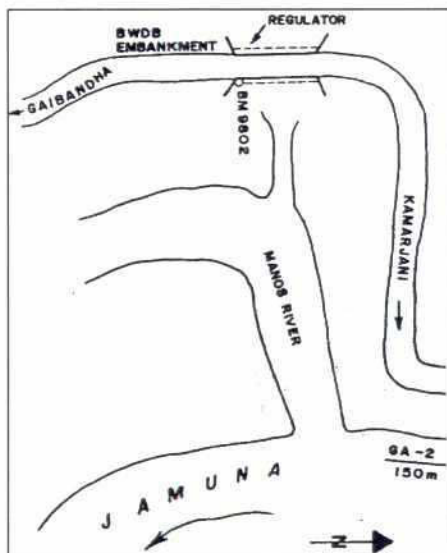


Photo:

Date: 04/07/98



BENCHMARK DESCRIPTION FAP 21

Point No.	9805
Location	Test Site I, Gidhari 32.2m from bankline of Jamuna river.
BM – Type	CC-Pillar (30x30x30cm ³)
Height above surface	0.00M
Instrument	EDM, Wild TC 1600
Surveyor	Osman Ghani
1st Installation	24/06/98
Access	By boat By motor bike starting from Gaibandha along left embankment of Ghagot river following embankment along groynes (30 min.)
Remarks	

Connecting Fixpoints

Location Point No.	Target Point No.	Horizontal Angle [gon]	Distance [m]
9805	2435	226.4206	2049.67
	9804	125.8982	2163.87

Coordinates

	Everest Modified	WGS '84
Easting (BTM) , [m]	462955.27	
Northing (BTM) , [m]	805758.51	
Height (PWD) , [m]	23.592	
Latitude [° , ' , '']	25°22.20722' N	25°22.23788' N
Longitude [° , ' , '']	89°37.90397' E	89°37.73510' E

Sketch:

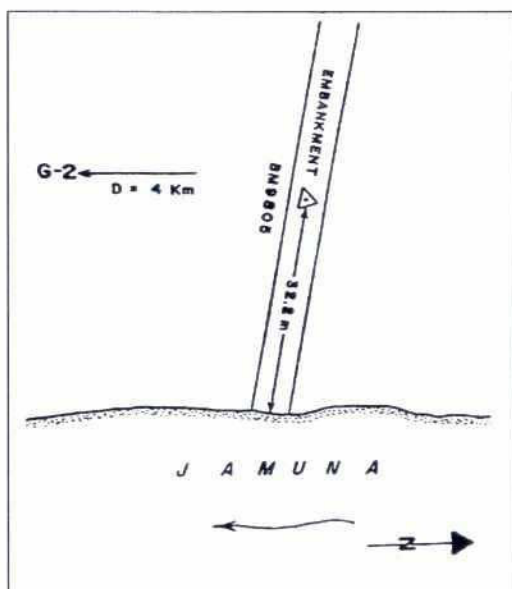


Photo:

Date: 04/07/98



BENCHMARK DESCRIPTION FAP 21

Point No.	2419
Location	Test Site I, Kamarjani – Groyne Field 46m upstream of GB-2, main Embankment
BM – Type	T-size R.C.C. Pillar
Height above surface	0.05m
Instrument	EDM, Wild TC 1600
Surveyor	Osman Ghani
1st Installation	1995
Access	By boat By car/motor bike from Gaibandha
Remarks	

Connecting Fixpoints

Location Point No.	Target Point No.	Horizontal Angle [gon]	Distance [m]
2419	2420	247.9410	62.10
	2421	221.4021	183.40

Coordinates

	Everest Modified	WGS '84
Easting (BTM), [m]	462148.94	
Northing (BTM), [m]	804671.44	
Height (PWD), [m]	23.881	
Latitude [°, ' , '']	25°21.61695' N	25°21.64765' N
Longitude [°, ' , '']	89°37.42485' E	89°37.25605' E

Sketch:

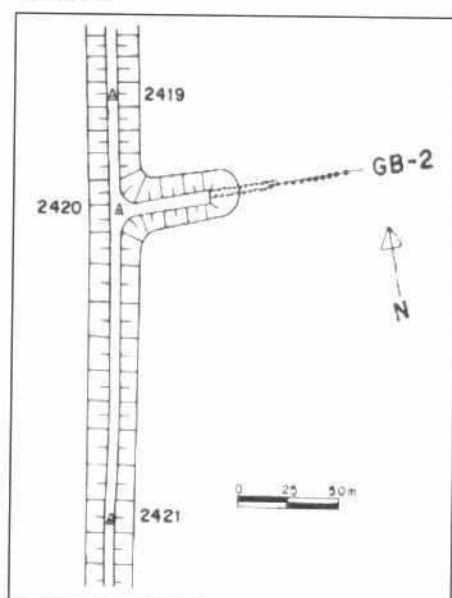


Photo:

Date: 31/08/98



BENCHMARK DESCRIPTION

FAP 21

Point No.	2420
Location	Test Site I, Kamarjani – Groyne Field Along the alignment of GB-2 (Centre of the Embankment)
BM – Type	T-size R.C.C. Pillar
Height above surface	0.20m
Instrument	EDM, Wild TC 1600
Surveyor	Osman Ghani
1st Installation	1995
Access	By boat By car/motor bike from Gaibandha
Remarks	

Connecting Fixpoints

Location Point No.	Target Point No.	Horizontal Angle [gon]	Distance [m]
2420	2419	47.9410	62.10
	2421	208.9211	129.08
	2433	203.6874	503.88

Coordinates

	Everest Modified	WGS '84
Easting (BTM) , [m]	462142.47	
Northing (BTM) , [m]	804626.13	
Height (PWD) , [m]	23.953	
Latitude [° , ' , '']	25°21.59238' N	25°21.62308' N
Longitude [° , ' , '']	89°37.42107' E	89°37.25227' E

Sketch:

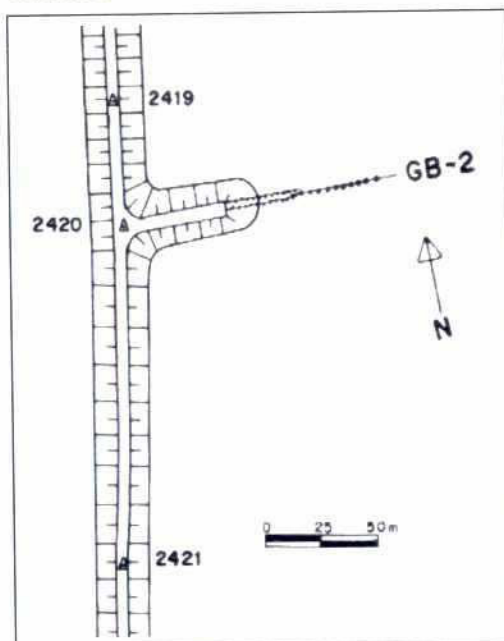


Photo: 193/35

Date: 12/04/97



BENCHMARK DESCRIPTION **FAP 21**

Point No.	2421
Location	Test Site I, Kamarjani – Groyne Field 129m downstream of GB-2 (Centre of the Embankment)
BM – Type	T-size R.C.C. Pillar
Height above surface	0.30m
Instrument	EDM, Wild TC 1600
Surveyor	Osman Ghani
1st Installation	1995
Access	By boat By car/motor bike from Gaibandha
Remarks	

Connecting Fixpoints

Location Point No.	Target Point No.	Horizontal Angle [gon]	Distance [m]
2421	2419	21.4021	183.40
	2420	8.9211	129.08
	2433	201.8896	375.38

Coordinates

	Everest Modified	WGS '84
Easting (BTM) , [m]	462124.44	
Northing (BTM) , [m]	804498.31	
Height (PWD) , [m]	24.145	
Latitude [° , ' , '']	25°21.52308' N	25°21.55380' N
Longitude [° , ' , '']	89°37.41053' E	89°37.24173' E

Sketch:

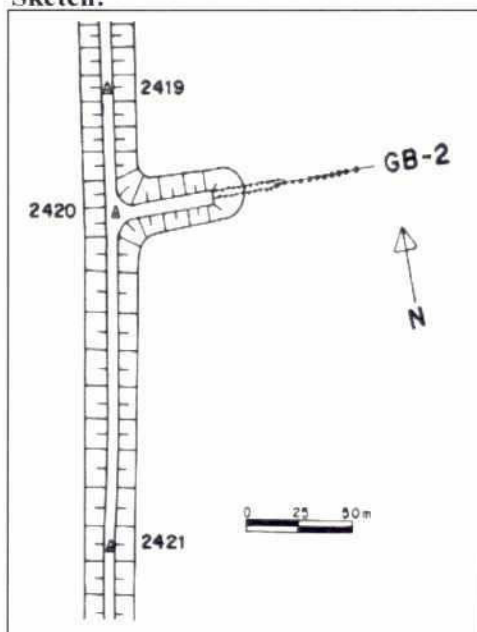


Photo: 193/34

Date: 12/04/97



BENCHMARK DESCRIPTION FAP 21

Point No.	2433
Location	Test Site I, Kamarjani – Groyne Field 40m from centre line of Embankment at G-1
BM – Type	T-size R.C.C. Pillar
Height above surface	0.10m
Instrument	EDM, Wild TC 1600
Surveyor	Osman Ghani
1st Installation	1996
Access	By boat By car/motor bike from Gaibandha
Remarks	

Connecting Fixpoints

Location Point No.	Target Point No.	Horizontal Angle [gon]	Distance [m]
2433	2420	3.6874	503.88
	2421	1.8896	375.38
	2434	248.2423	130.38

Coordinates

	Everest Modified	WGS '84
Easting (BTM) , [m]	462113.30	
Northing (BTM) , [m]	804123.09	
Height (PWD) , [m]	23.156	
Latitude [°.'''''''']	25°21.31975' N	25°21.35048' N
Longitude [°.'''''''']	89°37.40452' E	89°37.23573' E

Sketch:

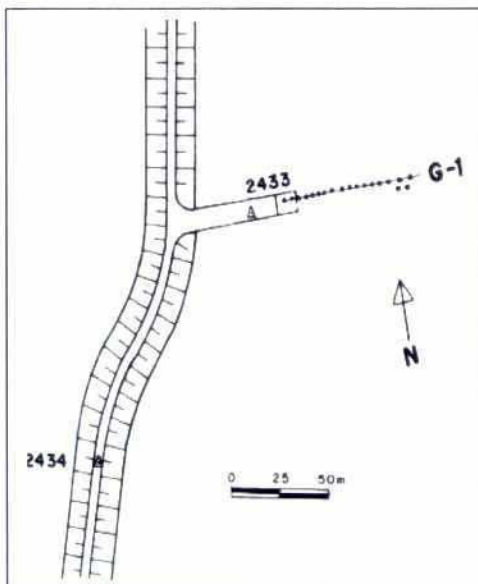


Photo: 193/33

Date: 12/04/97



BENCHMARK DESCRIPTION **FAP 21**

Point No.	2434
Location	Test Site I, Kamarjani – Groyne Field 108m downstream of G-1 (Centre of the Embankment)
BM – Type	T-size R.C.C. Pillar
Height above surface	-0.10m
Instrument	EDM, Wild TC 1600
Surveyor	Osman Ghani
1st Installation	1996
Access	By boat By car/motor bike from Gaibandha
Remarks	

Connecting Fixpoints

Location Point No.	Target Point No.	Horizontal Angle [gon]	Distance [m]
2434	2433	48.2423	130.38
	2436	225.6930	217.10
	2440	219.5364	754.43

Coordinates

	Everest Modified	WGS '84
Easting (BTM) , [m]	462023.69	
Northing (BTM) , [m]	804028.39	
Height (PWD) , [m]	23.674	
Latitude [°,'. ''''''']	25°21.26830' N	25°21.29903' N
Longitude [°,'. ''''''']	89°37.35123' E	89°37.18245' E

Sketch:

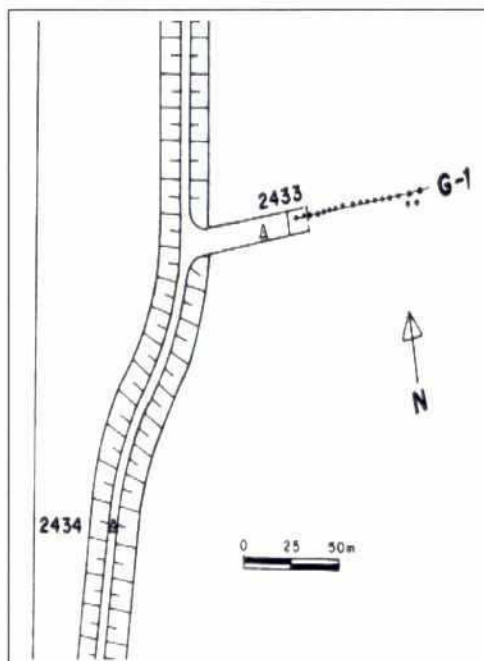


Photo: 193/32

Date: 12/04/97



BENCHMARK DESCRIPTION FAP 21

Point No.	2435
Location	Test Site I, Kamarjani – Groyne Field G-2 gangway, NE Corner
BM – Type	T-size R.C.C. Pillar
Height above surface	0.00m
Instrument	EDM, Wild TC 1600
Surveyor	Osman Ghani
1st Installation	1995
Access	By boat By car/motor bike from Gaibandha
Remarks	The point is used as reference point for orientation only

Connecting Fixpoints

Location Point No.	Target Point No.	Horizontal Angle [gon]	Distance [m]
2435			

Coordinates

	Everest Modified	WGS '84
Easting (BTM) , [m]	462128.84	
Northing (BTM) , [m]	803882.83	
Height (PWD) , [m]		
Latitude [° , ' , '']		
Longitude [° , ' , '']		

Photo: 54/17

Date: 23/08/95



BENCHMARK DESCRIPTION FAP 21

Point No.	2436
Location	Test Site I, Kamarjani – Groyne Field 68m downstream of G-2 (Centre of the Embankment)
BM – Type	T-size R.C.C. Pillar
Height above surface	-0.08m
Instrument	EDM, Wild TC 1600
Surveyor	Osman Ghani
1st Installation	1996
Access	By boat By car/motor bike from Gaibandha
Remarks	

Connecting Fixpoints

Location Point No.	Target Point No.	Horizontal Angle [gon]	Distance [m]
2436	2437	218.4821	102.43
	2438	218.0365	243.36
	2439	215.9669	374.07

Coordinates

	Everest Modified	WGS '84
Easting (BTM) , [m]	461938.43	
Northing (BTM) , [m]	803828.73	
Height (PWD) , [m]	23.584	
Latitude [° , ' , '']	25°21.15998' N	25°21.19072' N
Longitude [° , ' , '']	89°37.30073' E	89°37.13195' E

Sketch:

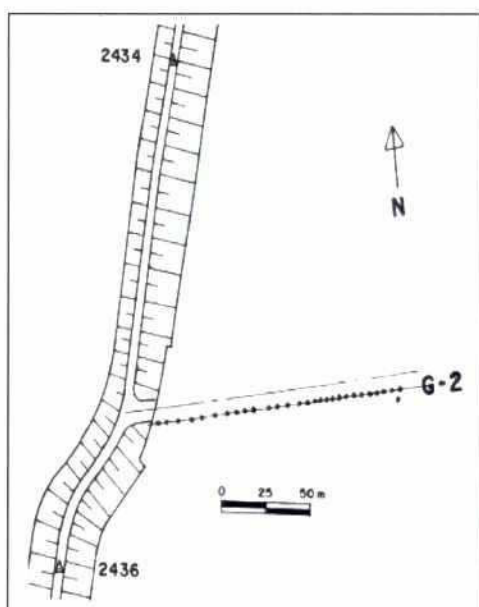


Photo: 193/E

Date: 12/04/97



BENCHMARK DESCRIPTION **FAP 21**

Point No.	2437
Location	Test Site I, Kamarjani – Groyne Field 91m upstream of G-3 (Centre of the Embankment)
BM – Type	T-size R.C.C. Pillar
Height above surface	-0.10m
Instrument	EDM, Wild TC 1600
Surveyor	Osman Ghani
1st Installation	1996
Access	By boat By car/motor bike from Gaibandha
Remarks	

Connecting Fixpoints

Location Point No.	Target Point No.	Horizontal Angle [gon]	Distance [m]
2437	2438	217.7128	140.94
	2439	215.0191	271.76
	2440	216.7247	436.35

Coordinates

	Everest Modified	WGS '84
Easting (BTM) , [m]	461909.11	
Northing (BTM) , [m]	803730.59	
Height (PWD) , [m]	23.537	
Latitude [°,''''''']	25°21.10675' N	25°21.13750' N
Longitude [°,''''''']	89°37.28340' E	89°37.11463' E

Sketch:

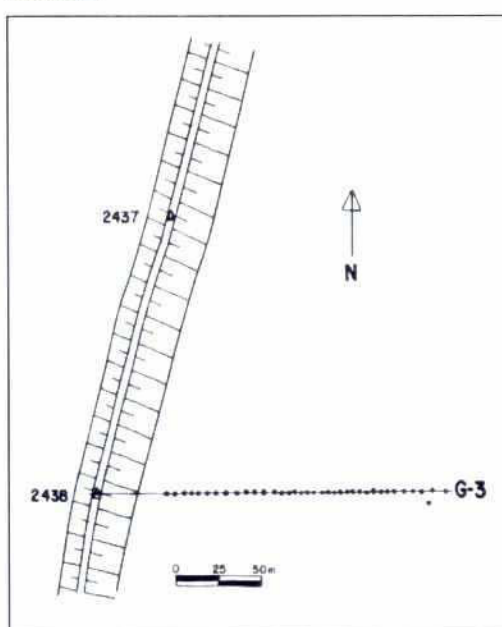


Photo: 193/27

Date: 12/04/97



BENCHMARK DESCRIPTION FAP 21

Point No.	2438
Location	Test Site I, Kamarjani – Groyne Field Along the alignment of G-3 (Centre of the Embankment)
BM – Type	T-size R.C.C. Pillar
Height above surface	-0.10m
Instrument	EDM, Wild TC 1600
Surveyor	Osman Ghani
1st Installation	1996
Access	By boat By car/motor bike from Gaibandha
Remarks	

Connecting Fixpoints

Location Point No.	Target Point No.	Horizontal Angle [gon]	Distance [m]
2438	2437	17.7128	140.94
	2439	212.1228	131.08
	2440	216.2533	295.44

Coordinates

	Everest Modified	WGS '84
Easting (BTM) , [m]	461870.40	
Northing (BTM) , [m]	803595.07	
Height (PWD) , [m]	23.424	
Latitude [°, ' , '']	25°21.03325' N	25°21.06402' N
Longitude [°, ' , '']	89°37.26055' E	89°37.09178' E

Sketch:

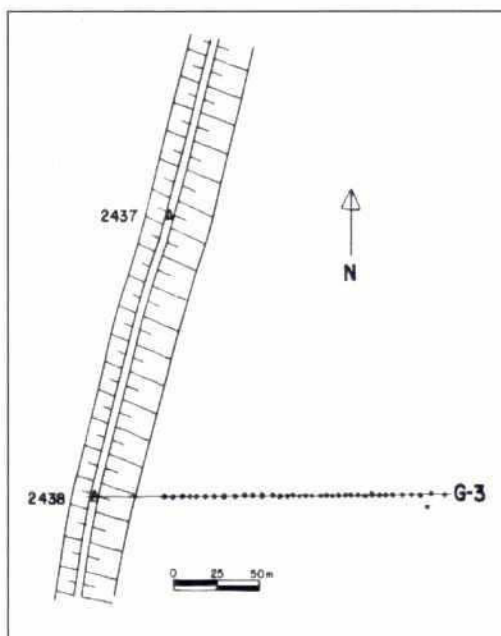


Photo:

Date: 31/08/98



BENCHMARK DESCRIPTION FAP 21

Point No.	2439
Location	Test Site I, Kamarjani – Groyne Field 150m upstream of GA (Centre of the Embankment)
BM – Type	T-size R.C.C. Pillar
Height above surface	-0.08m
Instrument	EDM, Wild TC 1600
Surveyor	Osman Ghani
1st Installation	1996
Access	By boat By car/motor bike from Gaibandha
Remarks	

Connecting Fixpoints

Location Point No.	Target Point No.	Horizontal Angle [gon]	Distance [m]
2439	2440	219.5368	164.85
	2438	12.1228	131.08

Coordinates

	Everest Modified	WGS '84
Easting (BTM) , [m]	461845.59	
Northing (BTM) , [m]	803466.36	
Height (PWD) , [m]	23.487	
Latitude [°,'.*****]	25°20.96348' N	25°20.99423' N
Longitude [°,'.*****]	89°37.24597' E	89°37.07722' E

Sketch:

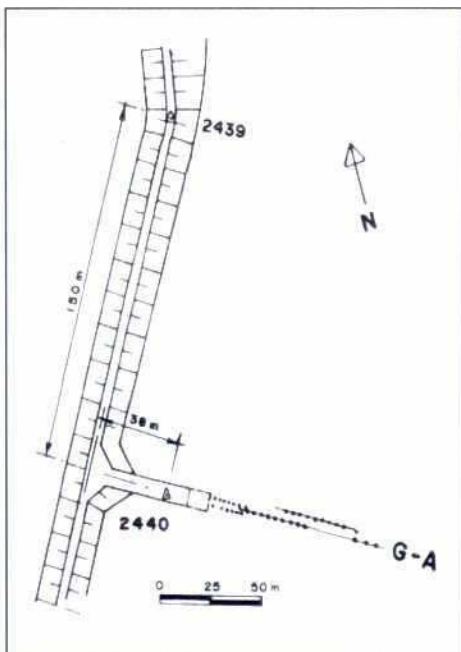


Photo:

Date: 31/08/98



BENCHMARK DESCRIPTION FAP 21

Point No.	2440
Location	Test Site I, Kamarjani – Groyne Field 38m from centre line of Embankment at GA
BM – Type	T-size R.C.C. Pillar
Height above surface	0.00m
Instrument	EDM, Wild TC 1600
Surveyor	Osman Ghani
1st Installation	1996
Access	By boat By car/motor bike from Gaibandha
Remarks	

Connecting Fixpoints

Location Point No.	Target Point No.	Horizontal Angle [gon]	Distance [m]
2440	2438	16.2533	295.44
	2439	19.5368	164.85
	2441	254.3031	119.24

Coordinates

	Everest Modified	WGS '84
Easting (BTM) , [m]	461795.79	
Northing (BTM) , [m]	803309.21	
Height (PWD) , [m]	23.105	
Latitude [° , ' , '']	25°20.87825' N	25°20.90902' N
Longitude [° , ' , '']	89°37.21653' E	89°37.04778' E

Sketch:

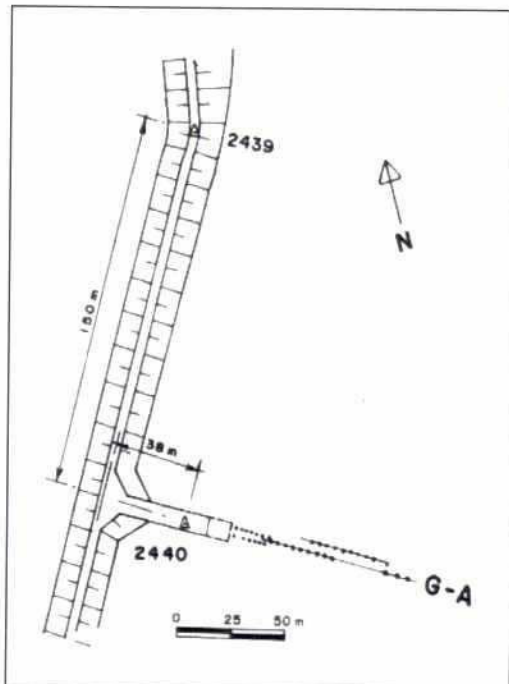


Photo: 193/21

Date: 12/04/97



BENCHMARK DESCRIPTION **FAP 21**

Point No.	2441
Location	Test Site I, Kamarjani – Groyne Field 87m upstream of GA-2 (Centre of the Embankment)
BM – Type	T-size R.C.C. Pillar
Height above surface	-0.08m
Instrument	EDM, Wild TC 1600
Surveyor	Osman Ghani
1st Installation	1996
Access	By boat By car/motor bike from Gaibandha
Remarks	

Connecting Fixpoints

Location Point No.	Target Point No.	Horizontal Angle [gon]	Distance [m]
2441	2440	54.3031	119.24
	2443	235.5312	148.91

Coordinates

	Everest Modified	WGS '84
Easting (BTM) , [m]	461705.97	
Northing (BTM) , [m]	803230.78	
Height (PWD) , [m]	23.727	
Latitude [° , ' , '']	25°20.83560' N	25°20.86637' N
Longitude [° , ' , '']	89°37.16310' E	89°36.99437' E

Sketch:

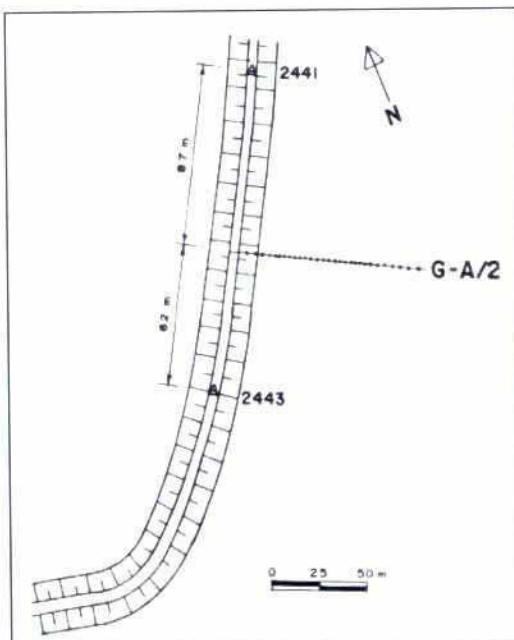


Photo: 193/24

Date: 12/04/97



BENCHMARK DESCRIPTION FAP 21

Point No.	2443
Location	Test Site I, Kamarjani – Groyne Field 62m downstream of GA-2 (Centre of the Embankment)
BM - Type	T-size R.C.C. Pillar
Height above surface	-0.10m.
Instrument	EDM, Wild TC 1600
Surveyor	Osman Ghani
1st Installation	1996
Access	By boat By car/motor bike from Gaibandha
Remarks	

Connecting Fixpoints

Location Point No.	Target Point No.	Horizontal Angle [gon]	Distance [m]
2443	2441	35.5312	148.91
	2440	43.8713	265.28

Coordinates

	Everest Modified	WGS '84
Easting (BTM) , [m]	461627.11	
Northing (BTM) , [m]	803104.47	
Height (PWD) , [m]	23.727	
Latitude [° , ' , '']	25°20.76703' N	25°20.79782' N
Longitude [° , ' , '']	89°37.11630' E	89°36.94755' E

Sketch:

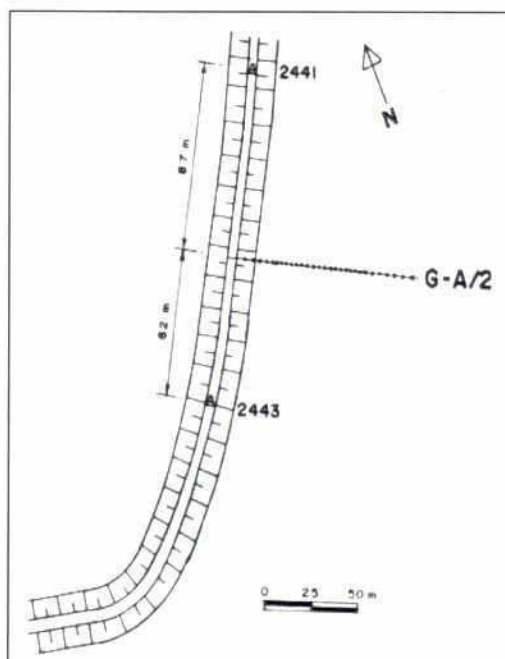


Photo: 193/26

Date: 12/04/97



BENCHMARK DESCRIPTION FAP 21

Point No.	9901
Location	Test Site I, Kundarapara Char
BM- Type	Steel Pipe
Height above surface	(-) 0.05m
Instrument	EDM, Wild TC 1600
Surveyor	Osman Ghani
1st Installation	26/07/99
Access	By boat
Remarks	

Connecting Fixpoints

Location Point No.	Target Point No.	Horizontal Angle [gon]	Distance [m]
9901	9902	48.210	178.86
	9903	210.673	277.96

Coordinates

	Everest Modified	WGS '84
Easting (BTM), [m]	465432.72	
Northing (BTM), [m]	803601.67	
Height (PWD), [m]	n/a	
Latitude [° . ' . '''''''']	25°21.04207' N	25°21.07285' N
Longitude [° . ' . '''''''']	89°39.38498' E	89°39.21593' E

Sketch:

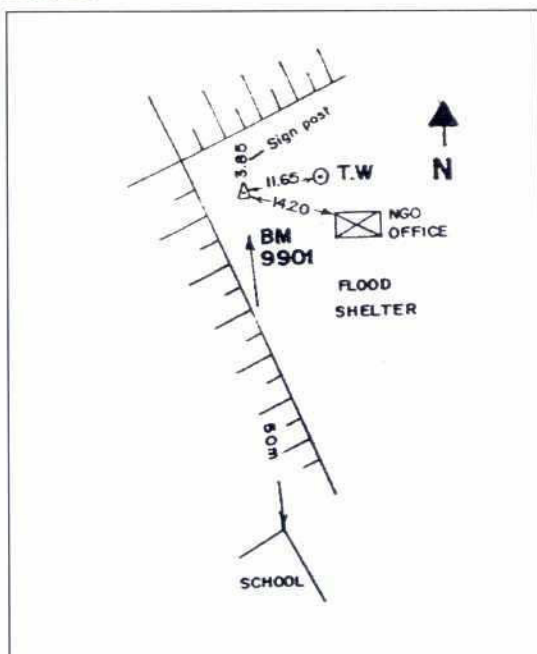


Photo: 344/1

Date: 26/07/99



BENCHMARK DESCRIPTION FAP 21

Point No.	9902
Location	Test Site I, Kundarapara Char
BM – Type	Steel Pipe
Height above surface	(-) 0.05m
Instrument	EDM, Wild TC 1600
Surveyor	Osman Ghani
1st Installation	26/07/99
Access	By boat
Remarks	

Connecting Fixpoints

Location Point No.	Target Point No.	Horizontal Angle [gon]	Distance [m]
9902	9901	248.210	178.86
	9903	225.254	438.06

Coordinates

	Everest Modified	WGS '84
Easting (BTM), [m]	465555.59	
Northing (BTM), [m]	803731.68	
Height (PWD), [m]	n/a	
Latitude [°, ' , '']	25°21.11267' N	25°21.14345' N
Longitude [°, ' , '']	89°39.45805' E	89°39.28900' E

Sketch:

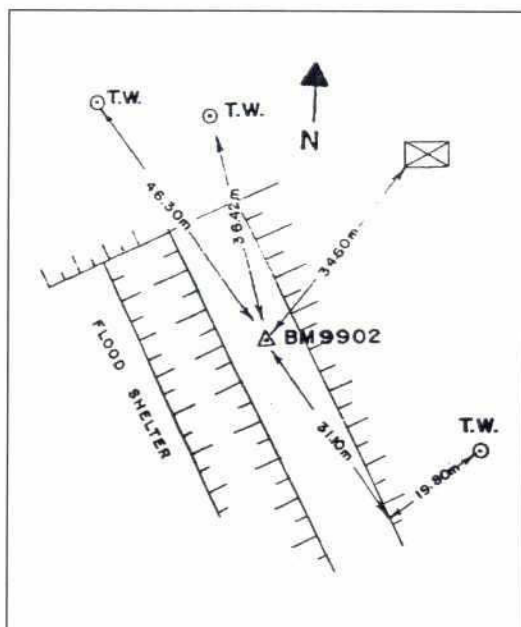


Photo: 344/3

Date: 26/07/99



BENCHMARK DESCRIPTION FAP 21

Point No.	9903
Location	Test Site I, Kundarapara Char
BM – Type	Steel Pipe
Height above surface	0.0M
Instrument	EDM, Wild TC 1600
Surveyor	Osman Ghani
1st Installation	26/07/99
Access	By boat
Remarks	

Connecting Fixpoints

Location Point No.	Target Point No.	Horizontal Angle [gon]	Distance [m]
9903	9901	10.673	277.96
	9902	25.254	438.06

Coordinates

	Everest Modified	WGS '84
Easting (BTM) , [m]	465386.34	
Northing (BTM) , [m]	803327.64	
Height (PWD) , [m]	n/a	
Latitude [° , ' , '']	25°20.89348' N	25°20.92430' N
Longitude [° , ' , '']	89°39.35773' E	89°39.18872' E

Sketch:

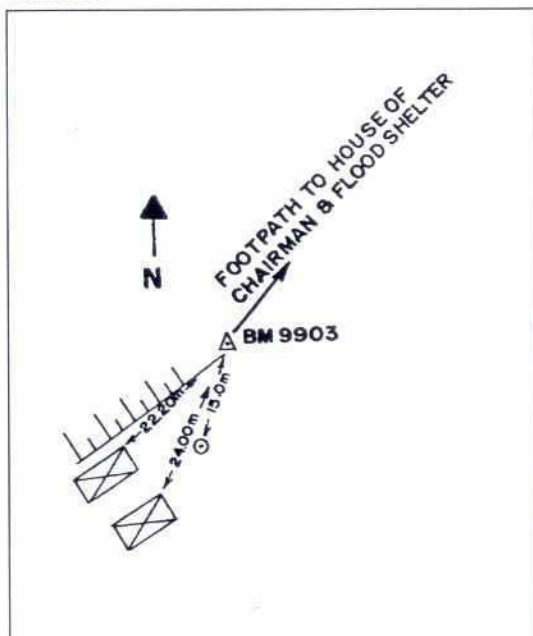


Photo: 344/4

Date: 26/07/99



BNCHMARK DESCRIPTION FAP 21

Point No.	9904
Location	Test Site I, Kamarjani – Syedpur
BM – Type	Steel Pipe
Height above surface	0.0m
Instrument	EDM, Wild TC 1600
Surveyor	Osman Ghani
1st Installation	24/07/99
Access	By car and motor bike
Remarks	

Connecting Fixpoints

Location Point No.	Target Point No.	Horizontal Angle [gon]	Distance [m]
9904	9905	268.520	410.81
	9906	239.783	1000.85

Coordinates

	Everest Modified	WGS '84
Easting (BTM) , [m]	461048.34	
Northing (BTM) , [m]	801111.33	
Height (PWD) , [m]	22.79	
Latitude [° , ' , '']	25°19.68610' N	25°19.71697' N
Longitude [° , ' , '']	89°36.77458' E	89°36.60592' E

Sketch:

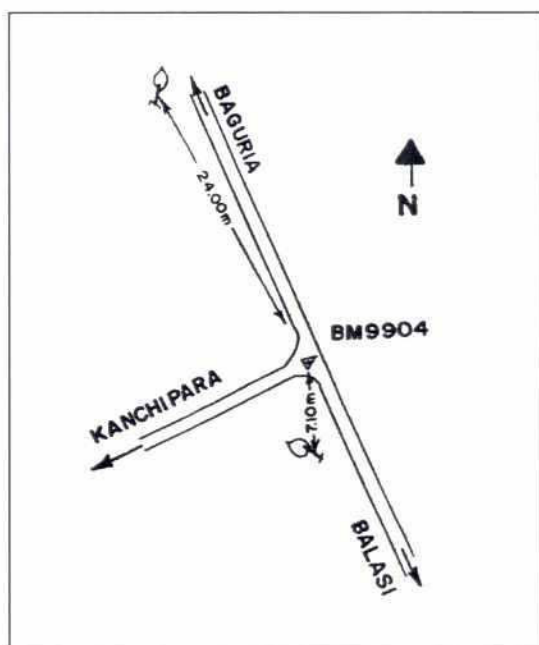


Photo: 344/6

Date: 26/07/99



BENCHMARK DESCRIPTION FAP 21

Point No.	9905
Location	Test Site I, Gholdaha (New Embankment)
BM – Type	Steel Pipe
Height above surface	0.0m
Instrument	EDM, Wild TC 1600
Surveyor	Osman Ghani
1st Installation	24/07/99
Access	By car
Remarks	

Connecting Fixpoints

Location Point No.	Target Point No.	Horizontal Angle [gon]	Distance [m]
9905	9904	68.520	410.81

Coordinates

	Everest Modified	WGS '84
Easting (BTM) , [m]	460686.74	
Northing (BTM) , [m]	800916.37	
Height (PWD) , [m]	23.01	
Latitude [° , ' , '']	25°19.57988' N	25°19.61075' N
Longitude [° , ' , '']	89°36.55932' E	89°36.39068' E

Sketch:

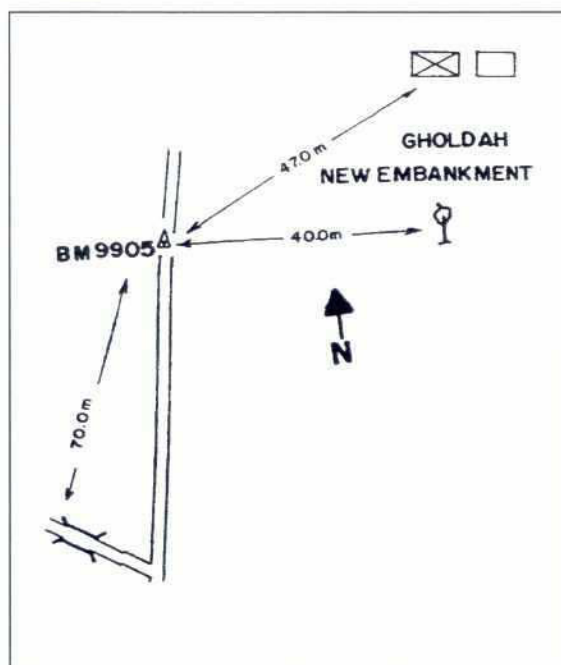
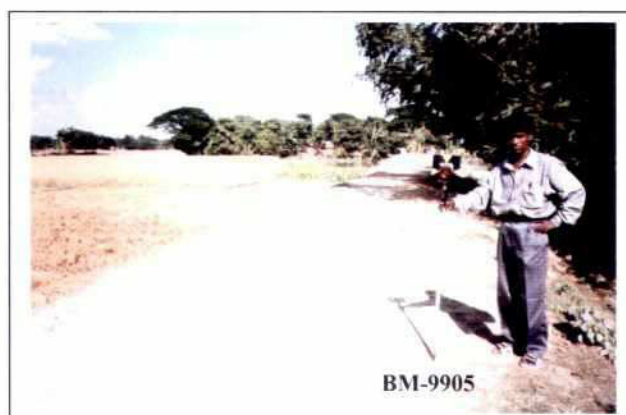


Photo: 352/13

Date: 20/11/99



BENCHMARK DESCRIPTION FAP 21

Point No.	9906
Location	Test Site I, Gholdaha
BM – Type	Steel Pipe
Height above surface	0.0m
Instrument	EDM, Wild TC 1600
Surveyor	Osman Ghani
1st Installation	24/07/99
Access	By car and motor bike
Remarks	

Connecting Fixpoints

Location Point No.	Target Point No.	Horizontal Angle [gon]	Distance [m]
9906	9904	39.783	1000.85
	9907	178.307	460.36

Coordinates

	Everest Modified	WGS '84
Easting (BTM) , [m]	460462.83	
Northing (BTM) , [m]	800299.62	
Height (PWD) , [m]	21.89	
Latitude [° , ' , '']	25°19.24533' N	25°19.27622' N
Longitude [° , ' , '']	89°36.42688' E	89°36.25827' E

Sketch:

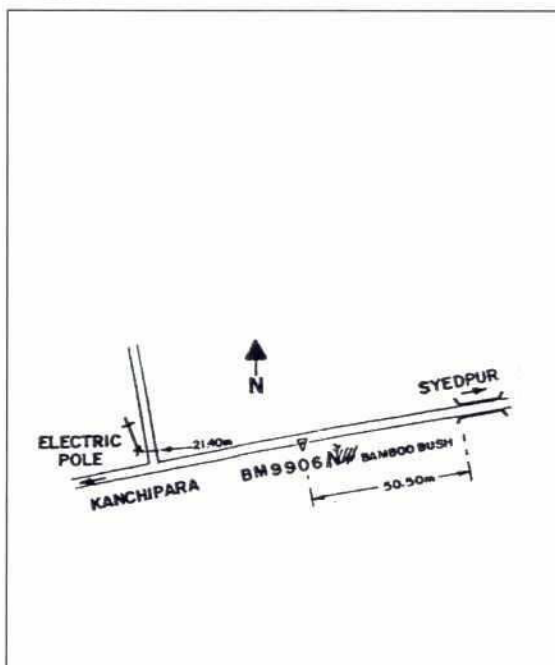


Photo: 352/14

Date: 20/11/99



20

BENCHMARK DESCRIPTION **FAP 21**

Point No.	9907
Location	Test Site I, Gholdaha
BM – Type	Steel Pipe
Height above surface	0.0m
Instrument	EDM, Wild TC 1600
Surveyor	Osman Ghani
1st Installation	24/07/99
Access	By car
Remarks	

Connecting Fixpoints

Location Point No.	Target Point No.	Horizontal Angle [gon]	Distance [m]
9907	9906	378.307	460.36

Coordinates

	Everest Modified	WGS '84
Easting (BTM) , [m]	460616.67	
Northing (BTM) , [m]	799865.73	
Height (PWD) , [m]	22.06	
Latitude [°,'''''''']	25°19.01045' N	25°19.04137' N
Longitude [°,'''''''']	89°36.51937' E	89°36.35075' E

Sketch:

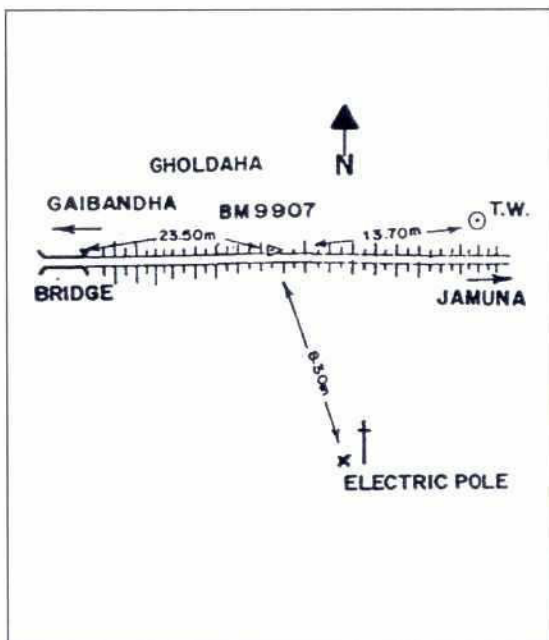


Photo: 344/5

Date: 26/07/99



BENCHMARK DESCRIPTION FAP 21

Point No.	9908
Location	Test Site I, Kamarjani Market
BM – Type	Steel Pipe
Height above surface	(-) 0.10m
Instrument	EDM, Wild TC 1600
Surveyor	Osman Ghani
1st Installation	25/07/99
Access	By car, motor bike and boat
Remarks	

Connecting Fixpoints

Location Point No.	Target Point No.	Horizontal Angle [gon]	Distance [m]
9908	9909	349.338	127.78

Coordinates

	Everest Modified	WGS '84
Easting (BTM) , [m]	463059.33	
Northing (BTM) , [m]	808268.90	
Height (PWD) , [m]	n/a	
Latitude [° , ' , '']	25°23.56768' N	25°23.59823' N
Longitude [° , ' , '']	89°37.96193' E	89°37.79302' E

Sketch:

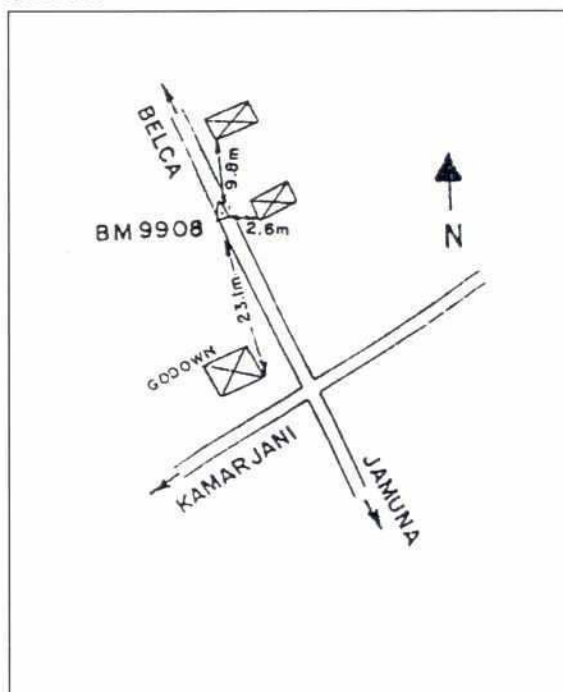


Photo: 358/1

Date: 04/02/2000



BENCHMARK DESCRIPTION FAP 21

Point No.	9909
Location	Test Site I, Kamarjani Market
BM – Type	Steel Pipe
Height above surface	0.0m
Instrument	EDM, Wild TC 1600
Surveyor	Osman Ghani
1st Installation	25/07/99
Access	By car
Remarks	

Connecting Fixpoints

Location Point No.	Target Point No.	Horizontal Angle [gon]	Distance [m]
9909	9908	149.338	127.78

Coordinates

	Everest Modified	WGS '84
Easting (BTM) , [m]	462968.04	
Northing (BTM) , [m]	808358.31	
Height (PWD) , [m]	n/a	
Latitude [° , ' , '']	25°23.61600' N	25°23.64655' N
Longitude [° , ' , '']	89°37.90732' E	89°37.73842' E

Sketch:

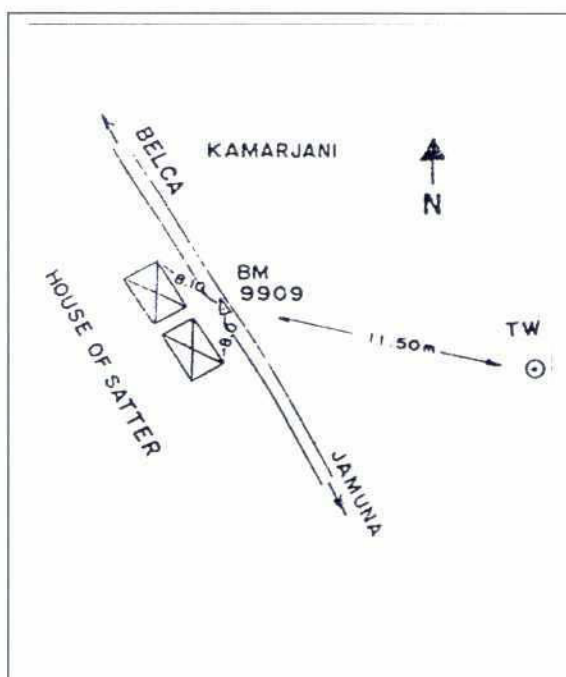
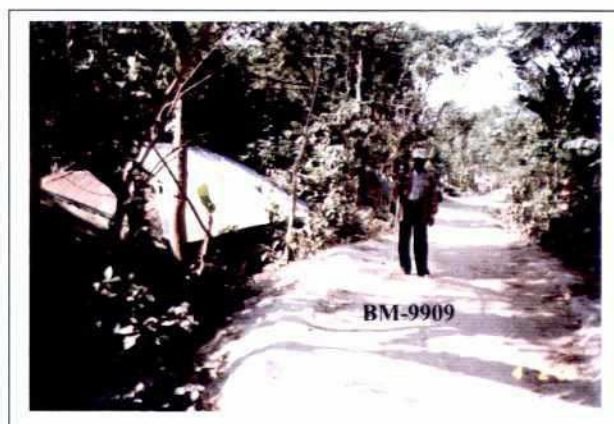


Photo: 358/2

Date: 04/02/2000



290

BANK PROTECTION PILOT PROJECT
FAP 21

FINAL PROJECT EVALUATION REPORT

ANNEX 7

**THE GROUYNE TEST STRUCTURE
EVALUATION OF HYDRAULIC LOADS AND
RIVER RESPONSE**

AUGUST 2001

FAP 21 - BANK PROTECTION PILOT PROJECT

FINAL PROJECT EVALUATION REPORT

ANNEX 7

Table of Contents

	<u>Page</u>
List of Acronyms	A-1
Glossary	G-1
List of Symbols	S-1
SUMMARY	0-1
1 INTRODUCTION	1-1
2 APPROACH FOR ESTIMATION OF HYDRAULIC AND LOCAL MORPHOLOGICAL PARAMETERS	2-1
3 BASIC DESIGN CONCEPT	3-1
3.1 INTRODUCTION	3-1
3.2 CENTRAL PART	3-1
3.3 UPSTREAM TERMINATION	3-1
3.4 DOWNSTREAM TERMINATION	3-4
4 FLOW VELOCITIES	4-1
4.1 INTRODUCTION	4-1
4.2 THE DESIGN DISCHARGE	4-1
4.3 THE DESIGN FLOOD PEAK FLOW	4-2
4.4 SHAPE OF THE DESIGN CHANNEL	4-3
4.4.1 Introduction	4-3
4.4.2 Design Channel Discharge	4-3
4.4.3 Determination of the Cross Sectional Shape	4-5
4.4.4 Design Bend Radius	4-11
4.5 FLOW VELOCITY DISTRIBUTION	4-11
4.6 THE EFFECT OF A SERIES OF GROYNES ON THE FLOW FIELD	4-14
4.6.1 Preliminary Remark	4-14
4.6.2 Oblique Flow Attack	4-14
4.6.3 Expansion Angle	4-15
4.6.4 Mixing Layer	4-17
4.7 EFFICIENCY OF A PERMEABLE GROYPNE TO REDUCE THE FLOW VELOCITY	4-17
4.7.1 Introduction	4-17
4.7.2 Comparison observed and design flow velocities	4-18
4.7.3 Reduction of Flow Velocities	4-20
4.8 CRITICAL FLOW VELOCITY FOR BANK EROSION	4-22

5	WAVES AND WIND	5-1
5.1	WIND	5-1
5.2	WAVES	5-4
6	SCOUR	6-1
6.1	INTRODUCTION	6-1
6.2	MAXIMUM LOCAL SCOUR DEPTH	6-2
6.2.1	Introduction	6-2
6.2.2	Analysis of the Scour Formula of Ahmad	6-4
6.2.3	Value of Coefficient K	6-5
6.2.4	Verification of FAP 21 Investigations	6-6
6.2.5	Further Results of the Physical Model Investigation	6-6
6.2.6	Results from Monitoring of Test Structure	6-7
6.3	TIME-DEPENDENT DEVELOPMENT OF SCOUR DEPTH AND SCOUR VELOCITY	6-9
6.3.1	Location of Maximum Scour	6-9
6.3.2	Scour Depth	6-12
6.3.3	Scour Velocity	6-13
6.4	FLOATING DEBRIS	6-14
6.4.1	Introduction	6-14
6.4.2	Presence of Floating Debris	6-14
6.4.3	Scour by Floating Debris	6-17
6.5	EXTRA STRUCTURE-INDUCED SCOUR	6-20
6.6	CONFLUENCE SCOUR	6-21
6.7	INTERACTION SCOUR	6-22
6.8	BANK EROSION AND FLOW SLIDES	6-22
6.8.1	Introduction	6-22
6.8.2	Sloughing at Groynes G-1, G-2 and G-3 in 1995	6-22
6.8.3	Slumping and Slides at Groynes G-1, G-2 and G-3 in 1995	6-23
6.6.4	Experience with Slides and their Prediction	6-33
7	DESIGN PARAMETERS	7-1
7.1	Introduction	7-1
7.2	Crest Level	7-1
7.3	Groyne Length	7-1
7.4	Bed Protection	7-4
7.5	Transition between Permeable and Impermeable Part	7-6
7.6	Groyne Spacing	7-6
7.7	Groyne Orientation	7-7
7.8	Groyne Permeability	7-7

8 RIVER RESPONSE**8-1**

8.1	Overall Morphological Changes	8-1
8.2	Changes in the Test Site Area	8-1
8.3	Changes Upstream and Downstream of the Test Structure	8-2

REFERENCES**R-1****LIST OF TABLES**

Table 4.3-1:	Maximum rise of the water level at the BWDB gauge station at Bahadurabad In a 24-year period	4-2
Table 4.6-1:	Examples of the expansion of angle β as function of h , C and L_g Assuming the same water depth in channel and groyne field	4-16
Table 4.6-2:	Recommended expansion angles if the main flow is parallel to the bank curvature	4-16
Table 4.7-1:	Reduction of flow velocities by a groyne consisting of a row of piles	4-23
Table 4.7-2:	Theoretical reduction of the flow velocities by a series of three groynes in a parallel flow with expansion angle $\alpha = 0$	4-23
Table 6.2-1:	Results of physical model tests by WL Delft Hydraulics	6-5
Table 6.2-2:	Recommended values of K for a single groyne of a vertical plate	6-5
Table 6.2-3:	Value of K for a vertical plate groyne in physical model test T5 at RRI, Faridpur	6-6
Table 6.2-4:	Values of K as function of the permeability of groynes with pre-shaped falling aprons (RRI, Faridpur)	6-6
Table 6.2-5:	Values of K for different types of groynes with varying permeability (RRI, Faridpur)	6-7
Table 6.2-6:	Table maximum scour depth in the local scour holes at Kamarjani test Structure	6-7
Table 6.2-7:	Value of coefficient K for Kamarjani test structure during 1995 monsoon	6-8
Table 6.2-8:	Coefficient K as function of the permeability	6-8
Table 6.2-9:	Coefficient k_{blockage} as a function of the permeability	6-9
Table 6.3-1:	Parameters for time-dependent scour development fitted to monitoring data, monsoon 1995	6-13
Table 6.3-2:	Maximum scour velocity of the deepest point of a local scour hole in 1995	6-13
Table 6.4-1:	Characteristic values of c_{fd}	6-20
Table 7.3-1:	Estimation of the length of a permeable groyne	7-3
Table 7.8-1:	Recommended pile arrangement of a permeable groyne	7-8

LIST OF FIGURES


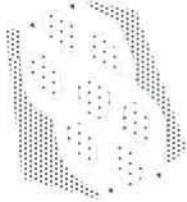

	Page
Fig. 3.3-1: Conceptual design of a scheme of groynes with bank erosion upstream and downstream from the scheme	3-2
Fig. 3.3-2: Conceptual design of a scheme of groynes along a meander bend, which Migrates downstream (no bank erosion upstream from the groyne)	3-3
Fig. 4.4-1: Bathymetry at Kamarjani (surveyed by FAP 24 and processed by EGIS)	4-4
Fig. 4.4-2: Sketch of a cross-section of an axi-symmetrical bend	4-6
Fig. 4.4-3: Comparison between calculated and observed inner-bend profile, Kamarjani during 1995 flood	4-8
Fig. 4.4-4: Comparison measured outer-bend profiles and the calculated outer-bend profile, Kamarjani	4-10
Fig. 4.4-5: Comparison of design outer bend profiles according to formula (4.4-8) and Annex 4	4-10
Fig. 4.5-1: Comparison of the flow velocity ratio in a bend as function of B_{ch}/r_c	4-14
Fig. 4.6-1: Sketch of a theoretical separating flow line	4-16
Fig. 4.6-2: Relationship between groyne length and expansion angle for several Groyne permeabilities	4-17
Fig. 4.7-1: Flow velocities between G-1 and G-2 and between G-2 and G-3 during the 1995 flood	4-19
Fig. 4.7-2: Control volume for application of momentum equation	4-21
Fig. 4.7-3: The drag coefficient determined from float observations during 1995 flood	4-22
Fig. 4.7-4: The drag coefficient determined from accurate flow observations during 1998 flood	4-22
Fig. 5.1-1: Measured wind speed and direction, wave heights during monsoon 1997	5-2
Fig. 5.1-2: Example wind speed during a storm on 12 September 1996	5-3
Fig. 5.1-3: Visually measured wave heights as function of wind speed, 1996 data	5-3
Fig. 5.2-1: Visually measured wave heights as function of wind direction, 1996 data	5-5
Fig. 5.5-2: Preliminary analysis of some observations made in 1995	5-5
Fig. 6.2-1: Scour pattern of permeable groynes	6-2
Fig. 6.3-1: Location of the maximum local scour depth downstream from G-2 during 1995 flood	6-10
Fig. 6.3-2: Location of the maximum local scour depth downstream from G-1 and G-2 during 1998 monsoon	6-11
Fig. 6.4-1: Thickness and area of floating debris at G-2 during 1996 monsoon period	6-15
Fig. 6.4-2: Area of floating debris as function of the water level	6-16
Fig. 6.4-3: The rise or fall of the waver level as function of the water level on days floating debris had been observed during 1996 monsoon	6-16
Fig. 6.4-4: Reduction of scour depth by increasing permeability of the groyne	6-17
Fig. 6.5-1: Different types of scour in Kamarjani during 1995 monsoon	6-20
Fig. 6.6-1: Bathymetry around groyne G-1, June 10, 1995	6-23
Fig. 6.6-2: Bathymetry around groyne G-1, June 24, 1995	6-24
Fig. 6.6-3: Bathymetry around groyne G-1, June 26, 1995	6-24
Fig. 6.6-4: Bathymetry around groyne G-2, May 22, 1995	6-56

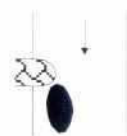


	Page
Fig. 6.6-5: Bathymetry around groyne G-2, July 08, 1995	6-26
Fig. 6.6-6: Bathymetry around groyne G-3, June 26, 1995	6-27
Fig. 6.6-7: Bathymetry around groyne G-3, August 16, 1995	6-28
Fig. 6.6-8: Bathymetry around groyne G-3, August 20, 1995	6-29
Fig. 7.3-1: Design projected total length of a groyne	7-3
Fig. 7.3-2: Example of the plan of stack dykes applied along Chinese rivers	7-4
Fig. 8.3-1: Bank erosion at Kamarjani between 1988 and 1999	8-2
Fig. 8.3-2: Impossibility to assess net effect of impeded bank erosion at test site and embayment formation immediately downstream	8-2

LIST OF ACRONYMS

FAP	-	Flood Action Plan
PWD	-	Public Works Department (datum level)
RRI	-	River Research Institute
SHW	-	Standard High Water
SLW	-	Standard Low Water
USWES	-	US Water Experiment Station

GLOSSARY

alluvial	related to deposits of sediments left by the flow of rivers	
approach-flow angle	angle between direction of approach flow and bankline	
axisymmetrical	related to idealized bends with uniform curvature	
bend scour	scour in outer bend	
braiding	formation of a river course with multiple channels, divided by bars that have a size on the order of the channel width	
Chézy coefficient	coefficient for hydraulic roughness	
confluence scour	scour occurring where two channels or rivers join	
conveyance	geometrical property of a cross-section which determines the relation between discharge and cross-sectionally averaged flow velocity	
effective groyne length	length of groyne projected onto a line perpendicular to the bankline	
expansion angle	angle between main flow direction and the flow line which separates the water area behind the groyne from the mixing layer which develops from the groyne head in downstream direction	
falling apron	suitably designed layer of granular material, such as concrete blocks or boulders, placed directly on the existing subsoil or river bed (i.e. without filter)	
fetch	length of uninterrupted contact between water surface and atmosphere, allowing water waves to grow by transfer of wind energy	
flow slide	bank erosion by means of relatively fast mass failure (liquefaction), resulting in deep bays in the bankline with a narrow neck	
groyne	elongated structure more or less transverse to the river flow and extending from a bank into the river	
hardpoint	local inerodible bankline, assumed to prevent a longer river reach from lateral migration (control point in river planform development)	
impinging flow	flow colliding on the bank	
interaction scour	scour enhancement due to structure-induced changes in the morphology on a larger scale	

launching apron	suitably designed integrated and articulating mattress system, such as sand-filled geosynthetics, concrete-filled geosynthetics or concrete blocks linked to a strong geotextile, placed on prepared slopes above and below water or in a horizontal excavation well above SLW. A launching apron contains a filter
lifetime	total time for which the structure is designed to remain in function
local scour	scour downstream of a local structure or obstruction
	
meandering	formation of a sinuous river course through bank erosion
	
mixing layer	transition zone around the interface of two parallel flows of different velocity, produced by turbulent exchanges
oversteepening	process by which erosion at the bank toe makes the bank so steep that it becomes unstable
peak flow	flow event with maximum flow velocities which does not necessarily come along with maximum water depths
planform	shape on map of banklines or water lines
point bar	bar at inner bend
	
protrusion scour	scour immediately upstream of a local structure or obstruction
recurrence time	return period, average time interval between subsequent events in which conditions are exceeded. When designing a structure, the recurrence time is usually larger than the projected lifetime, because, for instance, if both would equal 50 years, the structure would have a 64% probability of failure during its lifetime
regime equations	empirical formulas for channel dimensions
regime formulas	empirical formulas for channel dimensions
return period	recurrence time, average time interval between subsequent events in which conditions are exceeded. When designing a structure, the return period is usually larger than the projected lifetime, because, for instance, if both would equal 50 years, the structure would have a 64% probability of failure during its lifetime
scour	deepening of the bed by erosive action of water
scour velocity	rate of deepening of the deepest point of a scour hole
shear failure	normal soil-mechanical slide
shear stress	force exerted by the flow on a lateral interface of unit area
Shields parameter	parameter expressing the mobility of particles of a given size under given flow conditions

shoaling	effect of shallow water on water waves
service time	period within the lifetime in which the structure is exposed to attack by the river
slide	collapse of large portions of the bank into the river during short events (mass failure)
thalweg	line connecting the deepest points of consecutive cross-sections
total scour	combined effect of different forms of scour



LIST OF SYMBOLS

A	-	cross-sectional area of river	(m ²)
A _{ch}	-	cross-sectional area of channel	(m ²)
A _{fc}	-	cross-sectional area of inundated floodplains and chars	(m ²)
A _{fl}	-	cross-sectional area blocked by floating debris	(m ²)
A _I	-	subarea I of channel cross-section	(m ²)
A _{II}	-	subarea II of channel cross-section	(m ²)
A _p	-	cross-sectional area occupied by piles	(m ²)
A ₁	-	cross-sectional area of upstream boundary of control volume	(m ²)
A ₂	-	cross-sectional area of downstream boundary of control volume	(m ²)
b	-	Protrusion length (= length of groyne measured from bankline)	(m)
B	-	width at water surface	(m)
B _{ch}	-	channel width at water surface	(m)
C	-	Chézy coefficient for hydraulic roughness	(m ^{1/2} /s)
C _{ch}	-	Chézy coefficient for hydraulic roughness of channel	(m ^{1/2} /s)
C _D	-	drag coefficient	(-)
c	-	constant for spiral-flow parameter	(-)
c _A	-	spiral-flow parameter	(-)
c _{d,fa}	-	coefficient in design formula for thickness of falling apron	(-)
c _{fd}	-	empirical coefficient for effect of floating debris	(-)
c _n	-	braiding index, defined as the number of channels in the cross-section of the river	(-)
c _{w,fa}	-	coefficient in design formula for width of falling apron	(-)
c ₁	-	empirical coefficient in regime relation between discharge and average water depth	(s ^{c2} /m ^{3c2-1})
c ₂	-	empirical exponent in regime relation between discharge and average water depth	(-)
c ₃	-	empirical coefficient in regime relation between discharge and average channel width	(s ^{c4} /m ^{3c4-1})
c ₄	-	empirical exponent in regime relation between discharge and average channel width	(-)
c ₅	-	empirical coefficient for channel alignment and groyne-field water depth in formula for expansion angle	(-)
c ₆	-	first empirical coefficient in relation for design depth-averaged flow velocity over the toe of the outer bank	(-)
c ₇	-	second empirical coefficient in relation for design depth-averaged flow velocity over the toe of the outer bank	(-)
D	-	block or stone size of loose bed protection elements	(m)
D ₅₀	-	median diameter of sediment particles on river bed	(m)
d	-	thickness of falling apron	(m)
F	-	force exerted by flow on pile of permeable groyne	(N)
Fr	-	Froude number	(-)
g	-	acceleration due to gravity	(m/s ²)
H _s	-	Significant wave height	(m)
h	-	local water depth	(m)
h ₁	-	local water depth upstream of scour hole	(m)
h _c	-	water depth at channel centre-line	(m)

h_{ch}	-	cross-sectionally averaged water depth of channel	(m)
h_{fd}	-	thickness of layer of floating debris	(m)
h_{tr}	-	local water depth at transition between permeable and impermeable part of groyne	(m)
h_0	-	water depth at deepest point of cross-section (thalweg)	(m)
h'_0	-	modified water depth at deepest point of cross-section (thalweg)	(m)
I	-	water level gradient	(-)
K	-	empirical coefficient in Ahmad-type scour formulae	$(s^{0.67}/m^{0.33})$
$K_{bed\ protection}$	-	factor for influence of bed protection in Ahmad-type scour formulae	(-)
K_{bend}	-	factor for influence of bend in Ahmad-type scour formulae	(-)
K_c	-	Conveyance	(m^3/s)
$K_{floating\ debris}$	-	factor for influence of floating debris in Ahmad-type scour formulae	(-)
K_L	-	empirical coefficient in rewritten form of Lacey's scour formula	(-)
$K_{structure}$	-	empirical coefficient of structure in Ahmad-type scour formulae	$(s^{0.67}/m^{0.33})$
K_{total}	-	total coefficient in Ahmad-type scour formulae	$(s^{0.67}/m^{0.33})$
k	-	empirical coefficient in Dietz-type scour formulae	(-)
k_b	-	blockage factor	(-)
$k_{bed\ protection}$	-	factor for influence of sill-shaped bed protection in Dietz-type scour formulae	(-)
k_{fd}	-	factor for influence of floating debris in Dietz-type scour formulae	(-)
$k_{floating\ debris}$	-	factor for influence of floating debris in Dietz-type scour formulae	(-)
$k_{blockage}$	-	factor for influence of blockage in Dietz-type scour formulae	(-)
k_s	-	Nikuradse equivalent sand roughness	(m)
$k_{s,0}$	-	Nikuradse equivalent sand roughness in thalweg	(m)
$k_{s,l}$	-	Nikuradse equivalent sand roughness of underwater bank slope	(m)
k_t	-	empirical coefficient in formula for characteristic time of scour hole development	$(m^{2.3}/s^{4.3})$
L_f	-	fetch length	(m)
L_g	-	effective groyne length, i.e. length of groyne projected onto a line perpendicular to the bankline	(m)
L_m	-	additional safety margin between bank and embankment, to be covered by impermeable part of groyne	(m)
L_s	-	distance from the tip of the groyne to the location of the deepest point of a local scour hole	(m)
m_1	-	mass of water entering at upstream boundary of control volume	(kg)
m_2	-	mass of water leaving at downstream boundary of control volume	(kg)
n	-	cotangent of transverse bed slope angle of outer bend, i.e. ratio between horizontal (H) and vertical (V) displacements when moving along transverse bed slope of outer bend	(-)
n_t	-	exponent in empirical formula for time-dependent scour development	(-)
n_{tr}	-	empirical coefficient in relation for additional safety margin between bank and embankment	(-)
p	-	permeability of groyne	(-)

Q_{ch}	-	discharge in design channel	(m ³ /s)
q	-	specific discharge	(m ² /s)
Q_1	-	higher discharge of two anabranches	(m ³ /s)
Q_2	-	lower discharge of two anabranches	(m ³ /s)
R	-	hydraulic radius	(m)
r	-	co-ordinate along bend radius	(m)
r_c	-	radius of bend curvature at channel centre-line	(m)
r_t	-	radius of bend curvature up to the tip of groyne	(m)
r_0	-	radius of bend curvature at deepest point of cross-section (thalweg)	(m)
S_g	-	spacing between groynes	(m)
t	-	Time	(s)
t_l	-	characteristic time of scour hole development	(s)
u	-	upstream depth-averaged flow velocity	(m/s)
u_c	-	depth-averaged flow velocity at channel centre line	(m/s)
u_{ch}	-	cross-sectional averaged flow velocity of channel	(m/s)
u_{cr}	-	critical depth-averaged flow velocity for initiation of motion	(m/s)
u_l	-	depth-averaged flow velocity at upstream boundary of control volume or upstream of a scour hole	(m/s)
u_w	-	average wind speed	(m/s)
u_0	-	depth-averaged flow velocity at deepest point of cross-section (thalweg)	(m/s)
u_1	-	depth-averaged flow velocity at upstream boundary of control volume	(m/s)
u_2	-	depth-averaged flow velocity at downstream boundary of control volume	(m/s)
V_{fa}	-	volume of falling apron per unit distance along a streamline	(m ³ /m)
W_{fa}	-	width of falling apron	(m)
Y	-	cross-channel vertical co-ordinate	(m)
y_s	-	maximum local scour depth	(m)
$y(t)$	-	time-dependent local scour depth	(m)
$y_{s,c}$	-	confluence scour depth	(m)
$y_{s,imp}$	-	maximum local scour depth at impermeable groyne or plate	(m)
$y_{s,tr}$	-	maximum local scour depth at transition between permeable and impermeable part of groyne	(m)
Z	-	vertical co-ordinate	(m)
z_w	-	water level	(m)
α	-	oblique-flow angle, defined as the angle between flow lines and bankline	(degrees)
α_{max}	-	maximum angle of oblique flow	(degrees)
α_t	-	empirical coefficient for effect of upstream geometry on characteristic time of scour hole development	(-)
β	-	expansion angle	(degrees)
γ	-	angle between flow lines and line perpendicular to groyne axis	(degrees)
Δ	-	relative submerged sediment density	(-)
δt	-	time step	(s)
ΔL	-	safety margin for design groyne length	(m)
ϕ	-	angle of incidence of anabranches or confluence	degree

ε	calibration coefficient in relation for transverse distribution of depth-averaged streamwise flow velocities in axisymmetrical bends	(-)
θ	Shields parameter based on local water depth and depth-averaged flow velocity	(-)
θ_c	Shields parameter at channel centre-line	(-)
θ_{cr}	- critical Shields parameter for initiation of motion	(-)
κ	- Von Karman constant	(-)
λ_w	- relaxation length for flow perturbations	(m)
ρ	- mass density of water	(kg/m ³)
ρ_s	- mass density of sediment	(kg/m ³)
ω	- empirical coefficient in Dietz' formula for equilibrium scour depth	(-)

SUMMARY

A Groyne Test Structure has been constructed at Kamarjani on the right bank of the Jamuna River according to the design presented in Annex 4. This design has been based on the best available knowledge at the beginning of the project as well as a series of laboratory investigations. As the structure had been conceived as a *test structure*, the possibility of damage and an associated learning from experiences had been anticipated. After its construction, the performance of the Groyne Test Structure has been monitored for a period of several years with the aim to develop and optimize design criteria and cost-effective construction and maintenance methods, which will serve as future standards most appropriate for the prevailing conditions at the Brahmaputra-Jamuna River and other rivers of Bangladesh.

The monitoring of the Groyne Test Structure is presented in Annex 6. This Annex 7 presents the evaluation of the findings from the monitoring period. Some of the findings merely confirm the suitability of the original design. Other findings lead to improvements of the design criteria.

After some comment on the design methodology in Chapter 2 and on the conceptual design in Chapter 3, a description of the flow velocities and of waves and wind at the test structure is given in Chapter 4 and Chapter 5 respectively. Various aspects of the development of the scour hole in front of the groyne structure are described in Chapter 6. Chapter 7 gives an overview about the improved design parameters. Finally, Chapter 8 covers the river response with respect to large-scale morphological changes.

1 INTRODUCTION

The reach of the Brahmaputra-Jamuna River in Bangladesh flows through a bed of alluvial subsoil consisting mainly of non-cohesive fine sand, which is characteristic for many delta areas. Consolidated cohesive layers in the river banks can act as temporary hard points, which is seen for example at the Arial Khan River (Winkley et al, 1994). Along the Brahmaputra-Jamuna River the old Brahmaputra flood plain deposits act as temporary control points with an increased resistance to bank erosion.

The presence of hard points in the riverbed has an influence on the river planform and hence on the design of river training works. These hard points might function as control points in the planform development and might have a significant influence on the design parameters.

In river training works, groynes are generally used for the following purposes (Garde and Ranga Raju, 1985):

- flood control and protection;
- improvement of navigation conditions;
- guiding the flow towards a hydraulic structure;
- creating of a smooth curvature of the channel to prevent migrating bars and shoals, and
- stabilization of river courses.

The Groyne Test Structure at Kamarjani has been designed primarily to provide protection against bank erosion and indirectly also against flooding.

2 APPROACH FOR ESTIMATION OF HYDRAULIC AND LOCAL MORPHOLOGICAL PARAMETERS

2.1 LIFETIME

River training structures along the Brahmaputra-Jamuna river are generally designed to resist a certain design flood. In Bangladesh, a flood with a recurrence period of 100 years has often been selected as the design flood for bank protections of primary importance. The lifetime of a river training structure has often been related to the recurrence period of the design flood. Therefore, it is assumed that the design will be based on a lifetime of about 50 to 100 years for a bank protection structure. For the present test structures the lifetime of individual components of the structure itself was not given first priority, because the design water level does not change much between recurrence periods of 25 or 200 years. However, it is likely that extreme planforms will have a significant influence on the design parameters, but this influence is still largely unknown. If the apparent tendency of the Jamuna river to shift to the west or to increase its width at the current rate, turns out to be a permanent tendency, then the lifetime of the present structure is certainly limited to a few (2 to 4) decades only.

The *service time* of a river training structure is only a fraction of the *lifetime*, because the structure experiences river attack only in a limited number of years, lying idle in other years. Design conditions with a *recurrence period* of 100 years thus have a much lower probability of occurring during the service time, which implies that such a recurrence period leads to overdesign. On the other hand, the most severe loads on the structure are not related to the most extreme flood events, so that recurrence periods derived from water level registrations or discharge registrations are not very representative for the design conditions. Therefore, the relatively long recurrence periods may be maintained for future structures.

In general, bank protection structures along the Brahmaputra-Jamuna river will not be free of maintenance during their lifetime, because the cost of maintenance-free structures are too high and therefore uneconomic. This is true in particular in view of the different approach flows due to upstream bank erosion and the large variations in the hydraulic load during the lifetime of river training structures. A cost-effective approach with maintenance requires regular monitoring as well as monitoring after extreme events.

2.2 DETERMINATION OF DESIGN PARAMETERS

A *standard method* to determine the hydraulic and morphological parameters for the design of bank protection measures along a braided river consists in principle of the following steps:

(1) Hydrological Data Analysis

Hydrological data consists mainly of daily water levels observed in gauge stations and of less frequently measured discharges. In an analysis of hydrological data, the following parameters will be determined: Design Water Level, Standard High Water Level and Standard Low Water Level. Water levels, which have been measured in a gauge station, can be combined with data from a calibrated mathematical model, which covers the area of the river training structure. The design water level is often based on extrapolation of measured maximum water levels and their recurrence periods. A freeboard has to be added to the design water level, if access to the groyne is required by a gangway (see Flood Hydrology Study, FAP 25, Krüger Consult et al. 1992).

The hydrological data analysis of the Revetment Test Structure in Annex 11 has shown that temporarily the water level gradient can increase to 4 times the average due to the development of a cut-off in front of the test structure. This can also develop in front of a series of groynes.

(2) Morphological Data Analysis

Morphological data of the Jamuna river consists of yearly measured standard cross sections (during the lean season). In addition to these data, irregular bathymetric surveys of the ferry routes are available. In the analysis of morphological data, the maximum water depth will be determined in a design channel as the difference between the maximum water level and the lowest bottom level in the channel. Analysis of measured cross-sections (morphological data) and regime equations results in a minimum bottom level. The maximum water level is related to a selected return period or safety level. However, cross-sections are usually surveyed less frequently than water levels. Therefore, the distribution of the minimum bed levels is often unknown due to a lack of data and the absolute minimum bed level is simply taken from the surveyed cross-sections. In an advanced study planform developments such as the development of a cut-off have been studied by the Jamuna Bridge project (Rendel Palmer & Tritton, NEDECO and BCL, 1990).

The design cross-sectional profile of a channel can be determined as an envelope of measured cross-sections. In principle, these cross-sections should not include river training structures. It is recommended to determine the statistical distribution of the enveloping curves and to select a curve with the same safety level (or return period) as for the water levels. The method applied for the design of the Kamarjani Test Structure consisted of the determination of an absolute enveloping curve, because of the limited number of surveyed cross-sections in channels with sharp bends. If no sufficient surveyed cross-sections are available, the size of the channel can be estimated by using a characteristic width and depth according to empirical regime formulas.

The design curvature radius of a channel bend should be chosen to 2.5 times the channel width (Subsection 2.3.4 of Annex 1).

(3) Definition of Design Flow Velocities

The maximum flow velocity results from a statistical analysis of measured and calculated velocities. Sometimes these flow velocities are measured in physical model tests or simulated in mathematical models.

The design flow velocities in the approach flow can be determined in various ways:

- through statistical analysis of observed flow velocities;
- through simplified calculation methods, as presented in the following chapters, and
- through flow velocities simulated in a 2-D (depth-averaged) mathematical model or in a physical model.

It has to be noted that the flow velocity can increase to its maximum as a steep water level gradient develops during a cut-off.

(4) Definition of Design Waves

In Bangladesh often no sufficient field data are available to determine design wave heights with sufficient accuracy and spatial detail. Therefore, it is recommended to measure wave heights at different locations near river training structures during storms to get information on the prevailing wave heights of rivers in Bangladesh.

(5) Definition of Design Scour

Local scour attracts braiding channels which creates overall scour in the channel. Consequently, the design scour depth has to take into account not only the interaction of local scour with bend scour but also with confluence scour. A first estimate of the interaction scour depth is presented in this Annex. The enveloping curve is modified by adding the maximum design scour depth to the minimum bed level for the design of the piles of a groyne.

(6) Floating Debris

A maximum thickness needs to be selected for the floating debris piling up against a permeable groyne with a crest above the design water level. Floating debris causes a reduction of the permeability and therefore increases the local scour depth. Simple calculation methods for these effects are presented in following chapters. It is recommended to design the top of the piles below the floodplain level to prevent floating debris from piling up.

(7) Determination of Geometric Design Parameters

The top level of the piles of a permeable groyne should be the design water level (with floating debris) or the flood plain level (without floating debris)

The length of a groyne depends on the envelope curve.

2.3 CONCLUDING REMARKS

The steps of the design process often require iteration because they influence each other. A small local scour depth reduces the interaction between the channel and the river training structure. As a consequence, the assessment of the interaction scour becomes less critical.

All design methods applied in previous projects to design river training structures along the main rivers in Bangladesh include the use of physical models and more recently also mathematical models. One of the objectives in this Annex 7 is to develop and to present an analytical method suitable for hand calculations or a spreadsheet program to determine the design parameters at an early stage of the design process (feasibility study). The goal is that engineers of BWDB can use this method without foreign assistance.

3 BASIC DESIGN CONCEPT

3.1 INTRODUCTION

The conceptual layout of a river training structure along a braided river is often based on a combination of a few guidelines and the experience of the design engineer. This means that no widely accepted formal method exists at present. Hence, only some guidelines are presented for the conceptual design of a series of groynes.

The conceptual layout of a river training structure depends mainly on the stability of the river planform and can be designed for the protection of meandering bends with the following characteristics:

- meandering bend with more or less stable upstream and downstream river banks;
- meandering bend, which migrates gradually in downstream direction, and
- meandering bend in a braided river with unstable banks, both upstream and downstream from the selected location.

The last situation is representative for river training works along the Brahmaputra-Jamuna river, which is a braided river with considerable yearly changes in planform. Here a series of groynes requires, in general, upstream and downstream terminations, which are discussed in Sections 3.3 and 3.4 respectively. Often upstream and downstream groynes are smaller than the central groynes (see Annex 18 of the Final Report of the Planning Study Phase, Consulting Consortium FAP 21/22, 1993). Some conceptual aspects of the central part of the structure (that is defined as the main part of the structure between the upstream and downstream terminations) are summarised in Section 3.2.

3.2 CENTRAL PART

The most important conceptual aspect of the layout of the central part of the structure is on one side the length of the reach to be protected and on the other side the erosion rate of the present bankline. Often the location selected for a structure is a town to be protected against ongoing bank erosion. Typically, no sufficient space is available to construct a structure at some distance from the present bank and to allow some more bank erosion. This is often the most economic design. Examples are the design made for the protection of Chandpur (Haskoning et al 1992), the protection of Sirajganj (Halcrow, 1994), and also the test structures of Bahadurabad and Gutail. If no sufficient space is available, then a revetment has probably to be selected instead of more economic groynes.

To assess the available space, the prediction of future bank lines as a result of continued bank erosion by meandering bends during the preparation and construction period of the structure is required.

3.3 UPSTREAM TERMINATION

If the planform analysis indicates that considerable bank erosion has to be expected in future upstream from the selected location an upstream termination is necessary to prevent that progressing upstream bank erosion will damage the structure. One of the following types of terminations can be selected:

- a nearby hard point, for example oxbow lakes silted up with clay and silt (Winkley et al, 1994), other erosion-resistant floodplain strata or an existing bridge;
- a guide bund;

- a guiding dyke;
- several short groynes, and
- combination of these solutions.

It can be considered to extend the first groyne(s) into the floodplain (for example, to connect them to an existing embankment, see Fig. 3.3-1 a), if future bank erosion is expected over a narrow strip of the floodplain. However, if the future bank erosion is considerable, then a series of short groynes is not sufficient. Instead, a guiding dyke or a guide bund should be applied (see Fig. 3.3-1 a). An upstream termination made as a guide bund protected by revetment-type top layers and falling aprons has the advantage that it can accommodate considerable bank erosion from upstream.

The following guidelines have been recommended in the literature for the location of the **upstream termination** of a scheme in a meandering channel:

- the upstream termination should be located at least 1.5 times the channel width upstream from the entrance of the outer bend, i.e. upstream from the intersection of the inner bend tangent with the outer bend (FHWA recommendation based on physical model investigation: Lagasse et al, 1995, and Brown, 1985). Although not mentioned specifically, it seems likely that this recommendation applies for rivers much smaller than the Jamuna river;
- the upstream termination should not extend further upstream than the stretch with bank erosion (recommendation of Lagasse et al, 1995).

A prediction of bank erosion and shifting of the thalweg should be made for at least one year ahead. Regarding prediction methods reference is made to Section 5.5 of Annex 1.

If these rules are applied analogously to the planform of the Brahmaputra-Jamuna river, very long stretches of the bank in a meander bend will have to be protected. In practice, shorter stretches near valuable infrastructure (a town or a regulator) will be protected by a series of groynes. This approach will result in a series of hardpoints along the river. These points should be part of a master plan for training of the river.

Groynes to improve navigation along a shoal in the river have to cover the bank over a distance, which roughly starts at about the length of a groyne upstream from the shoal. According to Shiyi Wang (1990), the protection should be extended over the whole length of the shoal.

The importance of an upstream termination is illustrated by the extensive damage of Sirajganj town protection, which had been caused partly by a unsuitable alignment of the upstream termination resulting in extra deep scour (Halcrow, 1994). This is a revetment type structure, but similar developments can be expected in case of a series of groynes.

If a morphological study indicates that no bank erosion will occur upstream from the structure during the lifetime of the structure, then it is often cost-effective to postpone the construction of an upstream termination (Fig. 3.3-1 b). This is the case, for example, downstream from existing river training works, barrages or bridges. It applies also to the Kamarjani Test Structure.

m2

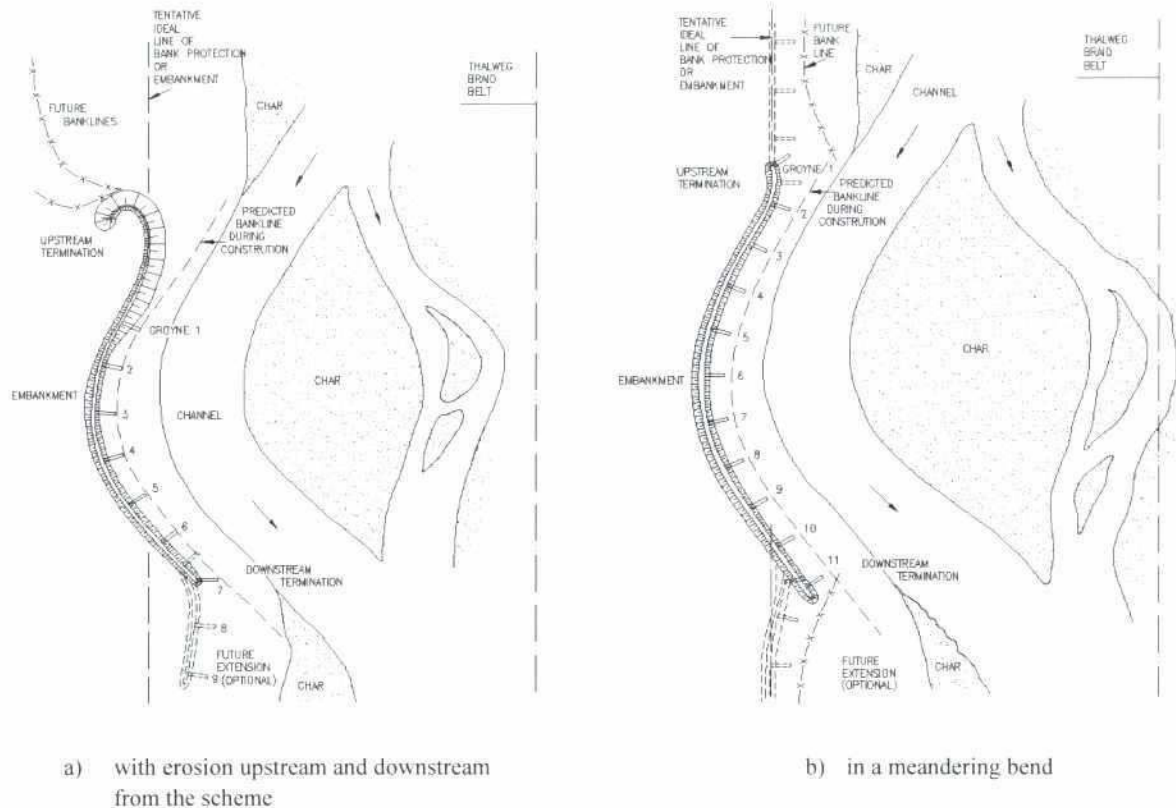


Fig. 3.3-1: Conceptual layout of groyne field

3.4 DOWNSTREAM TERMINATION

A downstream termination is generally necessary in case of a revetment-type structure, but less necessary in case of a series of permeable groynes. The gradual gradient in the flow velocities from the bank to the tip of permeable groynes results in a gradual widening and less deep scour at the downstream termination than for revetments. Downstream from the scheme, the river will most likely start to widen again in future. For a gradual transition some shorter groynes are recommended to be located slightly shielded by the upstream groynes.



4 EVALUATION OF HYDRAULIC LOADS FOR THE DESIGN

4.1 INTRODUCTION

The flow pattern in a meander bend is strongly three-dimensional and a scheme of groynes at its outer bend makes this flow pattern even more complicated. This complicated flow pattern has been simplified into a combination of several phenomena or elements of depth-averaged flow velocities to arrive at a simple and detailed calculation method for the design of such a scheme in the feasibility phase of a project. This method is also a valuable tool for the design of a physical model or a mathematical model. The calculation method to determine design flow velocities described in this section is not only valid for the design of permeable groynes, but also holds for the design of a revetment. The following aspects, which can be generally applied, are distinguished:

- the hydrological data analysis results in the determination of the design discharge (Section 4.2) and design flood peak flow (Section 4.3);
- the morphological data analysis results in a theoretical design channel profile (Section 4.4), and
- a calculation method to estimate approach flow velocities upstream from the series of groynes in a design channel with a design discharge (Section 4.5).

Moreover, the effects of a series of permeable groynes on a flow field are described. The following aspects are mentioned:

- the interaction between the flow and the series of groynes is described in Sections 4.6 and 4.7 viz. the effect of oblique flow attack and a mixing layer on the flow field between the groynes (Section 4.6) and the efficiency of a permeable groyne in reducing the flow velocity (Section 4.7), and
- the critical flow velocity for bank erosion (Section 4.8).

4.2 THE DESIGN DISCHARGE

The design discharge is often obtained from an analysis of hydrological data, especially the extrapolation of the stage-discharge relation at water level stations, where also discharge measurements have been executed regularly. An analysis of the recurrence period associated with a certain peak discharge results in an estimate of the design discharge. The nearest hydrological station along the Brahmaputra-Jamuna river is at Bahadurabad, where the design discharge for the test structures had been estimated at 88.000 m³/s (recurrence period 25 years). The design discharge with a recurrence period of 100 years is estimated at 95.000 to 100.000 m³/s (Delft Hydraulics and DHI, 1996, River Survey Project, Annex 3). This range in the design discharge is mainly caused by an inaccurate estimation of the overland flow during these extreme floods.

If no sufficient data on the stage-discharge relation are available, then the design discharge can be estimated as being equal to about twice the bankfull discharge. The design discharge is the same as the maximum discharge according to Inglis (1968). The bankfull discharge of the Brahmaputra-Jamuna river near Bahadurabad varies between 45,000 and 50,000 m³/s. The recurrence period of the bankfull discharge is about 1 to 2 years (Delft Hydraulics and DHI, 1996, River Survey Project, Special Report 6).

In addition to the analysis of hydrological data, mathematical modelling of the river can provide supplementary data for the selection of the design discharge.

If hydrological data of various stations along the river are available, then the design water level gradient can be determined in the same analysis.

4.3 THE DESIGN FLOOD PEAK FLOW

The design discharge is part of a design peak flow. In the monsoon hydrograph 4 to 5 peak flows can be distinguished. In the applied design method it is assumed that the maximum water level coincides with the maximum discharge. This assumption is doubtful because the maximum flow velocity occurs a few days before the maximum water level is reached. Therefore, it is physically more accurate to consider a design peak flow instead of a design discharge. A design peak flow includes the maximum flow velocity. A typical peak flow in the Jamuna river has a duration of about 2 weeks.

In the following, the assumption is made that the maximum flow velocity occurs as the water level gradient reaches its maximum value. The water level gradient can be estimated from two water level stations. The average water level gradient between these two stations is calculated. Another approach is to relate the maximum water level gradient to the maximum rise of the water level at a station via the propagation velocity of the peak flow. Furthermore, the duration and the rate of increasing discharge (also water levels and flow velocities) determine the rate of scour development. In the Study Phase (Consulting Consortium FAP 21/22, 1993, Annex 5) the maximum rises in water level per 1, 2, 3 and 5 days have been determined from the analysis of a data set observed in the permanent water level gauge station operated by BWDB at Bahadurabad (see Table 4.3-1). This data set covers a period of 24 years. It seems likely that these maximum rises of water level are also valid in the Kamarjani reach of the Jamuna river. A statistical analysis shows that a maximum daily rise of 0.85 m has an estimated return period of 50 years.

Interval (days)	Maximum rise of water level (m)	
	cumulative rise (m)	per day (m)
1	0.85	0.85
2	1.5	0.75
3	1.9	0.63
5	2.8	0.56
7	3.2	0.46

Table 4.3-1: Maximum rise of the water level at the BWDB gauge station at Bahadurabad in a 24 years period

These data have been used to determine a design peak flow. The maximum flow velocity occurs 3 to 4 days before the maximum water level has been reached. During these days the water level rises sharply as presented in Table 4.3-1. Using a simple kinematic wave approximation (Janssen et al, 1994), it can be shown that this rise of the water level does increase the water level gradient maximum 30 %. The Chézy coefficient increases also (that means the riverbed becomes smoother), say around 20 %. Both effects result in an increase in the flow velocity of 30 to 40 % during the rising limb of a peak flow (as can be shown by substitution of both effects in the Chézy formula). This rise in flow velocities has been observed during the monitoring period.

However, these peak flows have been analysed to determine the deterministic part of them. It is recommended to perform such an analysis in more depth because the required water level data are available.

4.4 SHAPE OF THE DESIGN CHANNEL

4.4.1 Introduction

The braiding Jamuna river has different channels. For the design of a river training structure it is assumed that a sharp meander bend is decisive in a design channel. The design channel profile is a function of the design discharge in the channel and the water depth.

The design channel profile depends on the design bend radius (Subsection 4.4.4), the thalweg of the channel and the centre line.

4.4.2 Design Channel Discharge

The design discharge in a braided river is distributed over various channels and a part will flow over the floodplain and inundate chars, see for example Fig. 4.4-1. The channel discharge Q_{ch} (m^3/s) is selected after an analysis of field data and the braiding index (i.e. the number of channels in a cross-section of the river). The braiding index in the Brahmaputra-Jamuna river varies from 1 to 5, on average between 2 and 3 (Final Planning Study Report). Since the design discharge in the whole river cross section is estimated at 95,000 to 100,000 m^3/s with a recurrence period of 100 years (Section 4.2) the design discharge, Q_{ch} , in a design channel is estimated at 40 % of the 95,000 to 100,000 m^3/s . This yields 38,000 to 40,000 m^3/s .

32/2

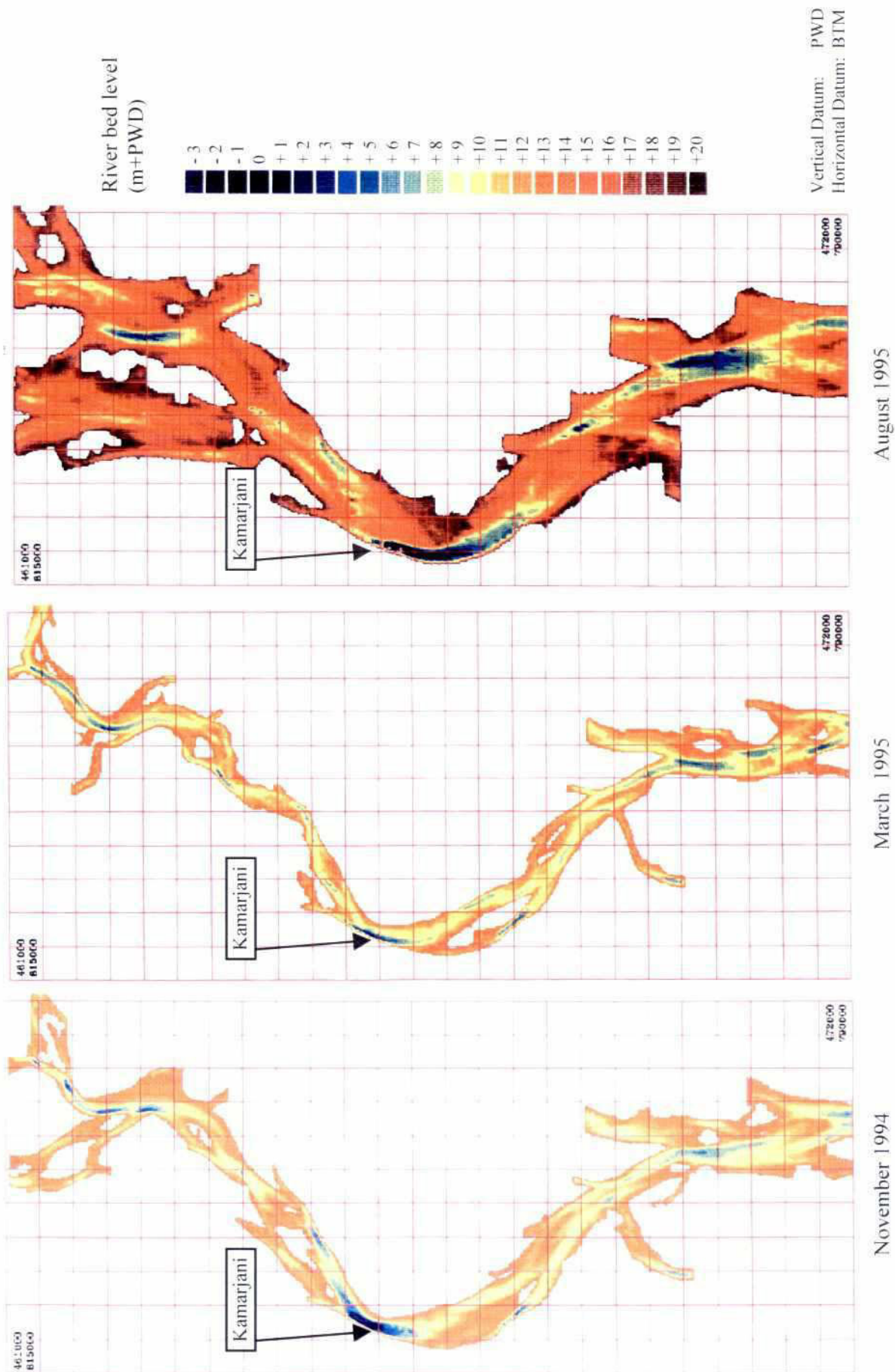


Fig. 4.4-1: Plan view of the Jamuna with bathymetry at Kamarjani
(Surveyed by FAP 24 and processed by EGIS)

4.4.3 Determination of the Cross-Sectional Shape

The cross-sectional area of a channel A_{ch} (m^2), can be expressed by

$$A_{ch} = B_{ch} \cdot h_{ch} \quad (4.4-1)$$

with

A_{ch}	=	cross-sectional of a channel	(m^2)
B_{ch}	=	average channel width	(m)
h_{ch}	=	average water depth within the channel	(m)

The cross-sectional area of the whole river is defined by

$$A = \sum_{j=1}^{j=c_n} B_{ch,j} \cdot h_{ch,j} + A_{fc} \quad (4.4-2)$$

with

A	=	cross-sectional area of the river	(m^2)
A_{fc}	=	cross sectional area above chars and floodplain	(m^2)
c_n	=	braiding index, defined as the number of channels in the cross-section of the river	(-)

The average channel depth h_{ch} and the average channel width B_{ch} at floodplain level can be determined from field surveys or estimated using regime equations as follows:

$$\begin{aligned} h_{ch} &= c_1 \cdot Q_{ch}^{c_2} \\ B_{ch} &= c_3 \cdot Q_{ch}^{c_4} \end{aligned} \quad (4.4-3)$$

c_1 to c_4 are empirical coefficients (-). They depend on the erodibility of the bank material (cohesive or non-cohesive soils) and are constants for the main rivers in Bangladesh (see for example Delft Hydraulics and DHI 1996, River Survey Project, Special Report 7, where these coefficients have been determined from field data for the Brahmaputra-Jamuna, Ganges-Padma rivers in Bangladesh). The graphs in that report give a good impression of the scatter of the data around the fitted curve.

Regime equations have been fitted to data related to channels in braided rivers with the water level below the bankfull level. Here, at-the-station relations are recommended, which can be extrapolated for the case the discharge is above bankfull discharge (Klaassen and Vermeer, 1988a).

The above parameters determine a simple rectangular cross section of the design channel and serve therefore only as a first approach. For more accurate calculation, the cross-section is separated in two parts: one part with the inner bend profile (area II) and a part with the outer bend profile (area I), see sketch in Fig. 4.4-2. The centre line of the cross section is defined by half the width B_{ch} .

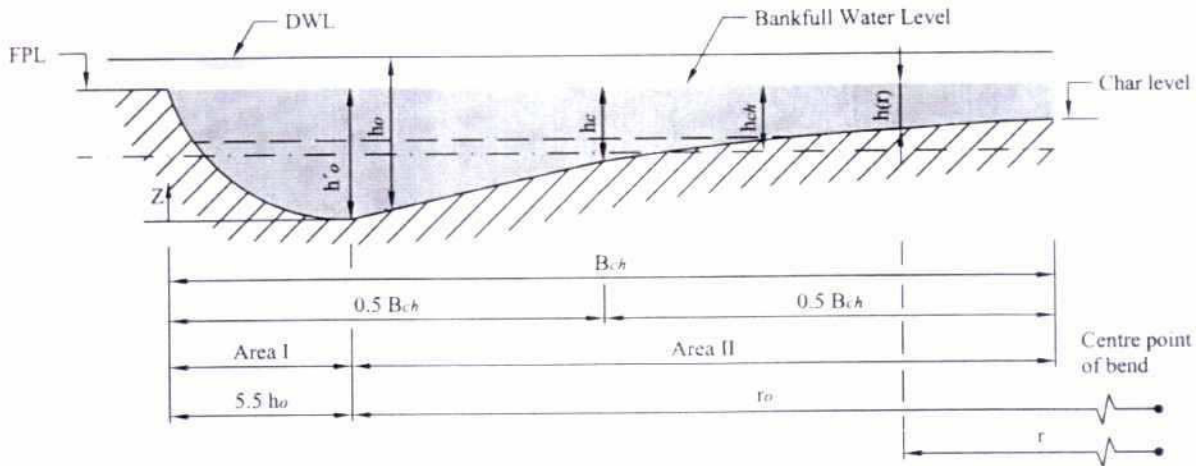


Fig. 4.4-2: Sketch of a cross-section of an axi-symmetrical bend

(1) Inner Bend Profile

Struiksmas has derived a general formula for the inner bend profile (Area II in Fig. 4.4-2) from an equilibrium of forces on a column of water in a bend. It is based on a schematised cross-section in an axi-symmetrical bend with several simplifying assumptions. One of these assumptions is $r_c / B_{ch} > 2$ (r_c = radius of bend curvature at channel centre-line in m and B_{ch} = channel width in m).

The bed profile in the inner bend is described by the formula according to Struiksmas et al (1985):

$$\frac{\partial h}{\partial r} = c_A \sqrt{\theta} \frac{h}{r} \quad (4.4-4)$$

where

c_A	=	spiral-flow coefficient	(-)
h	=	local water depth	(m)
r	=	co-ordinate along bend radius	(m)
θ	=	Shields parameter based on local water depth and depth-averaged flow velocity	(-)
or $\theta = \frac{h \cdot I}{\Delta \cdot D_{50}}$			
I	=	water level gradient	(-)
D	=	relative density of sediment	(-)
D_{50}	=	median diameter of sediment in the river bed	(m)

The spiral flow coefficient c_A in extreme design bends is defined as follows:

$$c_A = \frac{c}{\kappa^2} \left(1 - \frac{\sqrt{g}}{\kappa \cdot C} \right) \quad (4.4-5)$$

in which

C	=	Chézy coefficient for hydraulic roughness	(m ^{0.5} /s)
g	=	acceleration due to gravity	(m/s ²)
κ	=	von Karman constant, $\kappa = 0.4$	(-)
c	=	see Equation 4.4-6	(-)

Talmon et al (1995) give the following approximation the parameter c in Formula (4.4-5):

$$c = 18 \left(\frac{D_{50}}{h} \right)^{0.3} \quad (4.4-6)$$

where

D_{50} = median diameter of sediment in the river bed (m)

Integration of formula (4.4-4) between h_c and h_0 and a series expansion of a logarithm results in:

$$\frac{h_0}{h_c} = [1 + c_A \sqrt{\theta_c} \{ \sqrt{\frac{r_c}{r_0}} - 1 \}]^{-2} \quad (4.4-7)$$

where

h_c	=	water depth at channel centre-line	(m)
h_0	=	water depth at deepest point of cross-section (thalweg)	(m)
r_c	=	radius of bend curvature at channel centre-line	(m)
r_0	=	radius of bend curvature at deepest point of cross-section (thalweg)	(m)
θ_c	=	Shields parameter at channel centre-line	(-)

This result depends on the type of series expansion, therefore other formulations are possible as well.

The inner bend profile can be calculated using (4.4-7), assuming $h_c \approx h_{ch}$ at $r = r_c$ and to replace r_0 by r and h_0 by $h(r)$. Fig. 4.4-3 shows the measured inner bend profile of February and July 95. For the latter, the flow depth below the average flood plain level (20 m +PWD) can be estimated $h_c = 6.7$ m at a distance of 600 m from the outer embankment. The radius of bend curvature at the channel centre-line was roughly $r_c = 2400$ m. With a channel width $B = 1200$ m, this still corresponds to the restriction $r_c/B > 2$. The diameter $D_{50} = 0.2$ mm and a Chezy-coefficient of $C = 70 \text{ m}^{0.5}/\text{s}$ yield a spiral flow coefficient of $c_A = 4.4$ (see formula 4.4-5). The Shields parameter can be calculated to $\theta_c = 1.32$.

Given h_c , r_c , c_A and θ_c then $h(r)$ is calculated by the formula. The calculated profile fits very well to the observed inner bend profile in Kamarjani during the 1995 flood, see Figure 4.4-3. The envelope curve is calculated using the same parameters but $h_c = 8.5$ m. It is mentioned that the assumption $h_c \approx h_{ch}$ at $r = r_c$ is valid in the wide cross sections of the Jamuna river.

The extreme depth h_0 in the thalweg of the design channel is calculated by (4.4-7)

7/3/2

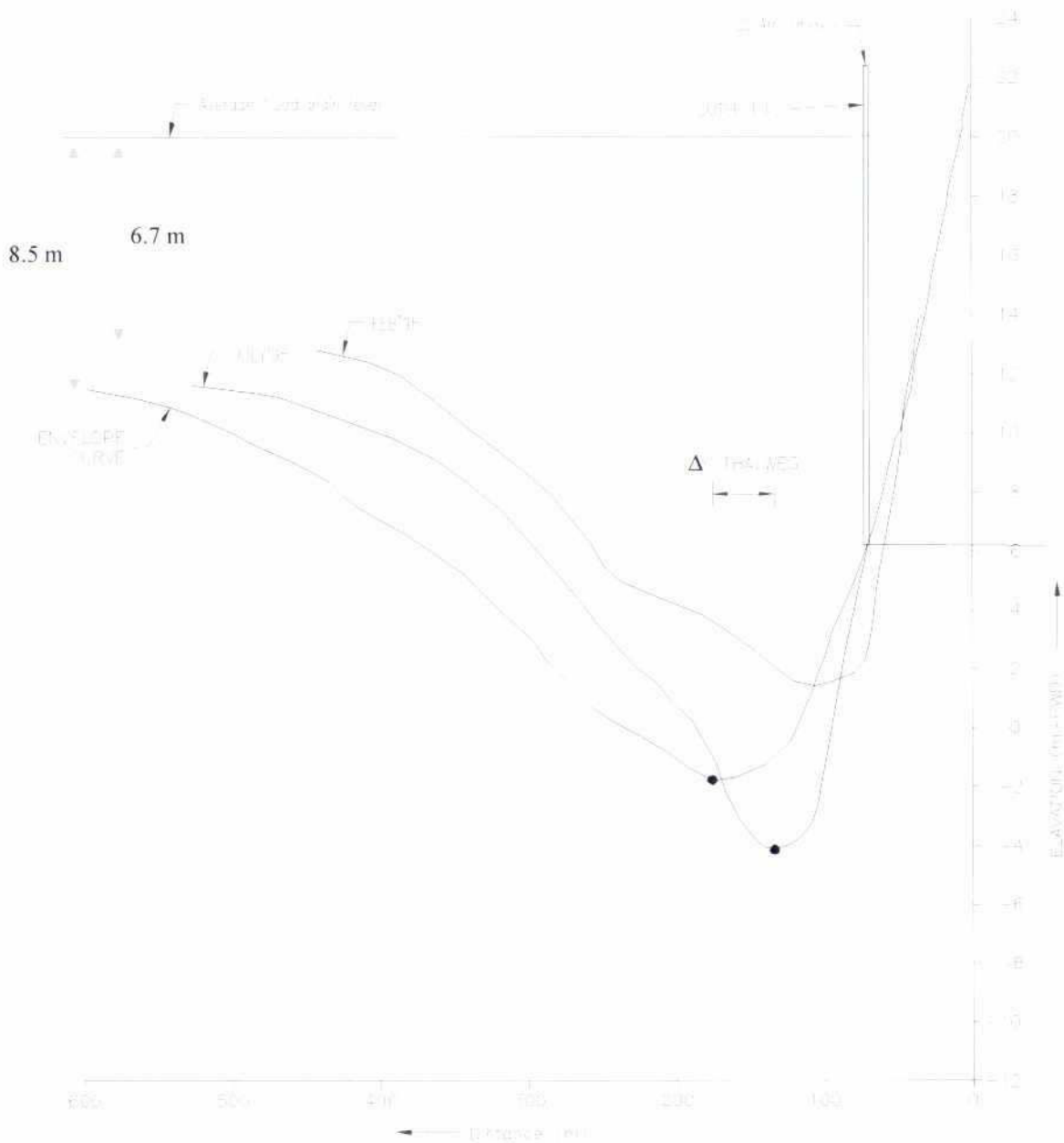


Fig. 4.4-3 Comparison between calculated and observed inner bend profile, Kamarjani during 1995 flood

(2) Outer Bend Profile

For the outer bend profile (Area I in Fig. 4.4-2) no formulations have been found in the literature. Therefore, an empirical formula has been derived based on enveloping curves from measured cross sections in the Jamuna river.

From the inner bend profile the water depth h_0 in the thalweg had been calculated related to the Design Water Level (DWL). The design water level is above the floodplain level (FPL). As only the part of the profile below the floodplain level is of interest, h_0 has to be substituted

$$h_0^* = h_0 - (DWL - FPL)$$

In area I of Fig. 4.4-2 the bed profile is given by an empirical envelope curve of surveyed cross-sections in the Jamuna river:

$$h(r) = h_0' - h_0' \left(1 - \frac{3B_{ch} - r}{5.5h_0'}\right)^2 \quad (4.4-8)$$

in which

$h(r)$	=	local water depth	(m)
B_{ch}	=	channel width	(m)
r	=	radius of channel bend	(m)
here: $r \geq 3B_{ch} - 5.5h_0'$			

This curve describes the envelope curve of all the surveyed cross-sections at selected locations. The width of area I in Fig. 4.4-2 is $5.5 h_0'$ and its cross-sectional area is $3.64 h_0'^2$. Theoretically, this area should be equal to $5.5 h_0' h_{ch}$ to maintain the average flow velocity calculated from the design channel discharge. In practice minor deviations from this condition can be accepted. The empirical bed profile can be used as an alternative to the design river bed profile given in Table 2.4-2 of Annex 4, h_0' is understood as the largest water depth at bankfull discharge. In other words, h_0' denotes the elevation difference between the floodplain and the lowest point. The comparison of the measured and calculated outer bend profiles show that the calculated outer bend profile is an envelope of the measured profiles. It seems likely that Formula (4.4-8) is valid for banks built up from non-cohesive soils as in Kamarjani. In case of cohesive banks steeper outer bend profiles seems likely. This has not been analysed.

Fig. 4.4-5 shows a few comparisons between the curve according to the formula and the straight lines according to the table. The resulting profiles are equivalent in the upper regions of the cross-section, but show deviations in the lower regions. In particular, the design riverbed profile appears to be too conservative, if SLW is much lower than floodplain level.

Cross Sections at Kamarjani from Aug '95 to Aug '98

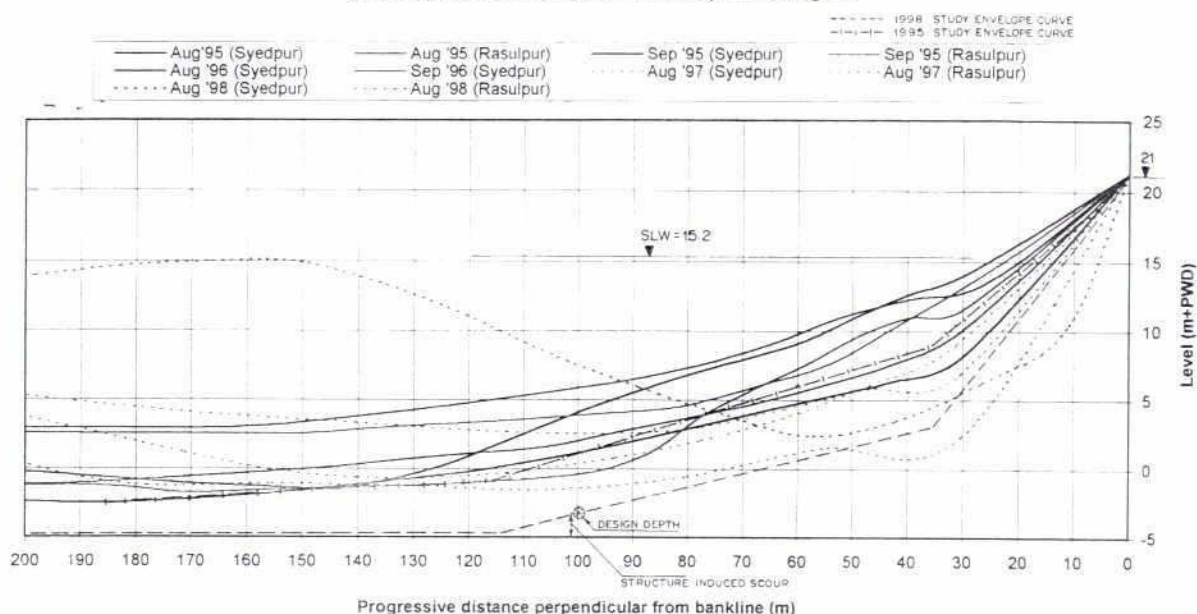


Fig. 4.4-4: Comparison measured outer bend profiles and the calculated outer bend profile, Kamarjani

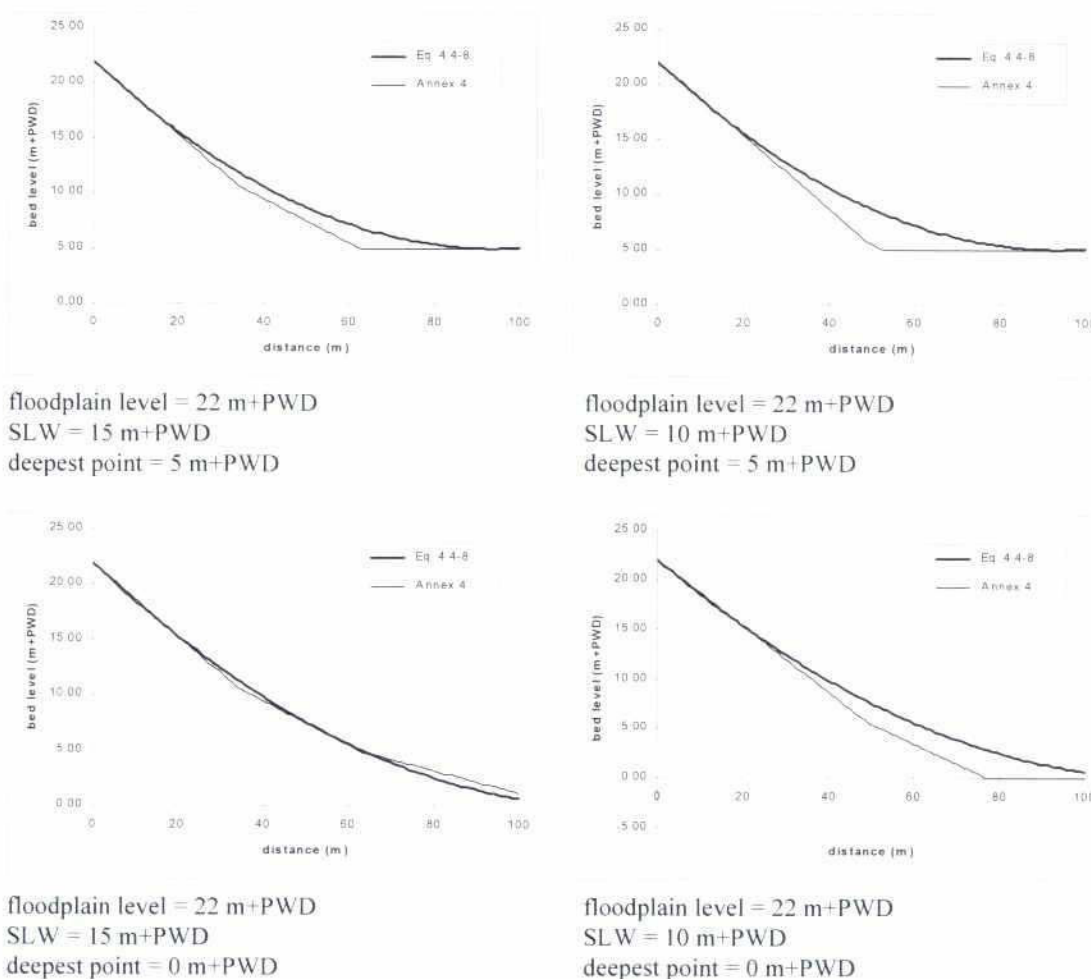


Fig. 4.4-5: Comparison of design outer bend profiles according to Formula (4.4-8) and Annex 4

This outer bend profile defines the thalweg where the water depth is $h = h_0$. This is at the location

$$r_0 = 3B_{ch} - 5.5h_0.$$

The condition $A_{ch} = A_I + A_{II}$ has to be fulfilled. Deviations can occur, if the assumption $h_c \approx h_{ch}$ is not valid. Then a more accurate calculation should be performed.

4.4.4 Design Bend Radius

In natural rivers the radius varies, as is demonstrated in the morphology report (see Annex 1). The minimum value of the radius determines the steepest bend profile, which is part of the design cross section. For design purposes the radius of a bend is schematised by a constant value.

It is recommended to use a design bend radius of 2.5 times the channel width ($B_{ch}/r_c = 0.4$, see Annex 1). This result is based on a study of bends in meandering rivers and has been verified for the Jamuna river as part of a planform study (see morphology report in Annex 1).

4.5 FLOW VELOCITY DISTRIBUTION

The flow velocity distribution is the approach flow towards the river training structure and it will be used to design the structure. The flow velocity averaged over the channel cross-section is defined as:

$$u_{ch} = \frac{Q_{ch}}{B_{ch} \cdot h_{ch}} \quad (4.5-1)$$

The Chézy-coefficient C_{ch} of the meandering channel is approximated by:

$$C_{ch} = \frac{Q_{ch}}{A_{ch} \sqrt{h_{ch} \cdot I}} \quad (4.5-2)$$

with I = water level slope (-)

In wide shallow river cross-sections, the averaged water depth h_{ch} is practically equal to the hydraulic radius R (m). Another approach, frequently applied in other studies of the Bangladesh rivers, is to use the conveyance K_c as a parameter to characterise cross-sections (Galapatti, 1993).

$$K_c = C \cdot A_{ch} \cdot R^{0.5} \quad (4.5-3)$$

where

A_{ch}	=	cross-sectional area of the channel	(m ²)
C	=	Chézy coefficient for hydraulic roughness	(m ^{1/2} /s)
K_c	=	conveyance	(m ² /s)
R	=	hydraulic radius	(m)

For all cross-sections in a certain river stretch with a constant discharge, a constant water level gradient and equilibrium bed topography, the conveyance is constant.

In general, the Froude number is less than 0.4 in alluvial rivers. If the Froude number is higher, then it is recommended to check carefully whether the theory presented in the following sections does apply. The flow in the design cross section is a function of the water level gradient I , the Chézy coefficient C , and Froude number Fr . The latter is given by

$$Fr = \frac{u_{ch}}{\sqrt{g \cdot h_{ch}}} \quad (4.5-4)$$

For the design of revetments the US Army Corps of Engineers (waterways Experiment Station) used design graphs to determine the flow velocity over the toe of the outer bank. The stone size is a function of this flow velocity. Thorne et al (1993) have analysed this design graph, and the design curve for natural channels is described by:

$$\frac{u_o}{u_{ch}} = c_6 - c_7 \log \left(\frac{r_c}{B} \right) \quad (4.5-5)$$

in which

c_6	=	1.75	
c_7	=	0.5	
B	=	channel width at the water surface	(m)
r_c	=	radius of the bend centreline	(m)
u_{ch}	=	cross section averaged flow velocity	(m/s)
u_o	=	depth averaged flow velocity in the thalweg	(m/s)

This design graph has been found to be on the safe side when used with sound engineering judgement and consideration of the limits of their applicability. However, a single parameter is probably not sufficient to characterise meandering bends as Thorne had supposed already (Thorne et al, 1993). Regression analysis was performed on the empirical data collected by Thorne et al to determine these coefficients more accurately without safety factor and $r/B > 2$:

- in natural rivers with straight approach conditions: $c_6 = 1.66$ and $c_7 = 0.42$
- in natural rivers with meandering approach conditions: $c_6 = 1.40$ and $c_7 = 0.24$.

In sequential meander bends the flow velocity over the toe is smaller than in bends with straight approach conditions.

(1) Inner Bend Flow Velocities

Based on the Chézy equation applied in a bend, the ratio of the flow velocities along the thalweg (u_o) and the centre-line (u_c) had been derived as:

$$\frac{u_o}{u_c} = \sqrt{\frac{h_0}{h_c} \left(\frac{r_c}{r_0} \right)^{(\varepsilon-2)/2}} \quad (4.5-6)$$

in which

ε	=	calibration coefficient.
---------------	---	--------------------------

Substitution of

$$r_0 = r_c + 0.5 \cdot B_{ch} - 5.5 \cdot h_0$$

leads to (see Struiksmma and Crosato, 1989)

$$\frac{u_0}{u_c} = \left(1 + \frac{B_{ch}}{2r_c} - \frac{n \cdot h_0}{r_c}\right)^{0.5 \varepsilon_c \sqrt{\theta} + 0.5 \varepsilon - 1} \quad (4.5-7)$$

in which

n	=	slope of the outer bend 1V:nH, with n = 5.5 (empirical value for Jamuna river)
ε	=	1: theoretical value without spiral motion 2: calibrated value for Waal river in the Netherlands 4: theoretical value with spiral motion

If no data are available to calibrate ε, then it is recommended to assume ε = 2. Assuming that $u_c \approx u_{ch}$, then follows u_0 from (4.5-7).

Some background information (with some typing mistakes in the formulas) on the theory behind these formulas is given by Mesbahi (1992), who was involved in a physical model investigation on the interaction between local scour around groynes and bend scour in the Study Phase of this Project.

The comparison with the US Water Experiment Station (USWES) design graphs shows reasonable conformity for $c_A \sqrt{\theta} = 10$, if B_{ch}/r_c varies between 0.05 and 0.2. This indicates a river with suspended load. For lower values lower flow velocities will be calculated. Compared with the USWES formula the influence of the hydraulic roughness of the channel has been introduced by Struiksmma and Crosato (1989) (see Fig. 4.5-1). Therefore, Formula 4.5-7 is recommended instead of the USWES formula and the coefficients determined by Thorne et al.

(2) Outer Bend Flow Velocities

The approach flow velocity above the underwater slope of the bank (area I in Fig. 4.4-2) is estimated by the Chézy formula and the Colebrook-White formula for steady uniform flow. The effect of spiral motion is neglected in this calculation. The ratio of the local depth-averaged flow velocity u_l above the underwater slope to the calculated depth-averaged flow velocity u_0 in the thalweg is given by:

$$\frac{u_l}{u_0} = \frac{\log \frac{12h_l}{k_{s,0}}}{\log \frac{12h_0}{k_{s,0}}} \sqrt{\frac{h_l}{h_0}} \quad (4.5-8)$$

where

h_0	=	water depth in the thalweg	(m)
$h_l(r)$	=	water depth above the underwater bank slope	(m)
$k_{s,0}$	=	Nikuradse equivalent sand roughness in the thalweg	(m)
$k_{s,l}$	=	Nikuradse equivalent sand roughness of underwater bank slope	(m)
u_0	=	depth-averaged flow velocity in the thalweg	(m/s)
$u_l(r)$	=	depth-averaged flow velocity above the underwater bank slope	(m/s)

If the u_0 is known from (4.5-7) then $u_l(r)$ can be calculated from (4.5-8). These flow velocities are the approach flow velocities to the groyne test structure. If the calculated flow velocities along the bank

are above the critical flow velocity for bank erosion, it is likely that the bank will erode without the protection by groynes. If the calculated design flow velocities are below the critical flow velocities for bank erosion, the calculation method might be unreliable in the considered case. For example, this is the case if the schematisation does not apply or other phenomena, which are not included in this calculation method, are dominant.

The presented calculation method will be a valuable tool for the design of a physical model or a mathematical model.

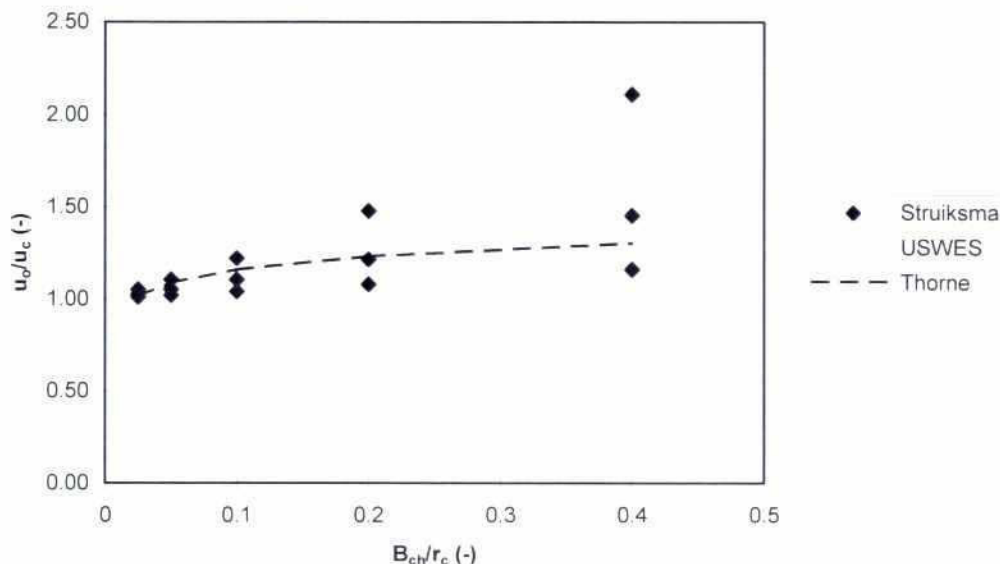


Fig. 4.5-1: Comparison of the flow velocity ratio in a bend as function of B_{ch}/r_c

4.6 THE EFFECT OF A SERIES OF GROYNES ON THE FLOW FIELD

4.6.1 Preliminary Remark

In case the approach flow is parallel to the bank, the reduced flow velocity downstream from a permeable groyne increases gradually in downstream direction to the undisturbed flow velocity. This process depends on an expansion angle combined with a mixing layer due to lateral transfer of momentum. This effect is intensified by an oblique approach flow. These aspects are described separately in the following Subsections.

4.6.2 Oblique Flow Attack

The flow in a meander bend had been described with an axi-symmetrical flow in the previous sections. Formulas have been presented to calculate the maximum flow velocity along the concave bank. In a braided river, meander bends tend to migrate in downstream direction. The migration of channels smaller than the design channel is often affected by the attraction of the flow induced by a bank protection structure (see Annex 1, Subsection 6.2.4). This results in an extreme oblique flow attack on the structure, which makes the flow velocities higher than in the parallel flow. Oblique flow is defined by the angle between the flow direction and the thalweg of a channel. This is also called a

flow impinging on a series of groynes. The curvature radius of the impinging flow can be very short in extreme design conditions.

Especially in bends or in individual channels of a braided river, the angle of oblique flow depends on the size of the local scour holes near the structure. A maximum angle is 40 to 50 degrees, if the depth of the local scour hole is slightly less than the water depth (see Annex 11).

4.6.3 Expansion Angle

The different values for the expansion angle β (see Fig. 4.6-1), which have been recommended in the literature, are summarised below.

Lagasse (1995) recommends an expansion angle with respect to the main flow of 17 degrees for impermeable groynes in concave bends, starting from the tip of the groyne, if the ratio of the projected groyne length L_g to the bankfull channel width B_{ch} satisfies $L_g/B_{ch} < 0.1$. This condition limits the disturbance of the main flow by a scheme of groynes. The expansion angle increases gradually to 20 degrees as L_g/B_{ch} increases to 0.4, probably because the depth of the scour hole increases. For a standard design of bendway weirs in sharp concave bends, an expansion angle of 20 degrees is recommended (Lagasse et al, 1997). This angle does not depend significantly on the groyne orientation.

Przedwojski et al (1994) quote Maza Alvarez' (1989) finding that the expansion angle varies between 9 and 14 degrees. In a study of the effect of push-tows on the water circulation around groynes in a straight river section, WL | Delft Hydraulics (1987) had measured a maximum angle of 35 degrees in the separating flow line, which corresponds to an expansion angle of about 13 degrees. The groyne spacing was four times the groyne length and two eddies developed in the groyne field, which was about half as deep as the navigation channel. Mathematical model simulations by WL | Delft Hydraulics (1991) show an expansion angle of about 10 degrees, assuming a fixed bed without scour holes, a shallow groyne field and a Nikuradse roughness height of 0.3 m. Field measurements in Druten along a straight section of the Waal river (WL | Delft Hydraulics, 1991, fig. 14) indicate a separation angle of 8 to 12 degrees in a shallow groyne field.

A groyne can be considered as a disturbance of the flow field. This disturbance diminishes in downstream direction and the relaxation length λ_w is a characteristic parameter for this process. This relaxation length follows from a linearized balance between the convective term and the friction term in a one-dimensional momentum equation:

$$\lambda_w = \frac{C^2 \cdot h}{2 \cdot g} \quad (4.6-1)$$

in which

λ_w	=	relaxation length	(m)
C	=	Chézy coefficient	(m ^{0.5} /s);
g	=	acceleration due to gravity	(m/s ²)
h	=	local water depth	(m).

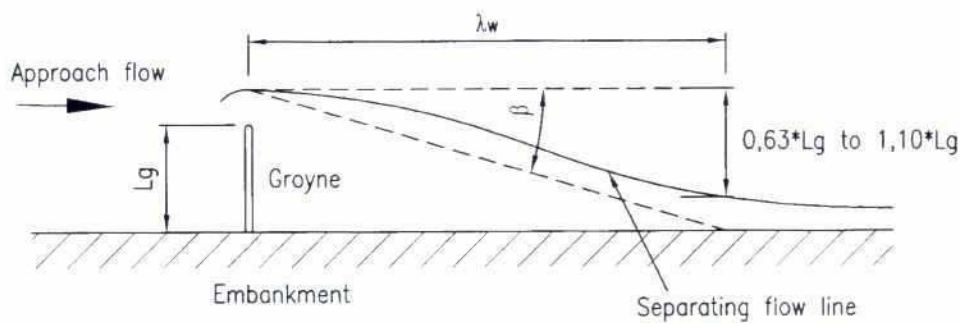


Fig. 4.6-1: Sketch of a theoretical separating flow line

The expansion angle can be calculated by

$$\tan \beta = 13.6 \cdot \frac{L_g}{C^2 \cdot h} \quad (4.6-2)$$

Table 4.6-1 gives examples of the application of this formula.

h (m)	C (m ^{0.5} /s)	L _g (m)	λ _w (m)	tan β (-)	β (degree)
3	40	60	245	0.170	9.7
5	60	200	917	0.151	8.7
5	40	200	408	0.340	19.5
10	40	300	815	0.255	14.6
8	40	250	652	0.266	15.2
8	40	300	652	0.319	18.3
8	40	350	652	0.372	21.3

Table 4.6-1: Examples of the expansion angle β as function of h, C and L_g, assuming the same water depth in channel and groyne field

The formula for the expansion angle can be generalised by including an empirical coefficient c₅ for channel alignment and groyne-field water depth

$$\tan \beta = 13.6 \cdot c_5 \cdot \frac{L_g}{C^2 \cdot h} \quad (4.6-3)$$

Values for c₅ are given in Table 4.6-2.

Channel alignment	Water depth in groyne field	Scour hole	Coefficient c ₅
bend	Deep	deep	1.25
straight	Deep	moderate / deep	1.00
straight	half of main channel depth	no / moderate	0.75

Table 4.6-2: Recommended expansion angles if the main flow is parallel to the bank curvature

Fig. 4.6-2 shows Brown's (1985) graph for the expansion angles at permeable groynes (Lagasse et al, 1995).

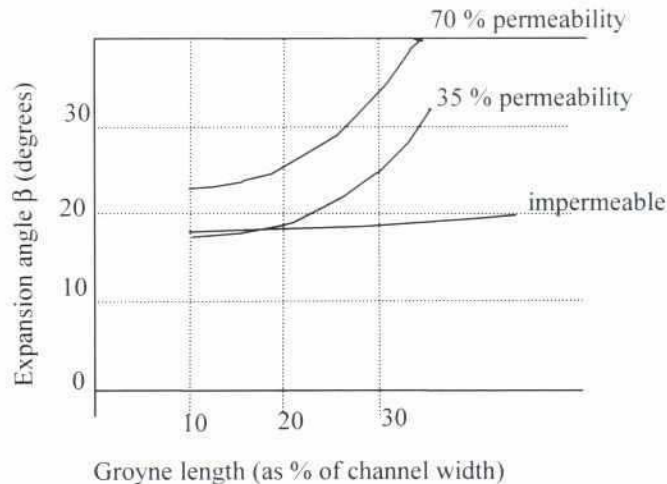


Fig. 4.6-2: Relationship between groyne length and expansion angle for several groyne permeabilities

In Kamarjani the expansion angle had been influenced strongly by the oblique approach flow and the bathymetry with considerable scour holes. The drifter measurements do not indicate clearly the expansion angle, also because the highly turbulent flow had disturbed the path followed by the drifter.

4.6.4 Mixing Layer

A mixing layer develops between the main flow in the channel and the flow passing through the permeable groynes. An approximate method to calculate this mixing layer has been set up by van Ellen (1988) for a situation where the main channel and the groyne field have different water depths and hydraulic roughness. Other information is given by Ikeda et al (1991). Rajaratnam (1976) gives a first approximation for situations in which the groyne field is as deep as the main channel and the influence of the hydraulic roughness is negligible.

In Kamarjani no mixing layer could be distinguished from the measurements, due to the complex bathymetry and groyne geometry.

4.7 EFFICIENCY OF A PERMEABLE GROUYNE TO REDUCE THE FLOW VELOCITY

4.7.1 Introduction

A pile row with and without bed protection is an obstacle in the flow. Downstream from the pile row the turbulence increases by the von Karman eddies and vortices. This increased turbulence in the flow results in reduced depth averaged flow velocities, which do not cause bank erosion in an equilibrium situation. The main effect of a pile row is the reduction of the flow velocities in the flow passing the pile row. In this section the observed flow velocities in the groyne field during the 1995 flood are compared with the design flow velocities (Subsection 4.7.2) and a method is presented to estimate this reduction of the flow velocities (Subsection 4.7.3).

4.7.2 Comparison of Observed and Design Flow Velocities

As soon as the impermeable part of the groynes became exposed to the flow during the 1995 monsoon, an unstable eddy developed just downstream from that part. This eddy was most of the time unstable: growing of the eddy was followed by a process of shrinking and it created a return flow along the embankment. After the slide near G-2 the eddy downstream from that groyne disappeared, and the flow pattern was changed in a straight flow without eddies and return current.

Some characteristic flow velocities, which were measured between the groynes G-1 and G-2 as well as between G-2 and G-3 by surface floats, are presented in Fig. 4.7-1 as a function of the distance to the axis of the embankment. These graphs show that the permeable groyne section from 60 to 110/130 m was very effective in reducing the surface flow velocities from 2.75 m/s to about 1 m/s near the transition to the impermeable part. In the impermeable part the reduction in flow velocities was very small, because this impermeable part generated eddies with return currents of maximum 0.8 to 1.0 m/s.

From these surface flow velocities the depth averaged flow velocities were estimated, see the curve in the graphs of Fig. 4.7-1. However, these maximum flow velocities were not measured at the same water level. Therefore, the tendency in these data points might be affected slightly by the different stages.

These flow velocities can be compared with the design flow velocities determined from the results of physical model tests and the generalised design flow velocities. The graphs show that the tendency in the measured flow velocities was similar to the tendency in the design flow velocities as function of the distance to the embankment and that the measured flow velocities were always below the design flow velocities. During the monsoons floods after 1995 the flow attack on the test structure was significantly less than during the 1995 flood. Therefore, those observations have not been presented here.

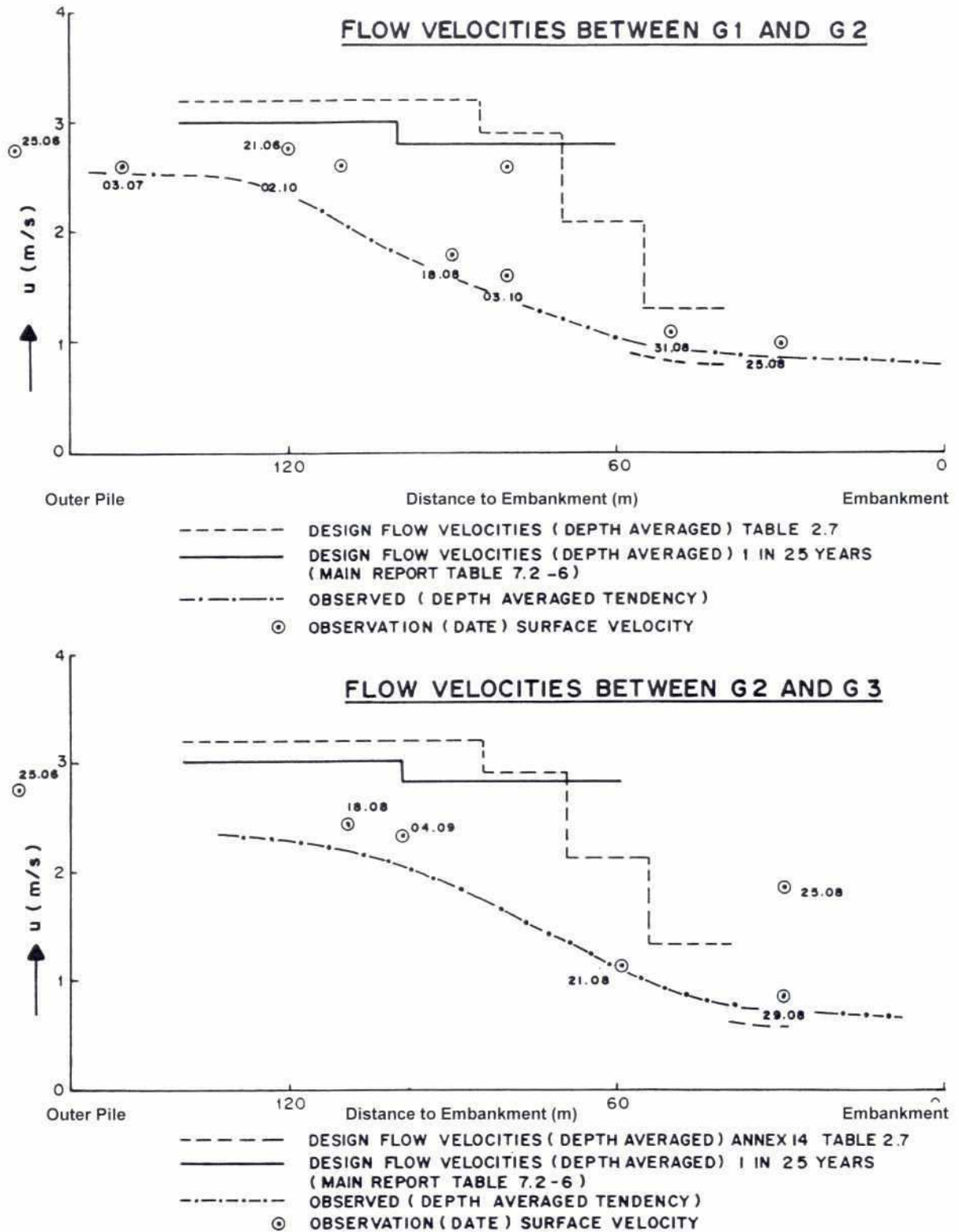


Fig 4.7-1: Flow velocities between G-1 and G-2 and between G-2 and G-3 during the 1995 flood

4.7.3 Reduction of Flow Velocities

Consider a control volume bordered by the flow lines, which intersect the permeable groyne in the centre of the spaces between a pile and its neighbouring piles (see Fig. 4.7-2). The momentum equation is applied to this control volume as follows:

$$F \cdot \delta t = m_1 \cdot u_1 - m_2 \cdot u_2 \quad (4.7-1)$$

in which

F	=	force load exerted by the flow on the pile	(N)
m_1, m_2	=	mass entering and leaving the considered control volume	(kg)
u_1, u_2	=	depth-averaged flow velocity at the side of the control volume	(m/s)
δt	=	time step	(s)

Subscript 1 refers to the upstream boundary of the control volume and subscript 2 to the downstream boundary. The formula can be written as:

$$C_D \cdot \frac{l}{2} \cdot \rho \cdot u_{ch,1}^2 \cdot A_p \cdot \delta t = \rho \cdot A_1 \cdot \cos \gamma \cdot u_{ch,1} \cdot \delta t \cdot u_1 - \rho \cdot A_2 \cdot \cos \gamma \cdot u_{ch,2} \cdot \delta t \quad (4.7-2)$$

in which

A	=	cross-sectional area	(m ²)
C_D	=	drag coefficient	(-)
u_{ch}	=	flow velocity averaged over A	(m/s)
γ	=	angle between flow direction and line perpendicular to the groyne axis	(degree)
ρ	=	density of water	(kg/m ³)

Subscript p in above formula refers to the pile.

It is assumed that the riverbed does not vary in the direction of the flow ($A_1 = A_2$) and that the flow velocity at the upstream boundary is equal to the approach flow velocity above the toe of an outer bend ($u_{ch,1} = u_o$). Then

$$\frac{u_2}{u_o} = \sqrt{1 - \frac{l}{2} \cdot C_D \cdot \frac{A_p}{A_l \cdot \cos \gamma}} \quad (4.7-3)$$

in which γ is the angle between the flow lines and a line perpendicular to the groyne axis. This angle is determined by the expansion angle and the oblique approach flow.

In Formula (4.7-3) the reduction of the flow velocity is a function of the drag coefficient C_D , the flow blockage by the pile row A_p/A_l , and the direction of the approach flow γ , which follows from the assumed oblique flow attack in the previous section.

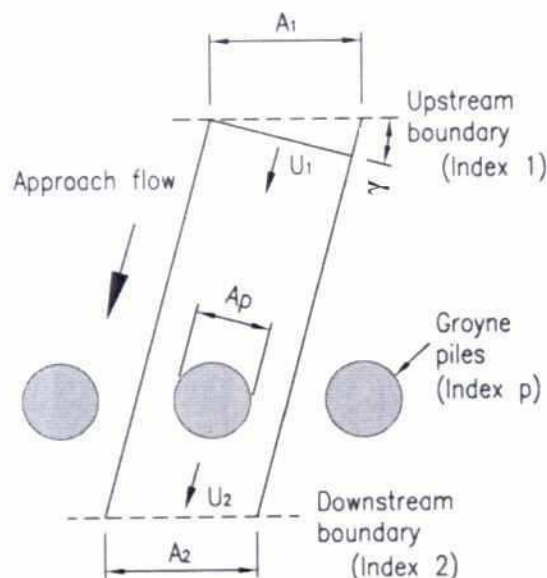


Fig. 4.7-2: Control volume for application of momentum equation

This formula has been compared with field measurements made during the 1995 and 1998 floods. This yields the following conclusion:

- $C_D = 0.7$ for smooth single piles in strong flows (design flow velocities 3 to 3.5 m/s);
- $C_D = 2$ for rough, closely spaced piles in moderate flows (at lower Reynolds numbers; approach flow velocities 0.5 to 0.9 m/s during monitoring).

These findings are described in more detail hereafter. The observed reduction of the flow velocities measured in the 1995 flood showed that C_D varied between 1.5 to 3 and had a slight tendency to increase as the permeability reduces from 90% to 50 % (see Fig 4.7-3). This is a known tendency when piles are close to each other, because the boundary layer around the piles contributes to the blockage of the flow. The scatter in the data can be ascribed to measurements on different dates, sometimes with a week between upstream and downstream measurements, and by irregular geometry of the riverbed and bank, which violates the assumption $A_1 = A_2$.

A similar analysis of the much more accurate float track measurements carried out in 1988 (Consulting Consortium FAP 21/22, 1998a) showed that $C_D = 2$ appeared to be a fair estimate (Fig. 4.7-4). The scatter in the 1998 data appeared to be less than in the 1995 data. The determination of this coefficient is very sensitive to the ratio u_2/u_b . The flow velocity downstream from the pile row is difficult to measure from float measurements because of the high turbulence level generated by the piles. This explains the scatter in the value of C_D .

For a single cylinder, Hallem et al (1978) recommend $C_D = 1.2$ in case of a circular cross-section and $C_D = 2$ in case of a square cross-section. A row of piles does increase C_D slightly from 1.2 to 2 for Reynolds numbers between 10^5 to 10^6 . These C_D values confirm the presented analysis of the monitoring data.

The conclusion is that the reduction of the flow velocities by the piles can be estimated by Formula (4.7-3) with $C_D = 2$ for the monitoring conditions with relatively low flow velocities. Sample values are presented in Table 4.7-1.



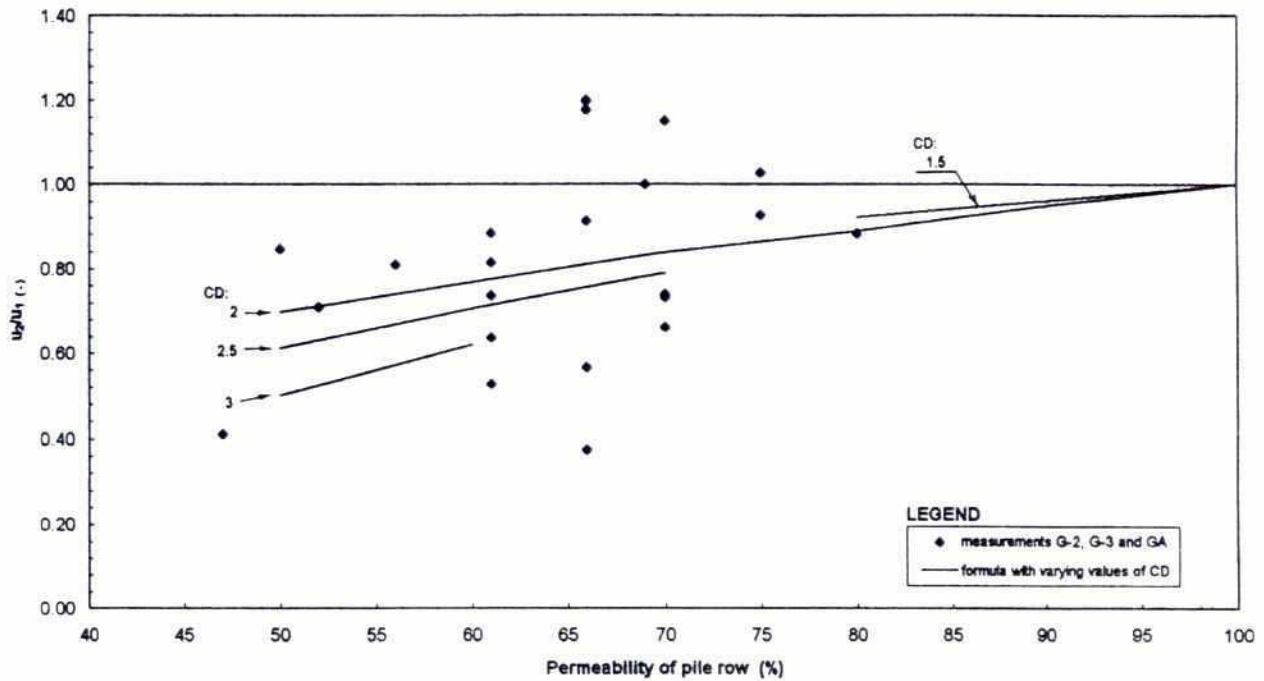


Fig. 4.7-3: The drag coefficient determined from float observations during 1995 flood

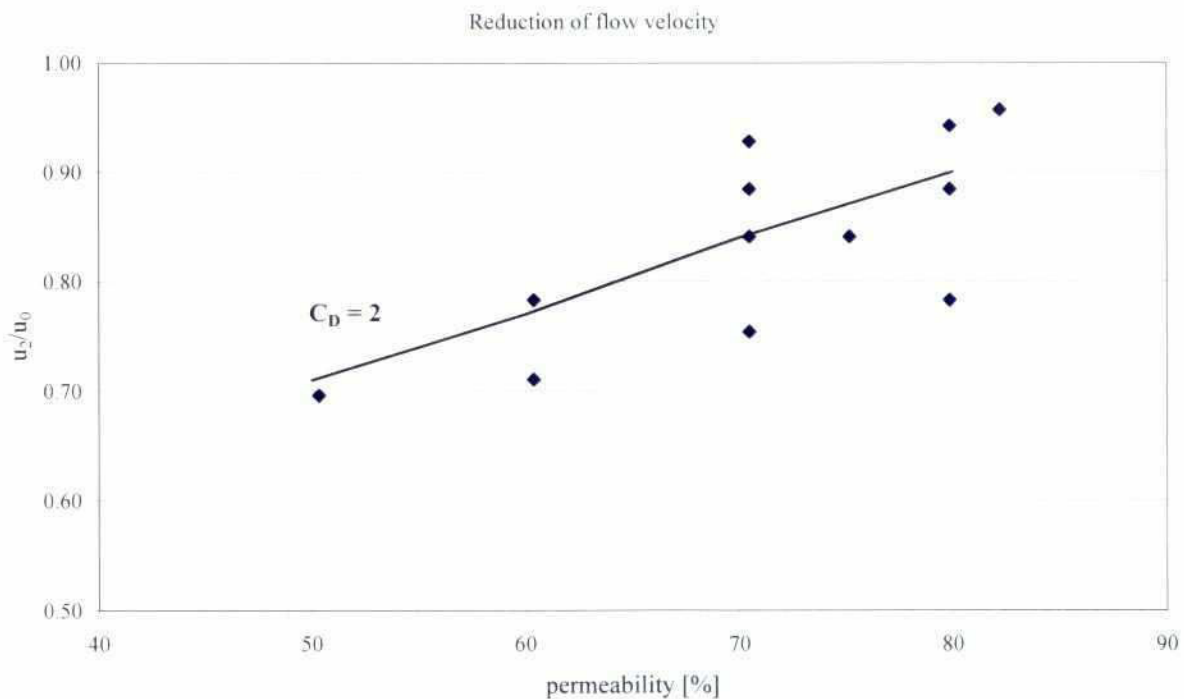


Fig. 4.7-4: The drag coefficient determined from accurate float observations during 1998 flood.

Permeability (%)	U_o/u_o (-)	
	observed	calculated (with $C_D = 2$ and $\cos \gamma = 1$)
80	0.8 to 1.0	0.90
70	0.7 to 0.9	0.84
60	0.65 to 0.8	0.77
50	0.6 to 0.7	0.71

Table 4.7-1: Reduction of flow velocities by a groyne consisting of a row of piles

The following formula given by Przedwojski et al (1994) overestimates the reduction and is therefore not recommended:

$$\frac{u_2}{u_o} = 1 - \frac{A_p}{A_1} \quad (4.7-4)$$

When a series of permeable groynes is attacked by parallel flow, the flow velocity is reduced from groyne to groyne in downstream direction by repeated application of Formula (4.7-3), see Table 4.7-2. This table shows that a series of permeable groynes can be very effective in reducing the flow velocities along the bank. However, lateral momentum transfer, expansion angle and oblique flow attack will affect this reduction of flow velocities adversely. Therefore, Formula (4.7-3) should not be applied more than three times to prevent too optimistic estimates of the flow velocity reduction. Nonetheless, the table shows that permeable groynes should be applied in series of at least three groynes to obtain a considerable reduction in flow velocities along the bank and to stop or to prevent bank erosion.

It is uncertain how the oblique flow attack and the expansion angle have to be combined. A first hypothesis is that they should be added to each other. But this still requires verification on the basis of monitoring data.

It is also uncertain how floating debris affects the flow reduction through a pile row. A first estimate is that A_p in formula (4.7-4) should be replaced by $A_p + A_{\Pi}$ where A_{Π} is the cross-sectional area blocked by floating debris (m^2).

Permeability (%)	u_2/u_o (-)		
	first pile row	second pile row	third pile row
80	0.90	0.81	0.73
70	0.84	0.71	0.59
60	0.77	0.59	0.46
50	0.71	0.50	0.36

Table 4.7-2: Theoretical reduction of the flow velocities by a series of three groynes in a parallel flow with expansion angle $\alpha = 0$

4.8 CRITICAL FLOW VELOCITY FOR BANK EROSION

The empirical critical flow velocity u_{cr} , is a depth-averaged flow velocity that induces the initiation of sediment motion. The u_{cr} depends on the local water depth and the subsoil (D_{50} , cohesiveness).

Instead of a critical flow velocity, a critical shear stress exerted on the river bed near the bank can be used as a parameter to indicate a stable or eroding bank. The critical value of the Shields parameter θ_{cr} based on shear stress (see also Annex 1, Subsection 1.5) varies between 0.03 and 0.1 depending on the D_{50} of the riverbed and bank. Following the Shields approach, a critical depth average flow velocity u_{cr} between 0.22 and 0.4 m/s can be determined. However, this approach is not correct because it holds only for uniform flow conditions and non-cohesive sediment with uniform grain size.

Due to the constrictions (mainly the cohesiveness of the material), the critical depth averaged velocity according to Shields has to be increased. It is 0.4 m/s for shallow water. For deep water it is expected that the turbulence intensities decay and that the bed particles are exposed to less turbulence velocity fluctuations as in shallow water. This is not accounted for by the Shields parameter, which is based on testing in physical models. It is suggested from experience to use a critical flow velocity of 1.0 m/s for deep water flow conditions.

If the flow exerts a critical shear stress everywhere in the bank section of a cross-section during a design event, the cross-section profile is just in equilibrium and no further bank erosion will occur. Various authors have determined the equilibrium profiles. This equilibrium ultimately determines the location of the stable bank. An embankment can be planned at a safe distance from this bankline.

5 WAVES AND WIND

5.1 WIND

The wind direction and the wind speed had been observed at the monitoring station (see Annex 6). A maximum wind speed of 12 to 16 m/s has been measured at the test structure during some moderate storms, see Fig. 5.1-1 showing the measurements during the monsoon 1997 and an example of wind speed measurements during a storm on September 12, 1996, see Fig. 5.1-2. In the year before a few observations are available, indicating an estimated maximum wind speed of 8 Beaufort, see Fig. 5.1-3. The maximum wind during extreme storms is most probably higher than these measured speeds. The maximum wind speed occurs during storms, most probably the storms which are called Northwesters (Rashid, 1991). During these storms the wind can change to all possible directions, but these storms occur mainly in the period from October to May, when the water level is below flood plain level. During the monsoon the dominant wind direction is SE, see Fig. 5.1-1.

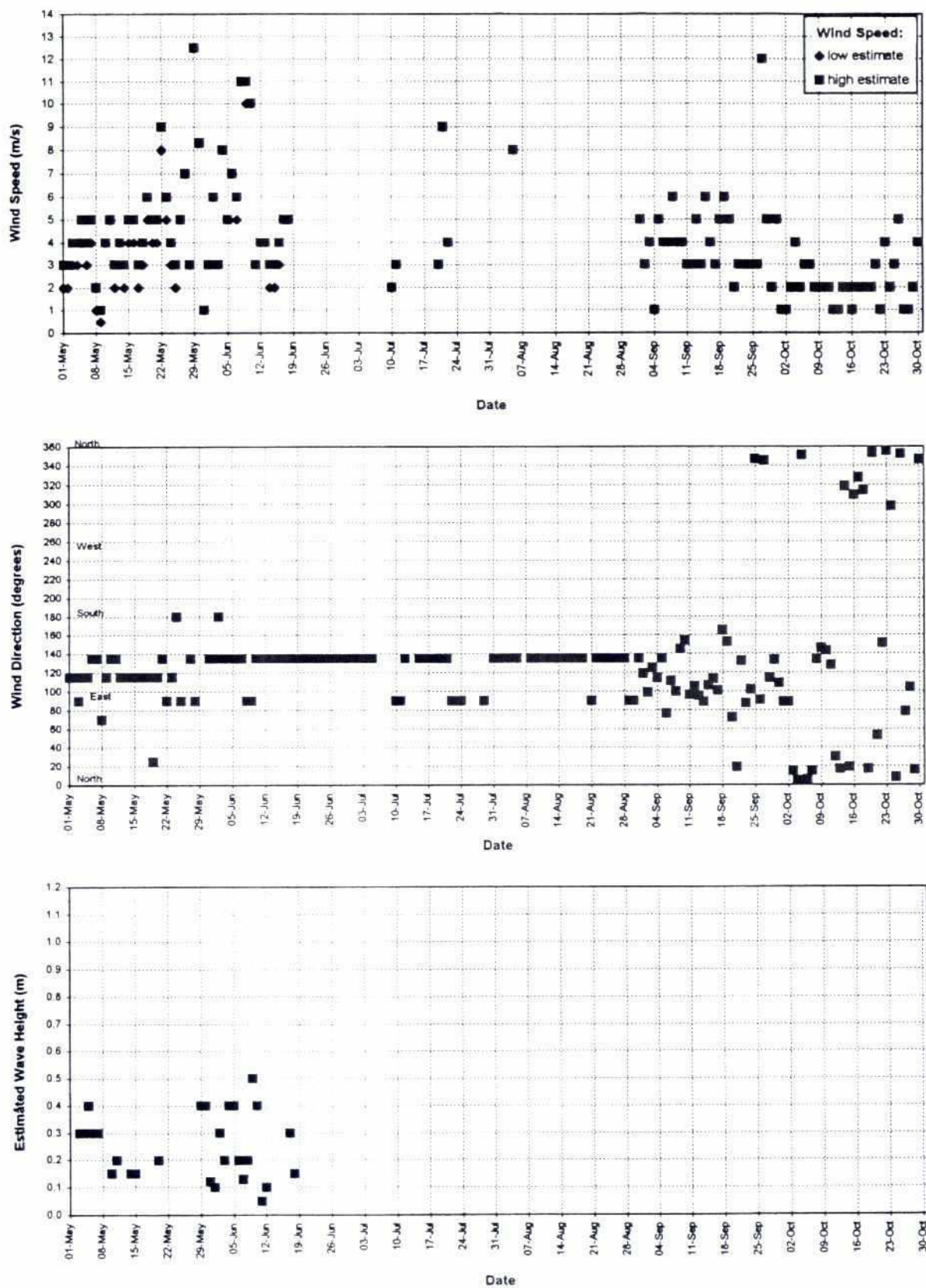


Fig. 5.1-1: Measured wind speed and direction, wave heights during monsoon 1997

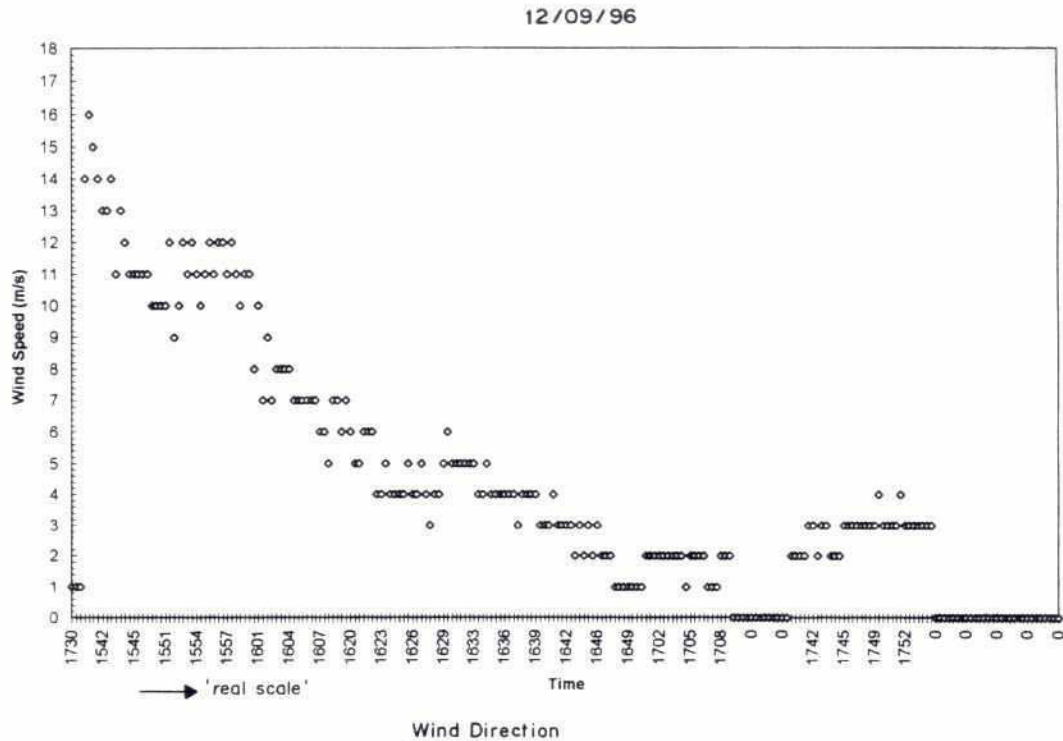


Fig. 5.1-2: Example wind speed during a storm on September 12, 1996

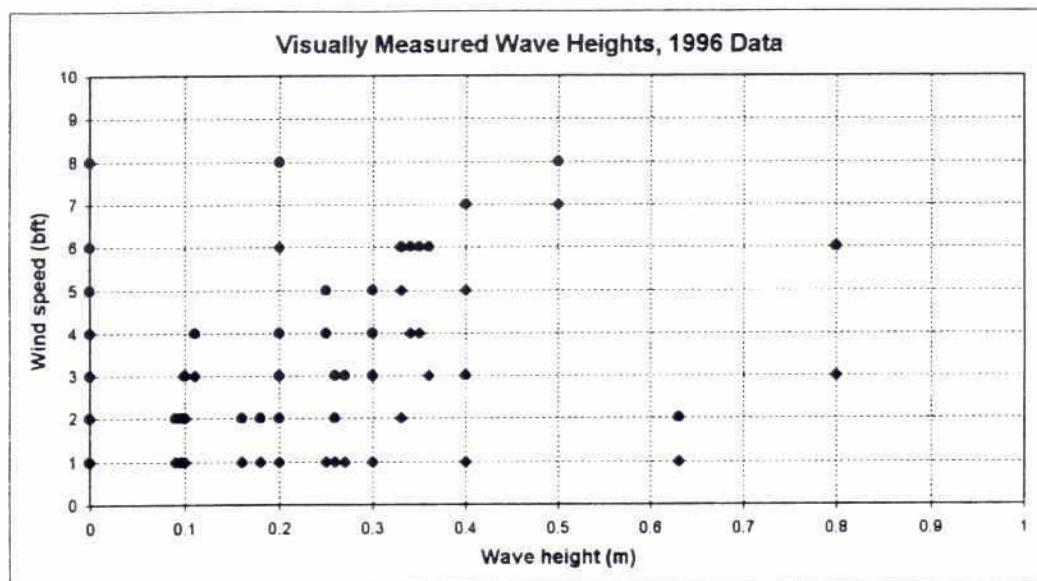


Fig 5.1-3: Visually measured wave heights as function of wind speed, 1996 data

5.2 WAVES

In general the maximum wave heights are caused by maximum wind speed over the longest fetch length. In Kamarjani the fetch length is maximum in SE and NE direction. From the few observations

in Fig. 5.2-1 it can be seen that the maximum estimated wave heights had been caused by wind from SE and E direction. This dependency on fetch length makes that the relation between wind speed and wave height shows some scatter, see Fig. 5.1-3 and Fig. 5.2-2 with some observations made during the 1995 monsoon. It is mentioned that the monitoring of wind was not fully operational at that time. Therefore, only a few observations are available from the 1995 monsoon. In general, these observations confirm the more accurate measurements in 1996 and 1997, when the flow attack on the test structure was less than in 1995 monsoon. The monitoring team had estimated maximum wave heights of about 1 m in the middle of the channel in front of the test structure, see Fig. 5.2-2. However, the effective height of waves attacking the groynes and the embankment was lower, with an estimated maximum of 0.8 m, see Fig. 5.1-3. This is slightly lower than the design wave height of 1 m. From these observations it is concluded that the maximum wave height with a return period of 100 years for the design of bank protection structures along the Brahmaputra-Jamuna river should be about 1.3 m. The significant wave height H_s , however, is lower than this maximum wave height, about 0.7 to 0.8 m.

The effective fetch length depends on the water level in the channel, the alignment of the channel compared to the wind direction and the banklines of the upwind water body. Therefore, the fetch length can vary widely. For the Brahmaputra-Jamuna river, a design fetch length of a few kilometres is recommended.

The design method is based on the formulas proposed in the Shore Protection Manual (CERC, 1977). For shallow water conditions, the significant wave height is calculated by:

$$H_s = 0.283 \cdot \tanh \left[0.530 \cdot \left(\frac{g \cdot h_{ch}}{u_w^2} \right)^{0.75} \right] \cdot \tanh \left\{ \frac{0.0125 \cdot \left(\frac{g \cdot L_f}{u_w^2} \right)^{0.42}}{\tanh \left[0.530 \cdot \left(\frac{g \cdot h_{ch}}{u_w^2} \right)^{0.75} \right]} \right\} \cdot \frac{u_w^2}{g} \quad (5.2-1)$$

in which

h_{ch}	=	average water depth in upwind area of water body	(m)
L_f	=	fetch length	(m)
g	=	acceleration due to gravity	(m/s ²)
H_s	=	significant wave height	(m)
u_w	=	average wind speed	(m/s)

Formula (5.2-1) holds for the deepest parts of the channel. The monitoring data have shown that the waves are lower in the shallower areas of the channel. It is recommended to take this phenomenon of shoaling into account when calculating the design wave attack on an embankment protected by permeable groynes.

Basically, the evaluation confirms the design assumptions. Reference is made to Attachment 1 of Annex 4 and Section 6.2 of Annex 6.

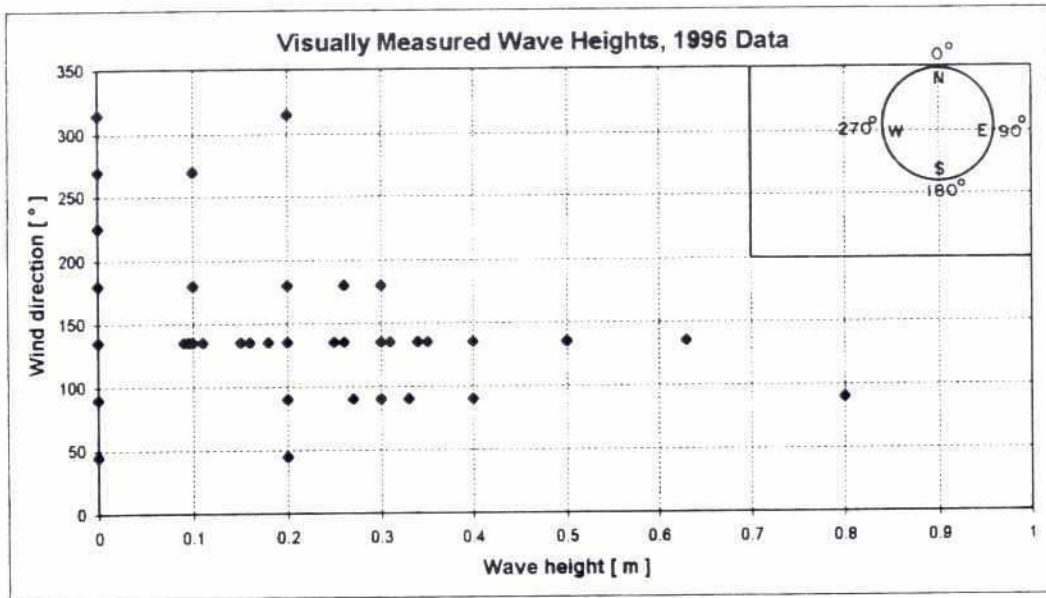


Fig. 5.2-1: Visually measured wave heights as function of wind direction, 1996 data

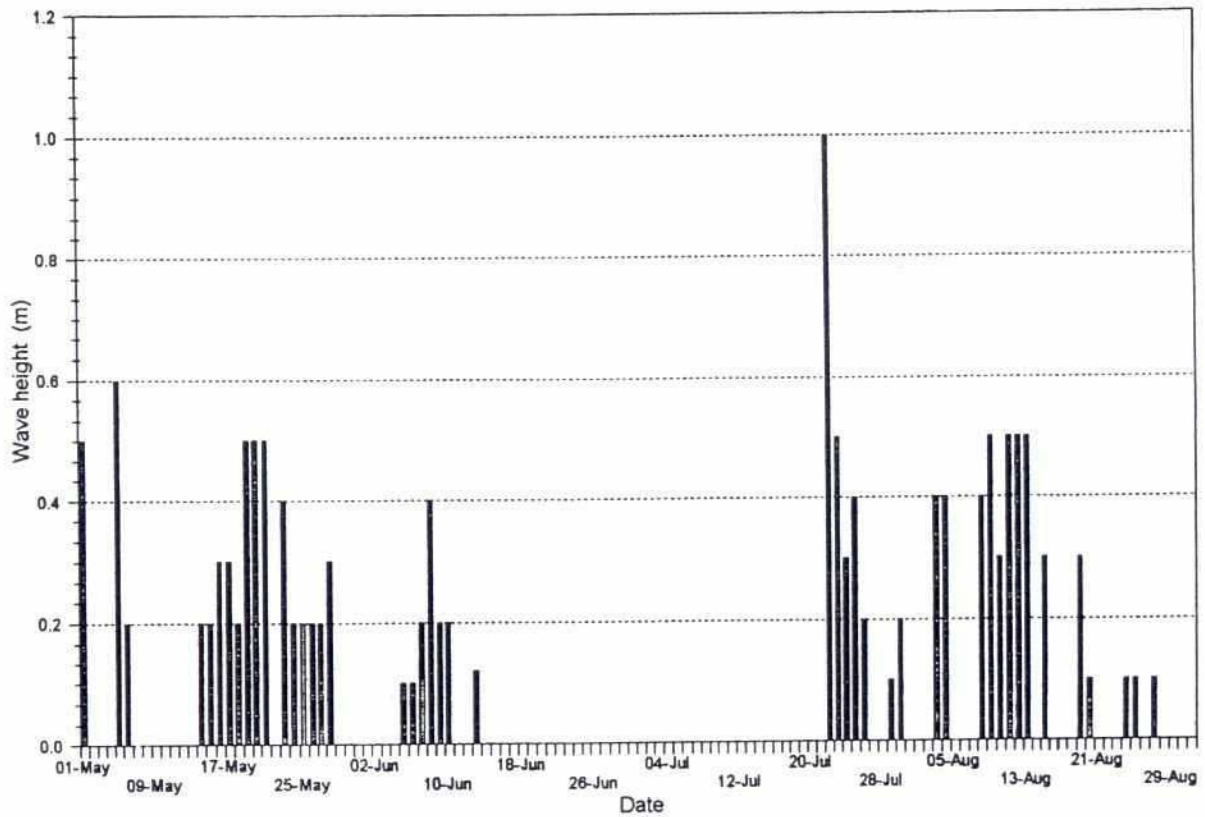


Fig. 5.2-2: Preliminary analysis of some observations made in 1995

6 SCOUR

6.1 INTRODUCTION

Downstream from each groyne a local scour hole developed during flow attack. The characteristic parameters of a local scour hole are its location, its growth rate ("scour velocity"), its maximum depth and the steepness of its side slopes. The maximum scour depth is defined as the difference between the depth in the deepest point of the scour hole and the averaged depth in the approach channel just upstream from a scour hole.

Near permeable groynes as constructed in Kamarjani the following scour phenomena can be distinguished:

1. local scour hole downstream from the tip of the groyne;
2. local scour around the piles (groyne without a bed protection);
3. local scour downstream from the transition from a permeable to an impermeable section;
4. local scour upstream from the groyne (protrusion scour), and
5. interaction scour, interaction between bend scour and local scour at the tip.

Theoretically, also an interaction scour between confluence scour and local scour, or confluence scour, bend scour and local scour is possible, and might result in very deep scour.

Add 1: In this chapter the local scour hole downstream from the tip of the groyne has received most attention, since it is most important for the design of the structure. It was investigated in physical model tests and it is described in detail in Section 6.2.

Add 2: The small local scour hole around piles is well known in the literature and the maximum depth is about 2 to 3 times the pile diameter if the water depth is larger than the pile diameter and if the groyne was designed without a bed protection (Breusers and Raudkivi, 1991).

Add 3: Physical model tests show that an abrupt transition from an impermeable part to a permeable part can cause the development of a secondary scour hole close to the bank (Fig. 6.1-1). Therefore, a gradual transition is recommended to prevent the development of such a secondary scour hole.

Add 4: This type of scour had not been included in the design of the test structures, but the monitoring data had shown that it could develop under certain circumstances. It will not be described in this chapter, because its small size does not require it to be included in the design procedure.

Add 5: This type of scour had also not been included in the design of the test structures, but the monitoring data had shown that it could also develop under certain circumstances. It will be described in Section 6.2 separately.

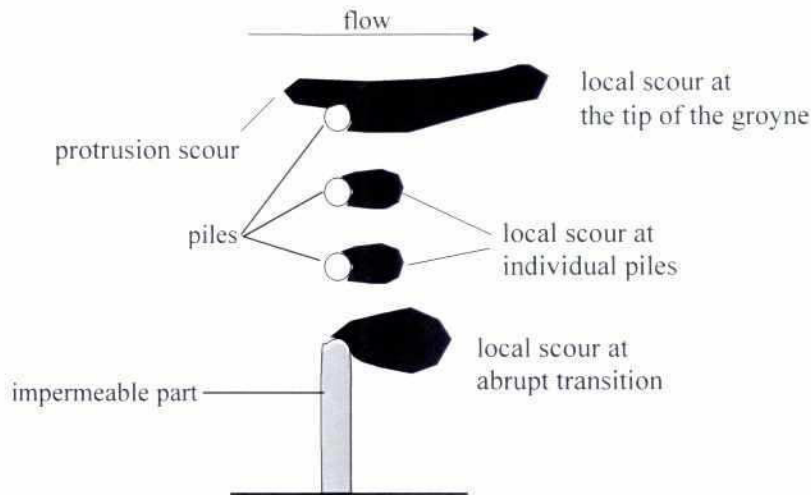


Fig. 6.1-1: Scour pattern at groynes with an impermeable and a permeable part

The expected maximum scour depth for the Kamarjani Test Structure had been determined from physical model tests. The scaling of the models to exclude scale effects is described in Section 6.2. The time-dependent development of the maximum scour depth and the maximum scour velocity determine the risk of the loss of stability of a part of the structure by flow slides. The development is described in Section 6.3. The width, the length and the side slopes of the local scour hole are of secondary importance. Floating debris causes additional scour, which is described in Section 6.4.

Two failure mechanisms, which could not be quantified satisfactorily for the design of the Groyne Test Structure at Kamarjani, appear to be important: extra structure-induced scour in rivers with rapidly changing bed levels and bank lines and large slides due to soil mechanical instability. These two mechanisms are presented briefly, but still little is known about them in quantitative terms. The extra structure induced scour is described in Section 6.5, followed by the estimation of confluence scour and interaction scour in Sections 6.6 and 6.7 respectively. Section 6.8, finally presents some aspects on the slides from mechanical soil instability.

6.2 MAXIMUM LOCAL SCOUR DEPTH

6.2.1 Introduction

Flow velocity gradients downstream from the tip of a groyne cause flow-separation vortices and a higher turbulence intensity, which produce a local scour hole.

The maximum local scour depth near the tip of a groyne is an important design parameter and has been investigated extensively in flumes and in the field. From a theoretical point of view the specific discharge in the upstream approach flow is equal to the specific discharge through the scour hole. Hence,

$$\{h(r_i) + y_s\} \cdot u_s = h(r_i) \cdot u \quad (6.2-1)$$

in which

$h(r_t)$	=	local water depth in the design cross-section at the tip of the groyne, calculated by Formula 4.4-8	(m)
$u(r_t)$	=	local flow velocity, calculated by Formula 4.5-8	(m/s)
u_s	=	depth averaged flow velocity in the scour hole	(m/s)
y_s	=	maximum local scour depth	(m)
r_t	=	bend radius up to the tip of the groyne	(m)

The standard length of a permeable groyne is recommended to reach up to the thalweg of the design channel. That means that $h(r_t) = h_0$ and that is the maximum water depth in the design cross-section. In general, a series of groynes includes also shorter groynes where $h(r_t) < h_0$. More about the groyne design can be found in Chapter 7.

The scour hole will be in equilibrium if $u_s = u_{cr}$, where u_{cr} is the critical depth-averaged flow velocity (m/s) for the initiation of motion. The effect of the shape of the structure and the increased turbulence is expressed in empirical coefficients. Different equations have been published based on this concept such as, for example, the formulas presented by Ahmad (1953) and Dietz (1968).

Ahmad (1953) considers the specific discharge, q (m^2/s) with $q = h \cdot u$, as main parameter in his flume experiments:

$$h_1 + y_s = K \left(h_1 \cdot u_1 \cdot \frac{B}{B-b} \right)^{\frac{2}{3}} \quad (6.2-2)$$

in which

K	=	empirical coefficient	($m^{-1/3} s^{2/3}$)
B	=	channel width upstream of the groyne	(m)
b	=	protrusion length	(m)
u_1	=	upstream depth-averaged flow velocity	(m/s)
h_1	=	water depth upstream from scour hole	(m)
y_s	=	maximum local scour depth	(m)

A disadvantage of this formula is that the coefficient K is not dimensionless ($s^{0.67}/m^{0.33}$). On the other hand this formula has been applied many times, so that appropriate values of the coefficient K are well known. They are presented in Subsection 6.2.4.

A disadvantage is also that the ratio b/B is very small in large rivers. The protrusion length b is produced by the part of the groyne which is in the water. It can equal, especially in physical model tests, the effective length L_g . The definition of B has to be changed to the width of that part of the river in which the flow is influenced by the groyne. Although this is physically more correct, it is much more difficult to determine B with this new definition than with the old definition.

Dietz (1967) considers the specific discharge $q = h_1 \cdot u_1$ for a two-dimensional situation:

$$h_1 + y_s = k \cdot h_1 \cdot \frac{u_1}{u_{cr}} \quad (6.2-3)$$

$$y_s = k \cdot h_1 \left(\omega \frac{u_1}{u_{cr}} - 1 \right) \quad (6.2-4)$$



in which k and ω are dimensionless empirical coefficients. The coefficient k in Dietz' formula for the equilibrium scour depth can be decomposed into various factors:

$$y_{s,e} = k_{bed\ protection} \cdot k_{floating\ debris} \cdot k_{permeability} \cdot h \left(\omega \frac{u}{u_{cr}} - 1 \right) \quad (6.2-5)$$

in which

$k_{bed\ protection}$	=	factor for the influence of a sill-shaped bed protection	(-)
$k_{floating\ debris}$	=	factor for the influence of floating debris (see Section 6.4)	(-)
$k_{permeability}$	=	factor for the permeability	(-)

6.2.2 Analysis of the Scour Formula of Ahmad

Ahmad's formula for the local scour depth depends explicitly on the length of the groyne L_g and the upstream specific discharge $h_1 \cdot u_1$. All other relevant effects, such as for example increased turbulence, are represented by the coefficient K .

The upstream flow velocity determines the sediment transport intensity upstream from the groyne. Live-bed scour occurs if $u_1 > u_{cr}$ and clear-water scour occurs if $u_1 < u_{cr}$. In all tests of Ahmad, live-bed scour was observed.

Recent investigations of bridge pier scour demonstrated that the maximum scour depth is a function of the sediment size and the flow velocity, if $u_{cr} < u_1 < 2.5 u_{cr}$ and that the scour depth is almost independent of the flow velocity if $u_1 > 2.5 u_{cr}$. In the latter case, the scour depth depends mainly on the geometry of a groyne (Breusers and Raudkivi, 1991). Only the velocity threshold depends on the sediment grain size.

Kandasamy and Melville (1989) show that these tendencies are not only valid for bridge pier scour, but also for scour near abutments (Breusers and Raudkivi, 1991). Provisionally, it is assumed that these tendencies are also applicable to local scour around groynes on the basis of similarities in the flow field around a groyne head and a bridge pier. The data of local scour near groynes suggest that the threshold of $2.5 u_{cr}$ in the criteria for bridge piers should be replaced by $2 u_{cr}$ for groynes.

Under FAP 21, physical model investigations have been carried out in Faridpur and France. The model discharge was selected to fulfil the condition $u_1 \geq 2 u_{cr}$ and therefore the local scour depth was almost independent of the type of sand or the model discharge. This means that with $u_1 \geq 2 u_{cr}$ the maximum local scour depth in the formula of Ahmad is a function of geometric parameters such as h_1 and $B/(B-b)$ only. Substitution of this criterion into the formula of Ahmad reads:

$$h_1 + y_s = K \left(h_1 \cdot 2u_{cr} \cdot \frac{B}{B-b} \right)^{\frac{2}{3}} \quad (6.2-6)$$

In the Brahmaputra-Jamuna river the critical flow velocity is about $u_{cr} = 0.6$ m/s depending on the water depth and the hydraulic roughness. Under design conditions the flow velocity u is always more than $2u_{cr}$. Formula (6.2-6) is similar to Lacey's formula if the length of the groyne is small compared to the width of the design channel. This is often the case in the Brahmaputra-Jamuna river. Lacey's formula can be written as (see Annex 1, Section 2.3):

$$h_1 + y_s = K_L h_1 \quad (6.2-7)$$

with

$$K_L \approx K \cdot \left(2u_{cr} \frac{B}{B-b} \right)^{\frac{2}{3}} \quad (6.2-8)$$

which is almost constant for a given geometry.

The remaining difference between Ahmad's formula and theory is the exponent of h_1 (0.67 compared with 1). This will cause some differences, which are probably compensated by the calibration of K_L .

6.2.3 Value of Coefficient K

Ahmad used sand with $D_{50} = 0.35$ mm and 0.695 mm respectively in his physical model investigation. He concludes that the sand type had no influence on the local scour depths. Presumably, this statement is based on an inaccurate extrapolation of the curve through his data points to determine the equilibrium scour depth, because the measurements were made only during a short period of 2 or 3 hours after the start of a test. This means that Ahmad did not measure the equilibrium scour depth. In the FAP 21 model investigations, the scour was measured during a period of 16 hours after the start of a test to determine the equilibrium scour depth. This yielded a new extrapolation curve, which was fitted through Ahmad's data points. The equilibrium scour depths determined by these extrapolated curves indicate that a coarse sand results in deeper scour holes. This effect was also observed in the studies of bridge pier scour, especially if $1 < u/u_{cr} < 2.5$ (Breusers and Raudkivi, 1991).

This means that the values for K recommended by Ahmad are too low. The values should be increased by approximately 20 %. For a single impermeable groyne (made of a vertical plate) and perpendicular to a straight bank line $K = 2 \text{ s}^{0.67}/\text{m}^{0.33}$ is recommended (Breusers and Raudkivi, 1991). After 20 % correction this value becomes $2.4 \text{ s}^{0.67}/\text{m}^{0.33}$. WL | Delft Hydraulics had earlier measured the development of a local scour hole near the head of a groyne made of a plate in a flume with a movable sand bed $D_{50} = 0.22$ mm. The scour measurements were made during a period of 24 hours. The results from two tests in which $1 < u_1/u_{cr} < 2$ and the application of formula 6.2-2 confirm this value of K (see Table 6.2-1).

Test	$h_1 + y_s$ (m)	u_{cr} (m/s)	$B - L_g$ (m)	$h_1 u_1 B / (B - b)$ (m ² /s)	K (s ^{0.67} /m ^{0.33})
T5	0.29 to 0.34	0.30	1.05	0.042	2.4 to 2.8
T7	0.35 to 0.40	0.39	1.35	0.058	2.3 to 2.6

Table 6.2-1: Results of earlier physical model tests in a flume by WL | Delft Hydraulics

The bend investigated in the Kamarjani model is rather sharp. The influence of bends on the recommended values of K is represented by a factor K_{bend} of 1.1 for a moderate bend and a factor 1.4 for a sharp bend (Breusers and Raudkivi, 1991). This is a rather simple method to include bend scour in the total scour depth, but it is sufficient for this evaluation. The bend in the Kamarjani model yields a factor of $K_{bend} = 1.3$.

In general, a series of groynes can be considered as single groynes, as far as the local scour holes are concerned. The recommended values for K are presented in Table 6.2-2. In the next section these values are compared with the values of K determined from the physical model investigations by FAP 21.

bankline for single groyne of a vertical plate	$K (s^{0.67}/m^{0.33})$		
	Ahmad	+ 20 % correction	bend effect
straight	2	$2 \times 1.2 = 2.4$	n.a.
curved	2	$2 \times 1.2 = 2.4$	$2.4 \times 1.3 = 3.1$

Table 6.2-2: Recommended values of K for a single impermeable groyne (vertical plate)

6.2.4 Verification of FAP 21 Investigations

In the Kamarjani model of FAP 21, test T5 has been performed with a series of three groynes made from plates and a vertical head. In all other tests more realistic permeable and impermeable groynes were built in. Based on the measurements of test T5, the value of K was estimated as accurate as possible from the Formula 6.2-6 with $h_1 = 0.202$ m, $u_{cr} = 0.18$ to 0.20 m/s, $B = 6.0$ m and $L_g = b = 0.80$ m.

The approach flow velocity was estimated to be about 0.35 to 0.40 m/s, which is just equal to $2 u_{cr}$. Therefore, it is expected that a further increase of the model discharge will not result in a significant increase of the scour depths and of the value of K , but would keep the value of K almost independent of the selected model discharge.

Table 6.2-3 shows that the calculated value of K varies between 2.9 and $3.6 s^{0.67}/m^{0.33}$ in test T5. These values confirm $K = 3.1 s^{0.67}/m^{0.33}$, which has been determined from literature in Table 6.2-2 with an accuracy of about ± 10 %. This confirmation is a good verification of the maximum scour depths measured in the Kamarjani physical model at the River Research Institute in Faridpur.

Groyne	$h_1 + y_s$ (measured in m, model)	K (calculated, $s^{0.67}/m^{0.33}$)
G1	0.62	3.0 to 3.3
G2	0.67	3.2 to 3.6
G3	0.595	2.9 to 3.2

Table 6.2-3: Value of K for a vertical plate groyne in physical model test T5 at RRI, Faridpur

For future physical model investigations it is recommended that the test programme includes a run with comparable parameters to verify the model set-up or to calibrate the model.

6.2.5 Further Results of the Physical Model Investigation

In the Study Phase, the first physical model investigation to optimise the layout of permeable groynes had been carried out at the River Research Institute in Faridpur. The groynes in that investigation had been schematised with a falling apron as bed protection in its final position after the process to fall had reached an equilibrium slope of $1V:2H$. With respect to the scour development these falling aprons

acted as sills. Values of K have been determined for different permeabilities from an analysis of the measured data (see Table 6.2-4).

Test No	permeability of the groyne with a pre-shaped falling apron	$K (s^{0.67}/m^{0.33})$
T4	50 %	2.4 to 3.0
T3, T8	70 %	2.2 to 2.3
T9, T10	80 %	1.7 to 1.9

Table 6.2-4: Values of K as function of the permeability of groynes with pre-shaped falling aprons (RRI, Faridpur)

In the Implementation Phase the groyne layout was further optimised by a physical model investigation in Faridpur (see Table 6.2-5). The permeability of the groyne was not kept constant, but varied from 80 % at the tip of the groyne to 50 % near the transition to the impermeable part of a groyne.

Type of groyne	$K (s^{0.67}/m^{0.33})$
permeable groyne with or without bed protection	1.5 to 1.6
permeable groyne with lowered top of the piles	1.7
cross-bar	2.2

Table 6.2-5: Values of K for different types of groynes with gradually increasing permeability (RRI, Faridpur)

6.2.6 Results from Monitoring of Test Structure

The development of the maximum scour depth with time was less regular in nature than observed in the physical model tests, probably because of peak flows in the hydrographs, flow slides and the occurrence of floating debris during some days. The maximum local scour depths during a flood have been observed in 1995 and 1996 (see Table 6.2-6).

Groyne	Maximum scour depth (m)	Date
G-1	7 to 8	August 10, 1995
G-1	11	May 15, 1996
G-2	8 to 9	August 20, 1995 (also July 10 after a flow slide)
G-2	8.5	June 25, 1996
G-3	9 to 10	August 14, 1995 (during the fourth flood peak and before the flow slide on August 19)
G-3	6.9	August 18 to September 05, 1996

Table 6.2-6: Observed maximum scour depth at Kamarjani Test Structure

Values of K are derived from the monitoring data. The water depth in the Kamarjani channel was about 15 to 18 m during the 1995 monsoon. The critical flow velocity for the deep water flow condition is assumed at $u_{cr} = 1.0$ m/s as depth-averaged flow velocity (see Subsection 4.8). The 1995 flow measurements indicate that the maximum surface flow velocity was 2.75 m/s at the tip of the

groyne. The maximum depth-averaged flow velocity is 2.5 m/s which is higher than $2 u_{cr}$. Consequently, the value of K has been estimated assuming $u_1 = 2 u_{cr}$ and using the maximum scour depth as mentioned in Table 6.2-6. Table 6.2-7 gives the results. With $u_{cr} = 1.0$ m/s, the values of K in the field and in the model are the same.

The resulting value of K due to the groyne geometry is $K = 1.7$ to $1.8 \text{ s}^{0.67}/\text{m}^{0.33}$. This confirms the model values for a groyne with a bed protection. Without bed protection, which acts like a sill, a slightly lower value of K should be expected 1.5 to 1.6 (according to the physical model results in Table 6.2-5). The lowering of the top of the piles seems to have minor influence on the maximum scour depth.

Type of permeable groyne	$K (\text{s}^{0.67}/\text{m}^{0.33})$ including floating debris	$K (\text{s}^{0.67}/\text{m}^{0.33})$ without floating debris
G-1 with bed protection	~2.30	~1.8
G-2 with falling apron	~2.15	~1.7
G-3 with lowered top of the piles	~2.15	~1.8

Table 6.2-7: Values of coefficient K for Kamarjani test structure during 1995 monsoon

These values of K based on monitoring of the test structure confirm the values of K found in the physical model investigation. They also yield a factor for the influence of floating debris of $K_{\text{floating debris}} = 1.2$ to 1.3 . The influence of floating debris on the maximum scour depth is analysed more in detail in Section 6.4. However, the field situation has to be strongly schematised for a determination of the dimensionless factors to calculate the total K from the coefficient $K_{\text{structure}} [\text{s}^{0.67}/\text{m}^{0.33}]$:

$$K_{\text{total}} = K_{\text{structure}} \cdot K_{\text{bend}} \cdot K_{\text{bed protection}} \cdot K_{\text{floating debris}} \quad (6.2-9)$$

in which

$K_{\text{structure}}$ for the Kamarjani Test Site according to Table 6.2-8.

permeability at the tip (%)	$K_{\text{structure}} (\text{s}^{0.67}/\text{m}^{0.33})$
80	1.2 to 1.3
70	1.4 to 1.6
60	1.5 to 1.8
50	1.6 to 2.0
0	2.4

Table 6.2-8: Coefficient K as function of the permeability

K_{bend}	=	1.3	(= 1.0 for straight channels)
$K_{\text{bed protection}}$	=	1.1	(= 1.0 without bed protection)
$K_{\text{floating debris}}$	=	1.2 to 1.3	(= 1.0 without floating debris)

The following, more general approach can be applied as an alternative for using the Ahmad formula:

$$y_s = k_{\text{blockage}} \cdot k_{\text{floating debris}} \cdot k_{\text{bed protection}} \cdot y_{s, \text{impermeable plate}} \quad (6.2-10)$$

The advantage is that $y_{s,imp}$, the local scour depth at an impermeable plate, can be calculated by any formula. The case of an impermeable vertical plate perpendicular to the flow with a vertical edge is a reference for which many different scour formulas exist. The individual values of K give an insight into the relative importance of the respective parameters.

For the Kamarjani test structure some of these coefficients k have been determined as:

permeability at the tip (%)	$K_{blockage}$ (-)
80	0.2
70	0.3
60	0.4
50	0.5
0	1

Table 6.2-9 Coefficient $k_{blockage}$ as a function of the permeability

The tendency in Table 6.2-9 results in a simple expression for $k_{blockage}$:

$$k_{blockage} = (1 - p) \quad (6.2-11)$$

in which

$$p = \text{permeability of the groyne} \quad (-)$$

The influence of floating debris is expressed by $k_{floating\ debris}$ (see Section 6.4):

$$k_{floating\ debris} = \frac{h}{(h - h_{floating\ debris})} \quad (6.2-12)$$

with

$$\begin{aligned} h &= \text{local water depth at the tip of the pile row} & (m) \\ h_{floating\ debris} &= \text{thickness of floating debris layer} & (m) \end{aligned}$$

These values are indicative, because in the analysis several assumptions have been made.

6.3 TIME-DEPENDENT DEVELOPMENT OF SCOUR DEPTH AND SCOUR VELOCITY

6.3.1 Location of Maximum Scour

The location of the maximum scour depth near the tip of the groyne depends on the width of the bed protection. It varies between 25 and 75 m downstream from the groyne axis, see for example the location of the maximum scour downstream from G-2 in Fig. 6.3-1. Near the other groynes similar results had been observed in 1995. However, during the 1998 monsoon the location shifted closer to the bank, because the river bed was higher than in 1995 and therefore the bed protection was below the bed level at that time. The scour developed as if there was no bed protection. The effect of the bed protection can be seen by comparing the location of maximum scour in Fig. 6.3-1 and 6.3-2. Without active bed protection the location of the maximum scour depth shifts towards the bank.

262

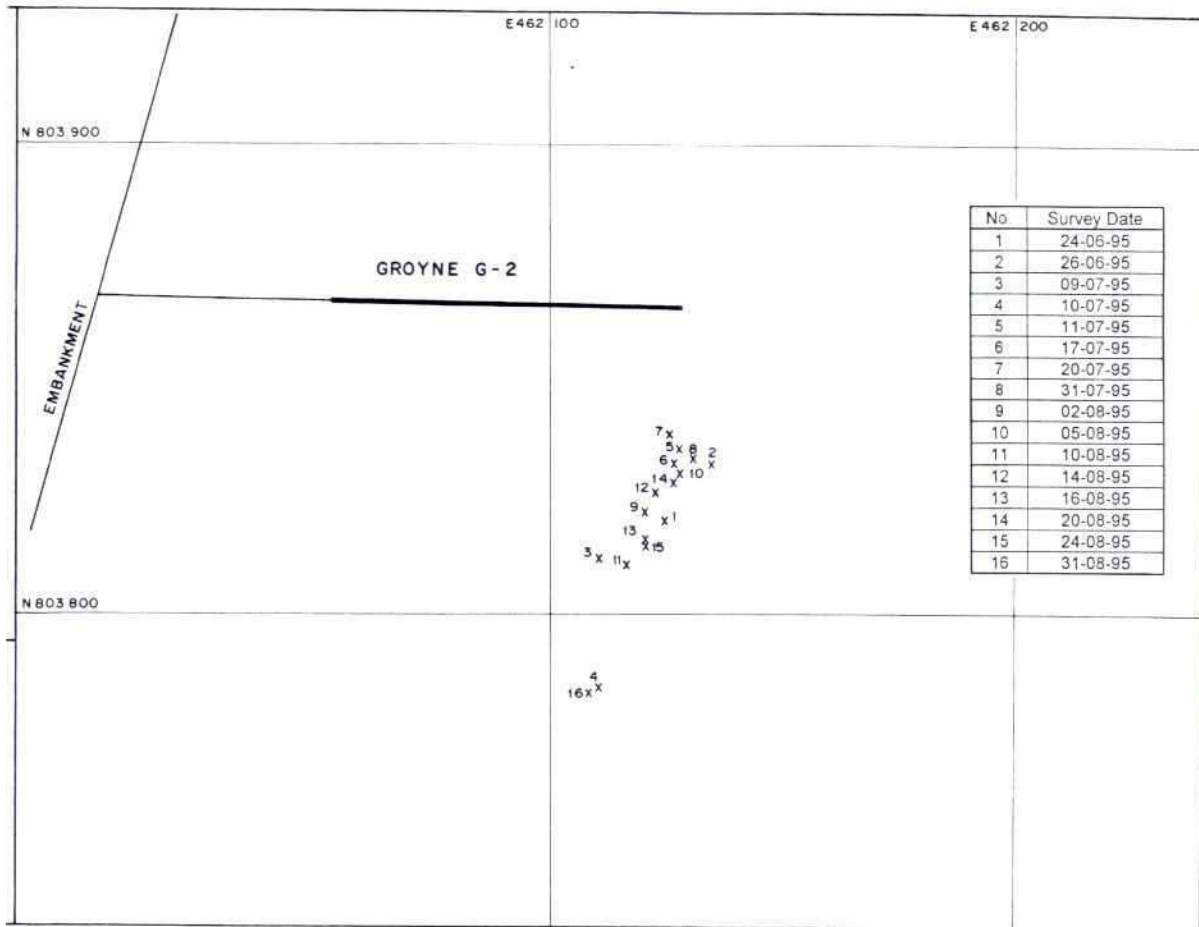


Fig. 6.3-1: Location of the maximum local scour depth downstream from G-2 during 1995 monsoon

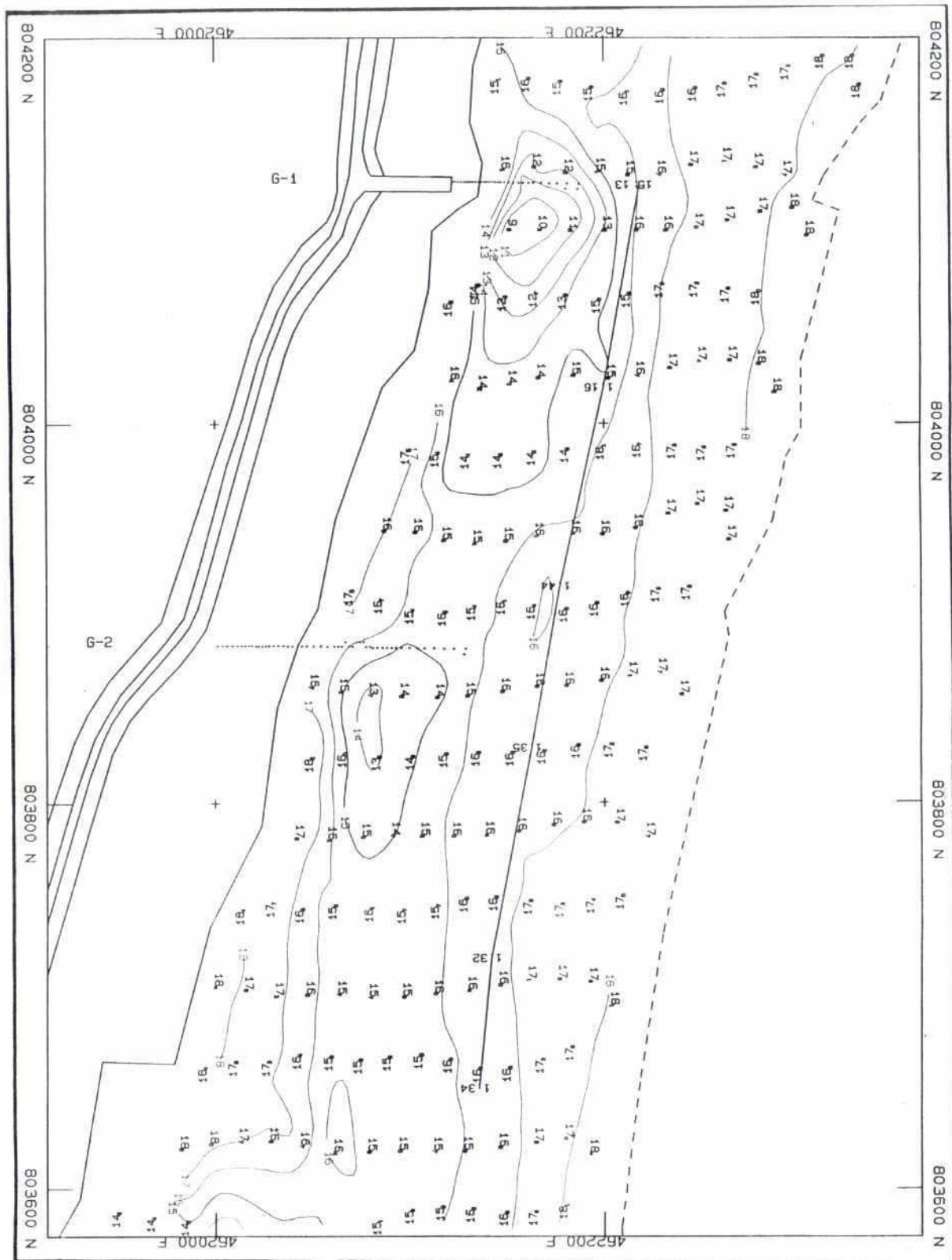


Fig. 6.3-2: Location of the maximum local scour depth downstream from G-1 and G-2 during 1998 monsoon

6.3.2 Scour Depth

The time-dependent development of scour holes is relevant for the following reasons:

- 1 fast scouring may trigger slides;
- 2 slow scouring may have the effect that the values predicted by Ahmad's formula are never reached.

The study of two-dimensional scour holes in the Netherlands has resulted in a semi-empirical calculation method for the local scour depth as a function of time. This method has also been applied successfully to three-dimensional scour holes as developed near the Kamarjani Test Structure. The formulas of this method are summarised in the following.

The *Chézy coefficient* is a measure for the flow resistance in the deeper part of the channel. The White-Colebrook formula reads:

$$C = 18 \log \left(\frac{12 \cdot h}{k_s} \right) \quad (6.3-1)$$

in which

C	=	Chézy coefficient	(m ^{0.5} /s)
h	=	local water depth	(m)
k _s	=	hydraulic roughness of the river bed	(m)

The *Shields parameter* has been rewritten to calculate the critical flow velocity for the initiation of sediment transport at the tip of a groyne:

$$u_{cr} = \sqrt{\theta_{cr} \cdot C^2 \cdot \Delta \cdot D_{50}} \quad (6.3-2)$$

in which

D ₅₀	=	median sediment diameter	(m)
Δ	=	relative density:	
	=	(ρ _s -ρ)/ρ	(-)
θ _{cr}	=	critical Shields parameter	(-)
ρ	=	mass density of water	(kg/m ³)
ρ _s	=	mass density of sediment	(kg/m ³)
u _{cr}	=	critical flow velocity	(m/s)

The formula for the characteristic time t_1 in hours at which $y_s = h_1$ reads

$$t_1 = \frac{k_t \cdot h_1^2 \cdot \Delta^{1.7}}{(\alpha_t \cdot u_1 - u_{cr})^{4.3}} \quad (6.3-3)$$

in which

k _t	=	empirical constant = 330	(-)
h ₁	=	upstream water depth	(m)
Δ	=	relative submerged density of river bed sediment (-)	
	=	1.65	
α _t	=	coefficient depending on the geometry upstream of the scour hole	(-)
u ₁	=	upstream depth-averaged flow velocity	(m/s)
u _{cr}	=	critical flow velocity for initiation of motion	(m/s)
	=	0.4 to 1.0 m/s	

Finally the time-dependent scour development can be calculated by:

$$\frac{y(t)}{h_1} = \left(\frac{t}{t_1} \right)^{n_t} \quad (6.3-4)$$

in which

h_1	=	water depth upstream from scour hole	(m)
$y(t)$	=	time-dependent local scour depth	(m)

Example

The monitoring data from the 1995 monsoon were used to calculate the time-dependent development of the local scour near the groynes. The calculation method consists of the following steps:

- the hydraulic roughness is estimated by substitution of $k_s = 0.05$ m and $h_1 = 20$ m in formula (6.3-1). This yields $C = 66 \text{ m}^{0.5}/\text{s}$.
- the critical flow velocity for the initiation of sediment transport is estimated by substitution of $C = 66 \text{ m}^{0.5}/\text{s}$, $\Delta = 1.65$ and $D_{50} = 0.002$ m in formula (6.3-2). This yields $u_{cr} = 0.71$ m/s.
- parameter t_1 is determined by extrapolation of the data points. Curve fitting shows that n_t is about 0.4 for two-dimensional scour holes but varies between 0.6 and 0.8 for three-dimensional scour holes (Breusers and Raudkivi, 1991).
- a calculation with the values in Table 6.3-1 appears to fit the observed scour development in time very well.

Groyne	Date	n_t	t_1 (hours)
G2	1 June	0.80	7,5
G3	1 June	0.65	30,0

Table 6.3-1: Parameters for time-dependent scour development fitted to monitoring data, monsoon 1995

6.3.3 Scour Velocity

The scour velocity is defined as the increase of the maximum scour depth in time. The maximum scour velocity in the local scour holes downstream from the groynes occurred during the first flood after completion of the construction (the 1995 flood), see Table 6.3-2. The lower scour velocity at G-1 might be the result of less flow attack compared to G-2 and G-3. It was furthermore observed that the supply of sediment from upstream affects the development of the scour hole at the downstream groynes. This extra supply of sediment delays the scour hole development as has been quantified in the analysis of the monitoring data from the Revetment Test Structure at Bahadurabad (Annex 11). This effect, together with a shift in the flow attack, causes a delay in the period of maximum scour velocity: first G-1 followed by G-2 and G-3 (see Table 6.3-2).

Groyne	Period of maximum scour velocity		Maximum scour velocity (m/day)
G-1	June 10 to 26, 1995	12 days	0.25
G-2	June 10 to 26, 1995	12 to 25 days	0.3
G-3	June 24 to July 9, 1995	14 days	0.4

Table 6.3-2: Maximum scour velocity of the deepest point of a local scour hole in 1995

6.4 FLOATING DEBRIS

6.4.1 Introduction

During the design of the Groyne Test Structure it was assumed that at the most upstream groyne floating debris may pile up to about 1 m depth below any water level, at the downstream groynes up to 0.5 m depth. These assumptions had been made because no measurements or observations were available at that time, see Procurement and Construction Report of January 1994. It was realised that the resultant loads on the piles are of major significance. Therefore, floating debris had been measured and excessive debris had been removed during the first monitoring years.

The presence of floating debris in the test structure is summarised in Section 6.4.2. The influence of floating debris on the flow velocities and the local scour had been studied in Section 6.4.3.

6.4.2 Presence of Floating Debris

Floating debris transported by the river is dominated by clusters of water hyacinths, banana trunks and other debris. The thickness and the area of the piled-up debris at the upstream side of each groyne was estimated from visual inspections, see for example Fig. 6.4-1 with the daily observations at G-2 during 1996 monsoon period. A maximum area of floating debris of about 10,000 m² with a thickness of about 2 m seems to occur in the Jamuna river. This is more than assumed during the design phase and also more than observed during the 1995 and 1996 floods, when area up to 300 and 600 m² and only one time a thickness of 2 m had been estimated. This might be due the decision after the first peak flow in 1997 to reduce the efforts to remove floating debris piled up against the groynes. In this connection it is mentioned that no bamboo rafts had hit the outer piles of the groynes after the 1995 flood. This type of accidents had happened a few times during the 1995 flood, just after completion of the construction of the groynes.

The highest amount of floating debris was observed during peak flows, because during a peak flow new flood plain areas upstream from the groynes were inundated and some of these areas were covered by water hyacinths which started to float with the flow. This means that floating debris can be observed when the water level rises above the flood plain level, see Fig. 6.4-2. In Kamarjani the lowest flood plain level is between 19 and 19.5 m + PWD.

The hypothesis that floating debris mainly occurs on days with a rising water level above flood plain level is not confirmed completely by the observations, see Fig. 6.4-3. Also on days with a falling water level some floating debris can occur, although not much. Probably the debris started to float during rising water levels and due to the travel time it arrived at Kamarjani when the water level started to fall.

In general, the thickness of the layer of floating debris increases as the flow velocity in the channel increases.

It is concluded that floating debris can exert considerable forces on the piles of the groynes, more than expected during the design of the groynes. Therefore, it might be considered to prevent floating debris. This is possible by designing the top of the piles of the groynes below the lowest flood plain level, in Kamarjani 19.2 m + PWD. This reduces the load on the piles, while this reduction of pile height has only a small effect on the flow velocities in the groyne field.

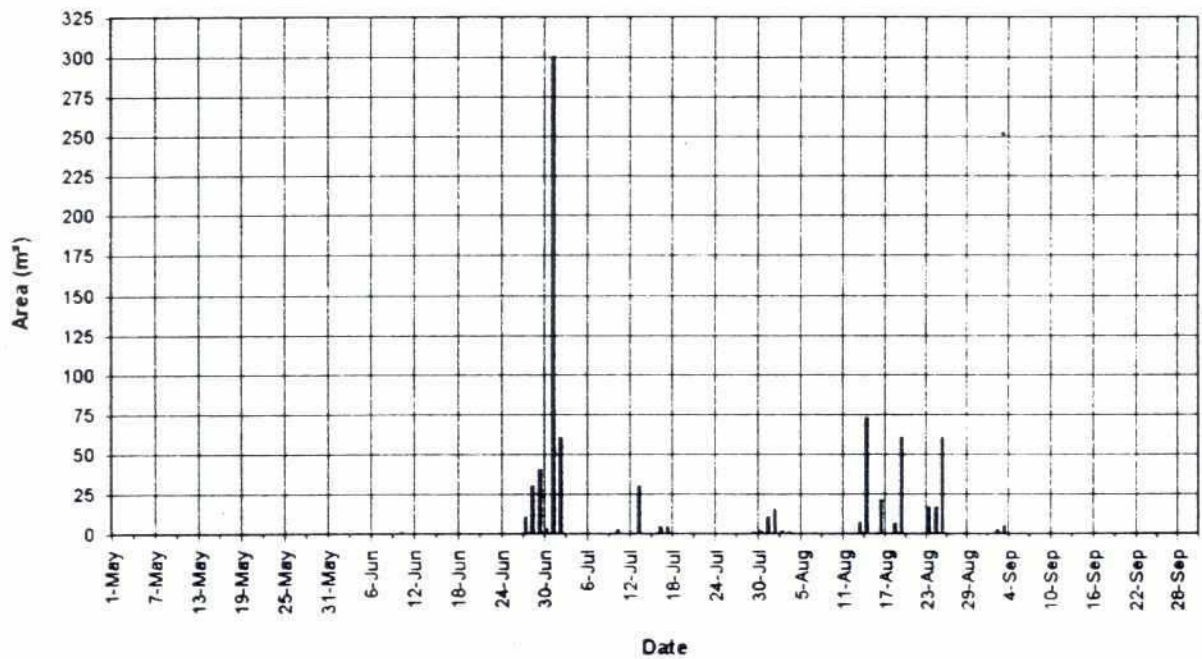
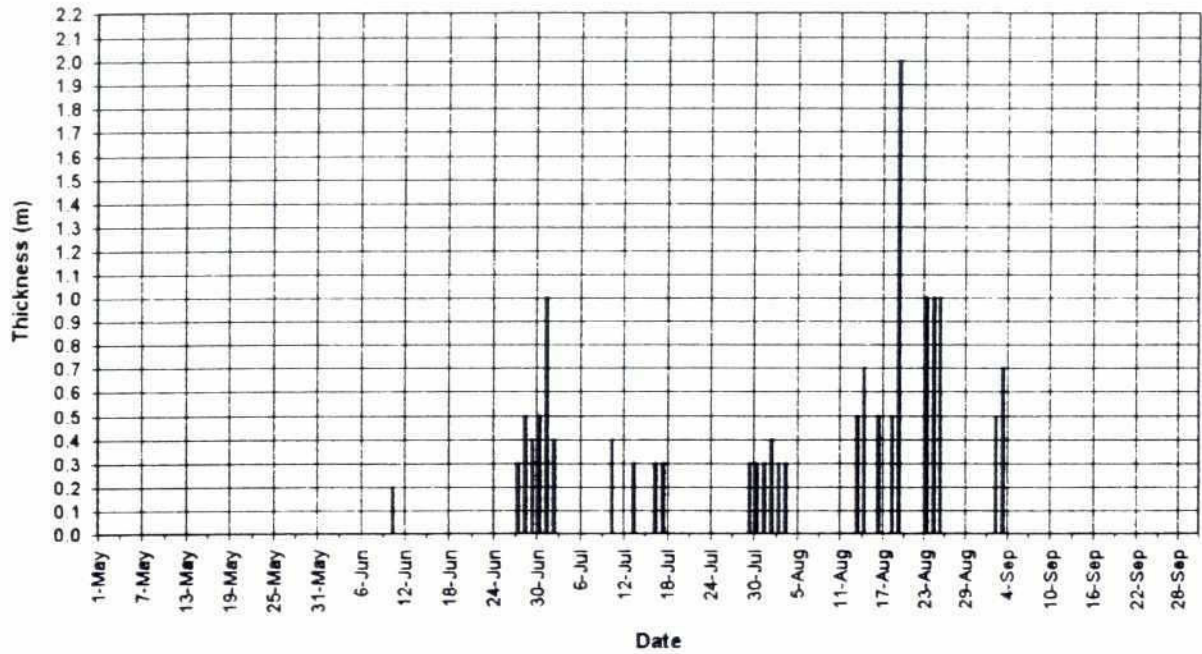


Fig 6.4-1 Thickness and area of floating debris at G-2 during 1996 monsoon period



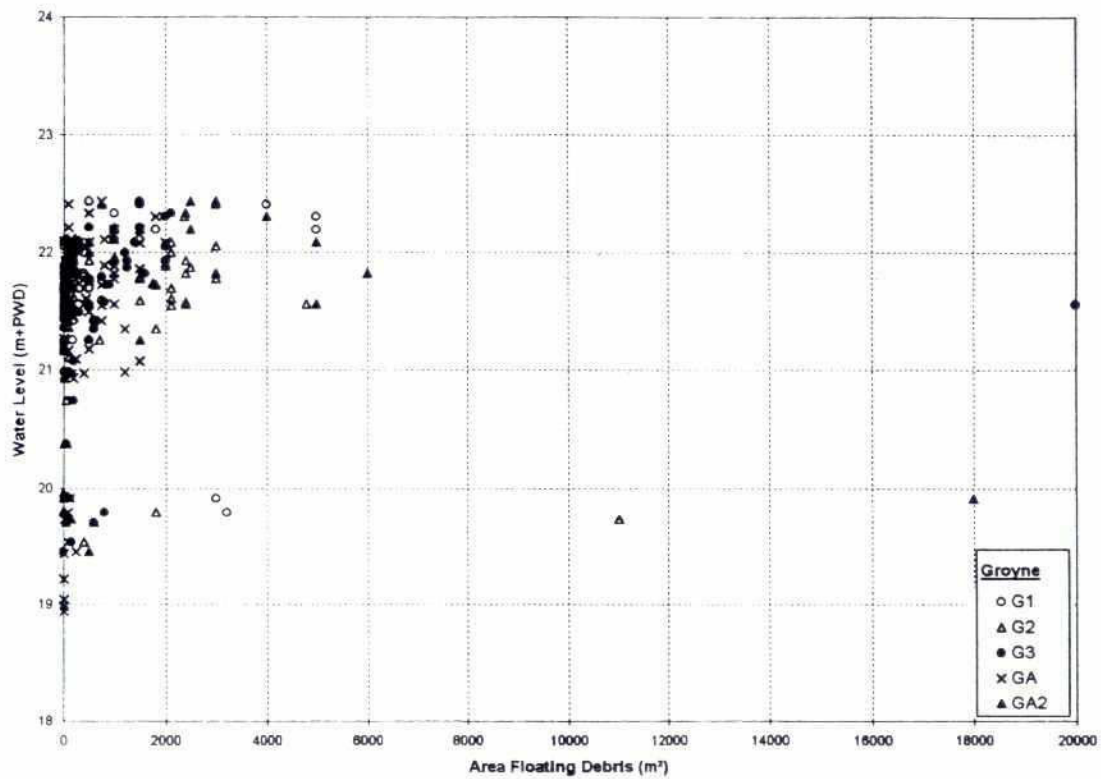


Fig. 6.4-2 Area of floating debris as function of the water level

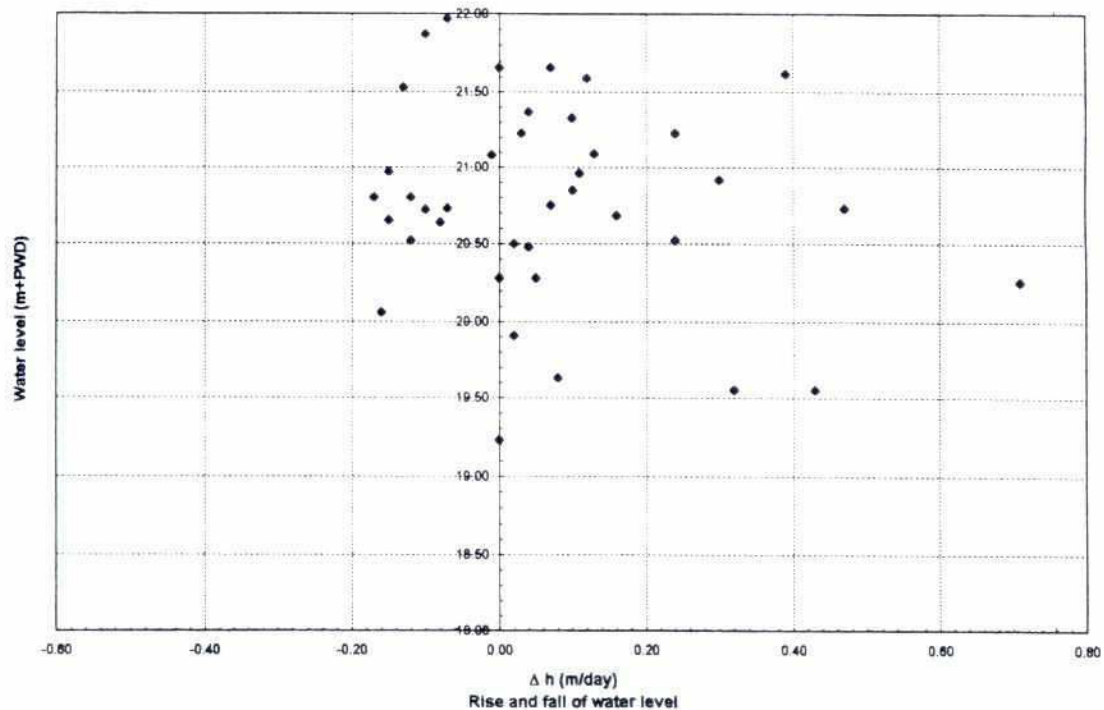


Fig. 6.4-3 The rise or fall of the water level as function of the water level on days floating debris had been observed during 1996 monsoon

6.4.3 Scour by Floating Debris

The physical model investigation had shown that an increasing permeability reduces the local scour depth, see Fig. 6.4-4:

$$y_s = k_{blockage} \cdot y_{s,imp} \quad (6.4-1)$$

in which

y_s	=	local scour depth	(m)
$y_{s,imp}$	=	local scour depth at an impermeable groyne	(m)
$k_{blockage}$	=	(1-p)	(-)
p	=	permeability of the groyne	(-)

The minimum value of p is 0 for an impermeable groyne and the maximum value is 1 when no groyne is present. An impermeable groyne has $k_b = 1$ and a groyne with 20 % blockage has $k_b = 0.2$.

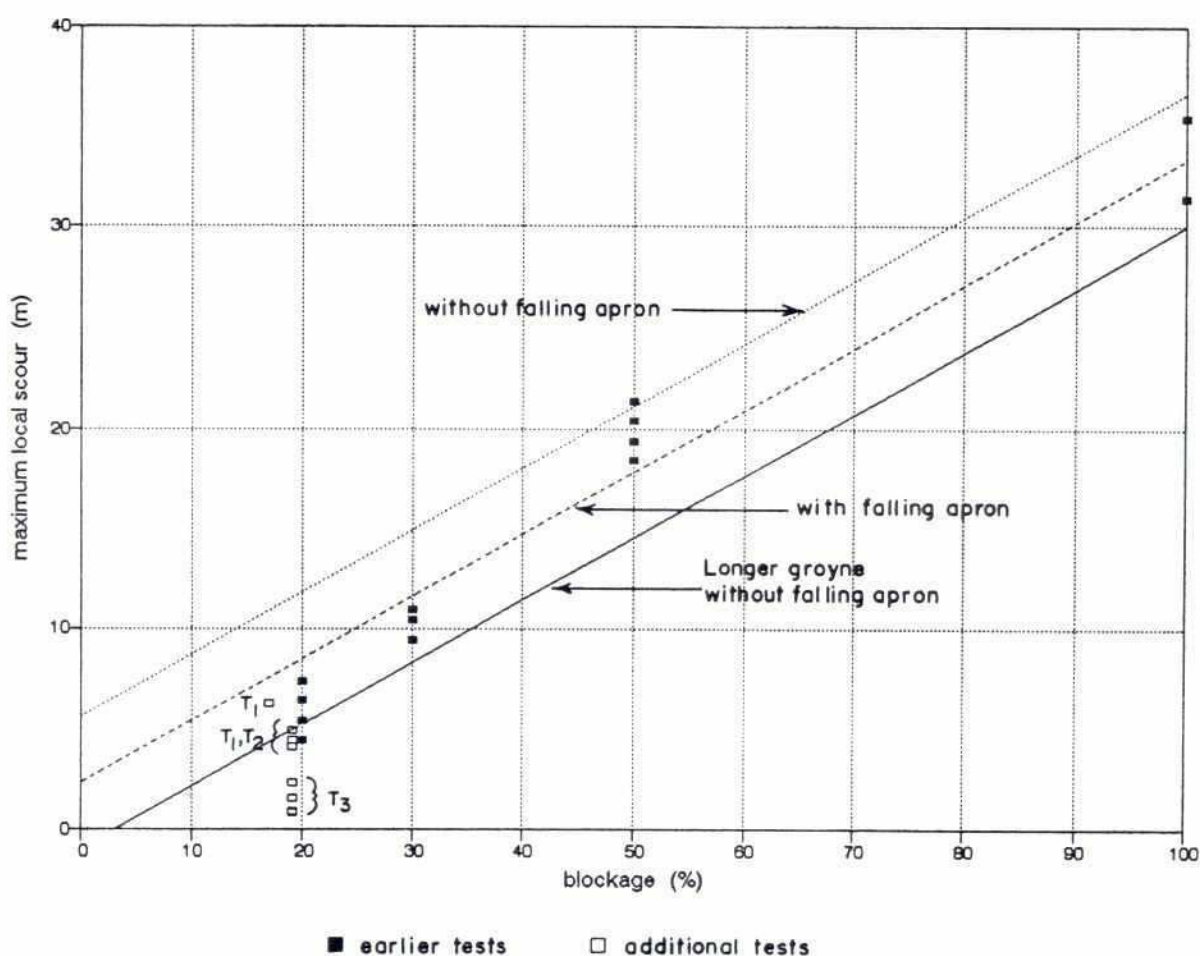


Fig. 6.4-4 Reduction of scour depth by increasing blockage of the groyne

Assume that the influence of floating debris on the local scour depth is similar to a reduction of the permeability of a pile row. This leads to the introduction of a factor

$$k_{fd} = \frac{h}{(h - h_{fd})} \quad (6.4-2)$$

in which

h	=	local water depth at the tip of the pile row	(m)
h_{fd}	=	thickness of the layer of floating debris	(m)
k_{fd}	=	factor for the influence of floating debris	(-)

The effect of floating debris is not only an additional blockage of the flow through the pile row, but also a redistribution of the approach flow velocity under the layer of floating debris, because a boundary layer starts to develop along the debris. This growing boundary layer causes a slight increase of the flow velocities near the bottom, because the specific discharge does not change. These increased bottom velocities cause a deeper scour hole. This effect can be translated as an increased blockage of the pile row $c_{fd} \cdot h_{fd}$ with $c_{fd} > 1$.

$$k_{fd} = \frac{h}{(h - c_{fd} \cdot h_{fd})} \quad (6.4-3)$$

in which

c_{fd}	=	empirical coefficient as per Table 6.4-1	(-)
----------	---	--	-----

In the physical model investigations, floating debris had been simulated by a smooth wooden plate or by small branches. The wooden plate had a well-defined thickness, but the bottom side was much smoother compared with floating debris from water hyacinths and banana tree trunks. This results in a relatively smaller increase in the local scour depth.

Results from field measurements and physical model tests lead to the values of c_{fd} given in Table 6.4-1. They show that the effect of the boundary layer is dominant over the effect of the additional blockage when the field of floating debris is large.

Up piling floating debris	c_{fd}	Comments
very small area ($< 200 \text{ m}^2$)	1	-
large area ($> 200 \text{ m}^2$) with hydraulic smooth layer of debris	3	for $h_{fd} < 0.15 h$
large area ($> 200 \text{ m}^2$) with hydraulic rough layer of debris	4	for $h_{fd} < 0.15 h$

Table 6.4-1: Characteristic values of c_{fd}

The thickness of floating debris had been monitored irregularly during the 1995 monsoon. Nonetheless, a maximum thickness of 1.0 to 1.5 m in a 300 m^2 area of up piling floating debris had been observed. The value of c_{fd} is estimated at about 3 for that case. Assuming a water depth of 18 m at the tip of the pile row, the floating debris factor k_{fd} takes a value of 1.2 to 1.3.

The analysis of the physical model tests results in a prediction for the local scour depth of 6 to 8 m in a situation of a permeable groyne without floating debris or $(6 \text{ to } 8) \cdot k_{fd} = 7.2 \text{ to } 10.4 \text{ m}$ with floating debris. The observed scour depths of 8 to 9 m coincide very well with this prediction. However, it is

uncertain whether a maximum layer of floating debris did occur at the time the maximum scour developed due to a lack of field observations. It is certain that the maximum layer of floating debris occurred during the developing stage of the scour hole. It might be that the layer of floating debris had accelerated the development of the local scour near G-2 and that in this way it had stimulated the large slide near that groyne in 1995, since a fast development of a scour hole can cause soil mechanical instability of the subsoil.

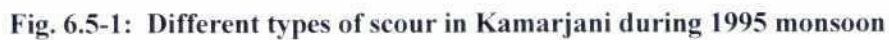
A thickness of 2 m of up piling floating debris is recommended for design conditions for river training works along the Jamuna river. If the blockage by the tip of the pile row is 20 % and the local water depth is 20 m (in design conditions), then floating debris causes an additional scour depth characterised by $k_{fd} = 1.4$ to 1.6. This can be considerable and therefore it is recommended to lower the crests of the piles below the level above which floating debris can occur. In the previous section it had been shown that this level is the lowest flood plain level.

6.5 EXTRA STRUCTURE-INDUCED SCOUR

Most quantitative methods for the prediction of structure-induced scour hold for relatively stable rivers where the bank lines are fixed and hence the geometry does not change. In unstable rivers where bed levels and bank lines change rapidly, however, bank protection structures may cause extra scour. This scour is extra to the local scour phenomena around the groynes and the bend scour. This *extra* scour occurs typically over the whole length of a series of groynes or over the whole length of a river bend. This means that the area affected by extra scour is much larger than the area of a local scour hole. In Kamarjani the deepest scour is the result of:

- *bend* scour due to the reduction of the bend radius resulting in a reduction of channel width and an increase of the average channel depth. This caused a deepening of about 2 m over the full length of the sharp bend. This deepening can be calculated by Equation 4.4-7.
- *extra* scour of at least 2 m in the thalweg of the channel. This phenomenon is largely unknown and can not be calculated. Some further considerations are given below.
- *local* scour around the groynes as investigated by physical model testing and as can be calculated by the formula of Ahmad (Equation 6.2-2) or other formulas: 6 to 8 m without floating debris, about 9 m (range from 7 to 10 m) with floating debris.

The deepest point in the thalweg follows from the summation of these three types of scour (Fig. 6.5-1). The channel at Karmanjani deepened from about +2 m in February 1995 to about - 11 m +PWD in July 1995 as is illustrated in Fig. 6.5-1.



- migrating rivers are overwide when point-bar deposition cannot keep up with bank erosion. The stopping of migration causes narrowing and associated deepening.
- the hindered migration deforms the bend. This increases the curvature and hence the bend scour of the channel along the predicted bend.

- the input of bank erosion material reduces the formation of near-bank scour. Stopping the input will consequently eliminate this reduction and hence lead to deeper scour.

The bend radius reduction mechanisms are presented in Fig. 7.2-1 of Consulting Consortium FAP 21/22 (1993, Vol. IA). They affect the overall morphology of the river. The extra scour mechanism has only an effect close to the banks and does not affect the overall morphology of lowland rivers, not even when they are rapidly migrating (Mosselman, 1992). A subsequent theoretical study of extra structure-induced scour in rapidly changing rivers (Shishikura, 1996; Mosselman et al, 2000) has increased the insight into this phenomena, but could not yield readily applicable design formulae yet.

Currently there are no quantitative methods to predict the extra structure-induced scour in rapidly changing rivers. For Test Structure I in Kamarjani the extra scour was therefore estimated through expert judgement (Consulting Consortium FAP 21/22, 1993, Volume III). The 20 % extra bend scour thus predicted complied with the physical model tests at RRI Faridpur and the prototype observations at Kamarjani.

6.6 CONFLUENCE SCOUR

In addition to the previously mentioned types of scour, confluence scour should be considered due to the following planform development:

The structure itself might induce a cut off channel in front of the groynes. A cut-off channel might induce confluence scour in front of the groynes. This has not been observed in Kamarjani during the monitoring period, but in Bahadurabad (see Annex 11). Therefore confluence scour should be included in the design conditions or situations.

Confluence Scour Phenomena were investigated by Klaassen and Vermeer (1988b) for the Jamuna River. The authors evaluated historical field data and a survey from 1987 and found from statistical regression the following empirical relation for the confluence scour depth $y_{s,c}$ (see also Annex 1):

$$y_{s,c} + h_1 = h_1 (1.292 + 0.037 \cdot \varphi) \quad (6.6-1)$$

with

φ	=	angle of incidence of anabranches or confluence	(degrees)
h_1	=	upstream water depth below SLW from the average of both approach channels	(m)

The basic boundary conditions for the data behind this formula are important to consider. Firstly, the angle of incidence was always $\varphi > 20^\circ$. The geometry of confluences changes easily, so that the design value of the incidence angle φ should not be measured from a temporary local situation. It is recommended to use a representative value of 45° for channels wider than 1 km and a representative value of 70° for channels narrower than 1 km.

Secondly, the ratio of the discharges in the two anabranches were roughly estimated to $1 < Q_1/Q_2 < 5/3$. For higher ratios no clear dependency could be detected (Q_1 is the higher discharge of the anabranches). It was also observed that the scour depth is most distinct for small discharges Q in the anabranches and also small ratios Q_1/Q_2 . The confluence scour depths observed were smaller than in gravel-bed rivers (Ashmore and Parker, 1983).

6.7 INTERACTION SCOUR

The reduction of the bend radius together with the extra scour acts in a much larger area (with a length of about the length of the series of groynes) than the local scour near the tip of a groyne. Therefore they act independently of each other and they can be added to each other (summation principle). However, confluence scour and local scour might have very similar horizontal geometric dimensions (width and length, but not depth). Therefore a strong interaction seems likely and the summation principle results easily in an overestimation of the total scour depth.

Therefore, it is recommended that the total scour depth due to interaction should be taken either from the summation of bend scour, extra scour and local scour or from the combination of bend scour, extra scour and confluence scour. The maximum value of both should be selected as expressed in the following formula for the design scour depth $y_{s,design}$:

$$y_{s,design} = y_{s,bend} + y_{s,extra} + \max \left[y_{s,local} ; y_{s,confluence} \right] \quad (6.7-1)$$

6.8 BANK EROSION PROCESS AND FLOW SLIDES

6.8.1 Introduction

The banks along the braided Brahmaputra-Jamuna river are eroded frequently as the planform changes are very dynamic. The natural erosion of unprotected banks should be understood well before analysing the possible erosion of a bank protected by groynes.

The natural bank erosion process depends among others on the composition of the soil in the banks. A typical situation is a layer of fine deposits of mainly silt on top of layers of fine sand. In a study of bank erosion along the Mississippi river, Fisk (1947) distinguished a gradual bank caving process by sloughing where sandy deposits make up the bed and bank, and slumping where fine grained, more cohesive deposits are present. In his study of the Jamuna river, Coleman (1969) mentioned the same two types of bank erosion. Torrey (1995) mentioned two types of slumping: a shear slide and a flow slide. A shear slide exhibits a U shape in plan and usually a rotational sliding surface in a section perpendicular to the river. A flow slide exhibits a bulb shape in plan with a narrow neck river wards and the bottom slopes in the scar are flatter than 20 degrees.

The natural bank recession in Kamarjani combined with the effects of the Groyne Test Structure has been partly a gradual process ("sloughing") and partly a process of sudden slides, which occur under certain conditions. These phenomena are described in Subsections 6.8.2 and 6.8.3 respectively.

6.8.2 Sloughing at Groynes G-1, G-2 and G-3 in 1995

Sloughing is a gradual process of bank erosion. It has been studied by comparing the contour lines of sequential bathymetric surveys from mid July to end of August 1995 (see for example Fig. 6.8-1 to 6.8-7). Thereby it was found that the natural bank erosion processes downstream from G-1 and G-2 averaged over the area proceeded at a rate of less than 2 m/day.

The natural bank erosion process depends on the development of the local scour hole. If the local scour deepens, then the bank tends to erode. If the local scour hole silts up, then the bank tends to be stable or to exhibit some sedimentation

It seems that the gradual bank erosion process between the groynes G-1 and G-3 does not depend so much on the maximum flow velocities, but on the development of the local scour hole. The function of the flow velocity in the bank erosion process is supposed to be mainly the transporting of eroded bank material. In an area with decreasing flow velocities, the eroded material will deposit at a short distance and the process will stop rather quickly.

The influence of a groundwater gradient on the gradual bank erosion process could not be assessed due to insufficient data. Some data show that after heavy rainfall the water level in the embankment is 0.2 higher or 0.4 m lower the river stage (see Consulting Consortium FAP 21-22 1998b).

6.8.3 Slumping and Slides at Groynes G-1, G-2 and G-3 in 1995

(a) Groyne G-1

The bathymetric survey on June 10, 1995 shows smooth bank profiles upstream and downstream from G-1 (see Fig. 6.8-1). A small slide near the head of the impermeable part of the groyne occurred on June 17, 1995 as the water level raised quickly to the first peak flow. In the period from June 13 to 20, a lot of floating debris had piled up against G-1. This floating debris may have caused a sudden increase of flow velocities and a small increase of the local scour depth, thereby triggering some small slides. The bathymetric surveys of the same area on June 24 and 26, 1995 show 3 to 4 small slides just downstream from the bed protection (see Figures 6.8-2 and 6.8-3). At that time the water level had started to recede just after the first peak flow.

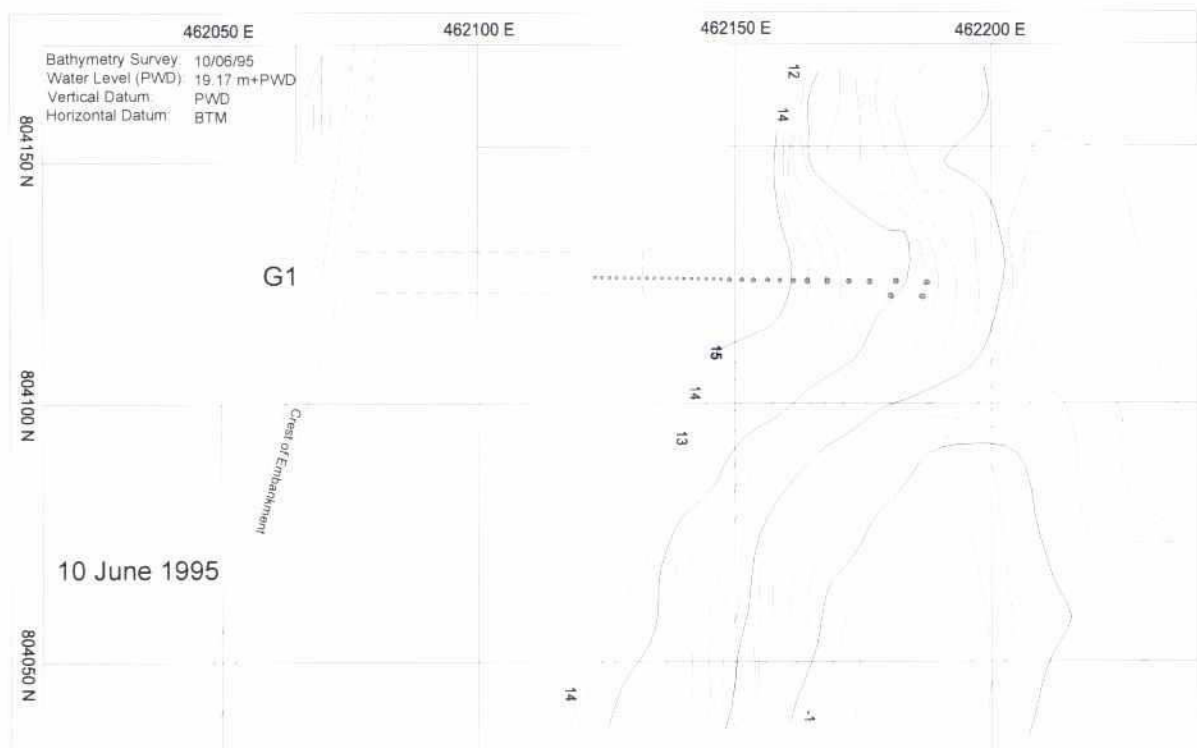


Fig. 6.8-1: Bathymetry around groyne G-1 on June 10, 1995

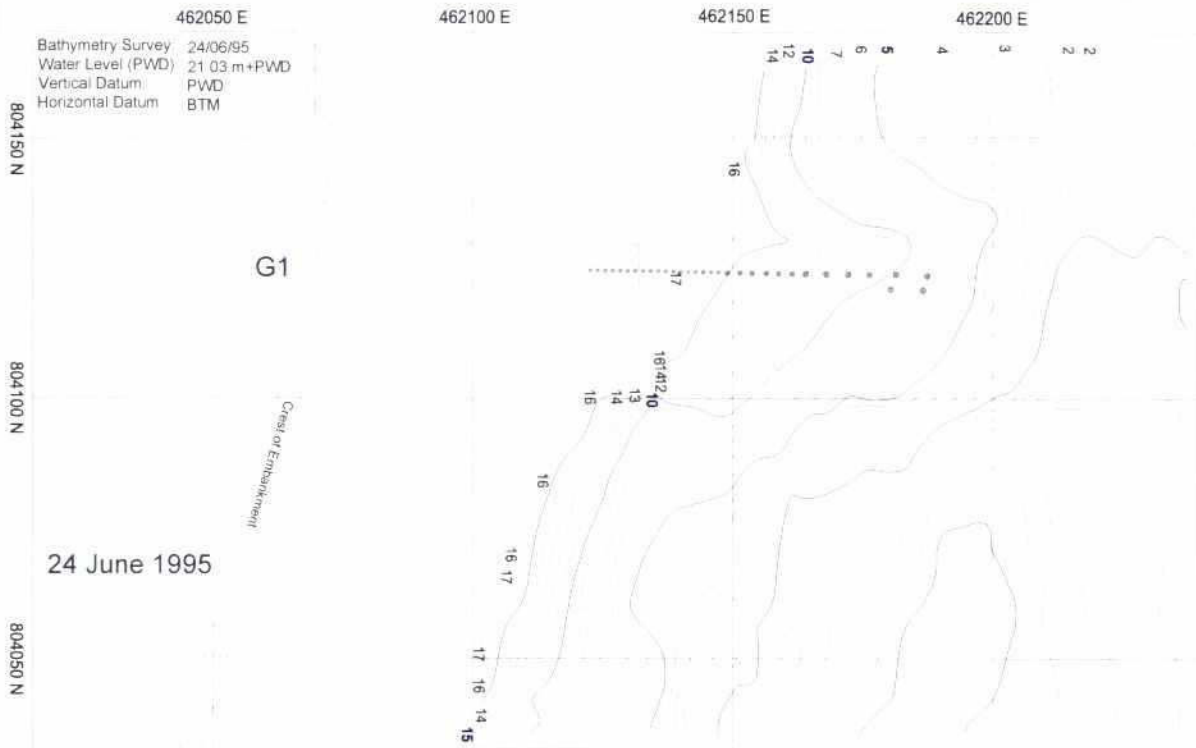


Fig. 6.8-2: Bathymetry around groyne G-1 on June 24, 1995



Fig. 6.8-3: Bathymetry around groyne G-1 on June 26, 1995

In general, small slides are difficult to identify on bathymetric maps based on surveys made by the monitoring team, because of the coarse spacing of the survey lines and the accuracy of the positioning system. The bottom slopes of the slides could not be determined accurately from the bathymetric maps.

(b) Groyne G-2

An initial small slide at the downstream toe of the impermeable part of groyne G-2 (downstream from the first pile) occurred already on May 21, 1995 when the water level started to rise sharply from about 18.00 to 19.00 m+PWD (see Fig. 6.8-4). High flow velocities were observed around the head of the impermeable part of the groyne. The scour hole was probably filled with material of the slide, reducing the maximum depth with several metres.

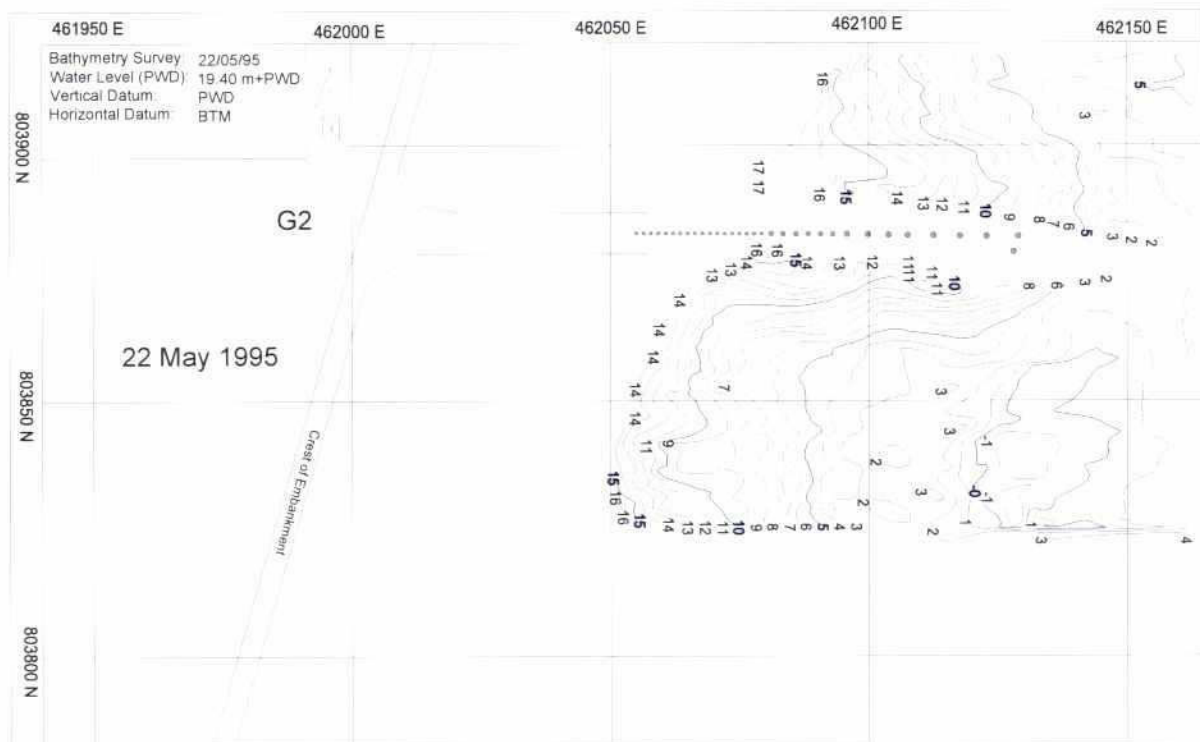


Fig. 6.8-4: Bathymetry around groyne G-2 on May 22, 1995

The big slide near G-2 occurred in the night from July 09 to 10, 1995. Bathymetric surveys of July 08 and 10 show, that just downstream from the groyne on an area of about 70 by 25 m about 10,300 m³ of subsoil eroded (see Fig. 6.8-5). These surveys did not cover the complete area of the slide, because this area extended also upstream from the groyne. Therefore, the total volume of the slide is estimated at about 20,000 m³. The maximum erosion depth in the slide was 12 m. The slide was concentrated near the pile row and extended up to the head of the impermeable part of the groyne. The falling apron was only 15 to 20 m from the axis of the groyne. This part was not able to resist a slide of that size and disappeared completely. Some short piles and a part of the gangway lost their stability. In the next weeks more piles were damaged.

Just before the slide, the maximum scour depth downstream from the groyne increased from 7 m on June 26 to 11 m on July 08/09, 1995. This increase of the local scour depth had also increased the side slopes. Local steep side slopes can result in over-steepening, which can trigger a slide.

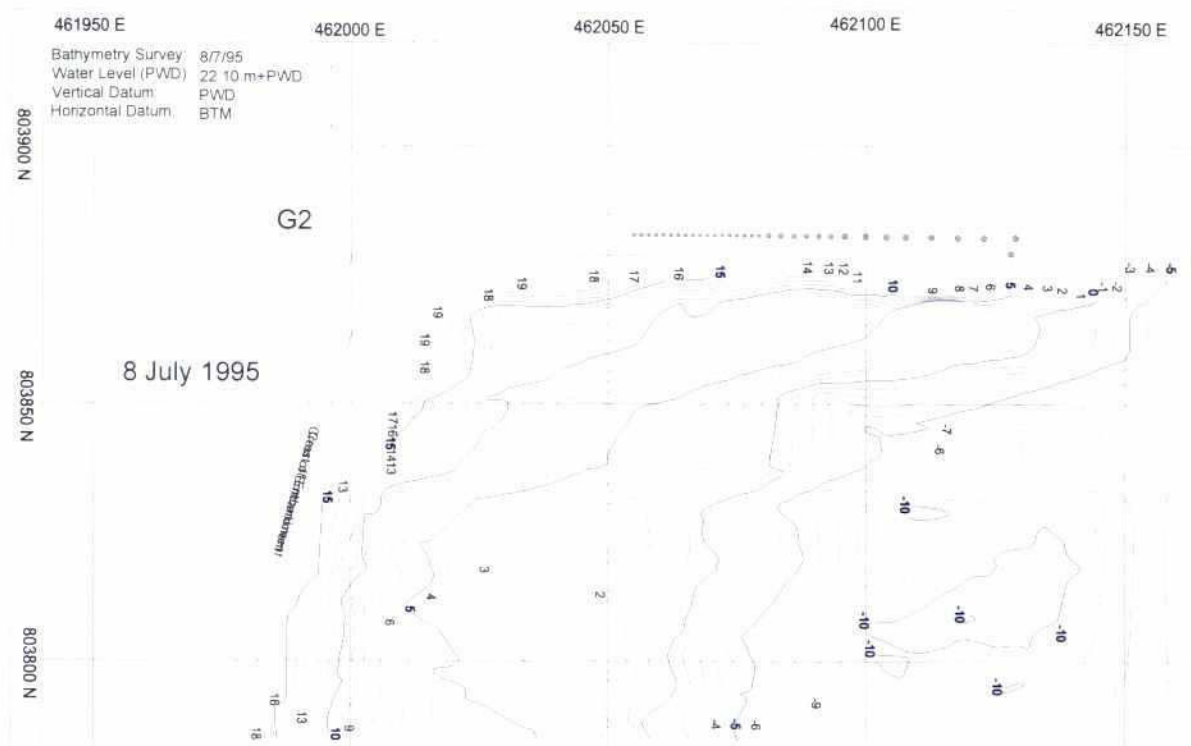


Fig. 6.8-5: Bathymetry around groyne G-2 on July 08, 1995

Floating debris may have contributed to this exceptional increase in scour depth in the days before the slide. Up to July 01 no floating debris was mentioned in the logbook. On July 02 and 03 some floating debris was observed between the groynes, but disappeared during the next days. A few days later a lot of water hyacinths and banana tree trunks were floating again between the groynes. On July 08 the amount of floating debris further increased and the whole area upstream from G-2 was fully covered. The amount of debris was reduced on July 09 because part of it flowed through the gap between the pile row and the impermeable dam. The current along the groynes was strong between July 02 and 09 and caused the thickness of the floating debris upstream from G-2 to increase. In general, the thickness of the layer of floating debris depends on the flow velocity.

The slide settled partly in the local scour hole and filled it with about 12,000 m³, thus reducing the scour depth from -11 to -5 m+PWD. The bottom slopes of the slide were very flat, estimated at 1:40 to 1:30 or 2 to 3 degrees in the centre-line of the slide.

(c) Groyne G-3

The first damage of groyne G-3 occurred after the first peak flow in the night of June 30 to July 01, 1995 just before the water level started to rise for the second peak flow. Within one hour, the rip-rap boulders with a median size of 0.25 m slipped down into the water on the downstream side of the head of the impermeable part of the groyne.

The erosion continued the following 4 to 5 hours and resulted in the loss of a part of the head with a length of 10 to 12 m and a width of several metres. In the impermeable part, a crack was observed at the top of the groyne. Probably this was a small slide as a result of soil mechanical instability. The development of the riverbed near the pile row in that period can be seen in Fig. 6.8-6 and Fig. 6.8-7. Between June 26 and July 09, the maximum local scour depth increased by 5 m, which was about 2 m more than the average trend in the development of the local scour depth. In the days before this slide

occurred, continuous erosion of the bank upstream and downstream from the groyne was observed. Sandbags were dumped the next three days to repair the damage.

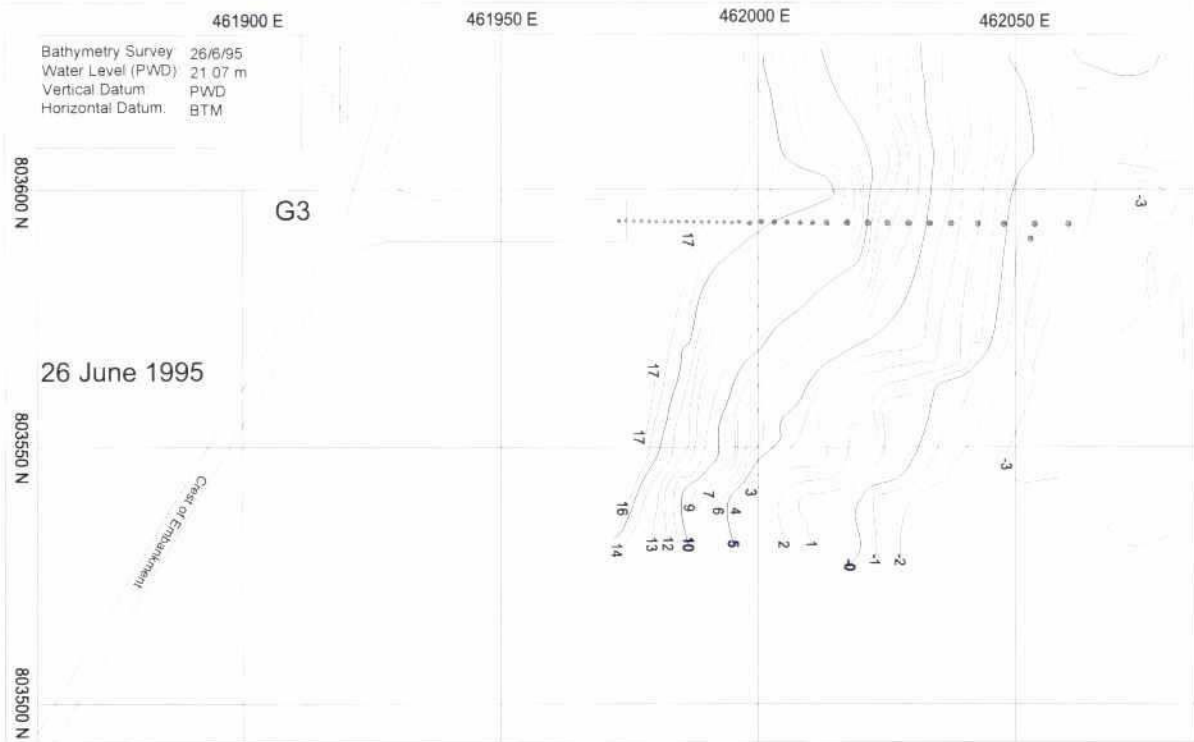


Fig. 6.8-6: Bathymetry around groyne G-3 on June 26, 1995

28

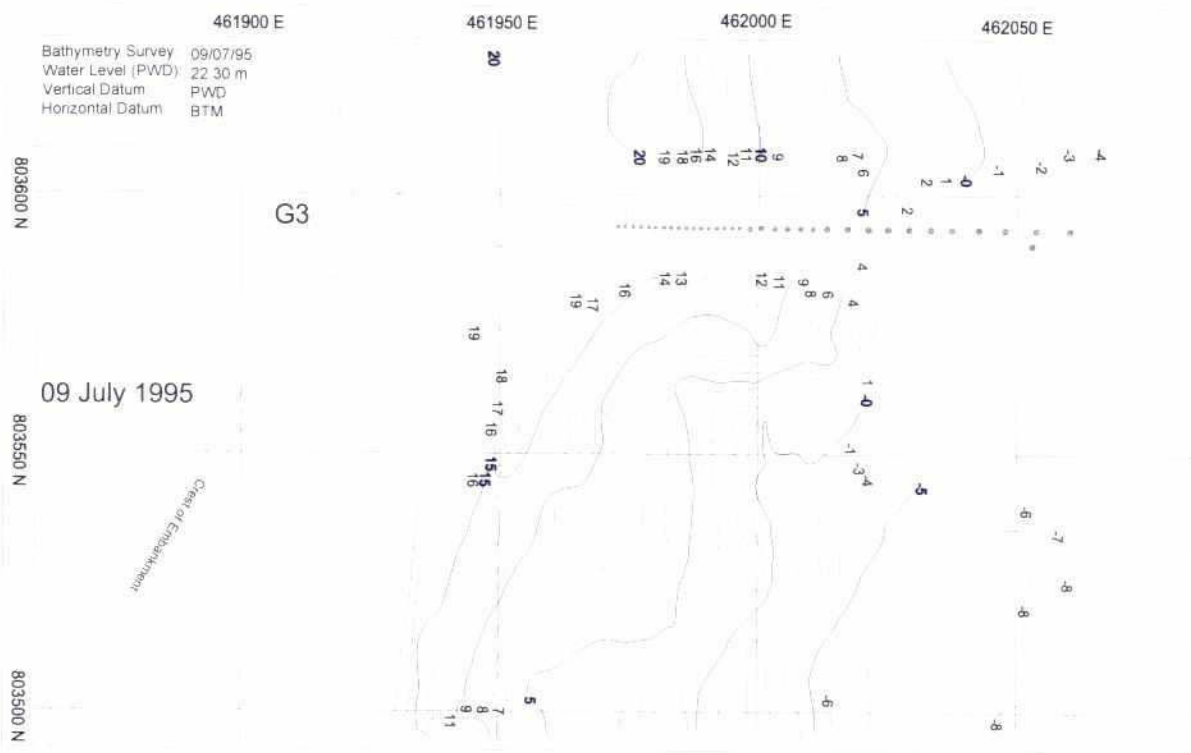


Fig. 6.8-7: Bathymetry around groyne G-3 on July 09,1995

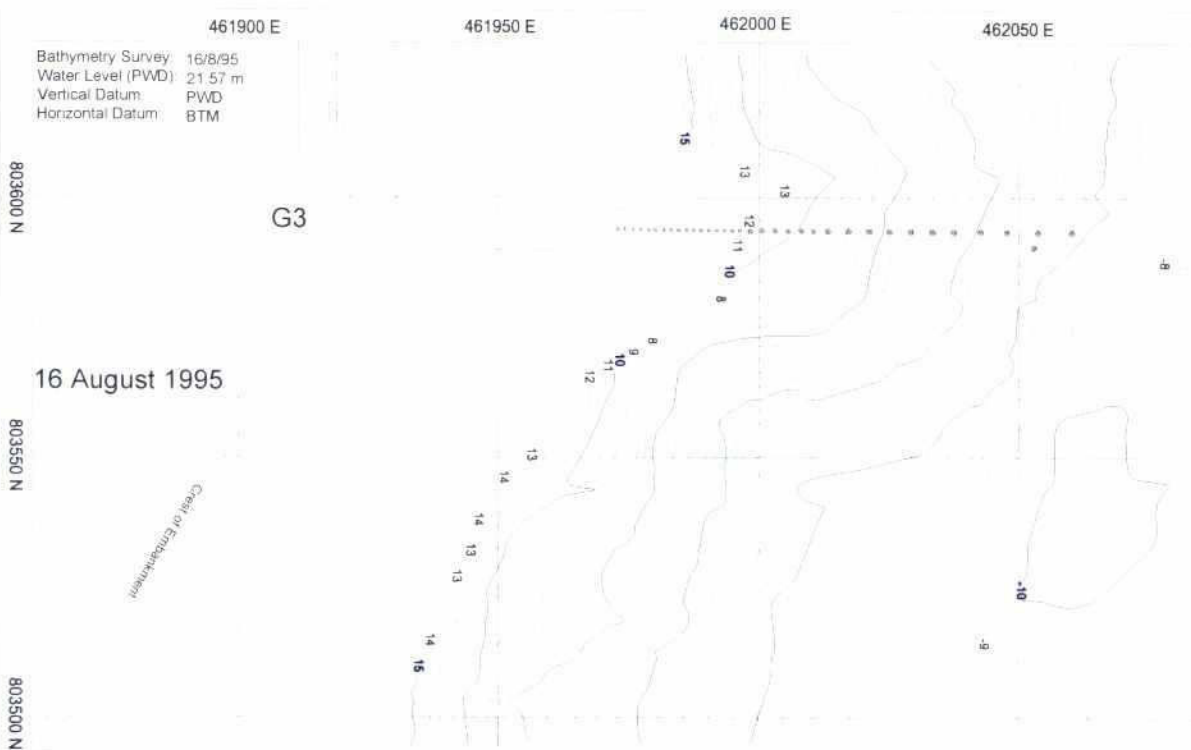


Fig. 6.8-8: Bathymetry around groyne G-3 on August 16, 1995

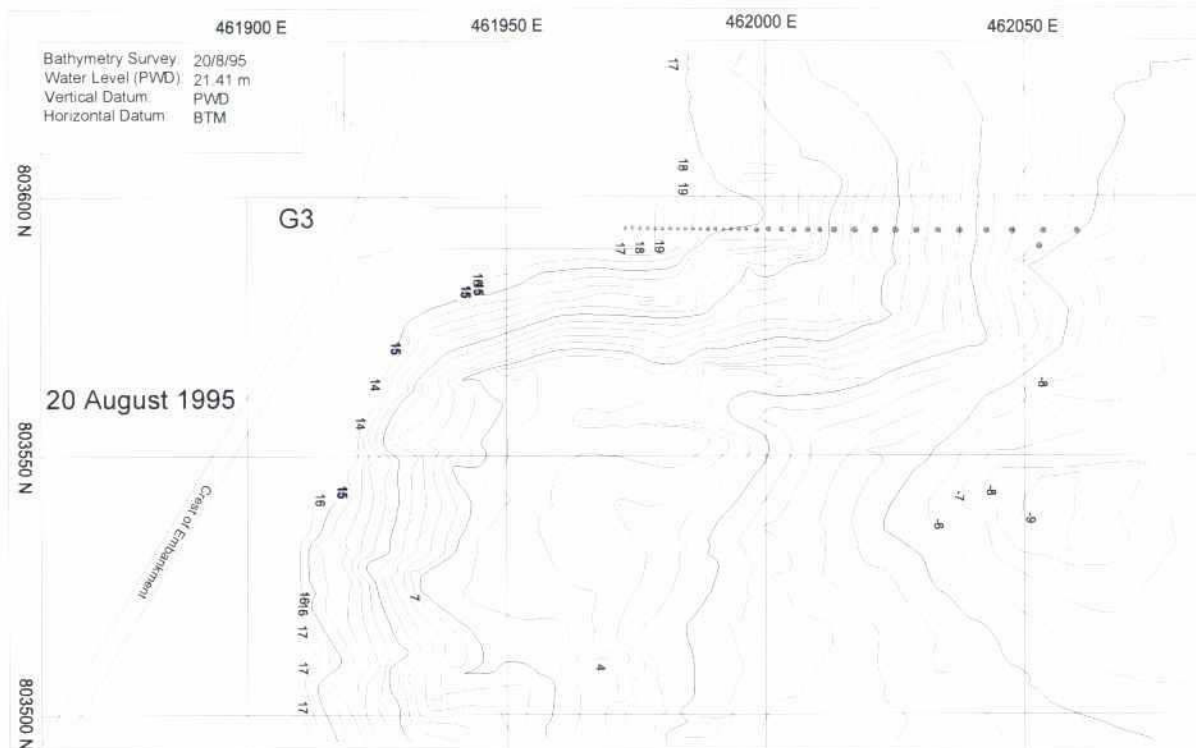


Fig. 6.8-9: Bathymetry around groyne G-3 on August 20, 1995

Just upstream from G-3, a medium size slide can be identified from bathymetric surveys between July 17 and 31. The +4, +8 and +12 m contour lines show erosion, whereas the 0 m contour line shows sedimentation of the eroded material.

An impressive big slide occurred near G-3 during day time on August 19 after an extremely quick rise of the water level of 0.8 m on August 12 as the water level started to rise for the third peak flow, which reached its maximum water level on August 17. The slide started in the morning at 9 hours when boulders slipped down and immediately a long straight crack parallel to the groyne axis developed in the middle of the impermeable part of G-3 (see Photographs 6.8-1 to 6.8-7). The head of the impermeable part started to disappear under the water surface at around 12 hours. The slide was completed several hours later in the afternoon. The next day some small erosion near the water line was observed near the remaining head of the impermeable part, which was more or less the part upstream from the initial crack. This indicates that the equilibrium was lost along one single slide plane rather than along a series of several slide planes during that event. However, the soil did not move in one large chunk as often observed along the Mississippi river (Torrey, 1995), but in smaller pieces. The bathymetric surveys of August 17 and 31, 1995 show that about 34,000 m³ eroded just downstream from the impermeable part of the groyne in an area of approximately 100 m by 75 m (see Fig. 6.8-8 and Fig. 6.8-9). The location of the maximum erosion depth in the slide was about 30 m downstream from the groyne axis. The falling apron around the impermeable part was made of concrete blocks with 0.15 and 0.2 m sides. The width of the falling apron was only 25 m from the axis of the groyne. This part was not able at all to resist a slide of that size and disappeared completely, together with a part of the impermeable groyne protected by brick mattresses. Based on the experience with earlier slides no actions were taken to repair the groyne by dumping materials (stones and cc-blocks).



Photo 6.8-1: Development of a crack in groyne G-3, August 1995



Photo 6.8-2: Development of a crack in groyne G-3, August 1995



Photo 6.8-3: Erosion process during slide at groyne G-3, August 1995



Photo 6.8-4: Erosion process during slide at groyne G-3, August 1995

202



Photo 6.8-5: Remains of earth dam protection after the slide at groyne G-3, August 1995



Photo 6.8-6: Transition between permeable pile row and earth dam after slide at groyne G-3, August 1995



Photo 6.8-7: Transition between permeable pile row and earth dam after slide at groyne G-3, August 1995

The flat bottom slopes in the centre of the scar after the slide are about 1:30, which is close to the average value of 1:25 found in slides in a Dutch estuary (Huis in't Veld et al, 1987).

Other possible causes for the big slide are the compaction of the subsoil of the groyne, changes in the groundwater levels by local rainfall and the temporary stock of cc-blocks on the top of the impermeable part of the groyne for repair work. It is mentioned that the maximum scour depth downstream from G-3 was rather stable in August 1995. It remained between -9 to -10 m + PWD without sudden changes.

6.8.4 Experience with Slides and their Prediction

(a) Introduction

Experiences with slides and bank erosion processes along the Brahmaputra-Jamuna in Bangladesh, the Mississippi in the USA and estuaries in the Netherlands are summarised in this subsection. Most attention is given to aspects which are relevant for the phenomena described in the previous section, i.e. the sizes of slides, the failure mechanisms, the conditions which increase the risk of a failure, and the different types of measures to reduce the risk of failure. In addition, the risk of slides at the second test site is assessed briefly.

(b) Sizes of Slides, Flow and Shear Failures

Coleman (1969) found on large-scale aerial photographs of the Brahmaputra-Jamuna river in 1963 an average of one slump per 300 m over a length of almost 50 km. The diameter of most slumps was less than 30 m, but also large ones with a diameter of more than 300 m occurred. The big slide in G-3 had a diameter of 75 to 100 m. Coleman concludes that flow and shear failures are among the most important processes by which the banks migrate. The experiences with the Kamarjani Test Structure seem to confirm his view.

In the Mississippi river, larger flow slides have been observed than those near the test structures at Kamarjani. A slide at Montz in 1973 had a total volume of 229,000 m³ and a slide at Wilkinson Point in 1949 had a volume of 3,000,000 m³ (Torrey, 1995). A few miles upstream from Baton Rouge, a flow failure occurred just after the peak of the 1950 flood. The total volume was more than four million cubic yards and the main levee was breached at more than 250 m from the bankline (Moore, 1972). The two biggest slides at Kamarjani had estimated volumes of only 20,000 and 34,000 m³.

(c) Failure Mechanism

Coleman (1969) opines that liquefaction of the subsoil causes flow failures. In his description, these flow failures occur either subaqueous or in the zone between the high water level and the low water level. Quite massive channel sands and silts underlie the stratified silts and silty clays of the natural levee deposits. During flood, a greater water pressure is applied to these sands below the river level, forcing water into the formation. This raises the pore pressure in the strata. As the water level in the river falls rapidly and the pressure against the channel walls is lessened, water moves back into the river. This causes a lateral flow with sand and silt into the channel. Normally this produces a bowl shaped shear failure in the overlying cohesive natural levee deposits. Along the banks of the Brahmaputra-Jamuna river many small shear failures can be observed. Several piezometers were placed in the embankment of the Kamarjani Test Structure just before the 1996 flood to investigate whether the same processes occur at that site.

The US Army Waterways Experiment Station has been investigating this type of failure along the banks of the Mississippi river since the 1940s. Steady-state void ratio testing on sands showed that in-situ densities implied from the field investigations were entirely too high to support the hypothesis of liquefaction as the flow failure mechanism. Instead, a locally oversteepened subaqueous slope, generated for example by rapid development of a local sour hole, could be sustained by the presence of negative (with respect to hydrostatic) pore water pressure generated by shear stresses immediately behind the steep face. Part of the eroded material will deposit directly downstream. A smooth slope will build up and gradually the height of the steep face reduces. The erosion process runs out if the upper boundary is reached. Chunks of the overburden fall and are also eroded by the flow. This retrogressive erosion may be the proper explanation for the slides observed near the test structures at Kamarjani.

(d) Empirical Criteria

The studies along the Mississippi river demonstrate that flow slides occur in point bar deposits with a typical vertical stratification. The ratio of the thickness of the overburden to the thickness of the underlying stratum should be less than 0.85. However, of all the sites predicted to be susceptible, less than one fourth had actually suffered a flow failure (Torrey, 1995). Torrey did not mention any criteria for shear failures.

Some rough criteria for the occurrence of flow slides have been established on the basis of field information on dike failures in the Eastern Scheldt area of the Netherlands (Pilarczyk, 1987). The subsoil in that area has some similarity with the subsoil of the Jamuna river, as it consists of fine sand with top layers of cohesive silt and clay. The criteria indicating a high risk for flow slides in a scour hole downstream from the bed protection of a sluice complex in a wide estuary channel are:

- the initial density of a subaqueous sand layer is an important parameter. In general loosely packed sand with porosity of more than 40 % is sensitive to flow slides (liquefaction), whereas in well packed sand only normal soil-mechanical slides can occur.
- for a subsoil consisting of loosely packed sand, the risk of a flow slide is high if:
 - the scour hole slope is steeper than 1:4 over a height of 5 m or more;
 - the average bank slope is steeper than 1:7 over the full scour depth if this scour depth amounts to 10 m or more.

These criteria do not apply straightforward to the soils near the test structure in Kamarjani, because the local scour hole downstream from the permeable groynes is close to an eroding bank. For the eroding bank other depth criteria should apply. These criteria still require further investigation.

Recent experience from the construction of the Jamuna Bridge shows that the risk of flow slides increases if the water depth is increased rapidly by dredging of thick sand layers at a time. The remedy is to dredge more slowly thinner layers at a time. The slope of the bank of the guide bund was adjusted from 1:5 in the initial design to 1:6 to increase its stability and to reduce the risk of flow slides. This slope 1:6 does not differ much from the overall 1:7 slope found in the analysis of Dutch dike failures.

(e) Measures to Reduce the Risk of a Slide

Both the maximum depth and the growth rate of local scour holes can be reduced by an optimisation of the hydraulic structure. Examples of optimisation are:

- prevention of floating debris, and
- construction of the even-numbered piles of the groyne in the first year and the odd-numbered piles in the next year to reduce local scour and other scour phenomena in the first year to reduce the scour velocity and therefore the risk on slides.

The bank stability can be improved by the following measures:

- long protection on a gentle slope into the local scour hole (Pilarczyk, 1987; experience from Jamuna Bridge);
- long groyne to shift the scour hole away from the bank;
- improved drainage of the subsoil, and
- compaction or replacement of the subsoil (Pilarczyk, 1987)

7 DESIGN PARAMETERS

7.1 INTRODUCTION

The hydraulic and morphological aspects of design parameters for a series of permeable groynes are described in the following sections, based on the experiences with the test structure of FAP 21 along a braided-river channel bend at Kamarjani. The analysis of monitoring data has been aimed at deriving general design rules, which can be used for a design manual. The following parameters have been distinguished:

- crest level (Section 7.2);
- groyne length (Section 7.3);
- bed protection (Section 7.4);
- transition between permeable and impermeable part of a groyne (Section 7.5);
- groyne spacing (Section 7.6);
- groyne orientation (Section 7.7), and
- permeability or pile spacing of a permeable groyne (Section 7.8).

7.2 CREST LEVEL

Permeable groynes generally consist of one or several rows of timber piles, steel piles or reinforced concrete piles, which must be designed to resist hydraulic loads and possibly the pressure of floating debris. The latter is always the case when the top of the piles is selected at the design water level for reasons of providing maximum bank protection for a given groyne length. If the load by floating debris should be avoided, then the top of the piles should be a certain margin below the minimum water level above which floating debris normally occurs. Experience has shown that this minimum water level corresponds to the lowest parts of the floodplain. The margin is recommended to be about 0.3 m so that the floating material can pass the structure unhindered. Near the embankment from which the groynes launch, the top of the piles should be raised gradually to the crest of the embankment. The piles in this transition have to be designed to resist not only the hydraulic loads but also the floating debris.

In case of submerged groynes, the installation of navigation signals is recommended.

7.3 GROYPNE LENGTH

The length of a groyne perpendicular to the bankline should be larger than the length needed for a natural slope profile between the local scour hole downstream from the groyne head and the toe of the embankment. For repelling groynes and attracting groynes, which are oriented obliquely, the lengths should be projected onto a line perpendicular to the bankline. This is called the "effective length".

As mentioned already in Section 4, the steepest natural profile in a concave outer bend of a sandy cohesionless river bed can be determined as the envelope of all near-bank cross-section profiles in a large dataset of measured cross-sections. The total scour depth is the summation of bend scour, extra scour and local scour or the combination of bend scour, extra scour and confluence scour. The maximum value of both should be selected as y_s (see Annex 6, Subsection 6.7).

A local scour hole develops near the tip of a groyne, if the main flow is parallel to the bank. The hole develops closer to the bank in case of oblique flow attack in a sharp bend. The **effective** length L_g of a permeable groyne in the mid-section of a scheme of groynes should satisfy the following conditions:

$$L_g \geq \Delta L + n \cdot (h_0^* + y_s) + 0.5 \cdot L_s \cdot \tan \alpha \quad (7.3-1)$$

and

$$L_g < 0.4 \cdot B_{ch} \quad (7.3-2)$$

in which

L_g	=	effective length of groyne	(m)
ΔL	=	safety margin, $\Delta L \geq 10$ m	(m)
n	=	5.5 for the slope 1(V) : n(H)	(-)
h_0^*	=	modified water depth at thalweg here: $h_0^* = h_0 - (DWL - FPL)$	(m)
y_s	=	maximum local scour depth	(m)
L_s	=	length of scour hole in main flow direction, with first estimate: $L_s = 4 y_s$	(m)
α	=	oblique-flow angle, defined as the angle between the flow line and the bankline	(degrees)
B_{ch}	=	width of the approach channel	(m)

The cotangent n for the slope should be smaller than for the angle of repose. Depending on the subsoil, values of 10 to 12 degrees are recommended. In the Brahmaputra-Jamuna river $n = 5.5$ for a safe design and $n = 4$ for a design with minor risk of damage during the lifetime of the groyne. A first approximation of the length of a scour hole is $4 \cdot y_s$. A minimum value of 10 m is recommended for the safety margin ΔL for the embankment.

The oblique-flow angle α equals zero, when the flow is parallel to the bank. The flow alignment, however, changes due to changes in river planform. The maximum value α_{max} should be determined from a planform analysis, which should include the effect of channel attraction by scour holes. For braided rivers, the recommended value is $\alpha_{max} = 45$ degrees.

Formulas (7.3-1) and (7.3-2) were applied to the groynes of the test structure at Kamarjani with $\alpha_{max} = 45$ degrees. The minimum observed channel width in 1995 was 700 m (see Table 7.3-1). However, this minimum width is smaller than the width of a design channel.

y_s (m)	n	h_0^* (m)	L_s (m)	L_g (m)	$0.25 B_{ch}$ (m)	L_g (m)	
						G-2	G-3
8	4	22	32	146	175	145	180
9	5.45	22	36	197	175	145	180

* h_0 includes confluence scour, bend scour and scour enhancement due to a change in approach conditions

Table 7.3-1: Estimation of the length of a permeable groyne

The depth h has to be selected from the envelope curve of the surveyed cross-sections. The maximum depth is the depth h_0 at the thalweg of the design channel based on the envelope curve. The structure-induced scour has to be added to it.

To the estimated length of the permeable groyne L_g another safety margin and the length of the groyne on the floodplain has to be added according to Fig. 7.3-1. For the latter, the minimum length is the expected bank erosion during the construction phase.

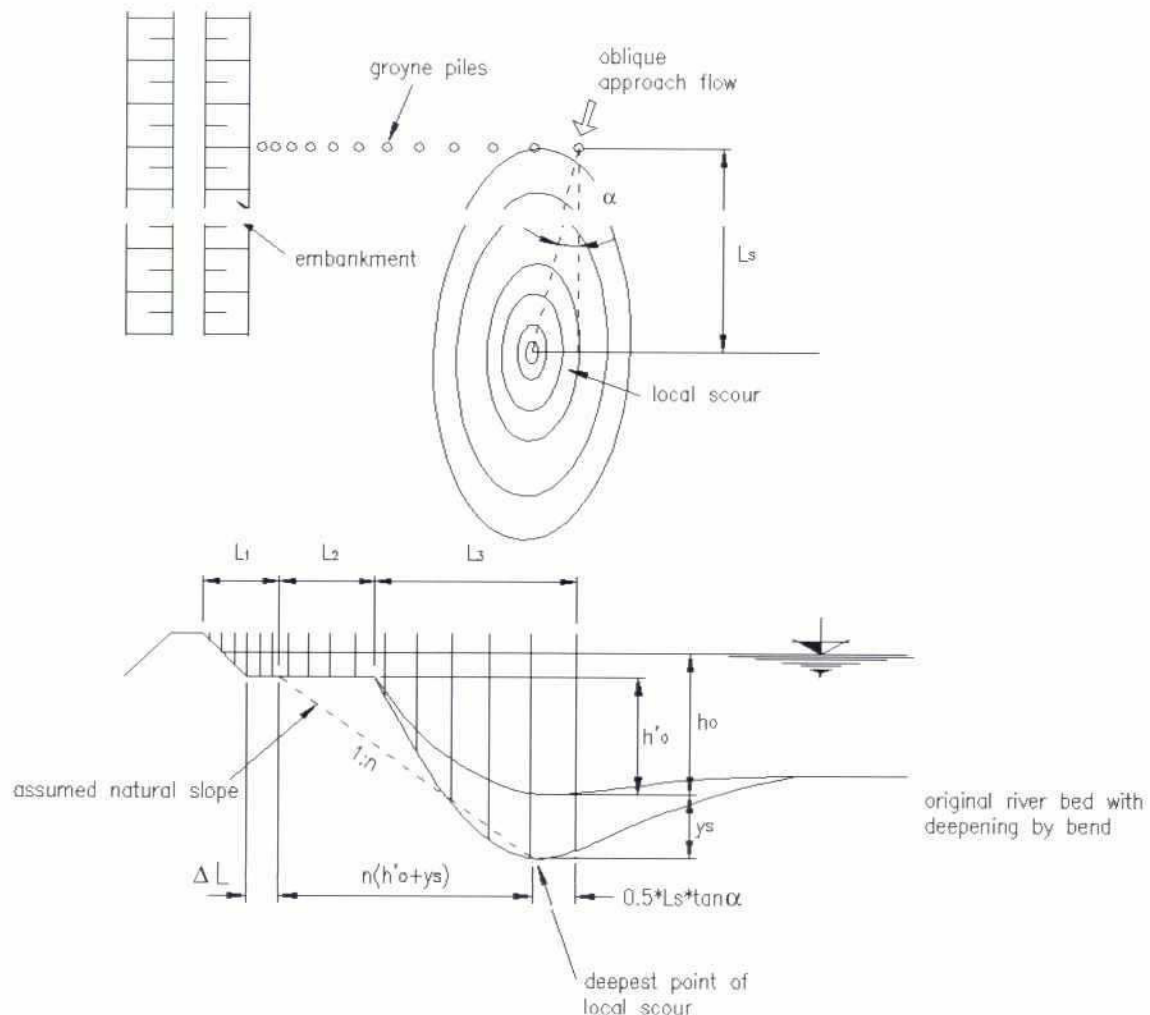


Fig. 7.3-1: Design projected total length of a groyne

It is most economic to construct the whole groyne as bored piles in the flood plain. But in that case the embankment should be at least 200 metres away from the present bankline. In practice, the embankment will be constructed closer to the river and that means that a part of the permeable groyne has to be constructed in the river.

In general, groynes in the upstream termination and in the downstream termination are shorter than calculated with the above formula. The underlying idea is that the flow will be guided along the structure with more or less smooth transitions.

Strong oblique flow attack on a scheme of groynes can exert the maximum load on the groynes and cause maximum erosion of the bank between the groynes. Therefore, this situation is decisive for the design of the groynes. Strong oblique flow attack in braided rivers has resulted in typical schemes of short groynes along the large braided rivers in China (Garde and Ranga Raju, 1985), as illustrated in Fig. 7.3-2.

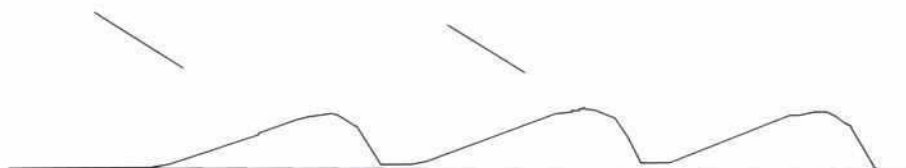


Fig. 7.3-2: Example of the plan of stack dykes applied along Chinese rivers

In the Chuanjiang River, the ratio between the highest and the lowest discharges is 8 to 15, which is comparable to the value of this ratio in the Brahmaputra-Jamuna river. The bed of the Chuanjiang river consists of sand, gravel and rock. Shiyi Wang (1990) gives some recommendations for the design of a scheme of groynes to improve navigation conditions. The groyne should not reach the area where 30 % of the design discharge flows. The first groyne is located about $0.8 \cdot L_g$ upstream from the shoal that has to be protected.

7.4 BED PROTECTION

A bed protection made of a granular or synthetic filter tends to assume a slope of 1 in 2 upstream and downstream from a pile row, if the riverbed erodes. This deformation damages the bed protection and causes the bed protection to fall as a falling apron of loose elements. If a bed protection has to remain undeformed, a very strong construction has to be selected, for example using gabions.

The main parameters of a bed protection are its width, its thickness and its level.

The influence of a bed protection layer on the *flow pattern* has the following characteristics:

- without any deformation of the bed protection and the river bed upstream, no changes are to be expected in the flow pattern, and
- a deformed bed protection acts like a sill and reduces the flow attack on the bank downstream from the groyne, in a similar way as the reduction due to permeability of the pile row.

The influence of a bed protection layer on the *local scour depth* has the following characteristics:

- the protection layer downstream from the pile row shifts the local scour away from the pile row in an area with less strong turbulence. This reduces the maximum scour depth, and
- the deformed protection layer will act as a sill, if the protection layer slides partially into the scour hole. A sill increases the local scour hole. This is illustrated by the results of the tests carried out under FAP 21 in Chanaz, France, and Faridpur, Bangladesh. In the tests in Chanaz, a pile row with bed protection but without sill caused no local scour. In the tests at RRI in Faridpur, a pile row with a prefixed falling apron caused a considerable scour hole.

Field observations confirm that the protection layer finds equilibrium at a slope of 1V:2H. This complies with the Indian experience with falling aprons (Spring, 1903; Varma et al, 1989). The bed protection around G-1 at Kamarjani had acted as a falling apron, because the erosion occurred as a gradual process with small flow slides, which had mixed up the layers of the bed protection. The falling apron around G-2 had fallen as expected.

The design width for a falling apron is (see also Annex 11)

$$W_{fa} = c_{w, fa} \cdot y_s \quad (7.4-1)$$

in which

W_{fa}	=	width of falling apron	(m)
$c_{w, fa}$	=	empirical coefficient	(-)
	=	2	
y_s	=	scour depth	(m)

A falling apron falls under a slope of 1 in 2 upstream and downstream from a pile row. Also lower values of $c_{w, fa}$, which represents the slope, have been reported. At G-2, the width of the falling apron is 15 m and the maximum observed scour depth is 8 to 9 m plus an interaction scour of 5 m. This indicates that the designed width is optimum for the local scour depth only. When including the interaction scour, i.e. the scour enhancement due to a structure-induced change in approach conditions, the width should have been increased.

Alternatively, if not the width but the thickness has to be selected as the decisive parameter, the design *thickness* d for a falling apron is

$$d = c_{d, fa} \cdot D \quad (7.4-2)$$

in which

δ	=	thickness of falling apron	(m)
$c_{d, fa}$	=	empirical coefficient	(-)
	=	3.5 for randomly placed cubes,	
	=	4.5 where turbulence is expected, e.g. at	
		upstream/downstream terminations, transitions, etc.	
D	=	block size or stone size	(m)



These relations (7.4-1) and (7.4-2) do not necessarily have to be valid at the same time. It is to be guaranteed that the parameters fulfil the following design formula 7.4-3 for the *volume* V_{fa} of the apron per running metre. It was determined from the physical model investigation. The volume should be :

$$V_{fa} = W_{fa} \cdot d = 5 \cdot y_s \cdot D \quad (7.4-3)$$

It is concluded, however, that permeable groynes should preferably be designed without a bed protection. The additional length of the piles, which is needed to compensate for the absence of a bed protection is often more economic. Moreover, the bed protection produces its own local scour, which contributes to the development of unfavourable approach conditions (flow attraction, interaction scour).

7.5 TRANSITION BETWEEN PERMEABLE AND IMPERMEABLE PART

The transition between the pile row and the impermeable part of the groyne may become exposed to heavy flow attack in due time, causing additional scour downstream, if the transition is abrupt. This additional scour may endanger the stability of the structure. Therefore, the transition requires careful design.

The transition between the groyne and embankment is of minor importance when the groyne consists solely of a pile row, because in that case this transition will lie in an area where the flow velocities are low. The impermeable part on the floodplain can be built as an earthdam or a cofferdam. Its purpose is to create a safety margin between the bank and the embankment.

The constructed transition in G-1 at Kamarjani had a designed slope of 1V:5H. The groynes G-2 and G-3 had a designed slope of 1V:3H, which had caused additional scour as deep as the local scour hole near the tip of the groynes. If a steep transition is necessary, then it is recommended to increase the length of the impermeable part of the groyne to accommodate for an additional safety margin for the embankment (see also Fig. 7.3-1):

$$L_m = n_{tr} \cdot (h_{tr} + y_{s,tr}) \quad (7.5-1)$$

in which

h_{tr}	=	local water depth near the transition	(m)
$y_{s,tr}$	=	local scour depth near the transition	(m)
n_{tr}	=	4, for the slope 1V:n ₁ H	(-)
L_m	=	length of the impermeable part of the groyne on the flood plain	(m)

In general, a gradual transition is recommended with a gentle slope, not steeper than 1:5. In that case no additional safety margin is required, since no additional scour will develop. A disadvantage is, however, that the distance between the toe of the impermeable groyne head and the main embankment will increase considerably.

7.6 GROYPNE SPACING

The spacing of the groynes in a scheme depends on the flow pattern in a design situation and the maximum allowable flow velocity along the bank, which is often the critical flow velocity for bank erosion. This flow pattern is governed among other parameters by the maximum angle of oblique approach flow and the expansion angle, depending on the water depth and the hydraulic roughness of the riverbed. The effective length of the groynes is an important parameter for the spacing. This holds as well for permeable as impermeable groynes.

The flow pattern can be calculated by a schematised method or can be derived from physical or mathematical model investigations. The accuracy of these calculations or simulations should be commensurate with the accuracy of the design situation. The major difficulty lies often in the accurate assessment of the extreme design situation with the corresponding planform and approach flow.

The spacing of groynes S_g in a flow parallel to the bankline is given by

$$S_g = \frac{0.67 \cdot L_g}{\tan \beta} \quad (7.6-1)$$

in which

L_g	=	effective length of permeable groyne	(m)
β	=	expansion angle	(degrees)

200

7.7 GROUYNE ORIENTATION

Considerations for the orientation of permeable groynes differ from those of impermeable groynes. The recommended orientation of permeable groynes is perpendicular to the main approach flow, because in that situation the designed blockage is equal to the effective blockage and the designed length is equal to the effective length. The direction of the approach flow can vary with stage and depends also on the planform of the river, especially in a braided river. The way in which the effective length of the groyne decreases in case of oblique approach flow can be determined by projecting the groyne onto a line perpendicular to the approach flow. From this procedure it is clear that permeable groynes become less effective as the approach flow becomes more oblique.

A permeable groyne does not change the direction of the flow passing through the piles. If the permeable groyne has a sill-shaped bed protection, however, this bed protection may deflect the flow direction towards a line perpendicular to the groyne axis. In that case, deflecting groynes are recommended pointing slightly upstream with an angle of 105 to 110 degrees with respect to the flow direction.

7.8 GROUYNE PERMEABILITY

The permeability of the groyne is characterised by the pile spacing. The pile spacing is determined by the pile diameter and the required blockage of the flow. The pile diameter is determined by the loads and the maximum water depth. The permeability of the groyne and its blockage obviously sum up to 100%.

The pile spacing is the same for a single pile row as for a double pile row if the flow is parallel. In case of oblique approach flow, the blockage of a double pile row has to be calculated as the blockage by both pile rows projected on a plane perpendicular to the oblique approach flow.

The pile arrangement at Kamarjani was made with a blockage, which decreased from the first pile near the embankment to the last pile in the river, in order to obtain a gradual reduction of the downstream flow velocities from the tip of the groyne to the bank. Consequently, the permeability increases.

It has been investigated that the efficiency of the structure is extremely influenced by changing water levels and bathymetry. The formation of a return current along the highly erodible bank downstream from the groyne was observed as a negative effect. The return current cannot be suppressed at all possible water levels. To increase the robustness of the system and to reduce the impact of the return current, the pile arrangement was further optimised by using a counter acting opening in the groyne close to the bank. A higher permeability of 70% was applied in the section between 0.1 to 0.3 L_g . This design optimisation was proved by physical model tests in Faridpur where also the best alignment for the increased pile spacing was investigated. Although the results of the investigations were obtained from a small number of experiments and not verified in detail, the optimisation has been applied in the extended groyne G3. The monitoring of the water motion proved that this measure works fine and very effective. Thus, the recommendation for the use of bank-near openings is given here for the future.

The recommended pile arrangement is given in Table 7.7-1. At Kamarjani, the permeability was kept constant within each of the individual sections.

296

Distance from embankment (as fraction of total groyne length)	Permeability (%)
0 to 0.1	50
0.1 to 0.3	70
0.3 to 0.4	50
0.4 to 0.6	60
0.6 to 0.8	70
0.8 to 1.0	80

Table 7.7-1: Recommended pile arrangement of a permeable groyne

8 RIVER RESPONSE

8.1 CHANGES UPSTREAM AND DOWNSTREAM OF THE TEST STRUCTURE

No structure-induced changes can be identified upstream from the test structure. Downstream from the structure, a typical 2 km long embayment has been formed by locally stronger bank erosion in the area of Syedpur, between Northings 801000 and 803000 (see Fig. 8.1-1). Given the limited predictability of distances of bank retreat, it is impossible to assess whether the bank in this area would have been eroded less or more in a situation without the Groyne Test Structure. This is illustrated in Fig. 8.1-2.

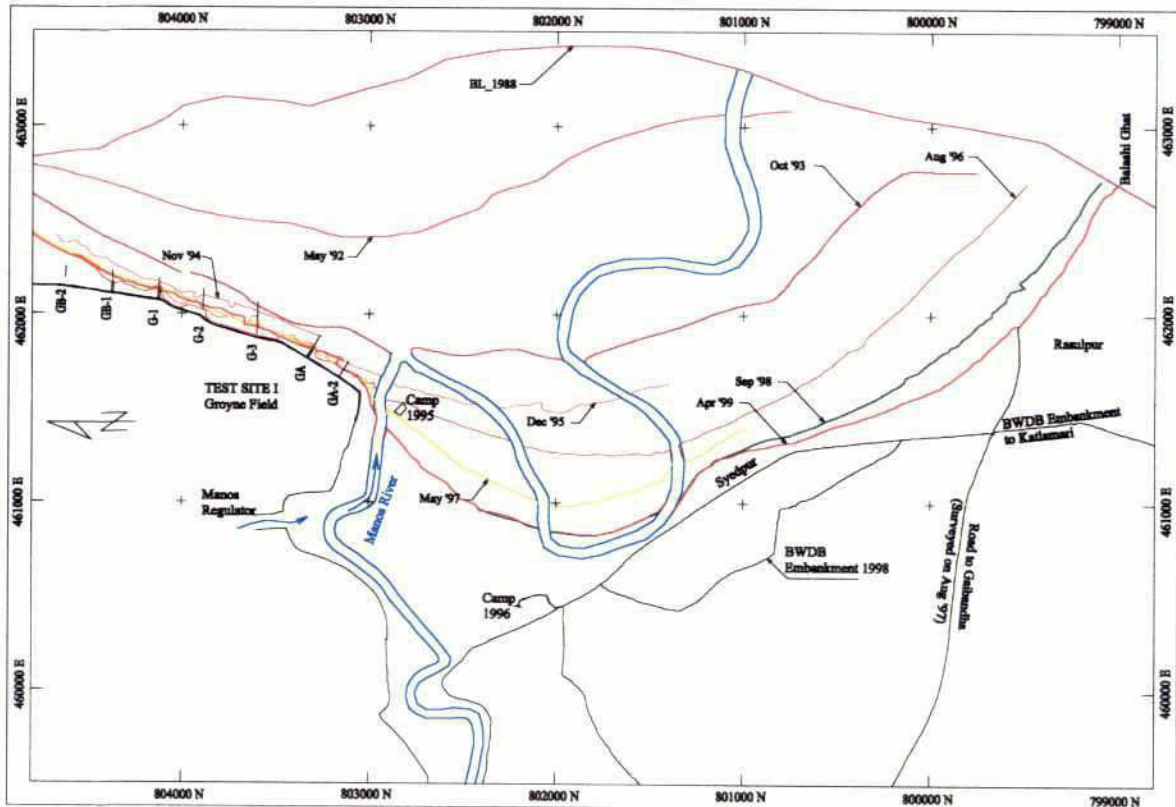


Fig. 8.1-1: Bank erosion at Kamarjani between 1988 and 1999

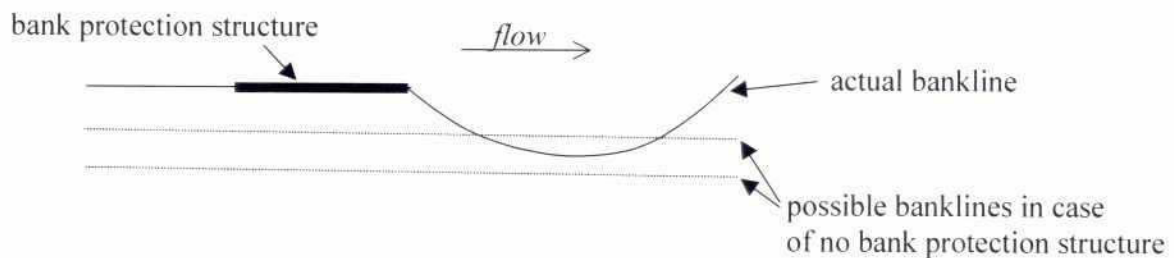


Fig. 8.1-2 Impossibility to assess net effect of impeded bank erosion at test site and embayment formation immediately downstream

Despite the impossibility to assess the net total effect of the Groyne Test Structure, one can argue that the presence of the structure enhances bank erosion in the area immediately downstream in two ways.

24
Firstly, the structure-induced local scour decreases bank stability through oversteepening. Secondly, flow attraction by the structure-induced scour hole leads to a more perpendicular flow impingement on the bank. Initially, the flow attraction at Kamarjani *reduced* the bank erosion downstream, because the migration of the downstream channel was slowed down. In December 1996, however, the point of flow impingement arrived at the downstream end of the structure, thus attacking the unprotected bank. This *enhanced* the erosion immediately downstream from the groynes while bank erosion further downstream remained weak (between Syedpur and Rasulpur).

The full bank erosion was resumed when the channel bend and the point of flow impingement had lost their contact with the Groyne Test Structure. The development of a bend cut-off could not prevent the resumption of severe bank erosion between Syedpur and Rasulpur. It is most likely, however, that the area of Rasulpur and Balashi Ghat would have experienced much more bank erosion if the Groyne Test Structure would not have been built.

It should be noted that the formation of the embayment between Northings 801000 and 803000 may also have been enhanced by overbank flows over the low-lying meander belt of the Manos river.

8.2 CHANGES IN THE TEST SITE AREA

The primary effect of the groynes has been the effective stopping of bank erosion at the site of the test structure. Furthermore, the structure has produced bed scour, which was most pronounced immediately after its construction in 1995. The dry-season channel along the test structure was deformed as a result of flow attraction by the structure-induced scour hole as explained in Subsections 6.2.3 and 6.2.4 of Annex 1. In December 1995, the deformation rotated the channel in a way that the resulting perpendicular flow impingement produced deep additional local scour. Section 8.3 provides more details on the local scouring at the Groyne Test Structure.

REFERENCES

- Ahmad, M. (1953), Experiments on design and behaviour of spur dikes. Proc. IAHR Conf. Minnesota, pp.145-159.
- Ashmore P. and G. Parker, (1983), Confluence Scour in Coarse Braided Streams, Water Resources Research, Vol. 19, No. 2, pp. 392-402.
- Breusers, H.N.C. and A.J. Raudkivi (1991), Scouring. IAHR Hydraulic Structures Design Manual, Balkema, Rotterdam, The Netherlands.
- Brown, S.A. (1985), Design of spur-type streambank stabilization structures. Final report, HWA/RD-84-101, Federal Highway Administration, Washington DC.
- CERC (1977), Shore Protection Manual. US Army Coastal Engineering Research Center.
- Coleman, J.M. (1969), Brahmaputra River: channel processes and sedimentation. Sedimentary Geol., Vol.3, Nos.2-3, pp.129-239.
- Consulting Consortium FAP 21/22 (1993), Final Report of the Planning Study Phase. Bank Protection and River Training (AFPM) Pilot Project FAP 21/22, June 1993.
- Consulting Consortium FAP 21/22 (1993), Annex 5. Bank Protection and River Training (AFPM) Pilot Project FAP 21/22, June 1993.
- Consulting Consortium FAP 21/22 (1998a), Current measurements at Kamarjani, Katlamari and Bahadurabad, June until August 1997.
- Consulting Consortium FAP 21/22, (1998b), Monitoring and Adaptation Report 1996.
- Delft Hydraulics and DHI (1996), Floodplain levels and bankfull discharge of the Jamuna, Ganges and Padma Rivers. River Survey Project, FAP 24, Special Report 6.
- Delft Hydraulics and DHI (1996), Geomorphology and channel dimensions. River Survey Project, FAP 24, Special Report 7.
- Dietz, J.W. (1969), Kolkbildung im feinen oder leichten Sohlmaterialien bei strömendem Abfluss. Mitteilungen Theodor Rehbock Flussbaulab., Karlsruhe, Heft 155, pp.1-119.
- Ellen, T. van (1988), Hydraulisch en morfologisch effect van open kribben. Afstudeerverslag Technical University Delft, Delft, The Netherlands (in Dutch).
- Fisk, H.N. (1947), Fine-grained alluvial deposits and their effect on Mississippi River activity. U.S. Army Corps of Engrs., Mississippi River Commission, Vicksburg.
- Galappatti, R. (1993), One dimensional morphological modelling in Bangladesh; Methodology and constraints. Int. workshop on morphological behaviour of the major rivers in Bangladesh, 6-9 November 1993, Dhaka.
- Garde R.J. and K.G. Ranga Raju (1985), Mechanics of sediment transportation and alluvial stream problems, Wiley Eastern Limited.
- Halcrow, Sir William & Partners, DHI, EPC and DIG (1994), River training studies of the Brahmaputra River, Final report, Bangladesh.
- Halcrow and Partners and EPC (1998), River bank protection project, Brahmaputra right bank priority works, Contract B2: Sirajganj, Engineer's review and action plan report on damages in 1998 monsoon, Dhaka, Bangladesh
- Hallem, M.G., N.J. Neaf and L.R. Wootton (1978), Dynamics of marine structures; methods of calculating the dynamic response of fixed structures subject to wave and current action. CIRIA, London SW1P 3AU, England.
- Haskoning, Delft Hydraulics & BETS (1992), Meghna River Bank Protection Short Term Study, FAP 9b, Final Report, February 1992.
- Huis in 't Veld, J.C., J. Stuip, A.W. Walther & J.M. van Westen (Eds., 1987), The closure of tidal basins, Delft Univ. Press.
- Ikeda, S., N. Izumi and R. Ito (1991), Effects of pile dikes on flow retardation and sediment transport. Journal of Hydraulic Engineering, Vol. 117, No. 11, November, pp. 1459 - 1478.

- Inglis (1968), Discussion on 'Systematic evaluation of river regime', Journal of Waterways and Harbour Division, ASCE, Vol. 94, No. WW1.
- Jansen, P.Ph., van Bendegom, L., van den Berg, J., de Vries, M. and Zanen, A. (1979), Principles of river engineering: The non-tidal alluvial river.
- Kandasamy, J.K. and B.W. Melville (1998), Maximum local scour depth at bridge piers and abutments. Journal of Hydraulic Research, Vol. 36, No. 2, pp 183-197.
- Klaassen G.J. and K. Vermeer (1988a), Channel characteristics of the braiding Jamuna River, Bangladesh, Proc. Int. Conf. on River Regime, Wallingford, England, pp. 173 - 189 .
- Klaassen G.J. and K. Vermeer (1988b), Confluence Scour in Large Braided Rivers with Fine Bed Material, Intern. Conference on Fluvial Hydraulics, Budapest, 1988
- Krüger Consult and BCEOM (1992), Flood Hydrology Study, Dhaka, Bangladesh, June 1992.
- Lagasse, P.F., J.D. Schall, E. Johnson, E.V. Richardson and F. Chang (1995), Stream stability at highway structures. Report no. FHWA HI 96-032 HEC-20.
- Lagasse, P.F., M.S. Byars, L.W. Zevenbergen and P.E. Clopper (1997), Bridge scour and stream instability countermeasures. Report no. FHWA HI 97-030 HEC 23.
- Maza Alvarez, J.A. (1989), Design of groins and spur dikes. Hydraulic Engineering Proceedings of the Nat. Conf. on Hydr. Eng., New Orleans, Louisiana, pp.296-301.
- Mesbahi, J. (1992), On combined scour near groynes in river bends, M.Sc. thesis IHE, Delft, The Netherlands.
- Mosselman, E. (1992), Mathematical modelling of morphological processes in rivers with erodible cohesive banks. Communications on Hydr. and Geotech. Engrg., No.92-3, Delft Univ. of Technol., ISSN 0169-6548.
- Mosselman, E., T. Shishikura & G.J. Klaassen (2000), Effect of bank stabilization on bend scour in anabranches of braided rivers. Physics and Chemistry of the Earth, Part B, Vol.25, Nos.7-8, pp.699-704.
- Pilarczyk, K.W. (1987), Stability of loose and cohesive materials. In: The closure of tidal basins, Eds. J.C. Huis in 't Veld, J. Stuip, A.W. Walther & J.M. van Westen, Delft Univ. Press, pp.355-365.
- Predwojski, B., R. Blazejewski and K.W. Pilarczyk (1994), River training techniques; fundamentals, techniques and applications. Part II, Rijkswaterstaat, Dienst Weg- en Waterbouwkunde, Delft, The Netherlands.
- Rajaratnam, N. (1976), Turbulent jets. Elsevier, Amsterdam, The Netherlands.
- Rashid, H.E. (1991), Geography of Bangladesh. Second revised Ed., Univ. Press, Dhaka.
- Rendel Palmer & Tritton, NEDECO, BCL (1990), Jamuna Bridge Project, Phase II Study, River Training Works, Design Report - Volume I, Bangladesh.
- Shishikura, T. (1996), Morphological changes due to river bank protection. M.Sc. Thesis H.H.285, IHE, Delft.
- Shiyi Wang (1990), Regulation of the transitional shoals in Chuanjiang river, China Port and Waterway Engineering, Vol. 4, No. 1, Series 7, January 1990, pp. 51-59.
- Spring, F.J.E. (1903), The training of certain great rivers in Northern India, so that they may not outflank the works which span them. Tech. paper No.153, Railway Board, Government of India.
- Struiksmā, N. and A. Crosato (1989), Analysis of a 2-D bed topography model for rivers, American Geophysical Union, pp 153 - 180.
- Struiksmā, N., K.W. Olesen, C.Flokstra and H.J. de Vriend (1985), Bed deformation in curved alluvial channels, Journal of Hydraulic Research, Vol. 23, No.1, pp 57 - 79.
- Talmon, A.M., N. Struiksmā & M.C.L.M. van Mierlo (1995), Laboratory measurements of the direction of sediment transport on transverse alluvial-bed slopes. J. Hydr. Res., IAHR, Vol.33, No.4, pp.495-517.
- Thorne, C.R., S.R. Abt and S.T. Maynard (1993), Prediction of near-bank velocity and scour depth in meander bends for design of rip-rap revetments, International Riprap Workshop, pp. 980 - 1007.

- Torrey III, V.H. (1995), Retrogressive failures in sand deposits of the Mississippi River. In: River, coastal and shoreline protection; Erosion control using riprap and armourstone, Eds. C.R. Thorne, S.R. Abt, F.B.J. Barends, S.T. Maynard & K.W. Pilarczyk, Wiley, pp.361-377.
- Varma, C.V.J., K.R. Saxena & M.K. Rao (Eds., 1989), River behaviour, management and training. Central Board of Irrigation and Power, Publ. No.204, Vol.I, New Delhi.
- Winkley B.R., E.J. Lesleighter and J.R. Cooney (1994), Instability problems of the Arial Khan River, Bangladesh. In: The variability of large alluvial rivers, ASCE Press, New York, USA, pp 269 - 284.
- WL | Delft Hydraulics (1987), Kribvakerosie door zes- en vierbaksduwvaart op de Waal. Verslag van modelonderzoek Q93/Q576 (in Dutch).
- WL | Delft Hydraulics (1991), Ontgronding bij een horizontale vernauwing. Report Q935, Delft, The Netherlands (in Dutch).

